UNIVERSITY OF SOUTHAMPTON

FACULTY OF ENGINEERING, SCIENCE AND MATHEMATICS.

SCHOOL OF CHEMISTRY

From linear to cyclic anion receptors: High affinity receptors and sensors for oxo-anions.

by

Simon James Brooks

Thesis for the degree of Doctor of Philosophy.

September 2006

UNIVERSITY OF SOUTHAMPTON

ABSTRACT

FACULTY OF ENGINEERING, SCIENCE AND MATHEMATICS.

SCHOOL OF CHEMISTRY

Doctor of Philosophy

FROM LINEAR TO CYCLIC ANION RECEPTORS: HIGH AFFINITY RECEPTORS AND SENSORS FOR OXO-ANIONS.

By Simon James Brooks

This thesis reports the synthesis and study of the coordination properties of a variety of novel organic anion receptors. A series of receptors based upon 1,2-phenylenediamine with varying hydrogen-bonding geometries have been investigated. Of these it has been observed that compounds that are based upon bis-urea functionality serve as excellent receptors for oxo-anions, in particular carboxylate anions, in DMSO solutions. Solid state analysis reveals that the carboxylate bis-urea interaction occurs through a 1:1 stoichiometry with all four of the NH donor groups coordinating to the anion. Extending the hydrogen bonding motif further, through additional appended amide groups, results in the formation of stronger complexes with anions although multiple stoichiometries become observed in solution. The bis-urea / carboxylate interaction has been further demonstrated as a useful synthon in the formation of higher order structure in the solid state.

A macrocyclic amido-urea derivative and various acyclic fragments of the structure have been synthesized and their anion binding properties determined. It has been found that the macrocycle displays significantly enhanced anion binding properties, in comparison to its fragments, with the especially high binding observed with carboxylates. Analysis of the binding data reveals that the macrocycle binds anions through differing binding modes depending upon anion size and shape.

Five 1,3-dicarboxamidoanthraquinone-based receptors have been synthesized and their anion binding properties investigated. In solution the receptors display moderate determinable selectivity for dihydrogen phosphate over the other oxo-anions, although fluoride interacts strongly the data could not be fitted to a binding model. The electrochemistry of the anthraquinone system has been investigated in both the presence and absence of fluoride and it has been determined that stabilizing interactions to the oxygen atoms from the amide groups may be overcome upon addition of fluoride anions, allowing electrochemical sensing of the fluoride species.

Various anthracene-based receptors have been synthesized in order to investigate differing hydrogen-bonding motifs. Two alternative amide motifs have been demonstrated to offer selectivities consistent with their respective hydrogen bonding arrays. A further examination of bis-urea based anthracene receptors reveal selectivity for carboxylates, with fluorescence quenching observed upon addition of coordinating anions.

ABBREVIATIONS.

Ar	Aryl
Br	Broad resonance (NMR)
Calc.	Calculated
cat	Catalytic
CV	Cyclic voltammogram
d	Doublet (NMR)
DCM	Dichloromethane
decomp.	Decomposed
DISP	Disproportionation (Electrochemical mechanism)
DMAP	4-Dimethylaminopyridine
DMF	Dimethylformamide
DMSO	Dimethylsulfoxide
ECE	Electrochemical-Chemical-Electrochemical (Electrochemical mechanism)
equiv.	Equivalent(s)
Et	Ethyl
ES	Electrospray (Mass Spectrometry)
g	Gram(s)
h	Hour(s)
HOBt	1-Hydroxybenztriazole hydrate
HRMS	High Resolution Mass Spectrometry
Hz	Hertz
i.e.	*Id est* (Latin: that is)
J	Coupling constant (NMR)
min	Minute(s)
m	Multiplet (NMR)
M	Molarity
Me	Methyl
mol	Mole(s)
m.p.	Melting point

m/z	Mass to charge ratio (Mass Spectrometry)
NMR	Nuclear Magnetic Resonance
Ph	Phenyl
ppm	Part per million (NMR)
PyBOP	Benzotriazol-1-yloxytripyrrolidinophosphonium hexafluorophosphate
q	Quartet (NMR)
R_f	Retention factor
s	Singlet (NMR)
t	Triplet (NMR)
TBA	Tetrabutylammonium

CONTENTS.

ACKNOWLEDGEMENTS.

I would initially like to thank my supervisor Dr. Philip A. Gale for all of his help and support during the last three years. Additionally I would like to thank all members of the Gale group both past (Korakot, Josep, Ismael and Louise) and present (Gareth, Matthew, Sergio and Jo) and all those temporary visitors (Somchai, Chantelle, Roberto, Tomas and Marta) who have both been a great source of support and encouragement. Additionally I would like to thank all of the three project students that I have had during my PhD (Peter, Pamela and Andrew) for their enthusiasm and hard work.

I would like to thank the University of Southampton and the EPSRC for funding and the NMR, MS and stores for all of their assistance.

An especially large thank you goes to Dr. Mark E. Light for all of his expertise in solving the numerous crystal structures that are outlined in this thesis. Additional thanks go to Dr. Peter. R. Birkin for his considerable help in the set up of the electrochemistry that is outlined and also for his elucidation of the mechanistics of the system. I would also like to thank Prof. Mike Gore and Dr Aimee J. Cossins for enabling the collaboration for the fluorescence section.

A huge thank you goes to my family especially my parents and Mathew, Mark and Leah for continuing to support me through the last three years. Finally I would like to thank Aimee for everything over the last few years.

1. INTRODUCTION.

1.1. SUPRAMOLECULAR CHEMISTRY

The field of supramolecular chemistry involves both the formation and investigation of systems in which discrete molecules are held together by non-covalent interactions. Unlike typical organic synthesis that involves the making and breaking of covalent bonds to produce a desired compound, the supramolecular chemist uses a variety of reversible intermolecular interactions in the formation of supermolecules. These supermolecules can be composed of two or more chemically distinct species that are held together through intermolecular binding interactions, with typically the larger component being referred to as the host, whilst the smaller component is the guest.

Host - guest interactions generally occur through particular binding sites that arise when the two components possess a combination of shape and charge that are complementary to one another, an idea first described by Fischer when considering the "lock and key" principle of enzyme-substrate interactions (Fig 1.1).[1]

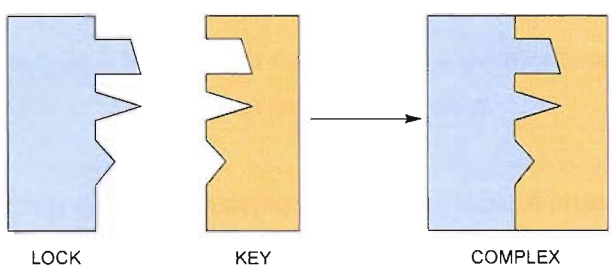

Fig 1.1: The "lock and key principle" – the two components display complementary shape allowing binding interactions to facilitate complex formation.

The most advanced examples of host - guest interactions come from nature, with perhaps the most notable being the double-helical structure adopted by DNA. The molecule is comprised of two distinct single chains that are held together through non-covalent hydrogen bonding interactions between complementary nucleotide base pairs. The reliable and specific interactions between the bases allow the DNA molecule to duplicate itself with an extremely high level of accuracy due to the fact that each of the bases binds its complementary base with a high level of selectivity (Fig 1.2).

The presence of multiple attractive interactions between both the donor and acceptor groups that stabilize the structure have been a great source of inspiration to supramolecular chemists with multiple research groups exploiting this and similar interactions for molecular self-assembly.[2, 3]

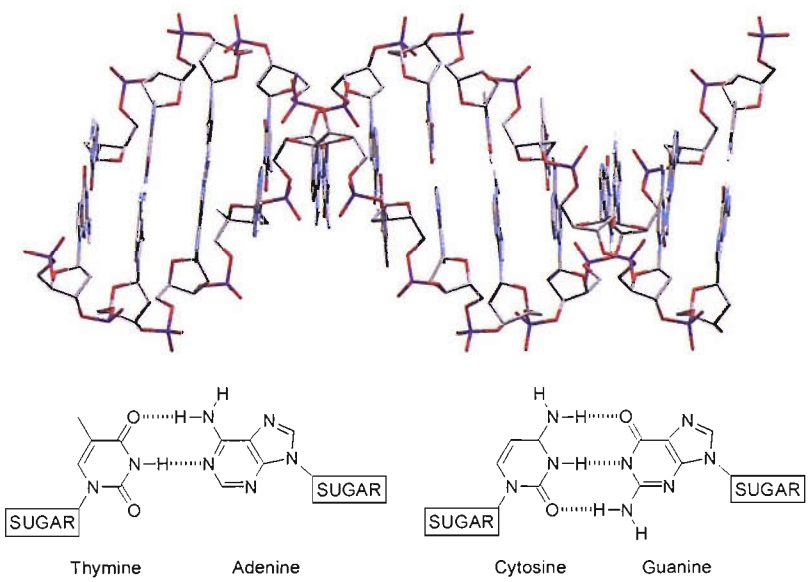

Fig 1.2: The DNA double-helix is held together through multiple specifically orientated hydrogen bonds between its component base pairs.

When considering synthetic receptors, a general design strategy is often employed consisting of either a cavity or a cleft, which can approximate the size and shape of either a part or the whole of the guest molecule. This binding site incorporates some chemical functionality that can be complementary both sterically and electronically to that displayed by the guest.

1.2. ANION COMPLEXATION.

Although often overlooked, the fact that anions are ubiquitous in Nature makes their study an important area of research. From the vast quantities of chloride found in the oceans, to nitrate and sulfate found in acid rain and carbonate in the form of mineralized rocks such as limestone, the presence of anions shapes a multitude of processes.

From a biological viewpoint, anionic substrates are involved in a multitude of physiogical processes, with approximately 70% of enzyme substrates and co-factors being anionic.[4] DNA itself is polyanionic, with the incorporated phosphate groups an important structural feature of the backbone of the molecule. Alternatively phosphate esters are commonly introduced to biologically active molecules through oxidative phosphorylation processes performed by molecules such as ATP and ADP in order to provide energy for chemical reactions to occur. Other biologically important anions include carboxylates that are present both in single amino-acids and proteins, whilst both chloride and sulfate are important in the maintenance of charge balance across cell membranes. In Nature both phosphate and sulfate are bound by certain bacteria[5,6] through the use of highly selective transport proteins known as phosphate binding protein (PBP) and sulfate binding protein (SBP) respectively (Fig 1.3).

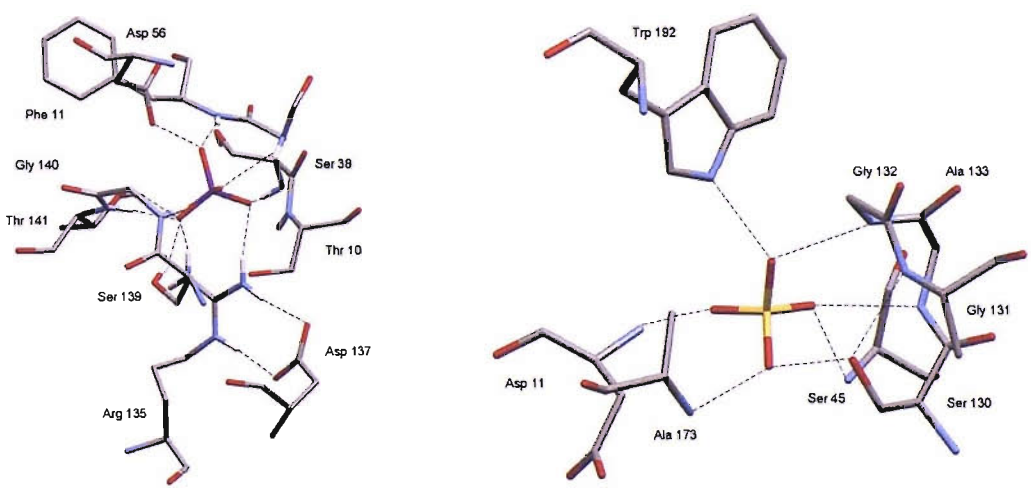

Fig 1.3: Tetrahedral phosphate and sulfate (left and right) are bound in nature specifically by their respective binding proteins.

Considering the similarity in terms of the tetrahedral shape of both phosphate and sulfate, these proteins are able to distinguish between the two anions with exceptional selectivity. This selectivity is achieved due to the differing protonation states of the anions at biological pH, phosphate is found in the mono-protonated form whilst sulfate is fully deprotonated. The PBP can form twelve hydrogen bonds with the anion, including the acceptance of a hydrogen bond from the anion to a negatively charged carboxylate residue. This interaction is one that is obviously unavailable to the non-protonated sulfate anion and provides a method of discrimination between the anions. SBP forms seven hydrogen bonds to the sulfate anion and lacks the ability to accept a hydrogen bond from the anion, therefore only fully deprotonated tetrahedral anions are able to fit with high specificity into binding site.

The field of anion coordination chemistry began in 1968 when Simmons and Park reported the first examples of synthetic receptors that displayed halide complexation properties (Fig 1.4).[7] This class of macrobicyclic hosts were termed 'katapinands' and analysis of their behaviour revealed the ability to encapsulate halide ions within their internal cavity upon protonation of the bridgehead nitrogen atoms. Later the chloride bound structure of **1** was confirmed by X-ray crystal structure determination and proved to be the first example of an anion bound by a macrocyclic host.[8]

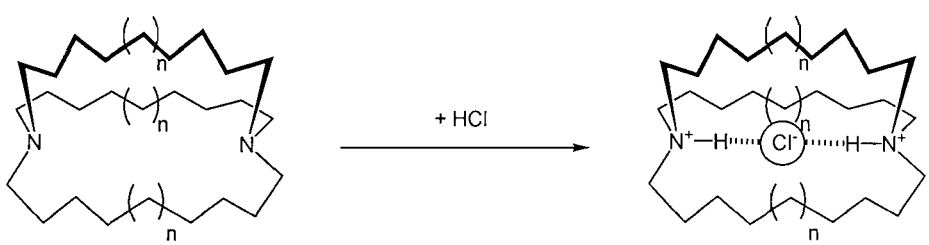

1 n = 1
2 n = 2

Fig 1.4: Simmons and Park's diprotonated katapinands **1** and **2** displayed chloride coordination properties.

In spite of this seminal early work, development in the area of anion coordination chemistry has been much slower in comparison to the more mature fields of both cationic and neutral substrate binding. This is due to a number of difficulties that make anion complexation both a challenging and exciting area of research.

- Anions are much larger when compared to their iso-electronic cationic counterparts (e.g. Na^+ = 1.02 Å, F^- = 1.33 Å) thus reducing their effective charge to radius ratio, making electrostatic interactions weaker.
- Even simple inorganic anions occur in numerous shapes and geometries, e.g. spherical (F^-, Cl^- and Br^-), linear (SCN^- and N_3^-), planar (NO_3^- and $PtCl_4^{2-}$), tetrahedral (PO_4^{3-} and SO_4^{2-}) and octahedral (PF_6^- and $Fe(CN)_6^{3-}$), along with numerous more complicated examples for biological oligophosphates.
- In comparison to cations of similar size, anions have higher free energies of solvation therefore requiring anionic hosts to compete more effectively than the solvent system employed.

The various supramolecular interactions that are available for the coordination of anions along with their relative strengths are displayed below (Fig 1.5).[4] Whilst ion-ion interactions are particularly strong they lack directionality and therefore make it difficult to introduce selectivity based upon shape recognition. Many groups have therefore focused their efforts into the synthesis of receptors that utilise hydrogen bonding interactions.

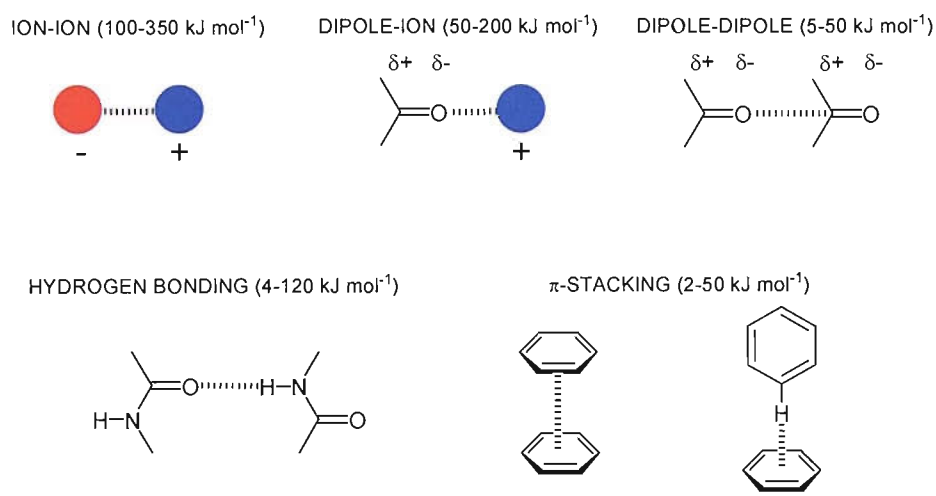

Fig 1.5: Non-covalent interactions and their relative strengths.

One of the most important factors that the anion coordination chemist is required to address is the solvent effect upon the system that is being studied. The use of weakly

coordinating solvents, such as chloroform, results in smaller interactions between the solvent and both the receptor and the anion. This therefore results in relatively low desolvation energies to be overcome before the binding interaction can occur and generally results in high stability constants. Unfortunately solution-phase analysis is impossible in weakly coordinating solvents for many receptors due to relatively strong self-association processes. The use of more competitive solvents such as dimethylsulfoxide introduces stronger solvent – receptor/anion interactions, allowing for greater solubilisation of receptor. The trade-off for this change of solvent is a higher desolvation energy which significantly reduces the observed stability constant.

In many ways the ultimate goal of the anion-coordination chemist is to bind anions both strongly and selectively under aqueous conditions. These environments are observed *in vivo* therefore receptors that can achieve this aim could potentially provide new medicines and diagnostic techniques. There are currently very few examples in which this goal has been achieved that reflects the great difficulty that is associated with achieving this aim.[9, 10]

The adoption of a single rigidified receptor conformation upon the coordination of an anion causes an unfavourable loss in entropy and has a detrimental effect upon the stability of the complex. This effect can be somewhat reduced in the case of acyclic receptors through the use of rigid frameworks to which binding units can be appended.[11] In addition the use of both steric and electrostatic effects in order to stabilise the binding conformation and predispose the receptor to adopt a more pre-organized structure have been investigated.[12,13] An alternative approach has been the development macrocyclic systems in which the binding sites are geometrically locked into a binding conformation.[14] In this case the entropic penalty is overcome during the synthesis of the receptor and therefore the binding process is more favourable.

Overcoming the various difficulties that have been outlined has been the aim of numerous research groups around the world over the last decade and as a result vast strides have been made into the development of new anion receptors that can bind both anions with both high levels of association and selectivity.

1.3. AMMONIUM BASED ANION RECEPTORS.

Ammonium based receptors combine both electrostatic interactions and hydrogen bonding interactions, in the case of protonated primary, secondary and tertiary amines, to facilitate the binding of anions. Protonation of the amine groups to the ammonium form increases the positive charge possessed by the receptor and as a consequence the anion stability constants are vastly improved over the non-protonated forms.

As previously demonstrated with Simmons and Park's early example,[7] polyammonium based anion receptors have provided both the earliest examples of synthetic anion receptors and also continued to be both a rich and diverse subset of anion coordination chemistry.[15-17]

During the 1970's Lehn and co-workers demonstrated the anion binding properties of a wide variety of both macrocyclic polyammonium derived anion receptors (Fig 1.6).[18-20]

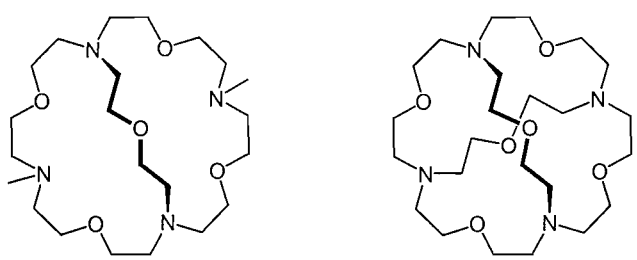

3 **4**

Fig 1.6: Lehn's macrobicyclic and macrotricyclic receptors **3** and **4** showed chloride selectivity when in the tetraprotonated form.

Protonation of the amine residues of **3** and **4** yielded the tetraprotonated ammonium forms for which the anion stability constants were determined. In both cases the receptors showed selectivity for chloride over iodide, reflecting the fact that the cavity within the systems in which the halide occupies is more suited to chloride than larger anions. This result that was subsequently confirmed *via* X-ray structure analysis of the chloride complex of **3**. The bicyclic receptor **3** which possesses lower conformational

rigidity, consistent with the removal of a strapping ring system, displayed considerably lower affinities for the anions investigated than analogous receptor **4**.

Investigation into quaternary ammonium receptors has been made by Schmidtchen and co-workers[21,22] in which the ammonium groups are arranged into a tetrahedral geometry through the use of alkyl spacer groups (Fig 1.7). Crystallographic characterisation of **5** revealed that one of the iodide counterions can be encapsulated within the cage-like cavity.

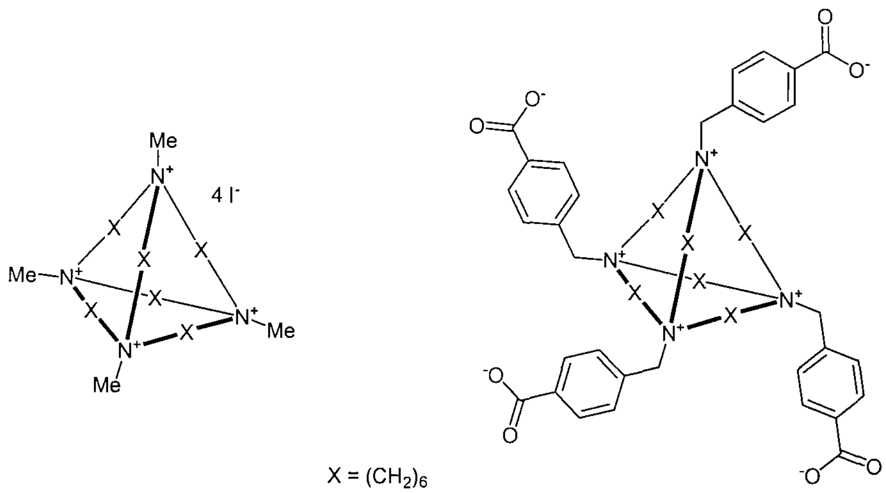

5 **6**

Fig 1.7: Schmidtchen's quaternary ammonium receptors 5 and 6.

The apparent high affinity of **5** for its own counter anion caused a competitive effect with anions for whose binding properties were under investigation. Therefore a zwitterionic form **6** was synthesized in which the appended carboxylate residues would not be able to occupy the binding site within the cavity. Comparison between the anion affinities of the two receptors performed by ^{1}H NMR titration experiments in D_2O confirmed that **6** displayed higher affinities for chloride, bromide and iodide than **5** indicating that removal of competition results in stronger complexes being formed.

More recently Martell and co-workers[23] have investigated the use of macrocyclic polyammonium receptors **7** and **8** in order to facilitate the binding of various anions in aqueous conditions (Fig 1.8). A variety of anion included crystal structures of the receptor **7** and **8** were obtained in which the anions were found to both occupy positions within the macrocyclic cavity and to be bound within crystal lattice.

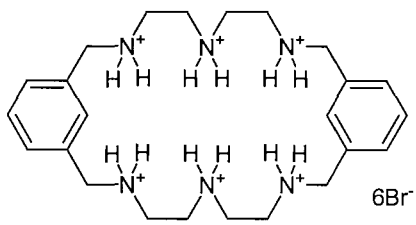

7

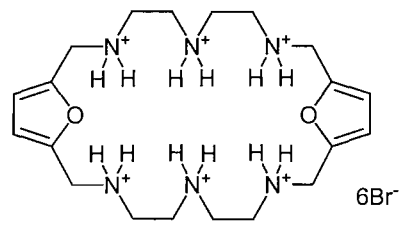

8

Fig 1.8: Martell and co-workers polyammonium receptors **7** and **8** bound a variety of phosphorylated anions.

Solution phase studies of both **7** and **8** with various anions were performed, with data obtained *via* potentiometric measurements performed in aqueous 0.1 M KCl solution. These results showed that the hexaprotonated form of both receptors bound anions more strongly in all cases with exceptionally high stability constants determined for the $P_3O_{10}^{5-}$ anion for each of the two receptors investigated.

1.4. AMIDE BASED ANION RECEPTORS.

Amides are essential in biological systems being the basis of polypeptide formation and playing structural roles in stabilising the tertiary structure of proteins. Amide NH groups are also used to coordinate anions in biological systems[24] and when combined with the extensive established chemistry that is already in place for their formation, have provided an accessible route to numerous anion receptors.

Organic amide based receptors typically have the amide binding units arranged in space so that they can act cooperatively within a convergent molecular architecture. This is typically achieved by either the lining of a macrocycle with amide NH groups or through appending groups onto an acyclic skeleton so that the amide moieties can arrange into a cleft or similar conformation.

In 1986 the first synthetic anion receptor that solely utilized amide NH···anion hydrogen bonding interactions was reported by Pascal and co-workers (Fig 1.9).[25] The C_3-symmetric cyclophane was synthesized *via* an acid chloride condensation reaction between the triamine **9** and triacid **10** and yielded the triamide **11** in 11% yield. The receptor **11** displayed evidence of binding of TBA fluoride in DMSO-d_6, however quantitative anion binding data was not reported.

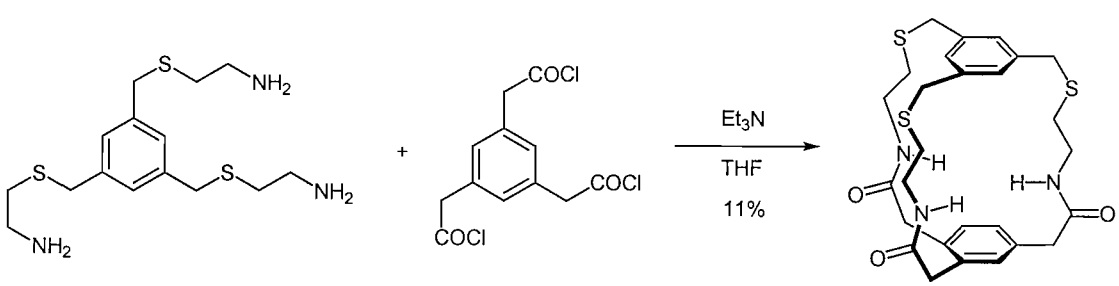

Fig 1.9: Pascal's cyclophane **11** displayed fluoride selectivity.

Subsequent work performed by Reinhoudt and co-workers[26] reported a class of acyclic C_3-symmetric tripodal receptors **12** and **13** that incorporated appended amide moieties (Fig 1.10). Association constants for these receptors with dihydrogen

phosphate, chloride and hydrogen sulfate were obtained *via* conductivity experiments performed in acetonitrile and revealed that phosphate was more strongly bound than the other two anions.

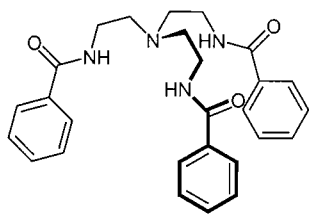

12

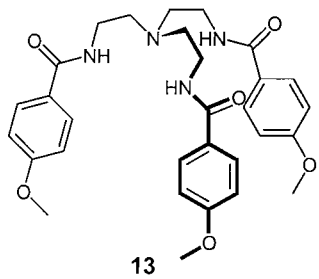

13

Fig 1.10: Reinhoudt's tripodal receptors **12** and **13** displayed selectivity for dihydrogen phosphate.

An alternate class of monocyclic C_3-symmetric receptors were reported by Hamilton and co-workers (Fig 1.11).[27,28] The anion complexation properties of these receptors were examined by NMR titration experiments performed in 98:2 $CDCl_3$ / DMSO-d_6 solution and revealed that the acyclic receptor **14** bound anions very poorly. Conversely macrocycle **15** displayed an increased affinity for anions with a 1:2 anion-receptor stoichiometry observed for iodide, chloride and nitrate whilst a 1:1 stoichiometry was observed for *para*-methyltosylate.

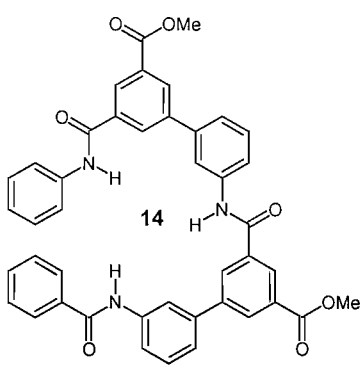

14

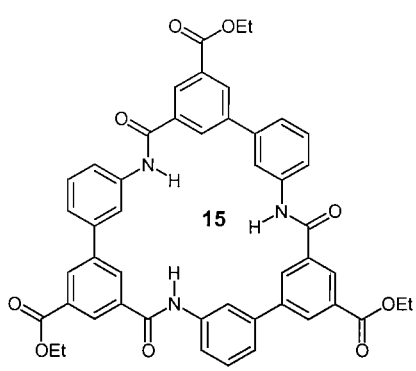

15

Fig 1.11: Hamilton's pseudo-C_3-symmetric acyclic **14** and C_3-symmetric macrocyclic **15** receptors.

Molecular modelling studies performed on the macrocyclic derivative with iodide indicated that the 1:2 stoichiometry could be due to the formation of a sandwich complex in which the anion sits between two molecules of the macrocycle with overall six amide NH hydrogen bonds to the anion.

Some of the most important acyclic amide-based receptors include the isophthalamide derivatives designed by Crabtree.[29,30] The use of isophthalamide derivatives in the binding of neutral guest species such as barbital had been previously investigated by Hamilton,[31] however it was Crabtree who first looked at the potential of the isophthalamide motif as a method of producing a convergent bis-amide cleft (Fig 1.12).

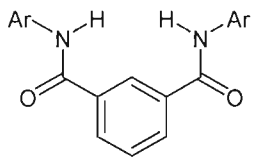

16 Ar = Ph
17 Ar = *p*-(n-Bu)C_6H_4

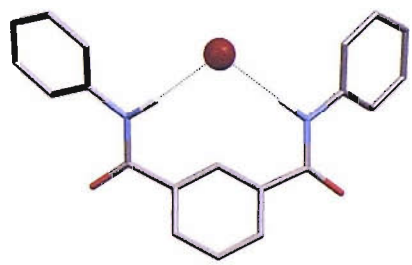

Fig 1.12: Crabtree's isophthalamide based anion receptors **16** and **17** and the bromide complex of **16**.

These receptors displayed a high affinity for halides due to their ability of the two amide groups to adopt a *syn-syn* geometry and form a convergent hydrogen bonding array. This conformation is ideally arranged for the coordination of spherical halide anions as well as allowing for the formation of almost linear hydrogen bonds. Solution phase studies of the anion association constants for these compounds were conducted *via* ^{1}H NMR titration experiments performed in CD_2Cl_2. These revealed that for **17**, chloride was bound stronger than bromide, presumably due to greater acidity and smaller size, showing that this class of compound is selective for halides under these conditions. X-ray crystal structure elucidation of the bromide complex of **16** reveals that the bromide is positioned slightly above the plane of the central aryl ring with the amide NH groups pointing directly at the anion in a *syn-syn* geometry.

Similarly a bis-amide approach based upon isophthalamide was developed independently by Smith and co-workers[32], in which a Lewis-acidic bononate group was appended through the peripheral aryl group (Fig 1.13). This was intended to utilize the boron-carbonate interaction to increase the binding affinity of the receptors relative to the non-derivatized isophthalamide.

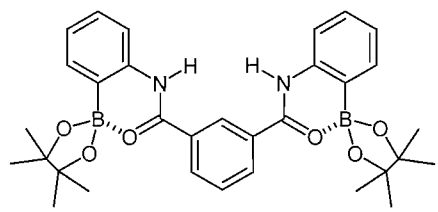

18

Fig 1.13: Smith's boronate isophthalamide receptor **18** displayed a significant increase relative to non-functionalized **16**.

Titration data performed in DMSO-d_6 revealed that **18** bound acetate with a constant of 2,100 M^{-1}, a ten-fold increase when compared to the isophthalamide derivative **16**. NOE experiments indicated that the receptor adopted a cleft conformation with the ^{11}B-NMR showing that an upfield shift occurred upon the addition of acetate. This behaviour appears to suggest that the binding of acetate by the receptor through the amide NH causes a cooperative polarisation of the carbonyl-boron bond.

Using a similar design rational of incorporating bis-amido groups, Prohen and co-workers[33] synthesized a range of squaramido-based receptors designed for the recognition of carboxylate anions in competitive solvent mixtures (Fig 1.14).

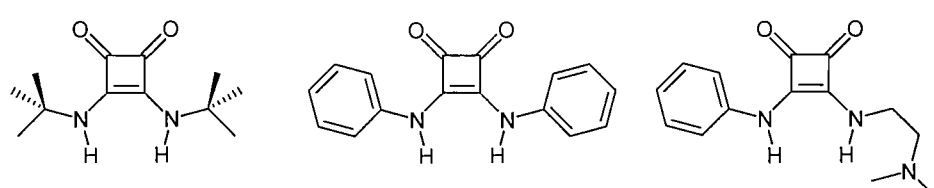

17 **18** **19**

Fig 1.14: Prohen's squaramido-based anion receptors **17-19** bound carboxylates in competitive solvents.

One of the main design features for this class of receptors is that the geometry adopted by the amide NH groups is far less convergent than the cleft geometries that can be adopted by isophthalamide receptors. This makes these receptors more efficient at coordinating bidentate anions through two approximately linear hydrogen bonds. Association constants relating to the strength of acetate binding for compounds **17-19** were determined in DMSO-d_6 to be 217, 1980 and 1120 M^{-1} respectively. This reflects the beneficial effect upon complexation caused by the increase in amide NH acidity through addition of electron deficient pendent aryl groups.

Kubik and co-workers[34] have developed cyclic hexapeptide-based receptors that contain both L-proline and 6-aminoicolinoic acid subunits that are placed alternately around the ring system (Fig 1.15).

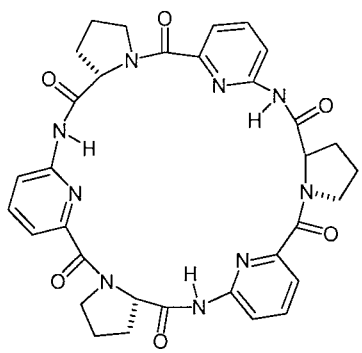

20

Fig 1.15: Kubik's cyclic hexapeptide **20** binds anions in highly competitive solvent mixtures.

The solution phase anion binding properties of **20** were investigated by ^{1}H NMR titration experiments performed in the extremely competitive solvent mixture of 80:20 D_2O/CD_3OD. In all cases for this receptor, a 2:1 host/guest stoichiometry was observed in solution with chloride, bromide iodide and sulfate all bound with high stability constants. The binding stoichiometry was confirmed *via* Job plot experiments whilst the iodide crystal structure revealed a 2:1 sandwich complex with the iodide in between the two hexapeptide macrocycles. Further derivisation of this motif was later performed with two hexapeptides covalently linked through various linker units[10], with the resulting receptor binding iodide in a 1:1 stoichiometry, confirmed by Job plot analysis and electrospray mass spectrometry. The manner in which the receptor can encapsulate an

anion, through the two hinged peptide subunits was subsequently described as a 'molecular oyster'.

Jurczak and co-workers[35] have synthesized a novel type of macrocycle **21** that incorporates both amide groups within a cyclic structure and a pendent amide group that can simultaneously coordinate to anions (Fig 1.16).

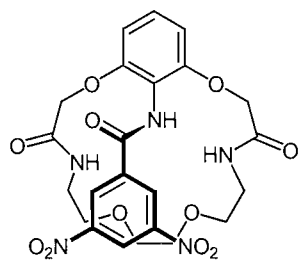

21

Fig 1.16: Jurczak's macrocyclic polyamide **21** allowed colorimetric detection of anions.

Determination of the anion binding properties of the macrocycle were investigated *via* ^{1}H NMR titration techniques in DMSO-d_6 and revealed a high selectivity for fluoride over other anions. A colourless solution of the receptor was observed to become deep blue on addition of fluoride, and yellow upon addition of chloride and dihydrogen phosphate.

The appendage of amide groups from various rigid scaffolds has proved to be a highly successful method of producing anion receptors that display both high association constants and selectivity. Calix[4]arenes have been shown in multiple examples to be particularly useful as rigid scaffold units upon which supramolecular host - guest assemblies can be based. This is due to the relative ease of derivatization of the calix[4]arene core and multiple positions from which functionalisation can be induced.[36,37]

Whilst earlier examples looked at the simple appendage of linear acyclic amide moieties to the scaffold, recently there have been various examples in which amide groups have been strapped across the calix[4]arene, providing extra rigidity to the receptor and the formation of stronger complexes with anions.

Ungaro and co-workers developed a novel series of C-linked 1,3-dialanylcalix[4]arenes (Fig 1.17).[38] Both receptors **22** and **23** include rigid aromatic groups within the strap itself that increase the rigidification effect induced by the strap.

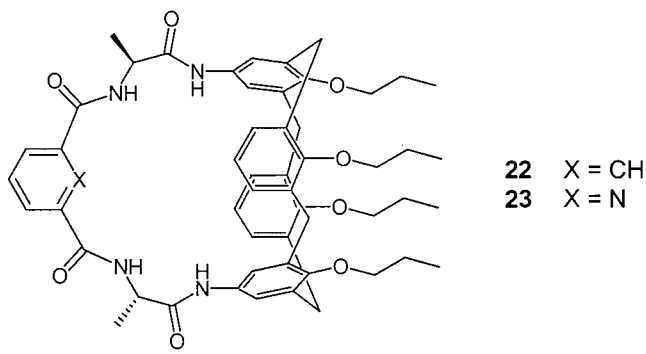

Fig 1.17: Ungaro's strapped calix[4]arene derivatives **22** and **23**.

The enhancement in both the rigidity and preorganisation of these receptors was reflected in the observed anion association constants for the receptors determined through ^{1}H NMR titration experiments performed in acetone-d_6. Carboxylate complexation was determined as particularly high, with benzoate and acetate bound with stability constants of 44,000 and 7,100 M^{-1} for **22** and 40,100 and 10,500 M^{-1} for **23**, for which also smaller degrees of both chloride and nitrate binding could be detected. The carboxylate stability constants are a deviation from those expected purely from the acidity of the anion. This difference can be explained by considering the possibility of additional stabilizing π-π interactions between the benzoate π-system and either the strap aromatic group and/or the calix[4]arene itself.

A more recent development by Beer and co-workers[39] has demonstrated a calix[4]arene bridged isophthalamide derivative **24** that can act as an AND logic gate, an important step in the use of supramolecular chemistry to produce molecular computing operations (Fig 1.18).

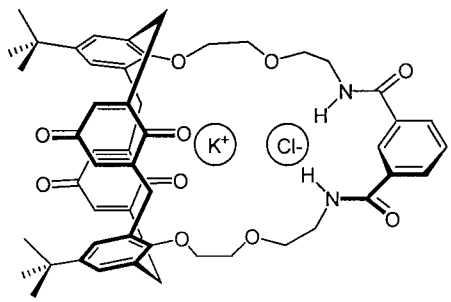

24

Fig 1.18: Beer's co-operative ditopic receptor **24**.

Calix[4]arene derivative **24** is functionalised through the appendage of an isophthalamide type strap across the lower rim attached by an ethylene glycol linkage. In addition oxidation of the non-appended calix[4]arene aryl systems has been performed to provide two quinone species that are redox active. This provides a method of monitoring the binding processes that occur with this receptor through changes in the electrochemical behaviour of the quinone / radical anion / dianion redox system.

Interestingly although the receptor is functionalised to bind both chloride (through the isophthalamide cleft) and potassium (through electrostatic interactions with the ethylene glycol and quinone oxygen atoms) the receptor only binds the contact ion-pair with any appreciable strength. As a result the presence of either of the anions alone does not significantly affect the redox behaviour of the system, whilst the addition of a solution containing both potassium and chloride results in a cooperative binding event with an observable change in the electrochemical behaviour.

Alternative scaffolds that have demonstrated considerable promise include steroidal-based receptors in particular those based upon functionalised cholic acid.[40] Davis and co-workers[41] have designed an acyclic system based upon sulfonamide bis-carbamate amide **25** and sulfonamide **26** groups that can be thought of as analogous to amide functionality. These are appended from cholic acid, with the resulting structures termed "cholapods' (Fig 1.19). The inflexibility of the fused ring system of the cholic acid scaffold forces the pendent sulfonamide groups in the 7α and 12α positions to adopt axial conformations that are ideally suited to form a convergent anion binding array.

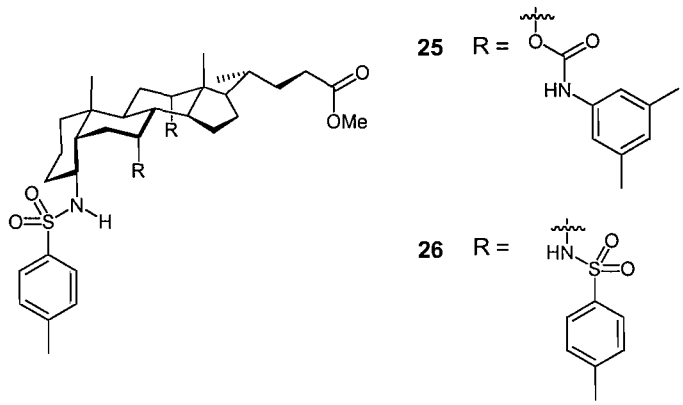

Fig 1.19: Davis' "cholapod" receptors **25** and **26** displayed halide selectivity.

Determination of anion stability constants was achieved from ^{1}H NMR titration experiments performed in $CDCl_3$. The structural rigidity and particular shape of these receptors provides a relatively small, well-defined binding site that is reflected by the fact that both receptors **25** and **26** showed selectivity for halides with particularly high affinities noted for fluoride with compound **25**. In the case of **26** the association with fluoride was too strong to determine by this method, however of the remaining anions that could be investigated chloride showed a similar trend of high anion association.

Overall the anion stability constant values for the sulfonamide derivative **26** were shown to be slightly higher than **25**, presumably due to the higher level of preorganisation of the molecule as predicted by molecular modelling experiments.

1.5. UREA BASED ANION RECEPTORS.

Ureas and their analogous thiourea derivatives have been employed as anion binding motifs in a diverse range of receptors within the last few years.[42,43] Among the advantages of using ureas and thioureas are that they form strong complexes with Y-shaped *oxo*-anions in particular (Fig 1.20). The methods of producing both ureas and thioureas are well documented and can be formed in high yielding reactions from either isocyanates or isothiocyanates making them readily synthetically available.

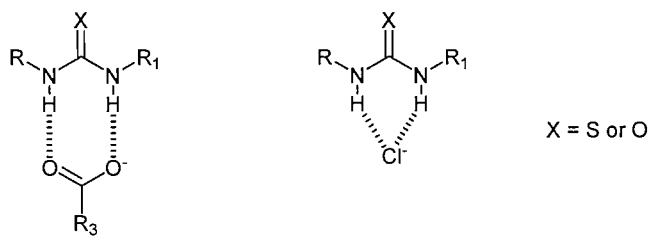

Fig 1.20: Urea and thiourea derivatives can form relatively strong complexes with both Y-shaped oxo-anions and halides.

Gunnlaugsson, Pfeffer and co-workers[44,45] have developed a class of thiourea substituted napthalimide derivatives **27-29** that can be used for the fluorimetric sensing of anions (Fig 1.21). 4-Amino-1,8-napthalimide was used as a fluorophore in order to develop sensors that fluoresce at longer wavelengths than those previously developed whilst retaining a high quantum yield.[46]

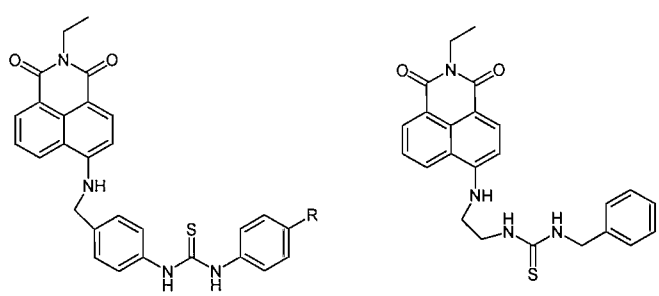

27 R = H
28 R = CF_3

29

Fig 1.21: Gunnlaugsson and Pfeffer's napthalimide based anion sensors.

Additionally the internal charge transfer state of napthalimide unit provides scope for modulation through the introduction of hydrogen bonding or deprotonation of the 4-amino group. This can provide an alternative way of sensing anions through a colorimetric change upon the addition of sufficiently interacting anions.

Evaluation of the anion stability constants of **27**-**28** with a variety of putative anions was performed *via* fluorescence quenching experiments performed in DMSO with data fitted using a non-linear least squares regression. Fluoride was bound with the highest affinity over both acetate and dihydrogen phosphate, with **28** which possesses an electron-withdrawing -CF_3 group displaying slightly higher stability constants. Receptor **29** incorporates a more flexible alkyl spacer unit between the urea moiety and the napthalimide moiety. This allows, in the case of dihydrogen phosphate, the amine residue to be used to coordinate the anion, due to the relatively large size and multiple oxygen atoms. This result is reflected in the anion having highest stability constant observed for this receptor. Simple amine derivatives of the same napthalimide moiety were later shown when in DMSO solution and in the presence of TBA fluoride to be able to sequester atmospheric carbon dioxide and cause its fixation in the form of hydrogen carbonate.[47]

Two bis- ferrocene substituted ureas were synthesized by Beer and co-workers[48] during the investigation of redox active anion sensors (Fig 1.22). Both a simple straight alkyl chain derivative **30** and a more sterically congested bis-*tert*-butyl ester urea **31** were synthesized to determine the effect of steric bulk upon the ability to coordinate anions.

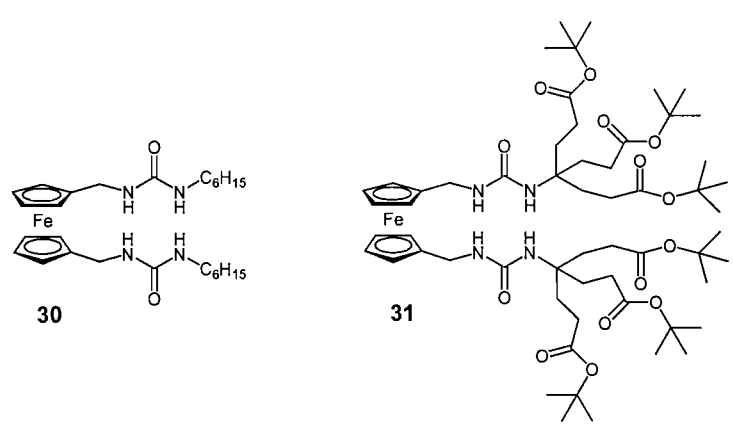

Fig 1.22: Beer's redox active alkyl chain **30** and sterically bulky **31** urea functionalised anion sensors.

Investigations into the coordination of both chloride and dihydrogen phosphate were performed *via* ^{1}H NMR titration experiments performed in acetonitrile-d_3 solution. Receptor **30** (in which there is no strong unfavourable interaction between the urea groups) shows selectivity for dihydrogen phosphate over chloride, with respective values of 1,150 and 350 M^{-1}. The presence of the larger, more bulky groups in receptor **31** appears to cause a change in observed selectivity. Both an increase in the chloride affinity to 880 M^{-1} and a decrease in dihydrogen phosphate to 150 M^{-1} attributed to unfavourable interactions between the larger phosphate anion and the tert-butyl ester groups.

Both naphthalene and binaphthalene appended thiourea derivatives were synthesized by Kondo and co-workers[49] in 2003 in order to investigate potential cooperative binding between the two thiourea moieties in compound **33** (Fig 1.23).

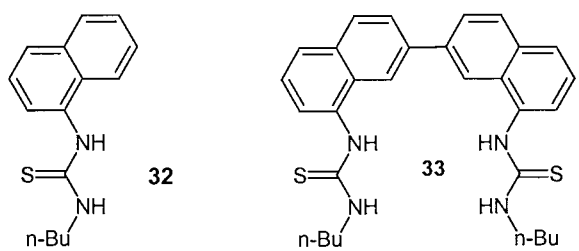

Fig 1.23: Kondo and co-workers based receptors upon naphthalene **32** and bisnapthalene **33** groups respectively.

The presence of binding was confirmed and evaluated through the use of UV-vis spectroscopy titration experiments performed in acetonitrile solution. Receptor **32** was observed to bind acetate, dihydrogen phosphate, fluoride and chloride with reasonable stability constants. The values obtained for the bis-thiourea derivative **33** however were observed to be approximately thirty times larger for the same anions. Job plot analysis indicated that even though multiple binding sites were present a 1:1 anion / receptor stoichiometry was observed for all of the anions investigated.

Pfeffer and co-workers[50] have investigated receptors **34-35** based upon thiourea groups appended upon the highly rigid polynorbornane scaffold unit (Fig 1.24). The incorporation of electron deficient aryl 4-trifluoromethylphenyl and 4-nitrophenyl

substituents was intended to increase the acidity of the thiourea protons and therefore enhance the anion binding properties. It was also envisaged that anion binding would result in a perturbation of the internal charge transfer character of the nitro-derivative and therefore allow colorimetric assessment of anion complexation.

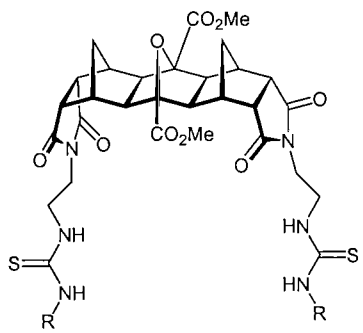

34 R = $C_6H_4CF_3$
35 R = $C_6H_4NO_2$

Fig 1.24: Pfeffer's and co-workers have used functionalised polynorbornanes as rigid scaffold unit for anion complexation.

Anion binding studies were performed *via* ^{1}H NMR titrations performed in DMSO-d_6 and revealed that both acetate and benzoate were strongly bound to both **34** and **35** with a 2:1 anion/receptor stoichiometry. In this case it is clear that each of the thiourea units is binding a single carboxylate. Addition of fluoride to a solution of **35** led to a strong colour change whilst a disappearance of the thiourea NH signals in the ^{1}H NMR spectrum was observed. Attempts to fit changes in alkyl CH resonances to a binding model proved difficult, however the appearance of a peak at $\approx$ 16.0 ppm was consistent with the presence of the semi-stable $[FHF]^-$ a species potentially formed following receptor deprotonation.

Fukazawa and co-workers[51] have produced a interesting example of a calix[4]arene derivative in which a bis-urea functionalized strap has been introduced in order to produce a ditopic receptor for dicarboxylates (Fig 1.25).

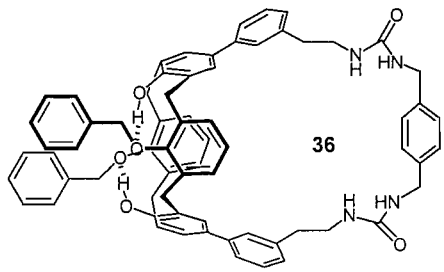

Fig 1.25: Fukazawa's calix[4]arene derived bis-urea receptor **36**.

Anion stability constants of receptor **36** with a variety of bis-carboxylates were investigated through the use of ^{1}H NMR titration experiments performed in DMSO-d_6 solution. The presence of 1:1 binding indicated that discrete binding of single dicarboxylate anions by the receptor was occurring, with strongest binding observed for anions based upon para-xylene spacer unit, indicating that the receptor possesses shape recognition properties for this type of anion.

Kilburn and co-workers[52,53] have devised a system for the enantioselective binding of aminoacids using of both acyclic and cyclic chiral receptors (Fig 1.26). In each case the presence of the pyridyl moieties acts to increase the rigidity of the receptors through intramolecular donor-acceptor interactions.

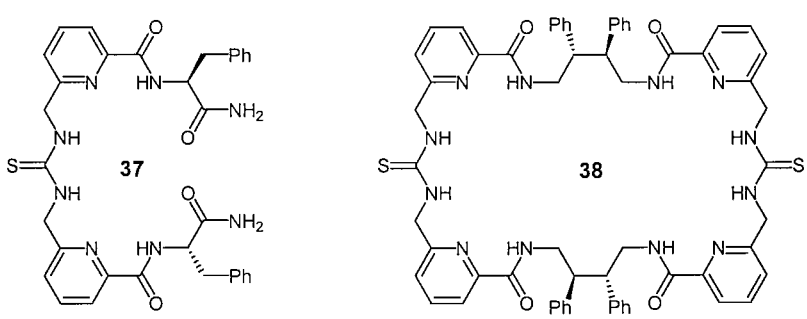

Fig 1.26: Kilburn's enantioselective receptors **37** and **38** bound the *D* form of N-Boc glutamate over the *L*-form.

Titration experiments were performed with a variety of both *L* and *D* forms of *N*-Boc protected chiral amino acid salts in the form of their TBA salts in $CDCl_3$. Discrepancies in observed stability constants between the two isomers would provide

evidence receptors displaying enantioselectivity. Whilst the acyclic receptor **37** displayed relatively modest enantioselectivity, the macrocyclic **38** displays high enantioselectivity for *N*-boc-L-glutamate in the form of the dicarboxylate anion in relatively polar solvents such as acetonitrile and DMSO. Interestingly **38** did not bind in $CDCl_3$ with the conclusion that it adopts a tightly wrapped conformation with intramolecular hydrogen bonding stabilizing this structure.

Recently Molina and co-workers[54] have developed a bis-urea system in which the combination of both ferrocene and naphthalene moieties has provided both electrochemical and fluorescent outputs upon the introduction of coordinating anions (Fig 1.27).

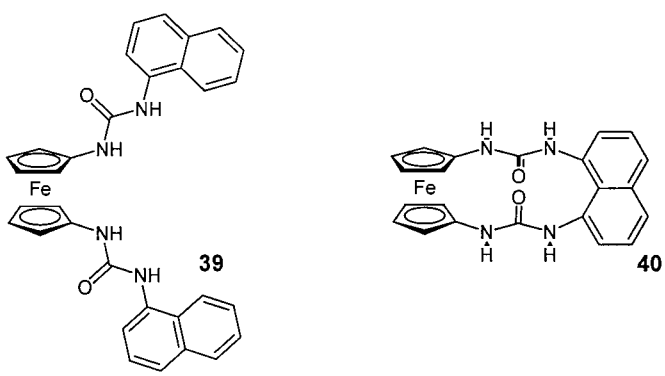

Fig 1.27: Molina's acyclic **39** and cyclic **40** ferrocene/naphthalene anion sensors.

Both receptors **39** and **40** demonstrated electrochemical responses in DMSO upon the addition of both fluoride and dihydrogen phosphate in the form of their TBA salts. Both oxidation and reduction peaks showed shifts towards more negative potentials upon addition of the anion, consistent with increasing difficult in reducing the negatively charged complex. Other anions investigated, including acetate, chloride and hydrogen sulfate produced no response in the redox chemistry.

Analysis of changes in the fluorescence of these compounds was performed in DMF were upon the addition of fluoride a significant enhancement in emission was observed. For compound **40** quantum yield increased from $\Phi_0 = 0.016$ to $\Phi = 0.21$, with a similar enhancement being observed for dihydrogen phosphate but to a lesser extent.

1.6. ARYL NH DONORS AS ANION RECEPTORS.

The use of aryl NH groups for anion complexation has been until recently less well documented in comparison to both amide and urea. The advantage of this group is an increase in solubility in organic solvents arising predominantly due to the lack of a hydrogen acceptor group (Fig 1.28). This effect lowers the level of self-association in solution making solvation of the receptor more favourable. Additionally the acidities of these NH protons are ideal for the formation of hydrogen bonds to anions and therefore the motif has been employed by numerous groups.[55, 56]

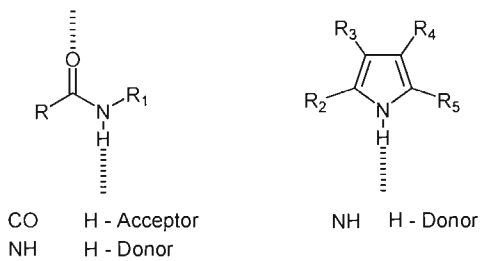

Fig 1.28: The lack of a H-acceptor group makes aryl NH groups less prone to self-association.

1.6.1. Pyrrole-based anion receptors.

The use of the pyrrolic NH group to coordinate anions has been a strategy employed by multiple research groups.[57,58] The first pyrrole-anion complex was obtained in 1999 by Gale and co-workers[59] through the co-crystallisation of pyrrole and TMA chloride (Fig 1.29).

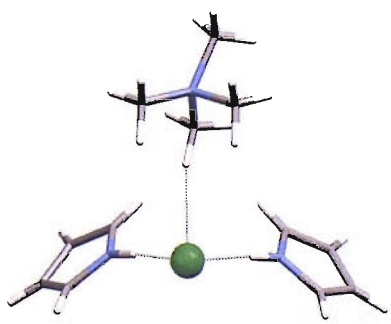

Fig 1.29: The first example of a pyrrole-bound anion complex.

Through the combination of pyrrole with a convergent bis-amide hydrogen bonding array, Gale and co-workers[60-62] have developed multiple systems based upon 2,5-dicarboxamidopyrroles. This motif facilitates the coordination of anions in through a combination of both convergent pyrrolic and amide NH groups to provide a three hydrogen bond donor motif (Fig 1.30).

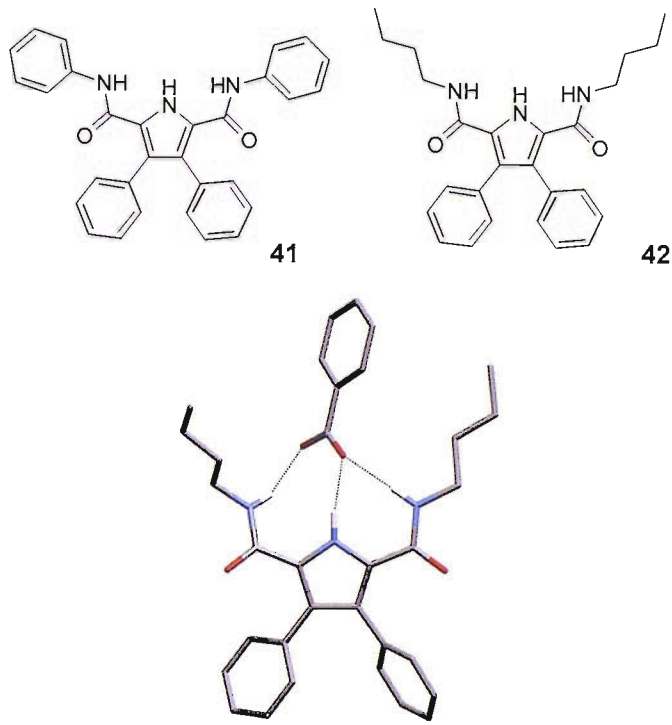

Fig 1.30: Gale's 2,5-dicarboxamido receptors **41** and **42** (above) and the benzoate complex of receptor **42** (below).

Investigation of the stability constants of compounds **41** and **42** were performed *via* ^{1}H NMR titrations in DMSO-d_6/0.5% water and acetonitrile-d_3 respectively arising from the differing solubilities afforded by the compounds. In both cases the receptors displayed a high affinity for oxo-anions, a reflection of the more open shape of the 2,5-dicarboxamidopyrrole cleft in comparison to similar clefts of the isophthalamide motif.

In the case of receptor **41** significant interactions were observed with both dihydrogen phosphate and benzoate, 1450 and 560 M^{-1} respectively, considering the high level of competition associated with the solvent mixture. This behaviour of oxo-anion

selectivity was mirrored in the case of **42** for which weaker stability constants (a consequence of the reduced acidity of the amide protons) for both dihydrogen phosphate and benzoate were obtained. The X-ray structure of the benzoate complex of compound **42** revealed a 1:1 receptor: anion stoichiometry in which the benzoate anion is bound to the receptor through three NH hydrogen bonds.[63]

More recently investigations into anion receptors that employ multiple pyrrole units have been performed.[64] One such example has included the functionalisation of the 2,5-dicarboxamidopyrrole motif with two additional groups through reaction of 2,5-dicarbonylchloride pyrrole with a 2-aminopyrrole derivative (Fig 1.31). It was hoped that the introduction of these additional pyrrole groups would lead to an increase in selectivity with oxo-anions.

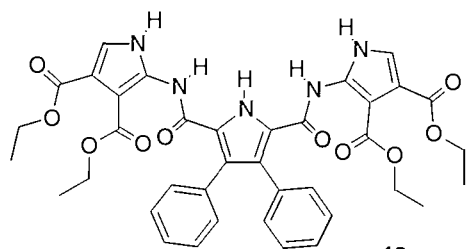

43

Fig 1.31: Sessler and Gale's receptor **43** employed two distinct types of pyrrolic NH donor.

Analysis of the solution phase anion complexation properties of receptor **43** performed in DMSO-d_6/0.5% water revealed that the compound displayed oxo-anion selectivity with an enhancement in stability constants for both dihydrogen phosphate and benzoate observed in comparison to analogous **41**.

Schmuck and co-workers[65-67] have investigated similar systems in their pursuit of both zwitterionic peptide receptors (utilising both anion and cation interactions) and self-assembling systems that can operate in extremely competitive solvent mixtures.

Zwitterion **44** was synthesized to provide insight into self-association processes in competitive solvents, with the incorporation of polyethylene glycol substituents onto the 3 and 4 positions of the pyrrole group in order to afford solubility in highly aqueous environments (Fig 1.32).

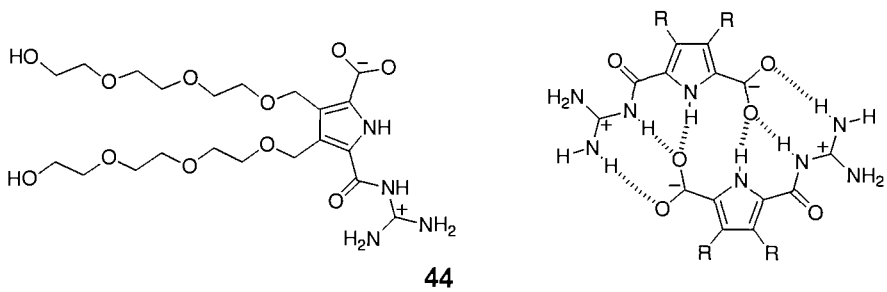

44

Fig. 1.32: Schmuck's pyrrole-based zwitterion **44** binds the carboxylate groups of the adjacent molecule through both pyrrolic and guanadinium hydrogen bonds.

Molecular modelling had indicated that that compound **44** could undergo dimerisation through intermolecular head-to-tail interactions between the carboxylate and guanidiniocarbonyl pyrrole moieties. Investigations revealed that the compound had an association constant of between 170-182 M^{-1} in a DMSO-d_6 / 2.5% water mixture.

This motif was later exploited further by Schmuck to produce a receptor **45** that displayed a huge affinity for dipeptides in aqueous environments.[68] The receptor design was assisted through the use of computational modelling with the aim to bind dipeptides that possess a free carboxylate group (Fig 1.33). The presence of a hydrogen bonded ion-pair interaction between the negatively charged carboxylate residue of the dipeptide and the guanidiniocarbonyl-pyrrole moiety of the receptor and additional interactions between the peptide backbone and the receptor was envisaged.

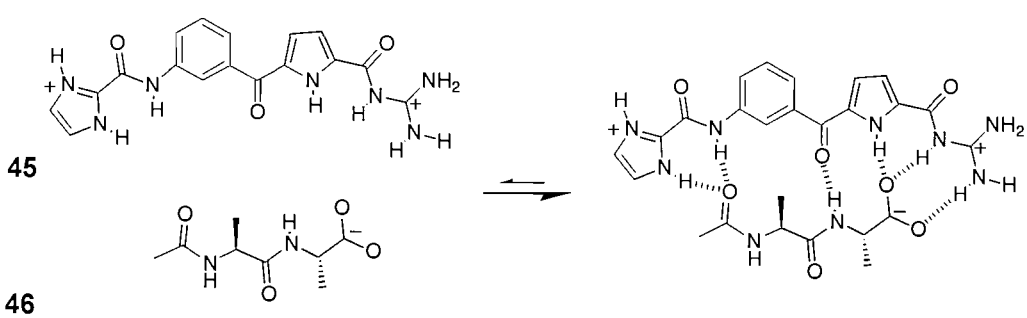

45

46

Fig 1.33: Schmuck's cationic guanidiniocarbonyl pyrrole receptor **45** displayed high affinity for dipeptide **46** in highly aqueous DMSO mixtures.

Initial data that the receptor could bind dipeptides came from ESI-MS experiments that displayed a distinct signal for 1:1 complexation between the receptor and the dipeptide shown **46**.

Solution studies further qualified this statement with ^{1}H NMR data indicating an association constant of greater than 10^6 M^{-1} in DMSO-d_6 / 40% water, with UV/vis experiments performed in the even more competitive solvent mixture of DMSO-d_6 / 90% water revealing an association constant of 43,800 M^{-1}.

1.6.2. Carbazole based anion receptors.

Analogous to pyrrole in terms of shape and geometry, the additional fused aryl rings that flank the central 5-membered heterocyclic ring have allowed chemists to append additional hydrogen bond donor groups to the rigid scaffold.

Insights into the use of carbazole-based acyclic anion receptors have been provided by Jurczak and co-workers[69] who produced two new receptors **47** and **48** in which the central motif is based upon a 1,8-diamino-3,6-dichlorocarbazole core (Fig 1.34).

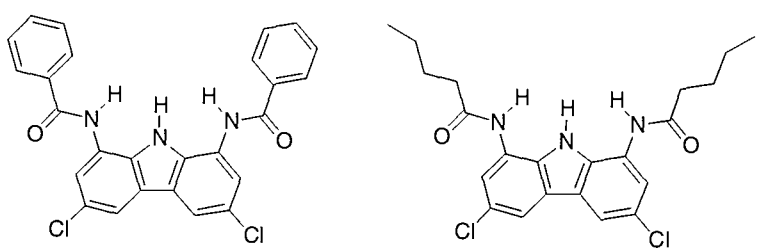

47 **48**

Fig 1.34: Jurczak's carbazole receptors **47** and **48** combine an aryl NH with a rigid scaffold.

Both aryl and alkyl derivatives were synthesized with the stability constants with a variety of putative anions determined *via* ^{1}H NMR titration experiments performed in DMSO-d_6 / 0.5% water revealing high association constants for both dihydrogen phosphate and benzoate. Interestingly while the bis-phenyl derivative **47** displayed association constants of 1230 and 1910 M^{-1} for benzoate and dihydrogen phosphate

respectively, the bis-butyl compound **48** revealed significantly higher constants of 8340 and 19,800 M^{-1}. This is an unusual observation considering the acidity of the amide protons and perhaps indicative of an unfavourable steric effect arising from the pendent aryl groups.

Sessler and co-workers[70] successfully combined both pyrrole and carbazole moieties in the formation of a novel expanded calixpyrrole receptor **49** (Fig 1.35). An advantageous property of carbazole is its high fluorescence (ϕ_f = 0.367) and therefore not only does it provide a NH donor group but also a means of sensing the anion through a fluorescence quenching mechanism.

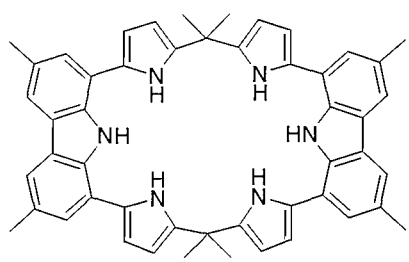

49

Fig 1.35: Sessler's calix[4]pyrrole[2]carbazole **49** displayed extremely high affinities for oxo-anions.

Elucidation of the association constants of compound **49** with a variety of anions was performed utilising fluorescence quenching titration experiments in dichloromethane. These results indicated that acetate was strongly bound by the receptor (K_a = 229,000 M^{-1}) with weaker interactions observed with larger, more complex, carboxylate anions such as benzoate, oxalate and succinate, 77,000, 31,000 and 9500 M^{-1}, respectively.

X-ray crystal analysis of the benzoate complex of **49** indicated in this case that the macrocycle adopts a "winglike" conformation with a single benzoate anion bound by the receptor through the four pyrrolic NH groups.

1.7. ARYL CH DONORS AS ANION RECEPTORS.

1.7.1. Imidazolium based anion receptors.

In the last few years increasing numbers of research groups have used positively charged aryl CH groups as a method of anion coordination, in particular imidazolium moieties have been employed for this end. Specifically examples in which 1,3-bis-substituted imidazolium moieties have been employed have been demonstrated to be able to perform as a anion binding units through both cation-anion electrostatic interactions and through the unconventional CH hydrogen bonds.

One of the earliest examples of this was shown by Sato and co-workers[71] who developed tripodal receptors **50** and **51,** both of which employed 1,3-bis-substituted imidazolium groups as a coordination site for anion binding (Fig 1.36).

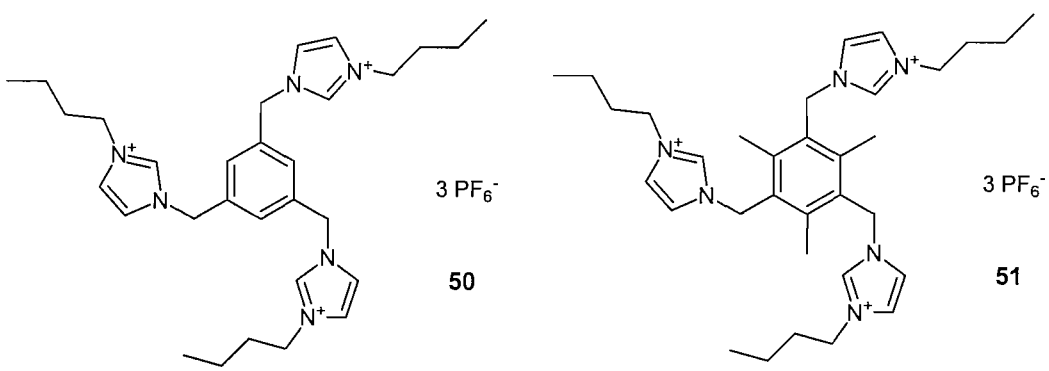

Fig 1.36: Sato's tripodal imidazolium based anion receptor **51** displayed chloride selectivity.

Investigations into the anion complexation properties of these compounds with variety of halides were performed *via* ^{1}H NMR titration experiments performed in deuterated acetonitrile solution. Receptor **51** displayed a high association constant with all of the anions reported, with chloride (75,000 M^{-1}), bromide (46,000 M^{-1}) and iodide (7,200 M^{-1}) all forming strong complexes with the receptor.

Interestingly the absence of the methyl groups appended to central phenyl ring in compound **50**, in comparison to **51**, resulted in a reduction in the reported chloride

association constant by approximately fifty-times (1,500 M^{-1}), with no association constant reported for either bromide or iodide in this case. This effect presumably arises from the greater conformational flexibility that receptor **50** displays through free rotation about the C_{aryl}-CH_2 bonds. Further development of this motif was reported by Kim and co-workers[72] who investigated the effect of nitro-substituted imidazolium moieties with these results displaying a similar overall behaviour to the non-functionalized derivatives.

Kang and co-workers[73] have also developed a tetraimidazolium receptor **52** based upon a functionalised glycouril molecule (Fig 1.37). Examination of the binding properties of this receptor revealed that the receptor bound halides in a 2:1 anion / receptor stoichiometry, whilst dicarboxylates such as succinate and glutimate were bound in a 1:1 fashion for which association constants were determined to be 1,800 and 2,700 in 90:10 acetonitrile-d_3/DMSO-d_6 solvent mixtures.

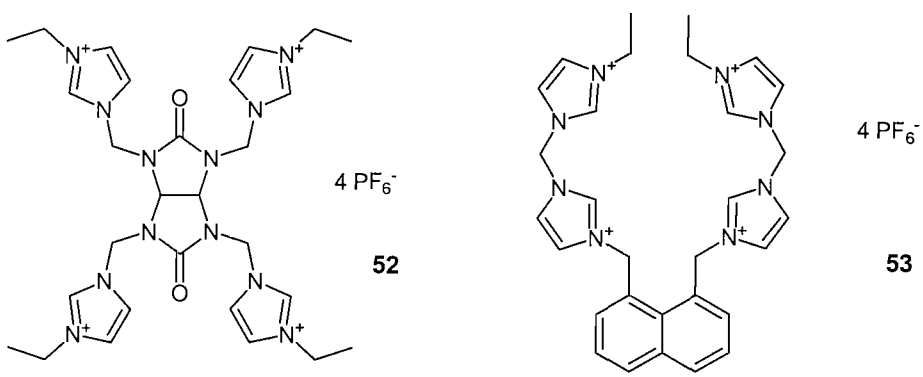

Fig 1.37: A variety of scaffolds allowed Kang to produce tetraimidazolium based receptors.

An alternative anion binding motif was also developed by Kang and co-workers[74] who synthesized a fluorescent anion sensor **53** based upon a naphthalene backbone to which imidazolium moieties were appended through 1,8-disubstitution of the naphthalene (Fig 1.37).

A methylene linkage between the naphthalene linked and pendant imidazolium groups facilitated the formation of a cleft predisposed for the complexation of halide anions. This arises from the fact that into the cleft it is possible for all of the imidazolium

2-positioned CH groups be orientated so as to simultaneously coordinate to a single anion.

Association constants were determined *via* fluorescence quenching experiments performed in 90:10 acetonitrile/DMSO solution. Anion association constants were obtained for iodide (5,000 M^{-1}), bromide (243 M^{-1}) and chloride (185 M^{-1}) and indicated that the cavity size of the receptor in this case is sufficiently large and rigid, so that binding of the larger iodide anion is favoured.

Macrocyclic imidazolium receptors have also been developed by a number of groups and have been demonstrated to display high association for anions. Xie and co-workers[75] investigated the halide binding properties of a novel class of imidazolium cyclophanes (Fig 1.38).

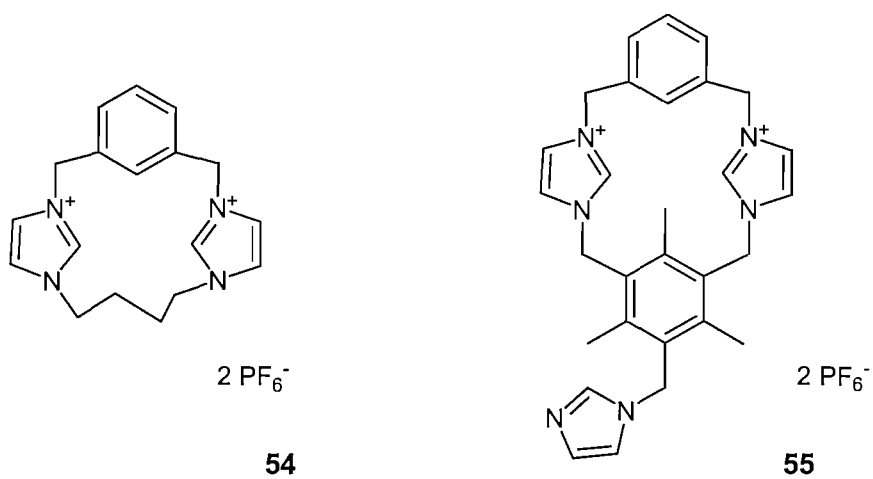

Fig 1.38: Xie's imidazolium cyclophanes **54** and **55** were observed to bind halide anions in acetonitrile solution.

Examination of the strength of association between a variety of halide anions and receptors **54** and **55** was achieved *via* UV/vis titration experiments performed in acetonitrile solution. Interestingly of the halides investigated bromide was bound most strongly by **54** with a stability constant of 17,900 M^{-1} determined although chloride was also strongly bound with a constant of 15,700 M^{-1} observed. In the case of the alternate receptor **55** upon which an additional imidazolium group was appended, an increase in stability constants were observed, however in this case the selectivity for bromide

previously observed was replaced by that for chloride with a value of 40,600 M^{-1} elucidated for its stability constant. This result indicates that the halide selectivity of system can be effectively tuned through relatively simple changes in the linkage groups.

Yet another example of appendage of anion binding units onto a rigid scaffold has been produced by Lee and Yoon[76] who have developed a receptor based upon the tetra-imidazolium substitution of a cavitand (Fig 1.39).

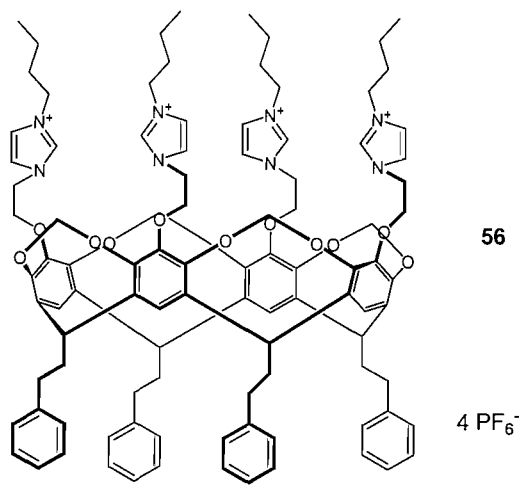

Fig 1.39: Lee and Yoon's tetraimidazolium receptor **56** was based upon a rigid cavitand scaffold.

Examination of the binding properties of receptor **56** was performed for both chloride and bromide and a selection of mono- and bis-carboxylates in DMSO-d_6 using ^{1}H NMR titration experiments. A 2:1 anion receptor stoichiometry was observed for the halides that were investigated (chloride and bromide) and acetate with values of 210, 100 and 400 M^{-1} determined for the combined stability constants.

The various bis-carboxylates for which spacer units of suitable length between carboxylate residues were employed were found to bind to **56** in a 1:1 anion / receptor stoichiometry strongly suggesting that all four of the imidazolium groups are able to simultaneously able to coordinate to anion, presumably with both of the carboxylate groups bound to a single receptor molecule. Of the bis-carboxylates investigated 1,4-phenylenediacetate, in the form of its TBA salt, was determined to form the most stable complex (16,200 M^{-1}).

Beer and co-workers[77] developed a series of macrocyclic tetraimidazolium based receptors in which the imidazolium groups are tethered through the use of various chain length alkyl linkage units in order to investigate the effect upon the anion complexation (Fig 1.40).

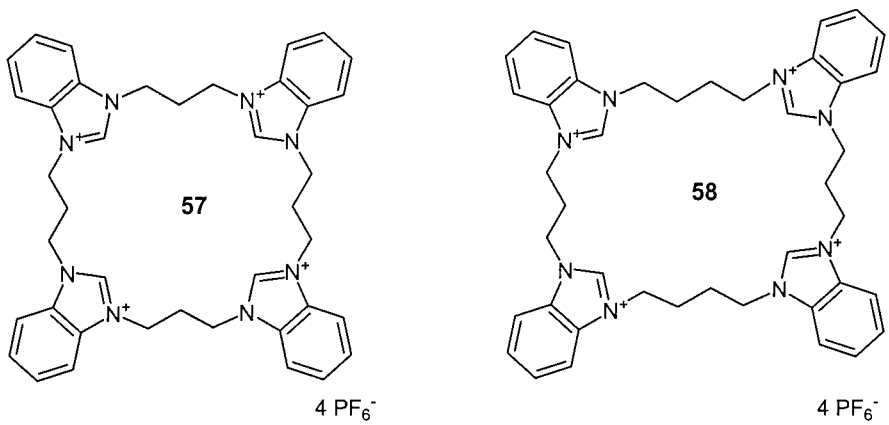

Fig 1.40: Beer and co-workers developed a new class of tetraimidazolium based anion receptors.

The anion stability constants for both receptors **57** and **58** were elucidated through NMR titration experiments performed in a mixed solvent system of 90:10 acetonitrile-d_3/water. Both receptors displayed very similar stability constants for the anions that were investigated with fluoride found to bind to both receptors with values of greater than 10,000 M^{-1}. Unfortunately exact values could not be determined in more competitive solvent mixtures due to solubility problems. All of the remaining halides investigated (chloride, bromide and iodide) were found to bind in a 1:1 ratio with the receptor with relatively high stability constants (1100 – 470 M^{-1}) considering the competitive nature of the solvent mixture used.

1.8. AIM OF THIS THESIS.

This introductory chapter has outlined a select few of the numerous ways in which anion coordination have been achieved by various research groups within recent years. The extensive use of hydrogen bonding arrays has facilitated much of the selectivity that has been observed with receptor design paramount in determining the ultimate selectivity that is observed. In an extension of this work, this thesis outlines the synthesis and analysis of various new anion binding receptors that use various hydrogen bonding motifs.

In particular this thesis discusses the synthesis and anion binding of both acyclic and cyclic receptors that show oxo-anion selectivity through a variety of differing design motifs. These include the formation of receptors based upon 1,2-phenylenediamine that have cleft conformations which have relatively large bite angles.

A novel class of macrocycle based upon amide clefts with additional hydrogen bonding groups, in the form of additional amide and urea groups, has been synthesized that displays differing anion binding modes depending upon the anion shape and size.

Deformation of regular amide cleft motifs into less convergent arrays through the use of steric interactions has been performed using amide cleft receptors based upon 1,3-anthraquinone derivatives. Furthermore the electrochemical behaviour of the quinone redox system has been investigated both in the absence and presence of coordinating anions.

The development of fluorescent anion sensors that combine both open clefts and anthracene as a fluorophore have been performed with the aim of producing sensors for oxo-anions in competitive solvent mixtures.

2. *1,2 - BIS-PHENYLENEUREA DERIVATIVES – ANION RECEPTORS AND CRYSTAL ENGINEERING SYNTHONS.*

2.1. INTRODUCTION.

The formation of a convergent hydrogen bonding cleft as a method for the complexation of anions has been the focus of numerous research groups. One approach that has been used has been the incorporation of multiple urea or thiourea moieties as hydrogen bond donor groups.[74, 78, 79] Both cyclic and acyclic designs have been shown to coordinate anions with varying levels of strength and selectivity.

Early examples employing thioureas were demonstrated by Umezawa and co-workers[80] with the complexation properties of both a flexible **59** and more rigid bis-thiourea derivative **60** investigated. The xanthene spacer group was intended to provide a more rigid framework upon which the appended thiourea moieties are attached.

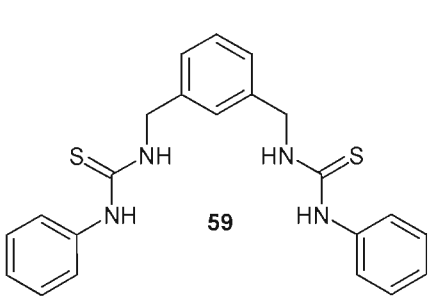

59

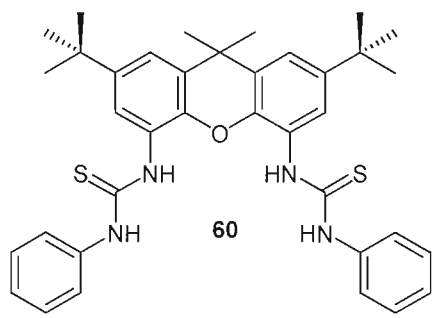

60

Fig 2.1: Umezawa's xanthene-based receptor **60** formed stronger complexes than its less preorganised analogue **59**.

Stability constants for both receptors **59** and **60** were determined via ^{1}H NMR titrations in which anions were titrated in the form of their TBA salts with experiments performed in DMSO-d_6. The stability constants for **59** with acetate and dihydrogen phosphate were determined at 2,300 and 1,600 M^{-1} respectively whilst the more pre-organised receptor **60** bound the same anions with higher constants of 38,000 and 55,000 M^{-1} in comparison.

Subsequent investigations into producing more rigid, macrocyclic receptors in which the urea moieties are geometrically locked into a conformation suitable for anion binding were undertaken by Reinhoudt and co-workers.[81]

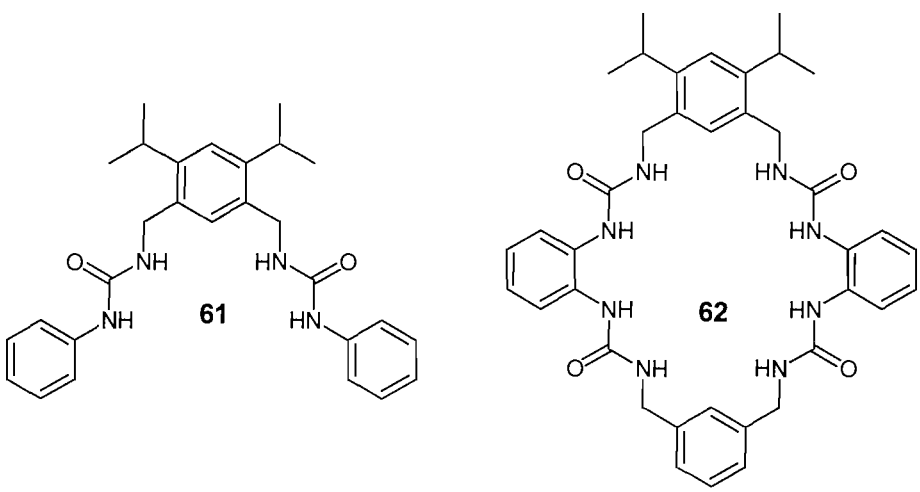

Fig 2.2: Reinhoudt's macrocyclic receptor **62** displayed significantly improved anion complexation properties relative to the acyclic analogue **61**.

Stability constants for receptors **61** and **62** with dihydrogen phosphate were obtained via ^{1}H NMR titration experiments performed in DMSO-d_6 and revealed that both receptors bound the anion in a 1:1 stoichiometry. The acyclic bis-urea derivative **61** was observed to have a stability constant of 900 M^{-1} whilst the macrocyclic **62** displayed an improved stability constant of 2,500 M^{-1}. This reflects the effect that a combination of macrocyclisation and the presence of additional hydrogen donors can enhance stability constants.

The synthesis of a naphthalene based bis-urea receptor **63** and subsequent analysis of both its fluro- and chromophoric properties were reported by Lee and Nam.[82] Fluorescence titration experiments were performed in acetonitrile: DMSO (9:1) and revealed that fluoride was bound with a constant of 14,200 M^{-1} whilst chloride contrastingly was complexed almost 40 times lower with a value of 380 M^{-1} obtained.

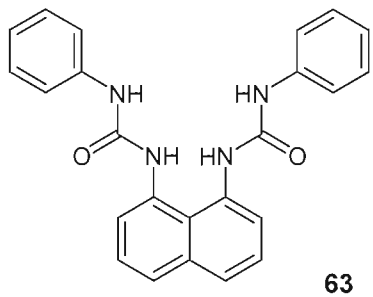

63

Fig 2.3: Lee and Nam's naphthalene receptor **63** displayed high affinity for fluoride in solution.

In addition to the selectivity observed the presence of a new emission peak was detected upon the addition of fluoride, an event that was attributed to the formation of highly charged hydrogen bonding in the anionic complex.

Steed and co-workers have developed numerous receptors based upon tripodal urea derivatives.[83] Receptor **64** was synthesized in the form of the tetrafluoroborate salt following metathesis from the bromide salt.

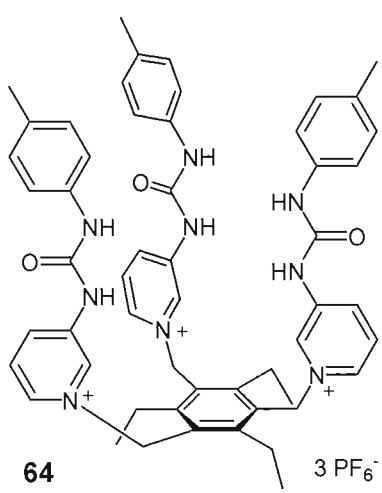

64 3 PF_6^-

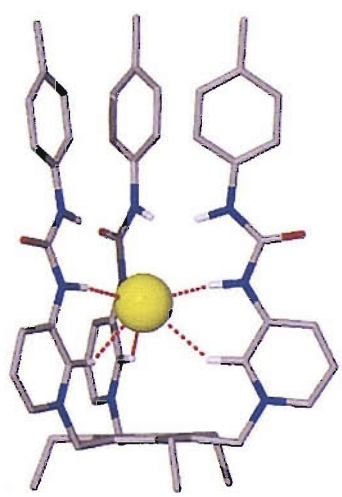

Fig 2.4: Steed's tripodal urea receptor **64** with the DFT minimised 1:1 chloride structure.

Determination of stability constants for compound **64** with a variety of coordinating anions was conducted via ^{1}H NMR titration experiments performed in acetonitrile-d_3. These revealed strong binding however as might be expected for a receptor in which the urea moieties are not forced into a single binding conformation multiple equilibria were observed in solution.

Some interesting investigations in the area of urea derived anion receptors have been performed by Fabbrizzi and co-workers.[84] Recently a chiral bis-urea derivative based on diaminocyclohexane **65** was demonstrated to bind chiral phosphates.

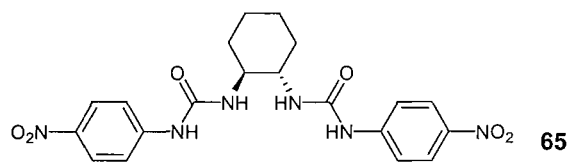

65

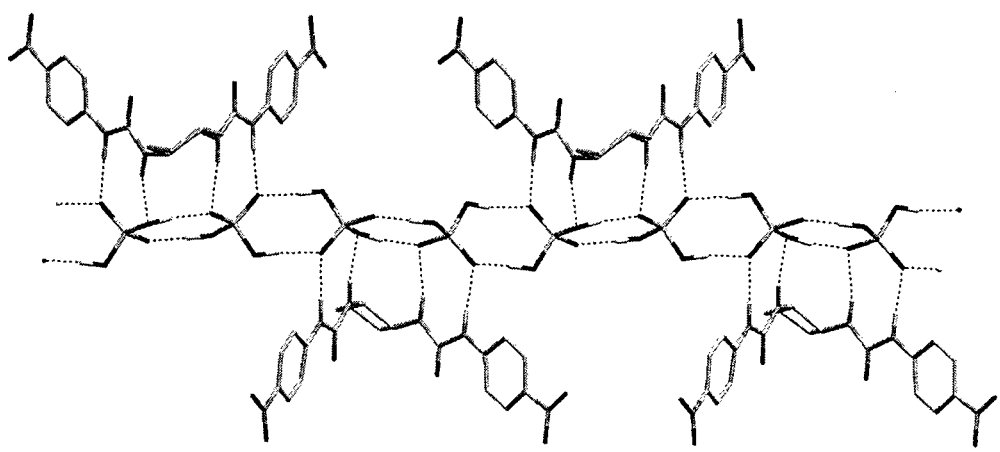

Fig 2.5: Fabbrizzi's chiral receptor **65** with crystal structure of the dihydrogen phosphate complex.

Stability constants for a variety of anions were obtained via UV-vis titration experiments performed in DMSO. Of these it was determined that acetate and benzoate were bound in a 1:1 stoichiometry with respective constants of 2,700 and 720 M^{-1}. In the case of dihydrogen phosphate a 1:2 receptor: anion stoichiometry was observed, K_1 = 920 and K_2 = 2900 M^{-1}, with unusually a higher constant for the second association observed. This effect is attributed to a cooperative binding mode evidence of which can be observed in the crystal structure of the dihydrogen phosphate 2:1 complex.

2.2. 1,2-PHENYLENEDIAMINE BASED CLEFTS.

Anion binding clefts containing both two and three hydrogen bond donor groups in the clefts have been shown to bind anions with high levels of association.[85,86] It also been demonstrated that by increasing the bite angle of the cleft it is possible to induce multiple sites within the cleft at which anion binding can occur.[63] This ultimately results in an increase in oxo-anion selectivity as the receptor becomes more suitable to coordinate to the various oxygen atoms that these anions possess.

We wished to develop receptors that possessed clefts that utilized a less convergent hydrogen bonding array so as to improve oxo-anion selectivity. In order to further improve the strength of complexes with anions we wished to investigate whether the effect of increasing in the number of hydrogen bond donor groups to four whilst still allowing a 1:1 anion / receptor stoichiometry to be formed.

2.2.1. SYNTHESIS AND CHARACTERISATION.

Three receptors **66**, **67** and **68** based upon a 1,2-phenylenediamine have been synthesized.[87-89] All of these compounds had been synthesized previously however only **67** had been analyzed for its anion binding properties and even then no oxo-anion properties were reported.

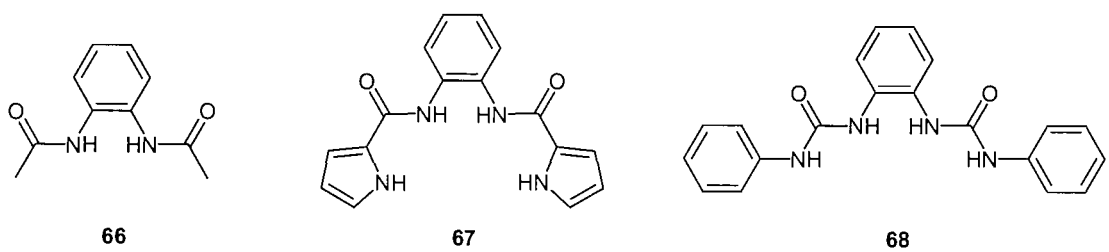

Fig 2.6: Previously reported compounds **66-68** were analyzed for their anion binding properties.

Although previously both the methanol and DMSO solvate crystals have been reported, the structure of the free receptor of **67** had not.[88] Crystals of the bis-pyrroleamide **67** that were suitable for X-ray analysis were obtained via slow evaporation

of an acetonitrile solution. The structure contains four crystallographically independent molecules which form extensive hydrogen bonding interactions to adjacent molecules through the pyrrole NH•••CO amide interaction. This interaction that has been previously observed in numerous structures involving both 2-carboxamido and 2,5-dicarboxamido-pyrrole derivatives.[61,90,91] The resulting sheet structure forms in the *bc* plane with the sheets stacking up in the *a* direction.

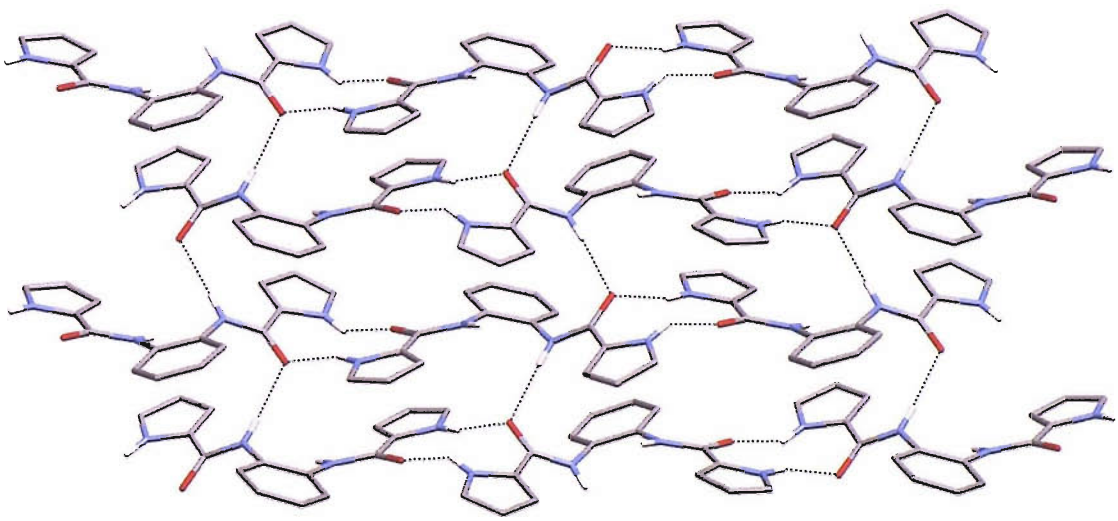

Fig 2.7: The crystal structure of **67** both lateral interactions through pyrrolic NH amide CO and axial amide NH amide CO are seen. Non-acidic protons omitted for clarity.

2.2.2. SOLUTION PHASE ANALYSIS.

2.2.2.1. ^{1}H NMR titration data.

Determination of the association constants for compounds **66-68** with a variety of anionic guests (added as their TBA salts) in DMSO-d_6 / 0.5% water were obtained via ^{1}H NMR titration experiments. Where possible perturbation in the chemical shift of the resonance equating to the central amide NH (or inner urea NH) upon the addition of aliquots of anion solution was recorded with data fitted using a 1:1 binding model.

Table 2.1: Anion association constants for compounds **66-68** in DMSO-d_6 / 0.5% water. Anions titrated in the form of their TBA salts. All experiments performed at 298 K. Data in all cases fitted to a 1:1 binding model using WINEQNMR[92] following the central NH resonances. All errors less than 12 %.

Anion	**66**	**67**	**68**
Chloride	13	12	43
Bromide	-	-	<10
Hydrogen Sulfate	-	-	10
Dihydrogen Phosphate	149	295	732
Acetate	98	251	3210
Benzoate	43	113	1330

In the case of both **66** and **67** the interaction with both bromide and hydrogen sulphate was insufficient to allow an association constant to be determined. The two hydrogen bond donor **66** displayed significantly lower association constants for all anions investigated than either **67** or **68** consistent with the presence of fewer anion coordinating groups.

The anion stability constants for compound **67** show a modest increase over those observed for **66**, with increases observed for dihydrogen phosphate, acetate and benzoate. Interestingly chloride is bound by **67** as weakly as its two hydrogen bond donor analogue, suggesting that the anion is bound in a similar manner in both of these systems.

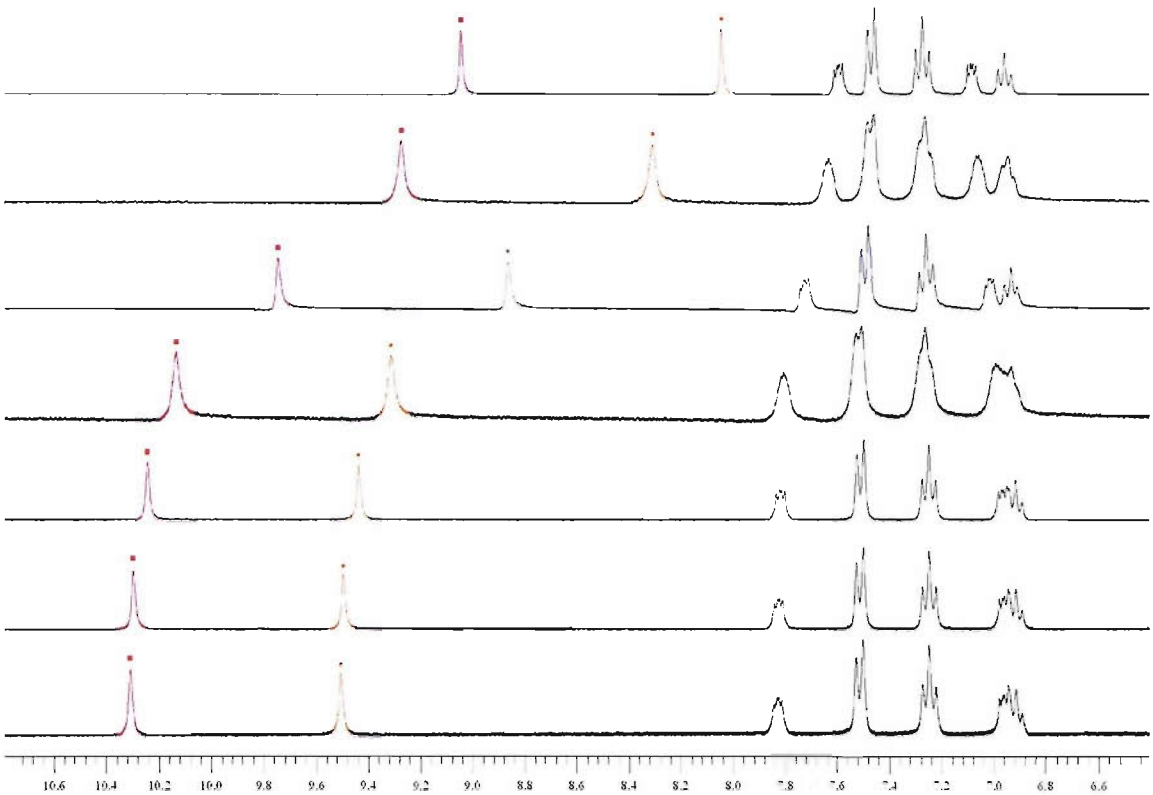

Fig 2.8: Stack plot of **68** showing the change in resonance of both the outer (red) and inner (orange) urea NH protons upon increasing acetate concentrations. Spectra recorded at 0.0, 0.21, 0.63, 1.05, 1.47, 3.15, and 5.26 equivalents of acetate.

Bis-urea derivative **68** binds all of the anions investigated to a higher degree than the previously discussed receptors (Graph 2.1). In particularly carboxylates are found to be bound by an order of magnitude greater than the analogous bis-amidopyrrole receptor **68** which also possesses four hydrogen bond donor groups. This significant improvement suggests that all four of the urea NH protons are ideally spaced geometrically to coordinate to carboxylate anions simultaneously. In contrast the pyrrolic and amide NH groups of the bis-amidopyrrole **67** are unable to simultaneously form four hydrogen bonds to carboxylates due to the decreased bite angle in this receptor resulting in lower anion stability constants.

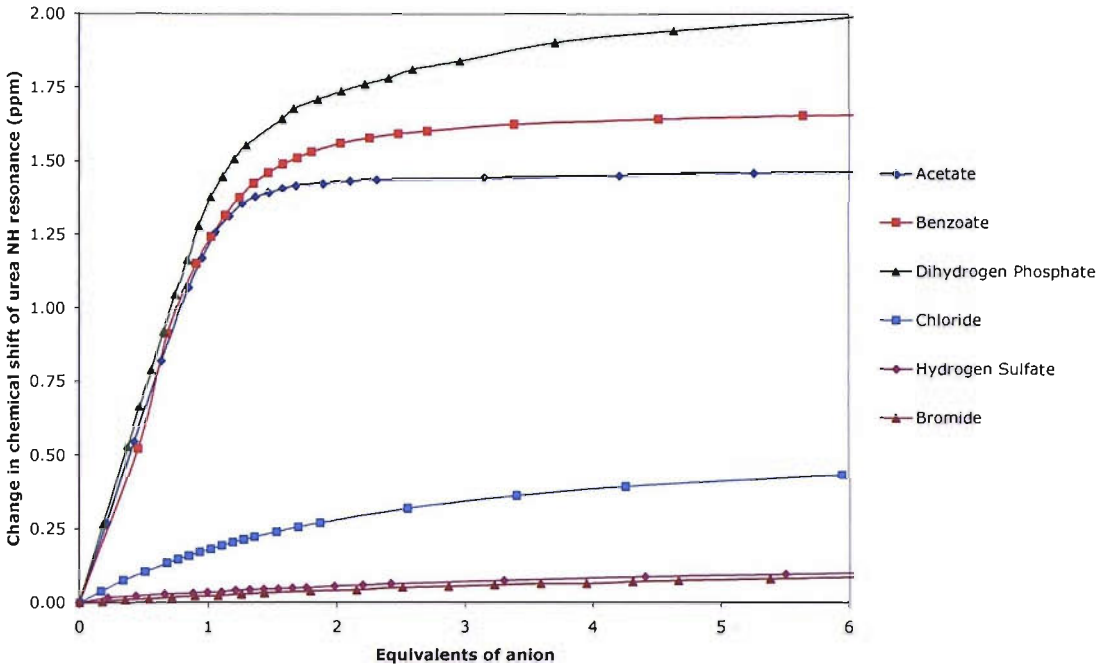

Graph 2.1: The effect of increasing anion concentration upon the chemical shift of the central NH urea resonance of compound **68**.

2.2.3 SOLID PHASE ANALYSIS.

In the case of compound **67**, the fluoride, chloride and acetate complexes were characterized crystallographically.

X-ray quality crystals of the fluoride complex of **67** were obtained via slow evaporation of an acetonitrile solution of **67** in the presence of excess TBA fluoride. The resulting structure showed that each host molecule bound a single fluoride ion through three hydrogen bonds, two from the amide NH groups [N2···F1 2.704(7) Å & N3···F1 2.666(8) Å] and a single pyrrolic NH group [N4···F1 2.656(5) Å] with bond angles between 158.9° and 170.3°. The remaining pyrrolic NH is involved in a reciprocated hydrogen bonding arrangement to an adjacent host molecule through the amide carbonyl group [N1···O1 2.798(8) Å].

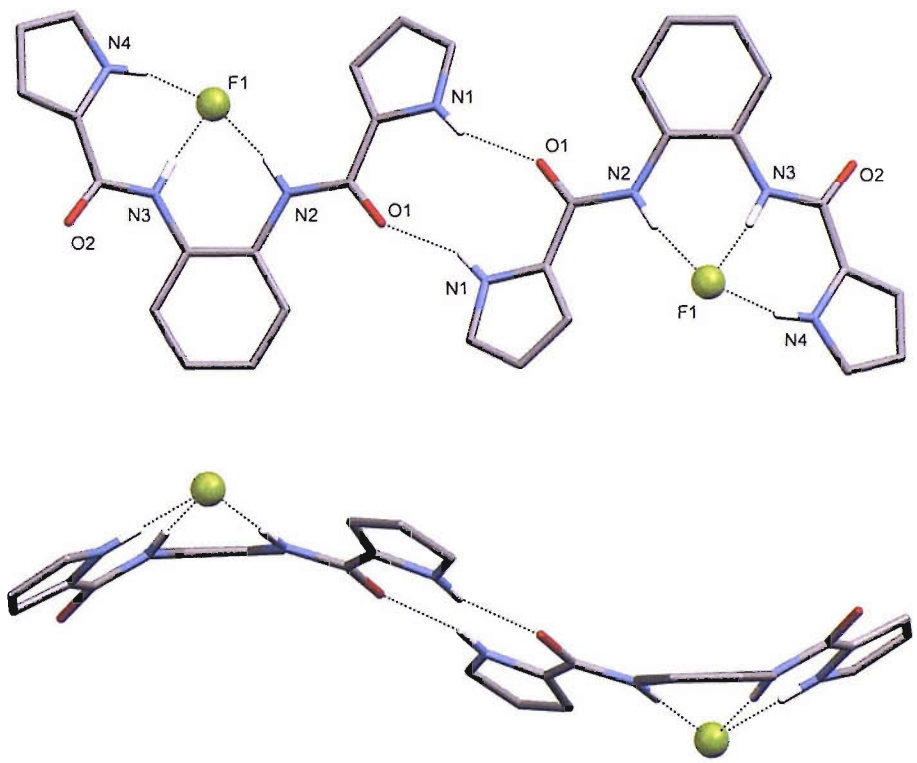

Fig 2.9: Receptor **67** coordinates the fluoride via three NH hydrogen bonds, with the remaining NH group involved in dimerisation. Non-acidic protons and TBA cations are omitted for clarity.

Slow evaporation of an acetonitrile solution of **67** in the presence of excess TBA chloride yielded X-ray quality crystals of the chloride complex of **67**. In this case each chloride ion is co-ordinated to the receptor only via the central amide NH groups [N2···Cl1 3.225(5) Å & N3···Cl1 3.165(6) Å] with bond angles of 164.5° and 165.6° respectively. Presumably the larger ionic radius of the chloride ion in comparison to fluoride prevents the pyrrolic NH groups having sufficient space to be able to coordinate to the ion.

Each of the pyrrolic NH groups is involved in hydrogen bonding to adjacent host molecules through interactions with the amide carbonyl groups as seen previously [N1···O1 2.809(7) Å & N4···O2 2.825(7) Å].

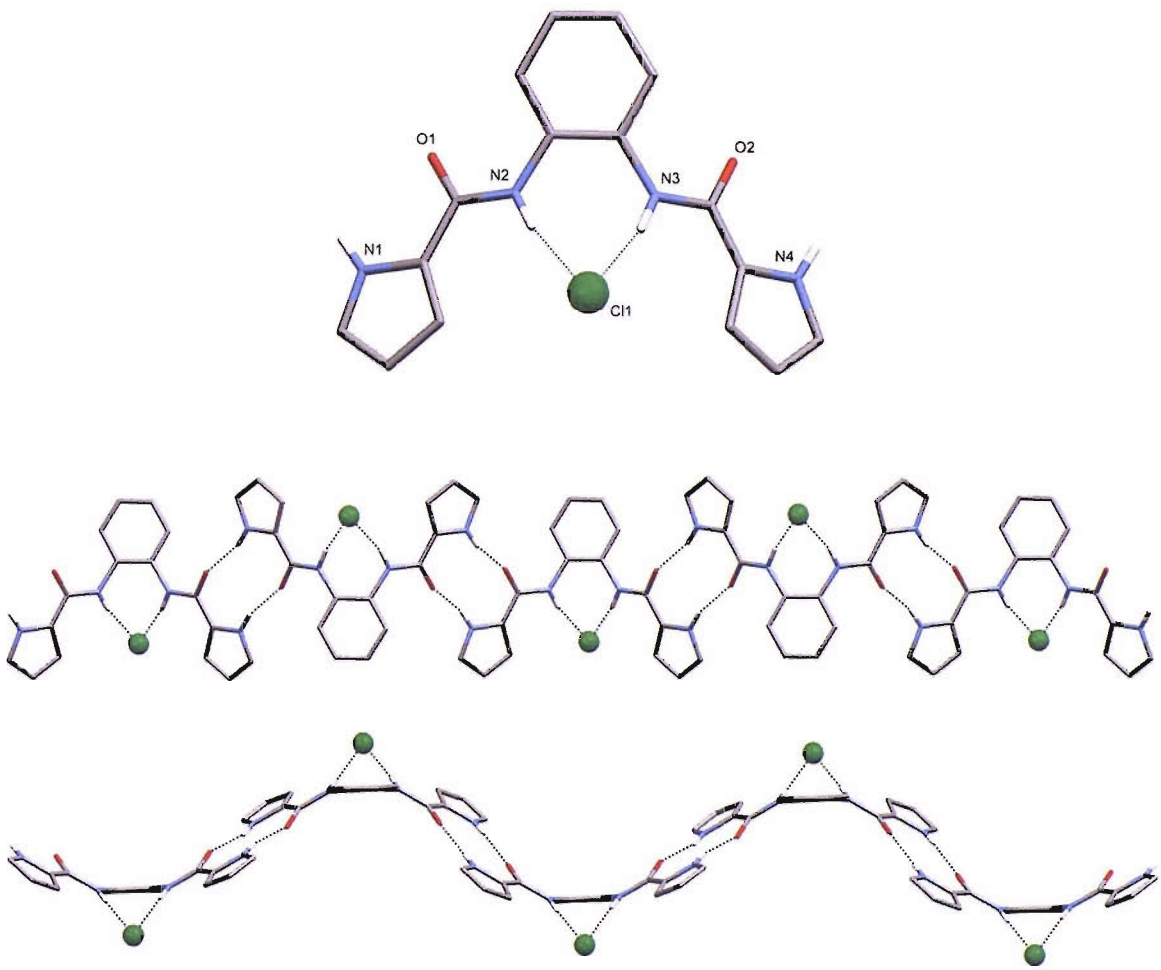

Fig 2.10: Receptor **67** binds chloride anion through the two central amide NH groups in the solid-state. Non-acidic protons and TBA cations are omitted for clarity.

X-ray quality crystals of the acetate complex of **67** were also obtained via slow evaporation of an acetonitrile solution of **67** in the presence of excess TBA acetate. The resulting structure shows that the two acetate oxygen atoms are coordinated to the receptor via the two amide groups [N2···O3 2.751(3) Å & N3···O3 2.731 (3) Å] and a single pyrrole group [N4···O4 2.781(3) Å] with bond angles between 151.0° and 160.2°.

The remaining pyrrolic NH is involved in the formation of non-reciprocated intermolecular hydrogen bonds with adjacent host molecules [N1···O2 2.874(3) Å]. The presence of three hydrogen bonds with the acetate appears to substantiate the assumption that not all NH groups can simultaneously co-ordinate with the anion in solution.

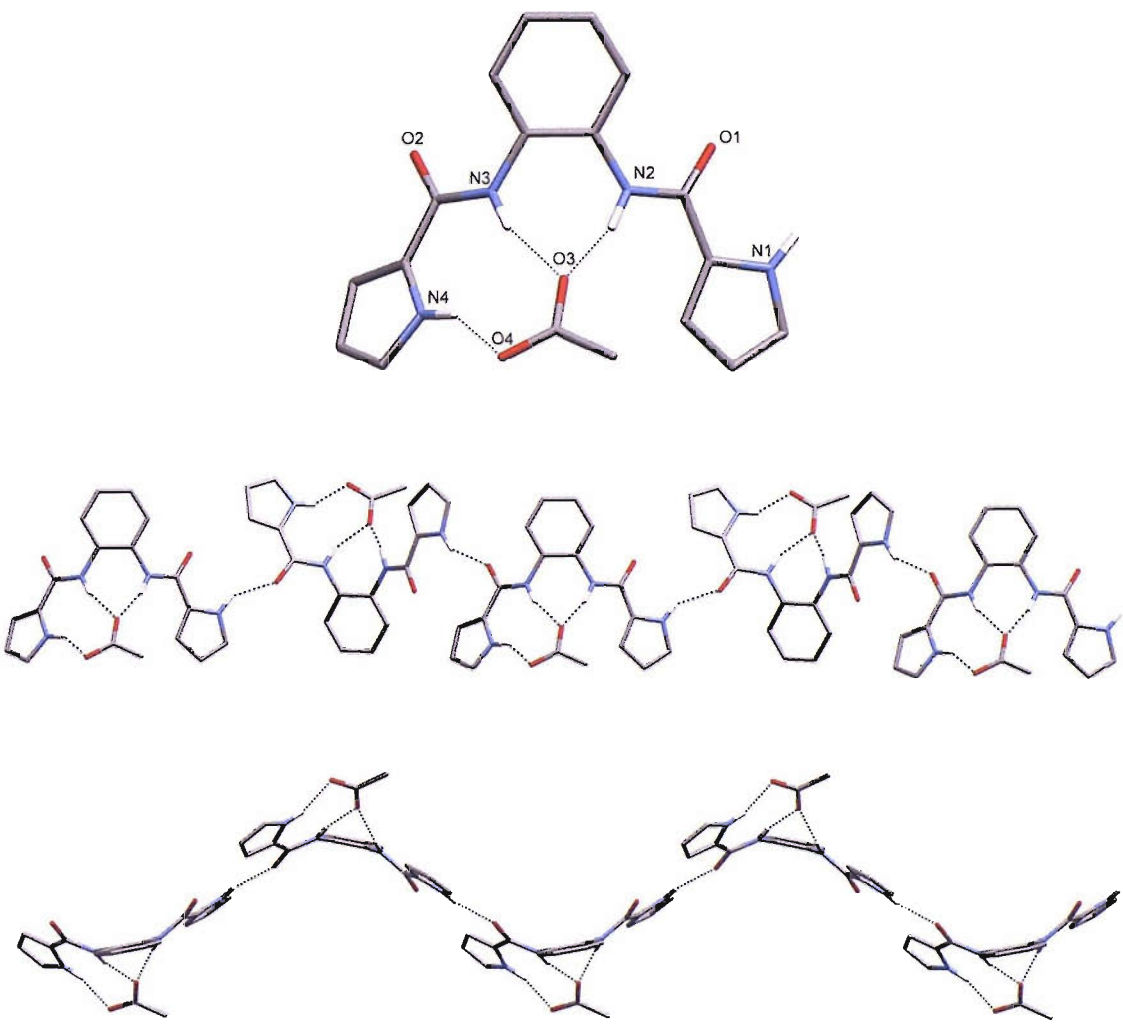

Fig 2.11: Receptor **67** binds acetate through three hydrogen bonds with the remaining pyrrolic NH groups involved in the formation of an infinite chain. Non-acidic protons and TBA cations are omitted for clarity.

X-ray quality crystals of the benzoate complex of **68** were obtained via slow evaporation of an acetonitrile solution of **68** in the presence of excess TBA benzoate. The resulting complex comprises a 1:1 anion receptor stoichiometry in which a four hydrogen bond donor / two hydrogen bond acceptor array (DDDD-AA) is observed. The structure consists of two distinct interactions, those from the internal urea NH groups [N2···O3 2.740(4) Å & N3···O4 2.939(4) Å] and the external urea NH groups [N1···O3 2.821(5) Å & N4···O4 2.820(5) Å], with all bond angles in the range of 151.0° and 161.1°.

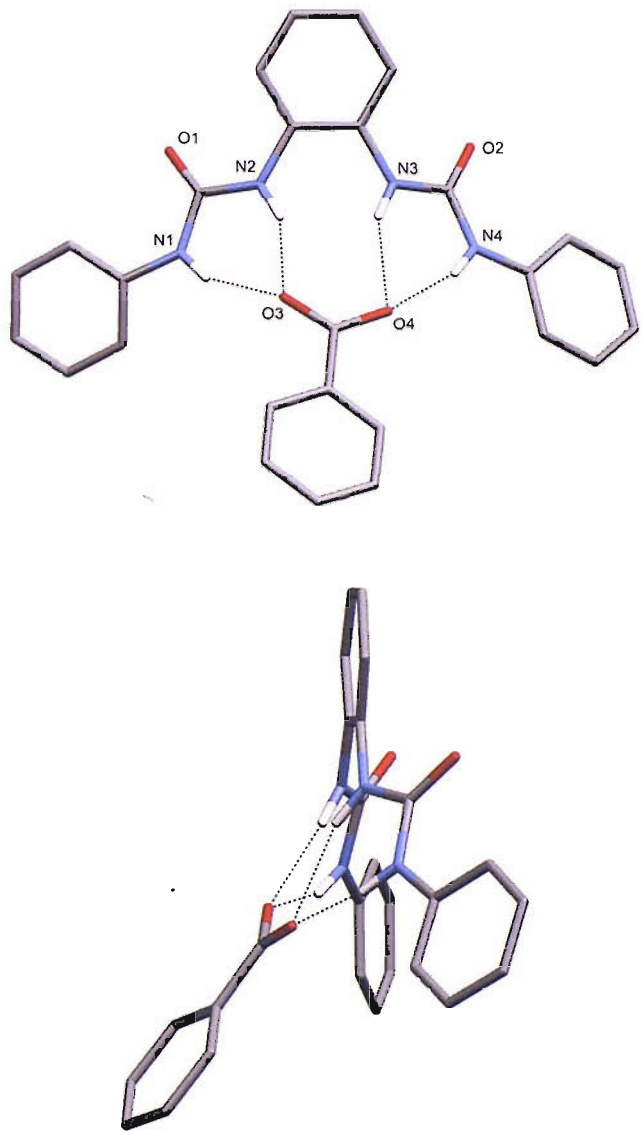

Fig 2.12: The benzoate complex of **68** displays a DDDD-AA hydrogen bonding array. Non-acidic protons and TBA cations omitted for clarity.

Crystals of the terephthalate complex of **68** of X-ray quality were obtained via slow evaporation of an acetonitrile solution of **68** in the presence of excess TBA terephthalate. The complex reveals that two distinct receptor groups encapsulate a single terephthalate anion. As observed previously with the benzoate complex of **68**, each of the carboxylate residues are bound by four hydrogen bonds from two internal urea groups [N2···O3 2.899(9) Å & N3···O4 2.843(8) Å] and two external urea groups [N1···O3 2.759(8) Å & N4···O4 3.083(8) Å]. In this case the pendent aryl groups of the each of the receptor molecules are orientated on the other face of terephthalate anion relative to the other receptor molecule.

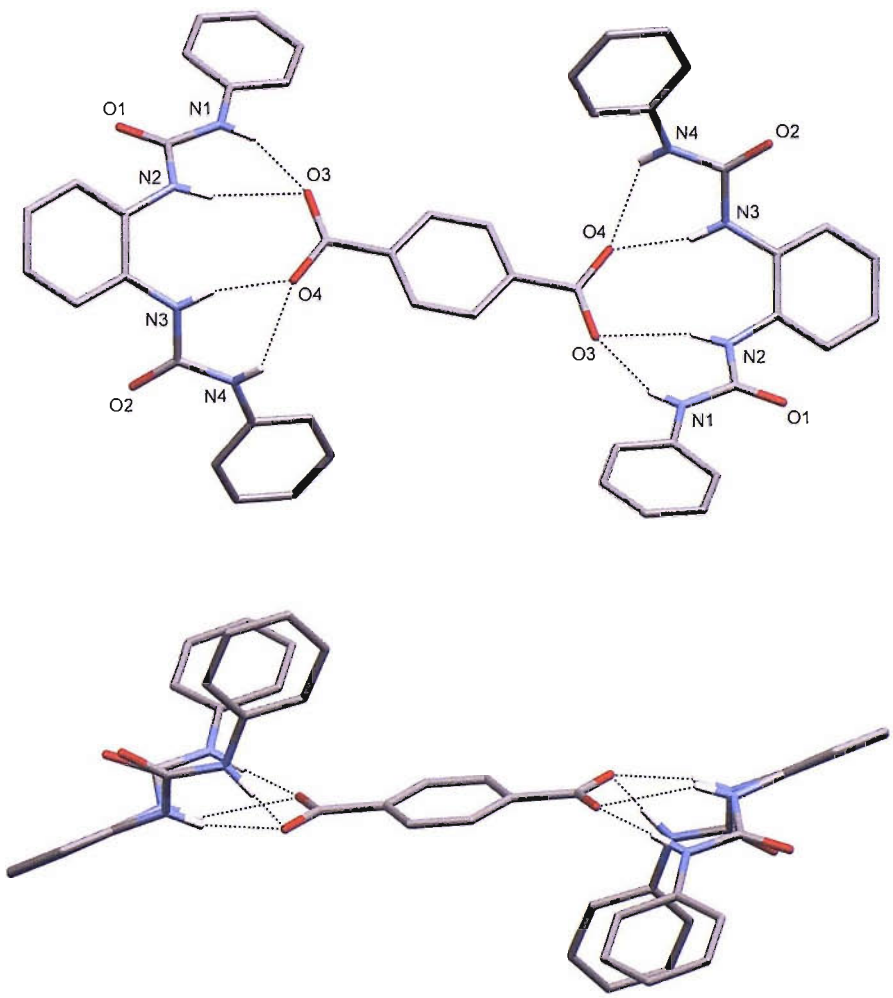

Fig 2.13: The terephthalate complex of **68** shows two independent molecules of **68** bound to the carboxylate residues via four hydrogen bonds. Non-acidic protons and TBA cation omitted for clarity.

2.3. BIS-UREA DERIVATIVES AS ANION RECEPTORS.

The high stability constants that were obtained with carboxylates for receptor **68** in competitive solvent mixtures merited further investigation. As a result it was decided to examine the motif further in an attempt to increase the anion binding ability of the motif through the inclusion of electron-withdrawing groups. This it was hoped would have the effect of increasing the acidity of the urea NH protons and lead to the formation of stronger host: guest complexes.

2.3.1. SYNTHESIS AND CHARACTERISATION.

Bis-urea based receptors **69-73** were synthesised via reaction between the corresponding functionalised diamine and phenylisocyanate / phenylisothiocyanate[93] (Scheme 2.1) giving the bis-urea/thiourea products in excellent yield.

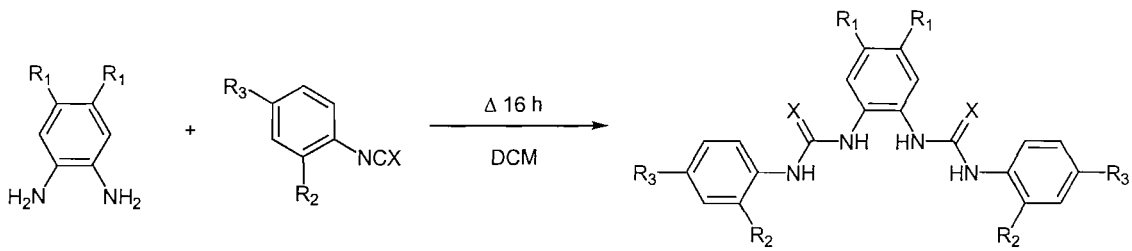

69	R_1 = Cl,	R_2 = H,	R_3 = H,	X = O.	82 %
70	R_1 = H,	R_2 = H,	R_3 = NO_2,	X = O.	98 %
71	R_1 = H,	R_2 = NO_2,	R_3 = H,	X = O.	98 %
72	R_1 = Cl,	R_2 = NO_2,	R_3 = H,	X = O.	68 %
73	R_1 = H,	R_2 = H,	R_3 = H,	X = S.	71 %

Scheme 2.2: Synthesis of bis-urea derivatives followed a simple procedure.

The crude reaction between the isocyanates and 3,4-dichloro-1,2-phenylenediamine yielded a mixture of both the bis-urea and the mono-urea mono amine with both compounds displaying low solubilities in a variety of organic solvents. Purification of these 3,4-dichloroderivatives was therefore subsequently achieved via trituration from hot acetone.

X-ray quality crystals of compound **73** were obtained via slow evaporation of an acetonitrile solution. The resulting sheet structure revealed extensive hydrogen bonding between adjacent bis-thiourea molecules. Neither of the sulphur atoms in this case are in the plane of the central aryl ring system whilst one of the thiourea groups can be seen to adopt an anti conformation [N3-N4]. Intermolecular hydrogen bonds are in the range of 3.347(2)-3.388 Å whilst an intramolecular interaction also observed [N3···S1 3.118(2) Å] in this heavily twisted system.

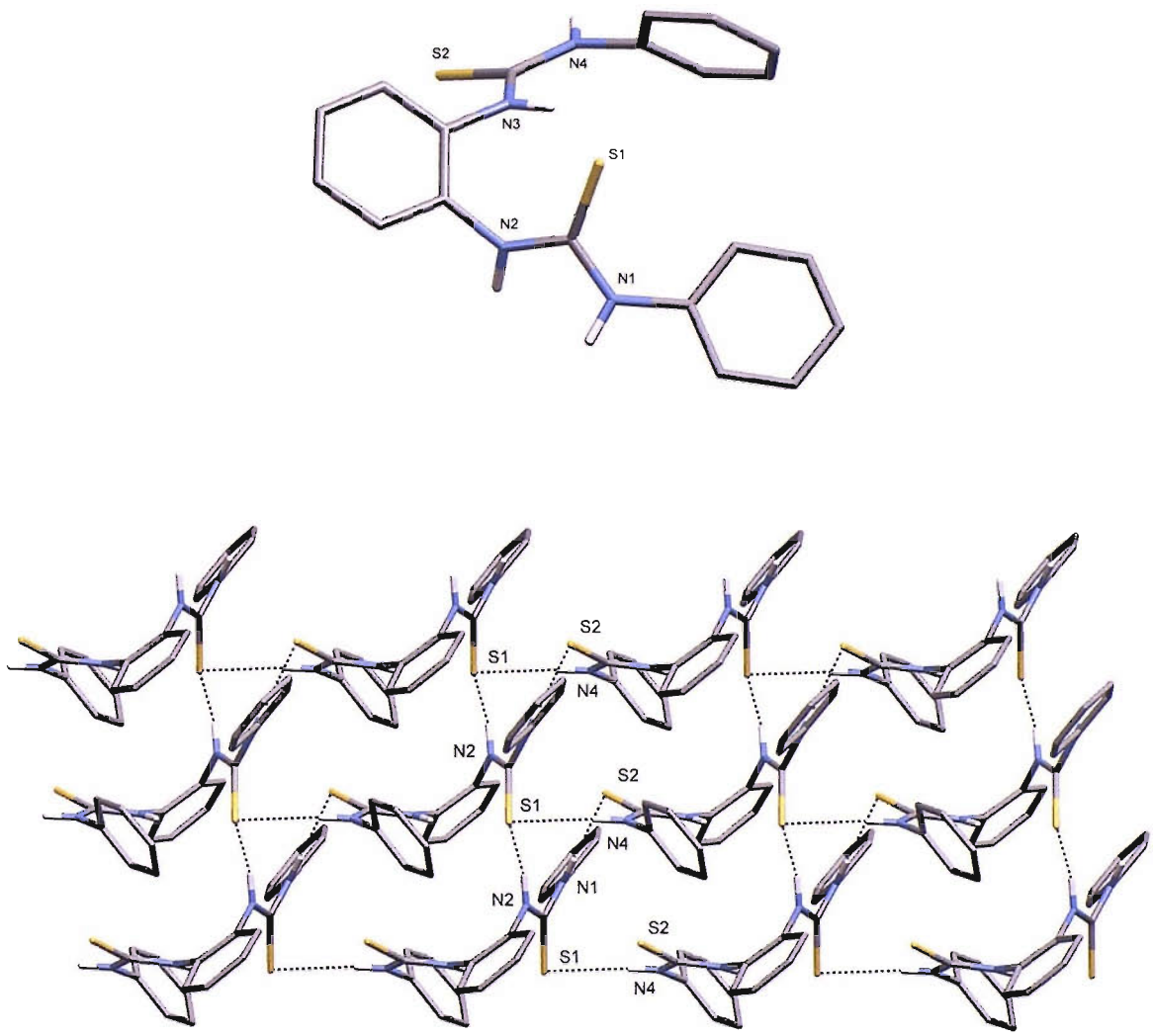

Fig 2.14: Thiourea derivative **75** forms hydrogen bonded sheets in the solid state. Non-acidic protons omitted for clarity.

2.3.2. SOLUTION PHASE ANALYSIS.

2.3.2.1. ^{1}H NMR titration data.

Association constants for a variety of anionic guests in the form of their TBA salts in DMSO-d_6 / 0.5% water were determined via ^{1}H NMR titration experiments with data fitted to a 1:1 binding model.

Table 2.2: Anion association constants (M^{-1}) for compound **69-73** in DMSO-d_6 / 0.5% water. Anions titrated in the form of their TBA salts at 298 K. All data fitted to a 1:1 binding model using WINEQNMR.[92] All errors <15%.

Anion	69	70	71	72	73
Chloride	67	78	-	18	18
Bromide	<10	<10	-	-	-
Hydrogen Sulfate	<10	<10	-	-	-
Dihydrogen Phosphate	4724	666[a]	349	1637	1490
Acetate	8079	4018	1739	-[b]	188[a]
Benzoate	2248	1399	541	1249	233[a]

[a] Slightly sigmoidal titration curves were obtained in these cases however data was most satisfactorily fitted to a 1:1 binding model. [b] Appearance of new peaks in the NMR spectra and a sharp colour change may indicate deprotonation.

Generally a similar trend in terms of oxo-anion selectivity is observed for the all of the receptors investigated however upon closer examination several interesting deviations are revealed.

The highest association constants are observed for compound **69** in which electron-withdrawing groups are located on the central aryl ring of the bis-urea cleft. The presence of these groups has the effect of increasing in the acidity of both the internal urea NH protons (chemical shift in DMSO for **69** = 8.21 ppm compared to 8.04 ppm for

68) and to a lesser extent those of the outer urea protons (**69** = 9.14 ppm whilst **68** = 9.04 ppm).

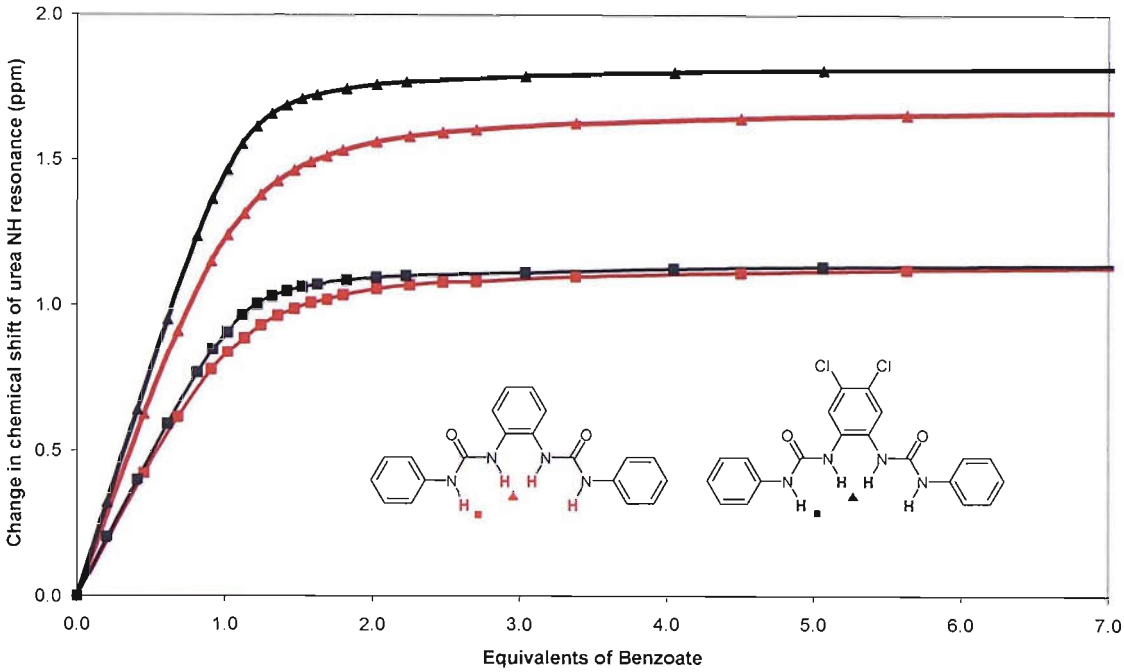

Graph 2.2: Change in chemical shift of internal and external urea NH resonances of **68** (red) and **69** (black) upon the addition of TBA benzoate.

Receptor **69** forms strong complexes in particular with both acetate and dihydrogen phosphate (8,079 M^{-1} and 4,724 M^{-1}) whilst benzoate also demonstrates an improvement in complex stability when compared to the non-derivatized receptor **68** (2,248 M^{-1} c.f. 1,330 M^{-1}). In order to determine how benzoate interacts with each of the receptors, the changes in chemical shift of both the internal urea proton resonance and the external urea proton resonance of compounds **68** and **69** were investigated (Graph 2.2).

In both receptors the external urea NH resonances are shifted downfield by almost identical amounts upon the addition of excess TBA benzoate indicating similar interactions with the benzoate anion. The internal urea NH protons are shifted downfield to a greater amount than their respective external urea protons indicating that the strongest interaction between the anion and the receptor occurs through these protons. The internal protons for the more acidic receptor **69** shift downfield to a greater extent

than those of **68** reflecting the formation of stronger hydrogen bonds with benzoate through these protons.

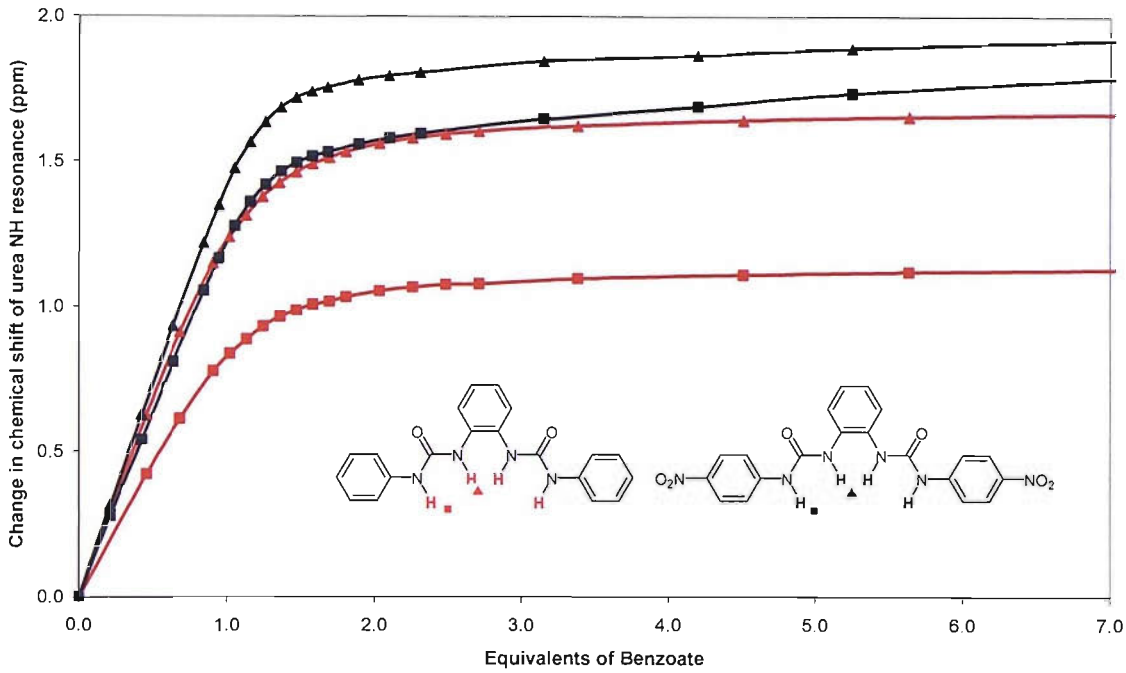

Graph 2.3: Change in chemical shift of internal and external urea NH resonances of **68** (red) and **70** (black) upon the addition of TBA benzoate.

Similarly the changes in both the internal and external urea resonances of receptors **68** and **70** upon the addition of TBA benzoate was monitored. In the absence of benzoate the external protons of **70** were observed at 9.81 ppm in comparison to 9.04 ppm making them considerably more acidic. Additionally the internal protons show a significant downfield shift to 8.28 ppm when compared to 8.04 ppm for **68**. In this case both the internal and external protons display downfield shifts greater than those exhibited by **68**, with the external protons in particular showing a significant increase in change in resonance chemical shift.

From this evidence alone it would appear that the nitro-functionalized receptor **70** contains the most acidic urea protons in comparison to the chloro-functionalised receptor **69** and would be expected to coordinate anions more strongly. Examination of the anion stability constants reveals that this is not the case there must therefore be a reason why

electron-withdrawing groups located on the 3- and 4- positions of the central aryl ring cause higher stability constants.

A likely possible explanation of this observation could arise from an increase in the rigidity of the anion binding conformation of **69** through intramolecular aryl CH···OC urea interactions.

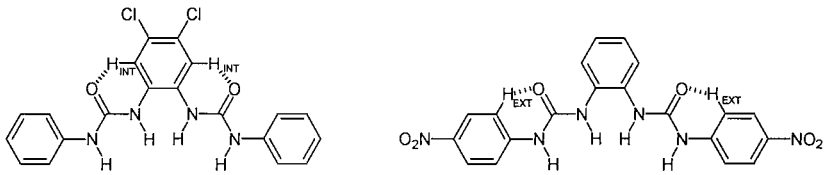

Fig 2.15: Receptor **69** can potentially form stabilising aryl CH···OC interactions to increase pre-organization.

The presence of electron-withdrawing groups can not only increase the acidity of the appended NH groups but also the aryl CH protons. In comparison to those of **68** the CH protons appended to the central aryl ring of **69** display a downfield shift of 0.32 ppm. The 2- and 6- positioned aryl CH protons of the pendent groups of **70** are shifted by 0.71 ppm when compared in a similar fashion whilst in both cases the protons on the non-substituted aryl ring systems are effectively unchanged. In the case of **69** greater hydrogen bonding between the H_{INT} protons and urea CO groups stabilizes the conformation of the two urea groups into a cleft conformation improving the pre-organization of the receptor. Interactions between the H_{EXT} protons and the urea CO group in **70** locks the pendent aryl groups relative to the urea, however this has no effect of controlling the conformation of the urea groups in terms of adopting a cleft conformation.

The improvements in anion stability constants observed for the 4-nitro receptor **70** can therefore be attributed purely to the increased acidity of the urea protons. As the outer urea proton becomes more dominant in the complexation of anions it appears that there is an increasing tendency for the urea groups to bind anions independently as indicated with a presence of sigmoidal titration curves. In this case however a 1:1 binding in solution still remains the dominant interaction.

Receptors **71** and **72** both possess nitro groups in the 2-position of the pendent aryl groups with **72** also functionalized with chloro- groups in the 3 and 4 positions of the central aryl group. In comparison to **68-70, 71** displays a significant reduction in anion binding properties whilst even with the presence of additional electron-withdrawing groups **72** only binds approximately as well as the non-functionalised receptor though strong colour changes observed upon the addition of acidic anions may indicate that deprotonation processes are occurring.

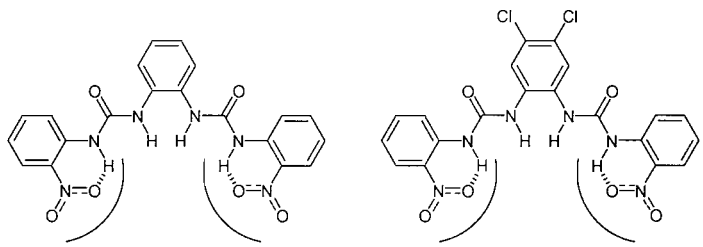

Fig 2.16: The location of nitro groups in the 2-position of receptors **71** and **72** could hinder anion binding.

The poor anion complexation properties of these receptors can be explained by considering the additional steric bulk within the cleft of the receptor having a repulsive effect upon the approaching anion. In addition much of the hydrogen bond donor effect of the external urea NH protons could be removed through the formation of intramolecular hydrogen bonds.

Typically anion receptors that contain thiourea moieties as a binding site display improved anion complexation properties in comparison to urea analogues however in this case thiourea based receptor **73** displays anion stability constants that are an order of magnitude smaller than analogous urea values. This could arise from the larger size of the sulphur atom causing repulsive effects with the aryl CH protons with a twisting of the cleft into a conformation unfavourable for anion binding, as suggested from the X-ray crystal structure.

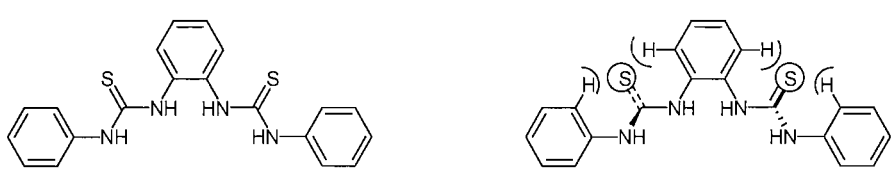

Fig 2.17: Bis-thiourea **73** could suffer twisting deformations due to the larger size of sulphur atom.

2.3.3. SOLID PHASE ANALYSIS.

X-ray quality crystals of the benzoate complex both **69** and **70** were obtained via slow evaporation of acetonitrile solutions of **69** and **70** respectively in the presence of excess TBA benzoate.

Unlike the previously observed structures that incorporate the bis-urea / benzoate interaction, the benzoate anion adopts a slipped conformation within the cleft. Whilst the two central urea NH groups coordinate to one of the oxygen atoms [N3···O4 2.782(4) Å & N2···O4 2.777(4) Å] the remaining benzoate oxygen coordinates to one of the external urea groups [N1···O3 2.837(3) Å]. The remaining bis urea NH group is too distant to effectively form a hydrogen bond to the anion, although it remains possible that an edge-to-face π-π interaction is present.

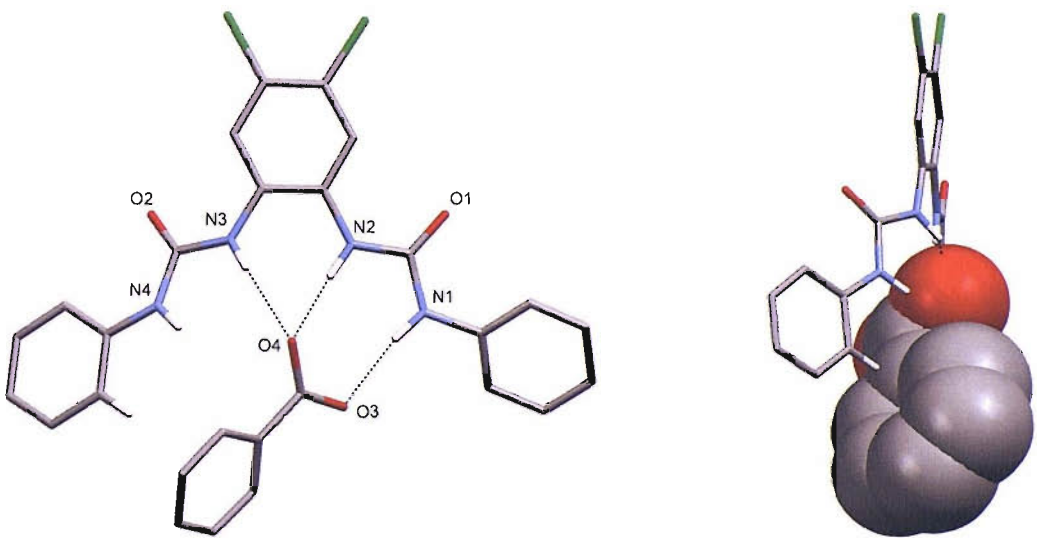

Fig 2.18: The benzoate complex of **69** shows the benzoate anion asymmetrically bound via three hydrogen bonds to the bis-urea and one CH···π interaction. Non-acidic protons and TBA cations omitted for clarity.

The crystal structure of **70** with benzoate adopts the four donor-two acceptor hydrogen bonding array as observed in the previous examples. In this case the anion is bound in a less symmetrical manner with both the two central urea NH groups [N4···O8 2.830(2) Å & N3···O7 3.022(2) Å] and external urea NH groups [N5···O8 2.812(2) Å & N2···O7 2.793(2) Å] coordinating to the anion. As observed before remarkably similar bond angles are observed in all cases in the range of 151.4° - 156.4°.

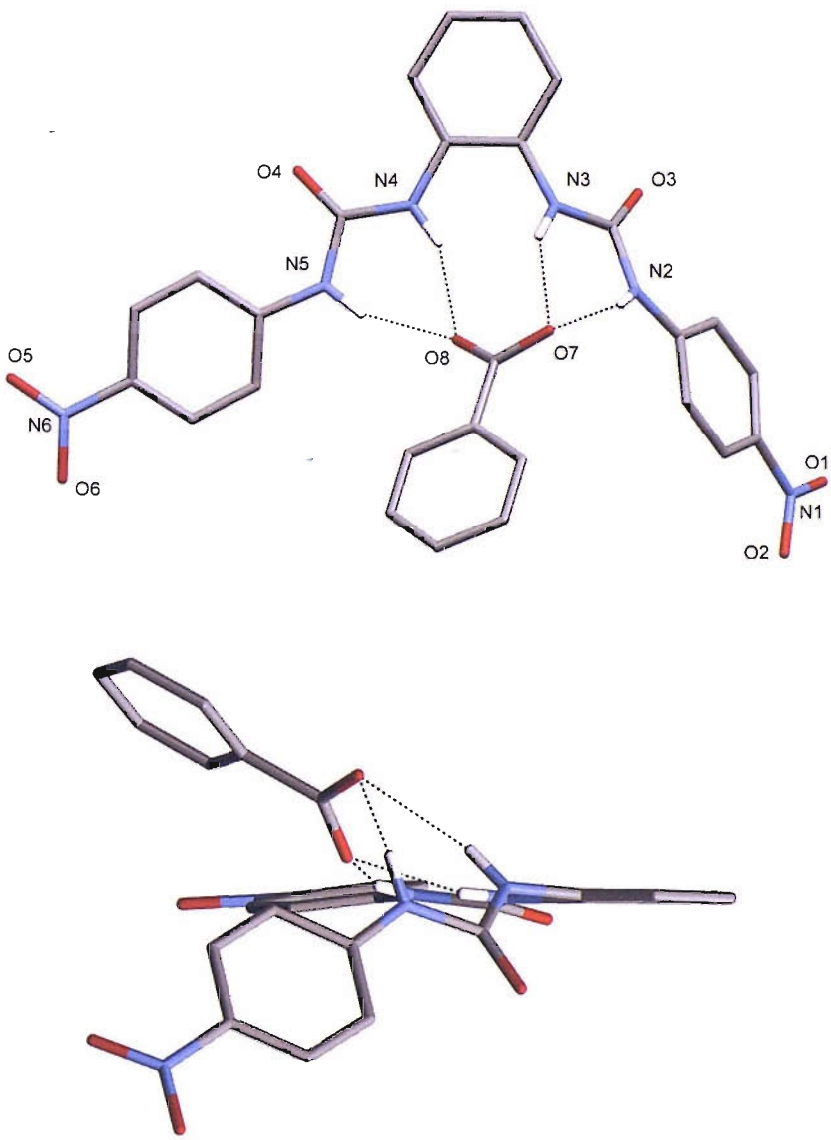

Fig 2.19: The benzoate complex of **70** has the anion bound centrally in the cleft. Non-acidic protons omitted for clarity.

2.4. BIS-AMIDE SUBSTITUTED BIS-UREA DERIVATIVES.

Altering the electronic properties of bis-urea receptors has been demonstrated as an effective method through which the strength of complexes with anions could be improved. An alterative method of achieving this aim is the incorporation of additional hydrogen bond donor groups. It was decided that in order to try and fully maximize the host / guest interactions further, substitution the system through the appendage of additional amide moieties would be employed. It was hoped that the presence of these groups could provide additional hydrogen bonds between the guest and the host, therefore providing more stable complexes in highly competitive solvent mixtures.

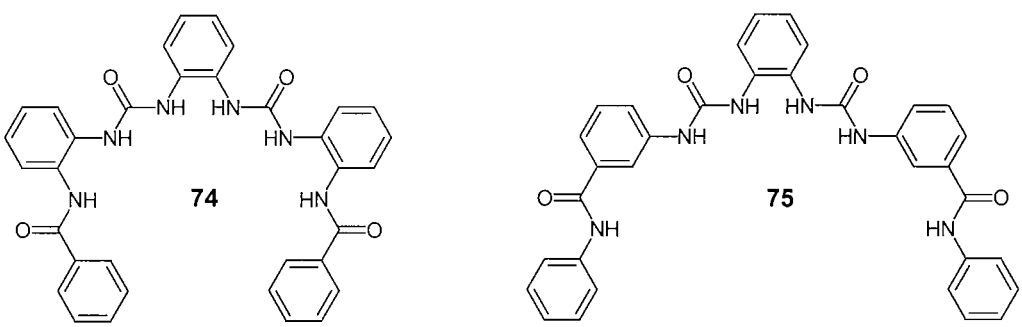

Fig 2.20: Bis-amide bis-urea derivatives were synthesized.

2.4.1. SYNTHESIS AND CHARACTERISATION.

Receptor **74** was synthesized via a route that initially saw the reduction of compound **71** using hydrazine monohydrate with palladium on carbon catalyst to give the bis-amine **76**. This was subsequently coupled with benzoyl chloride **77** in the presence of triethylamine and a catalytic amount of DMAP to afford the bis-urea-bis-amide in 29 % yield (Scheme 2.3).

Compound **75** was formed in two steps with the first the reaction between 1,2-phenylenediamine **78** and 3-ethylisocyanatobenzoate **79** to give the bis-urea-di-ester **80** in quantitative yield. Gelation of the reaction mixture occurred soon after the reaction started however it was found that the addition of a small quantity of anhydrous methanol

reverted the mixture back into solution with no appreciable loss of yield. The bis-urea-di-ester was than subsequently reacted with aniline **81** in the presence of trimethylaluminium at reflux conditions for 5 days which gave the bis-amide **75** in 94 % (Scheme 2.4).

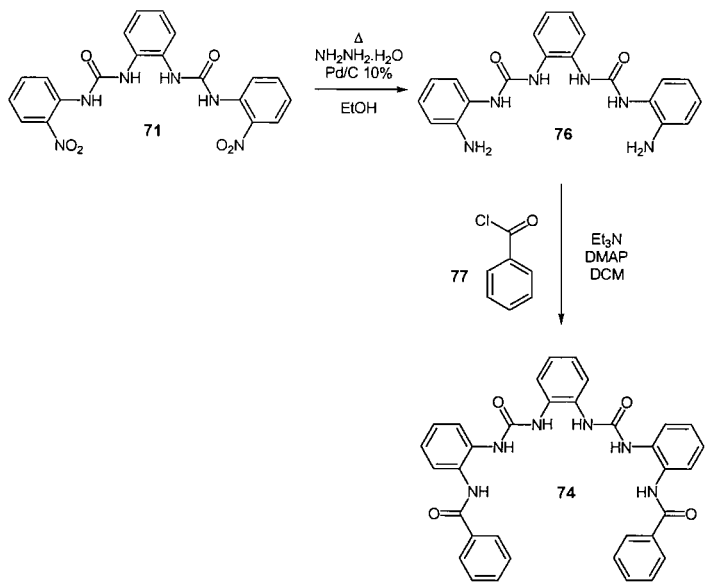

Scheme 2.3: Reaction scheme for the synthesis of compound **76**.

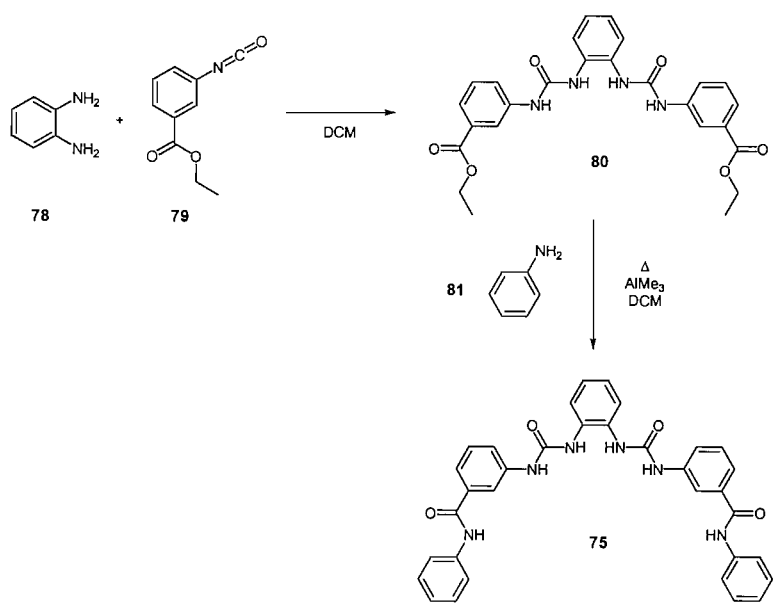

Scheme 2.4: Reaction scheme for the synthesis of compound **81**.

X-ray quality crystals of the free receptor of **74** were obtained via slow evaporation of a DMSO solution of **74**. The resulting structure shows that the receptor forms infinite tapes in which the each of the urea groups in conjunction with their appended amide moieties lie in opposing directions. Each of the urea groups coordinate to the urea oxygen atoms of the adjacent group [N2···O3 2.9110(15) Å, N3···O3 2.8228(15) Å, N4···O2 2.8528(15) Å & N5···O2 2.9810(15) Å], whilst the amide groups form similar interactions [N1···O4 2.7775(16) Å & N6···O1 2.7902(16) Å].

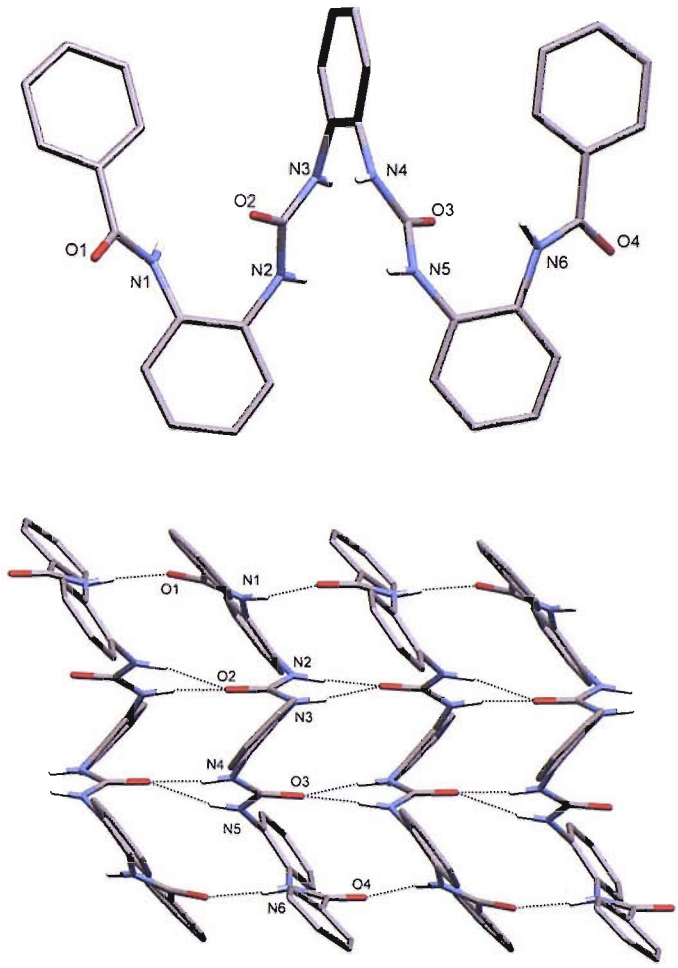

Fig 2.21: Bis-amide substituted derivative **74** displays intermolecular hydrogen bond interactions through both amide and urea moieties. Non-acidic protons omitted for clarity.

2.4.2. SOLUTION PHASE ANALYSIS.

2.4.2.1. ^{1}H NMR titration data.

Association constants for a variety of anionic guests in the form of their TBA salts in DMSO-d_6 / 0.5% water were determined via ^{1}H NMR titration experiments.

Table 2.3: Anion association constants for compounds **74** & **75** in DMSO-d_6 / 0.5% water. Anions titrated in the form of their TBA salts at 298K. Data fitted to 1:1 and 1:2 binding models using WINEQNMR.[92] All errors less than 15 %.

Anion	**74**	**75**
Chloride	17	52
Dihydrogen Phosphate	$K_1 = 7777$ $K_2 = 24$ $\beta = 185,000$	2289
Hydrogen Sulfate	-	12
Acetate	$K_1 = 6008$ $K_2 = 9$ $\beta = 55,230$	3199
Benzoate	$K_1 = 10110$ $K_2 = 2$ $\beta = 16,554$	974

Receptor **74** that includes amide groups in the cleft, shows an increase in more complex species in solutions are observed as shown by an increase in the sigmoidal nature of the NMR titration curves. The data was most satisfactorily fitted to a 2:1 binding model for acetate, benzoate and dihydrogen phosphate. The value for β reflecting the overall complex stability indicates that in these cases dihydrogen phosphate is bound by the receptor with exceptionally high association constants in DMSO solution, whilst both acetate and benzoate are also bound with considerable strength. The relatively weak second stability constant indicates that the predominant interaction in

solution is a 1:1 interaction between the anion and the receptor. The also remains the possibility of higher ordered systems in solution (Fig. 2.22).

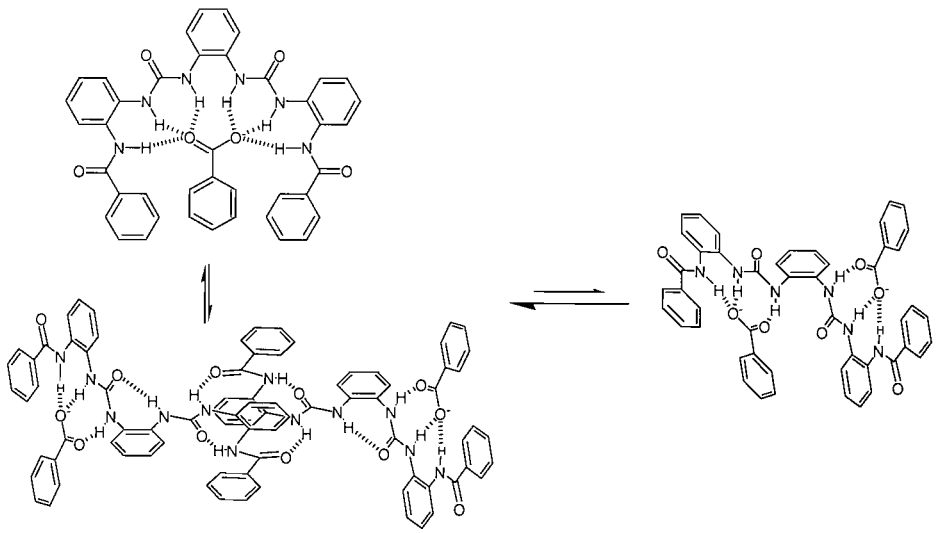

Fig 2.22: Weak secondary association constants for **74** with a variety of oxo-anions indicates the likelihood that a 1:1 anion receptor binding stoichiometry is predominant in solution at lower anion concentrations.

The observed stability constants for receptor **75** are similar to those obtained with **68** suggesting that in this case the additional amide groups are not resulting in a deformation of the bis-urea cleft. In the case of carboxylates, the amide NH groups are too remote to effectively cause additional hydrogen bonding interactions with insignificant shifts observed during the NMR titration. Dihydrogen phosphate is bound more strongly by this receptor than the non-functionalised receptor, potentially due to the larger size of the phosphate anion making simultaneous urea – amide interactions possible.

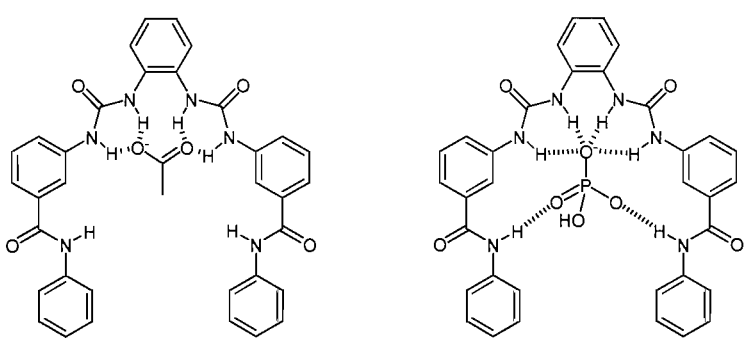

Fig 2.23: Alternative anion binding modes of receptor **75** with acetate and dihydrogen phosphate.

2.4.3. SOLID STATE ANALYSIS.

X-ray quality crystals of the acetate complex of **74** were obtained via slow evaporation of a DMSO solution of **74** in the presence of excess TBA acetate. The dimeric structure contains an extensive network of hydrogen bonding with intra- and intermolecular interactions between receptors in addition to interactions between the receptor and the anion.

The acetate anion is bound to the receptor through a combination to two urea NH interactions [N4···O5 2.803(4) Å & N5···O6 2.750(3) Å] and a pendent amide interaction [N6···O6 2.953(4) Å]. Intramolecular hydrogen bonding interactions from the NH groups not involved in anion coordination between the urea moieties [N3···O3 2.738(4) Å] and from the remaining pendent amide group [N1···O2 2.682(3) Å] are present. Intermolecular hydrogen bonds exist between the two receptors [N2···O1^{i} 2.924(4) Å].

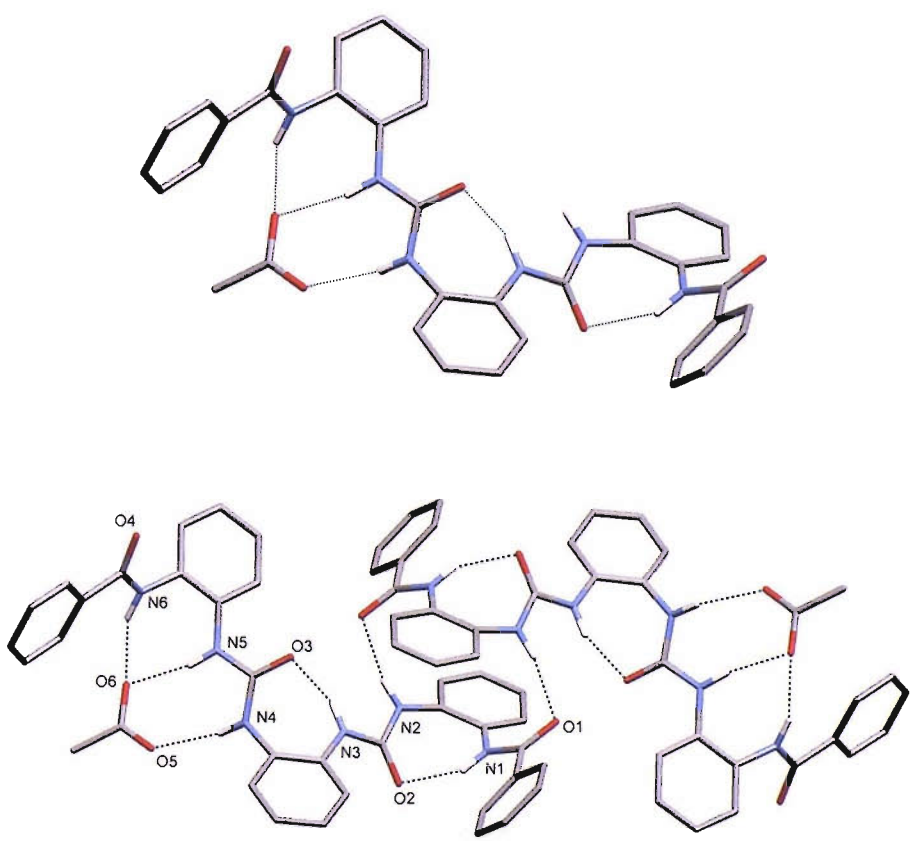

Fig 2.24: The acetate complex of **74** binds one anion via a urea and adjacent amide moiety. The remaining NH groups are involved in dimerisation. Non-acidic protons and TBA cations are omitted for clarity.

X-ray quality crystals of the benzoate complex of **74** were obtained via slow evaporation of a DMSO solution of **74** in the presence of excess TBA benzoate. A similar dimeric structure was observed with benzoate as had previously been observed with acetate with the presence of extensive intra- and intermolecular hydrogen bonding.

The benzoate anion is bound by two urea NH interactions [N4···O5 2.761(4) Å & N5···O6 2.830(4) Å] with an additional interaction from the pendent amide group [N6···O6 3.016(4) Å]. Intramolecular hydrogen bonding interactions from the NH groups not involved in anion coordination between the urea moieties [N3···O3 2.709(4) Å] and from the remaining pendent amide group [N1···O2 2.698(4) Å] are present. Intermolecular hydrogen bonds exist between the two receptors [N2···O1^{i} 3.030(4) Å].

Fig 2.25: The benzoate complex of **74** has one anion via a urea and adjacent amide moiety. The remaining NH groups are involved in dimerisation. Non-acidic protons and TBA cations are omitted for clarity.

2.5. TETRA-UREA DERIVATIVES – BUILDING BLOCKS FOR CRYSTAL ENGINEERING.

Solution phase analysis of the bis-urea / carboxylate interaction has demonstrated to be particularly favourable in competitive solvent mixtures. The multiple X-ray crystal structures that have been obtained have shown the carboxylate anion generally bound within the bis-urea cleft with all four of the urea NH groups coordinating. Of particular interest was the terephthalate structure of **68** that revealed that two receptors could simultaneously coordinate to a single anion.

It was therefore decided to investigate whether the interaction could be utilised in the formation of higher order supramolecular structures. In particular it was hoped that the use of a tetra-urea substituted receptor in combination with a dicarboxylate would result in the formation of anionic hydrogen bonded polymers.

Two tetra-urea derivatives were synthesized, one of which has each of the bis-urea groups attached to separate biphenyl connected aryl rings whilst the other derivative has all of the urea groups appended to a single aryl component.

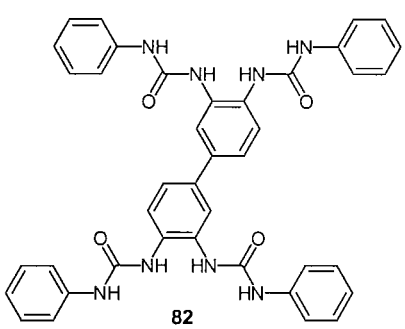

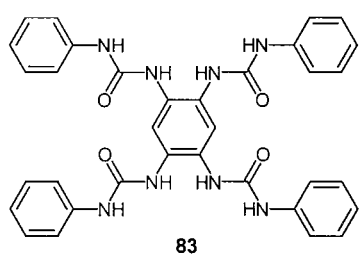

Fig 2.26: Tetra-urea based receptors for the formation of self-assembling structures.

2.5.1. SYNTHESIS AND CHARACTERISATION.

Compound **82** was prepared reaction between phenylisocyanate **84** and 3,3′-diaminobenzidine **85** in DMF yielding **82** in 58 % yield (Scheme 2.5). Compound **83** was prepared according to literature.[94]

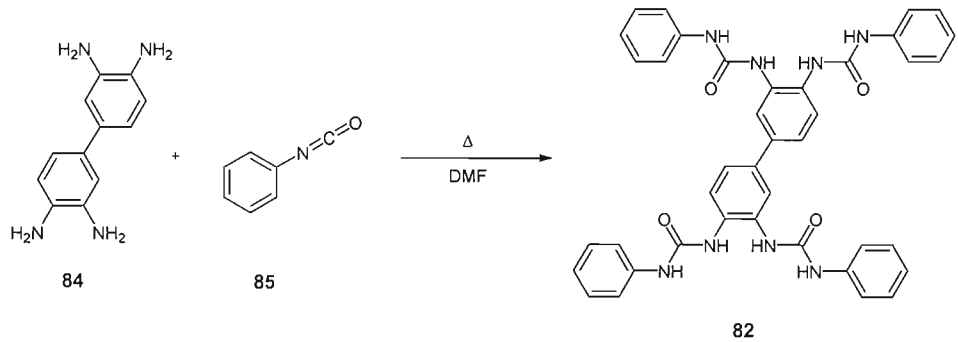

Scheme 2.5: Synthesis of tetra-urea derivative **84**.

2.5.2. SOLID PHASE ANALYSIS.

Slow evaporation of a saturated hot DMSO solution of tetra-urea derivative **82** in the presence of excess TBA benzoate yielded the benzoate complex of **82**. The structure reveals that each of the respective bis-urea moieties binds a single benzoate anion in an asymmetrical manner. One of the benzoate anions is bound in an almost symmetrical arrangement with the internal urea NH groups providing two hydrogen bonds [N6···O6 2.940(9) Å & N7···O5 2.794(10) Å] and the external urea NH groups a further two [N5···O6 2.850(8) Å & N8···O5 2.819(9) Å]. The other benzoate anion adopts a more slipped conformation in the bis-urea cleft with two urea NH of one urea group coordinating to a single benzoate oxygen [N4···O8 3.019(10) Å & N3···O8 2.715(11) Å] whilst the remaining urea group coordinates to both of the benzoate oxygen atoms [N2···O8 3.152(8) Å & N1···O7 2.769(8) Å].

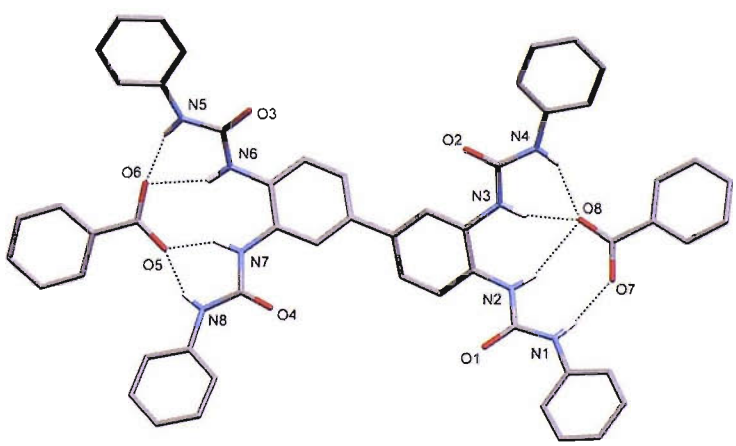

Fig 2.27: The benzoate complex of **82** shows two benzoate anions bound to one molecule of **84**. Non-acidic protons, DMSO molecules and TBA cations omitted for clarity.

X-ray quality crystals of the acetate complex of **82** were obtained via slow evaporation of a saturated hot DMSO solution of **82** in the presence of excess TBA acetate. As in the case of the benzoate complex of **82** each of the bis-urea binding sites coordinates to a single acetate anion, however in this case each of the two acetate anions were coordinated in an identical manner. A slipping of the anion in the cleft was observed once more with one of the urea groups coordinating to a single acetate oxygen atom [N4···O4 2.918(7) Å & N3···O4 2.726(7) Å]. The remaining urea group coordinates to both of the acetate oxygen atoms [N2···O4 3.275(7) Å & N1···O3 2.845(7) Å]. A further less significant interaction is present between one of the central urea NH groups and the outermost acetate oxygen [N2···O3 3.340(8) Å].

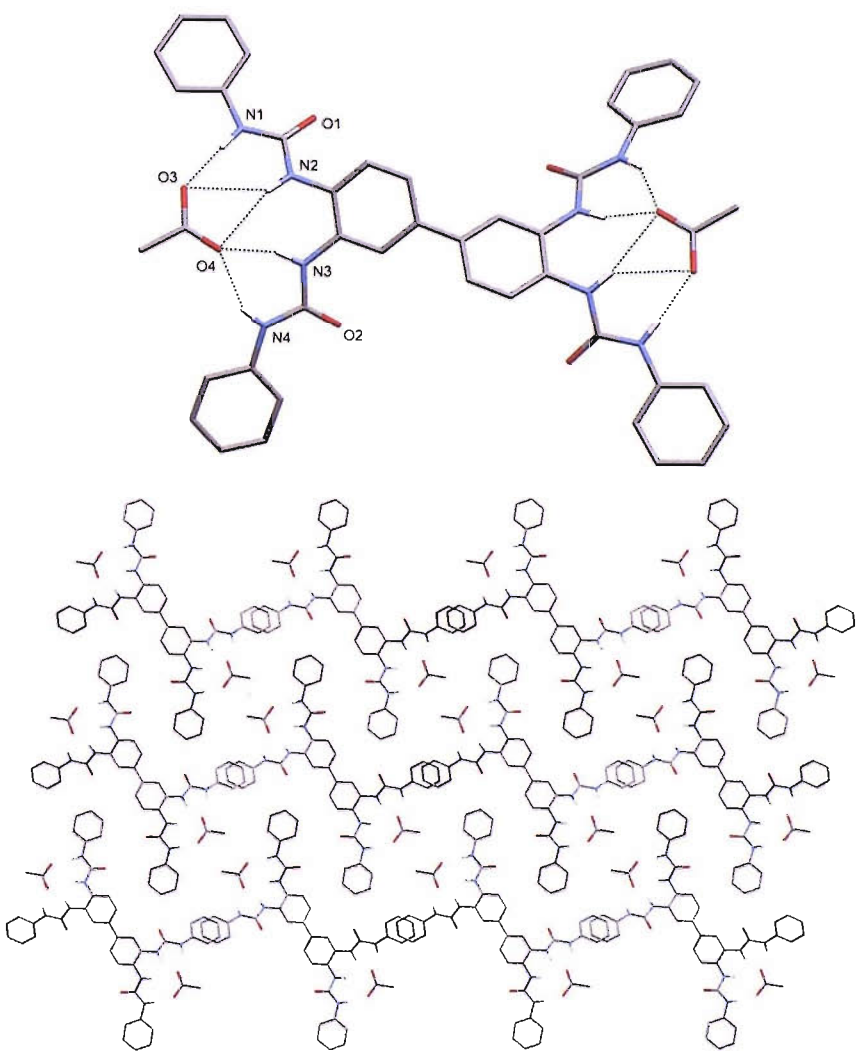

Fig 2.28: Acetate complex of **82**. Non-acidic protons, DMSO and TBA cations omitted for clarity.

Slow evaporation of a saturated hot DMSO solution of **82** in the presence of excess TBA terephthalate yielded X-ray quality crystals of the terephthalate complex of **82**. The resulting structure contained infinite hydrogen bonded chains of alternating terephthalate – tetra-urea units. Each of the carboxylate residues of the terephthalate were bound identically with a slightly slipped conformation within the bis urea cleft. The internal urea NH groups coordinate to both of the oxygen atoms [N2···O3 2.824(7) Å & N3···O4 2.919(6) Å] whilst the exterior urea NH are also coordinated [N1···O3 2.805(8) Å & N4···O4 2.857(7) Å]. A further long interaction between one of the internal urea NH groups and the distant oxygen is also in evidence [N3···O3 3.216(6) Å]. There also appears to be some evidence of π-overlap of the outer pendent aryl groups with the distance between groups consistent with π –stacking.

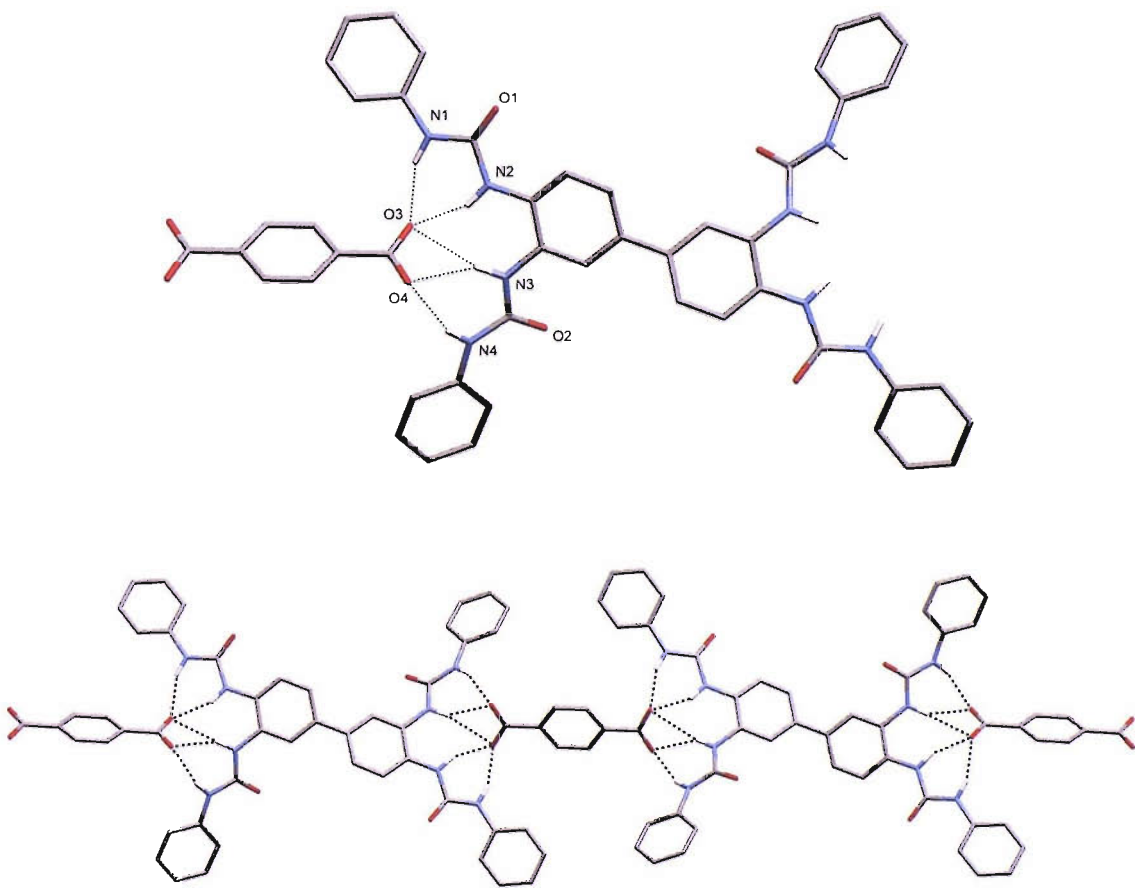

Fig 2.29: The **82** terephthalate complex forms infinite chains in the solid state. Non-acidic protons, DMSO molecules and TBA cations omitted for clarity.

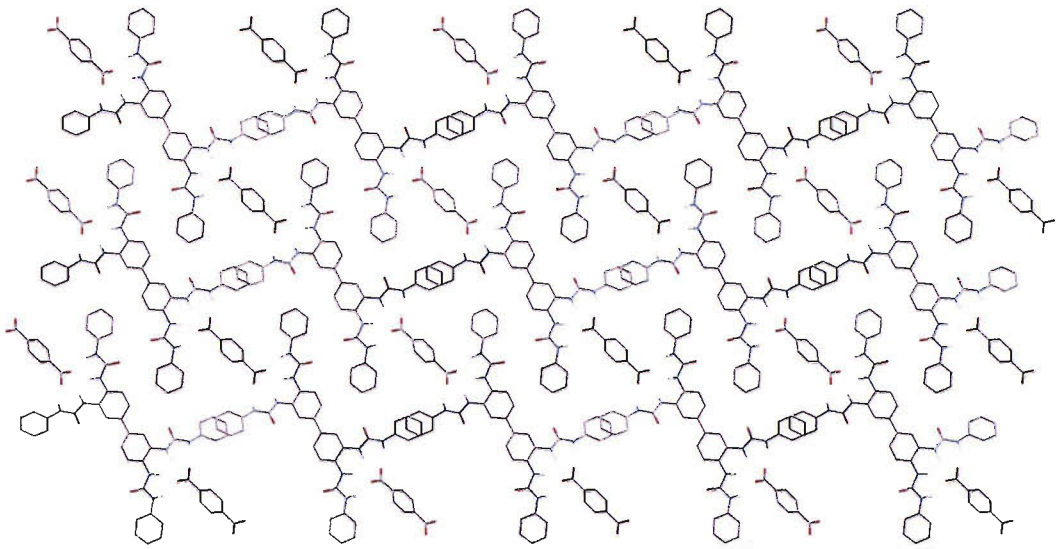

Fig 2.30: The terephthalate complex of **82** shows evidence of π-stacking between pendent aryl groups. Non-acidic protons, DMSO molecules and TBA cations omitted for clarity.

X-ray quality crystals of the acetate complex of **83** were obtained via slow evaporation of a saturated hot DMSO solution of **83** in the presence of excess TBA acetate. Incorporated water molecules in this structure results in a disruption of the simple anion / bis-urea interactions that have previously been demonstrated. Two crystallographically independent molecules of **83** are contained within the unit cell, each of which coordinate acetate in an identical manner through each bis-urea binding site.

The first molecule binds the acetate through a slipped conformation with one urea group coordinating a single oxygen atom [N4···O5 2.920(3) Å & N3···O5 2.744(3) Å] whilst the other urea group coordinates to both acetate oxygen atoms [N1···O6 2.814(3) Å & N2···O5 3.003(3) Å].

The second molecule binds both an acetate and water molecule within both of the binding sites. The acetate is held by two hydrogen bonds from the internal urea protons [N7···O7 3.095(3) Å & N6···O7 2.878(3) Å] and a further interaction including an external urea NH [N5···O8 2.817(3) Å]. The remaining external urea NH coordinates to a single water molecule [N8···O9 2.805(3) Å] which in turn forms hydrogen bonds to the acetate bound in the cleft [O9···O7 2.720(3) Å] and to one of the acetate oxygen atoms

coordinated to an adjacent complex [O9···O6 2.701(3) Å]. The overall result is the formation of a hydrogen bonded chain in the solid state

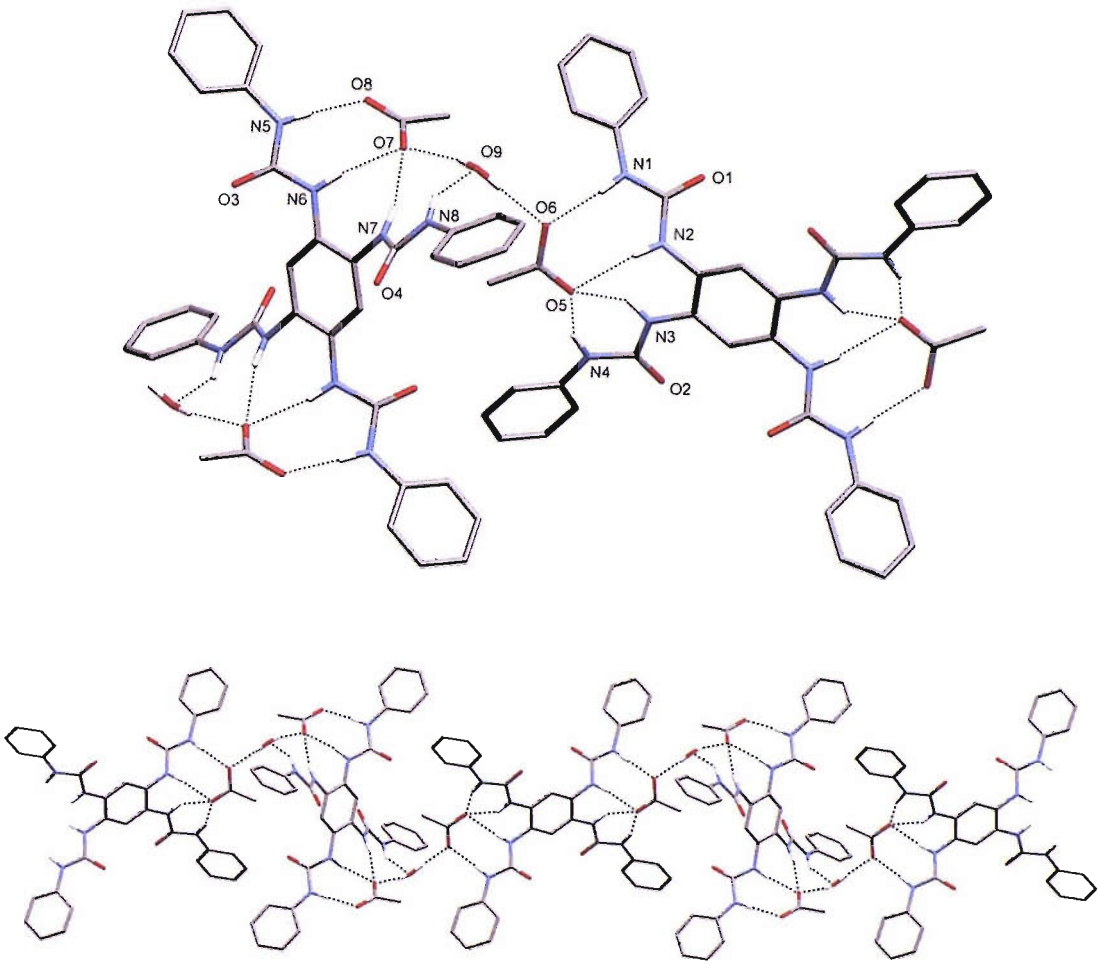

Fig 2.31: The hydrated acetate complex of **83** forms a hydrogen bonded chain in the solid state. Non-acidic protons, DMSO molecules and TBA cations omitted for clarity.

Slow evaporation of a saturated hot DMSO solution of **83** in the presence of excess TBA isophthalate yielded X-ray quality crystals of the isophthalate complex of **83**. Each of the carboxylate residues of the isophthalate are bound by the receptor asymmetrically, however in both cases a slipped conformation of the carboxylate within the bis-urea cleft is observed. As has been observed previously one of the urea groups coordinates to a single oxygen atom [N3···O7 2.7463(18) Å & N4···O7 3.0054(18) Å] [N5···O5 3.0209(19) Å & N6···O5 2.7399(18) Å], whilst the remaining urea group

coordinates to both of the isophthalate oxygen atoms [N1···O8 2.8320(18) Å & N2···O7 3.0989(18) Å] [N7···O5 3.262(2) Å & N8···O6 2.7473(18) Å]. The resulting structure forms an anionic hydrogen bonded chain in the solid state.

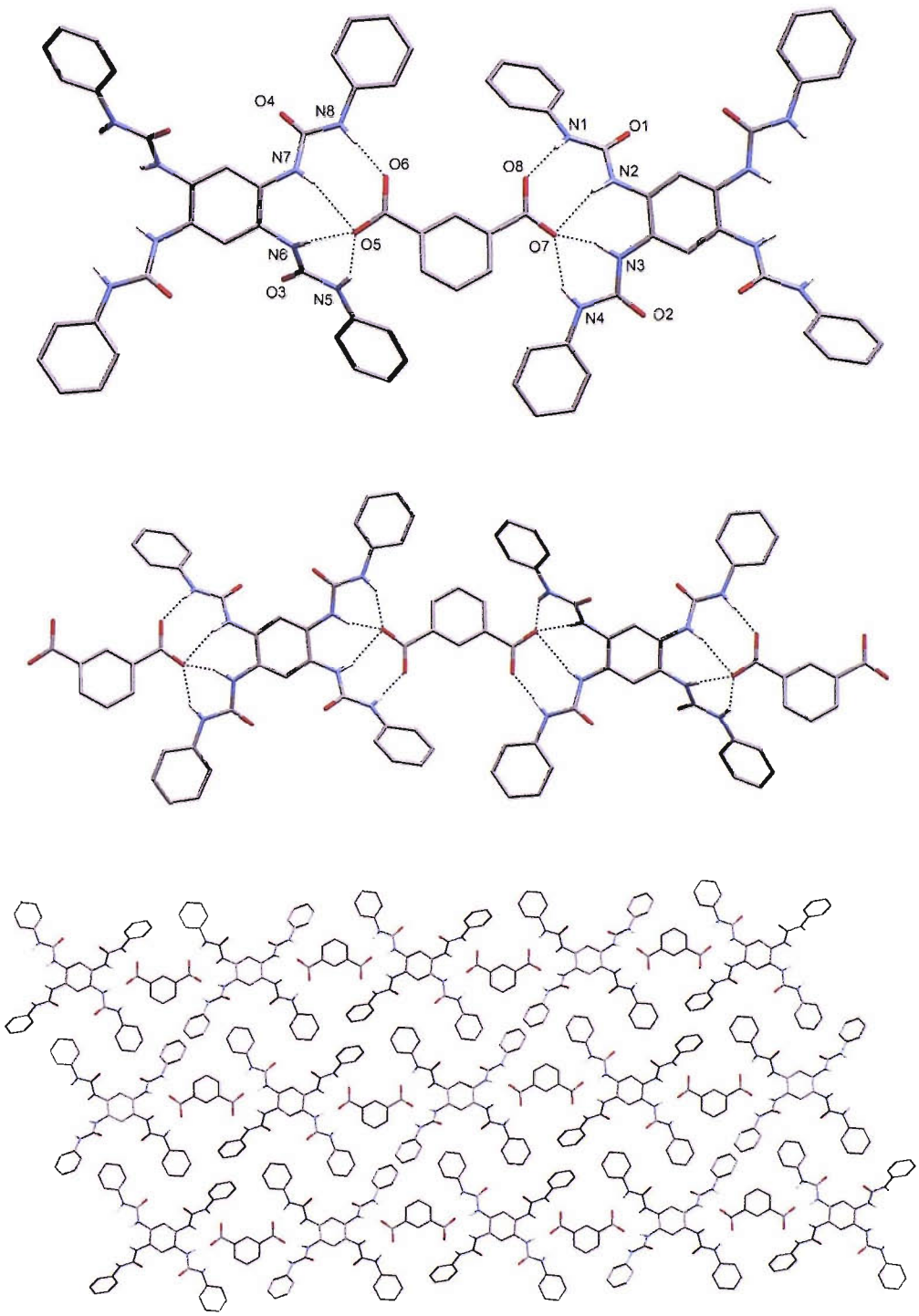

Fig 2.32: The isophthalate complex of **83**. Non-acidic protons, DMSO molecules and TBA cations omitted for clarity.

2.6. CONCLUSION.

A series of 1,2-phenylenediamine based receptors **66-68** have been synthesized and their anion coordination properties investigated by ^{1}H NMR titration techniques performed in DMSO-water solvent mixtures. The studies revealed that the bis-urea motif displayed exceptional oxo-anion coordination properties, particularly for carboxylates.

Further investigation of the solution phase properties of various substituted bis-urea clefts **69-73** have shown that the introduction of electron-withdrawing groups upon the central aryl ring of these systems can produce a further enhancement in the stability of complexes, whilst substitution of electron-withdrawing groups upon the pendent aryl groups of these receptors only yields moderate improvements in anion coordination.

The appendage of additional hydrogen bond donor groups in the form of amides **74** and **75** can cause an improvement in the anion stability of complexes with inorganic oxo-anions and depending upon the location of the substitution pattern a further improvement upon carboxylate complexation.

Bis-urea derivatives readily form X-ray quality crystals in the presence of carboxylates in the form of their TBA salts, using a combination of rigid dicarboxylates and tetra-urea derivatives **82** and **83** it has been shown possible to form extended hydrogen bonded anionic polymers.

3. CARBOXYLATE SELECTIVITY IN AN AMIDO - UREA HYBRID MACROCYCLE.

3.1 INTRODUCTION.

The development of macrocyclic anion receptors based upon the 2,6-pyridinedicarboxamide cleft is recent area of anion coordination chemistry. In the last decade following the first reported use of the amide clefts as a motif for binding anions, [29,32] numerous research groups have developed different designs producing an array of macrocycles and cryptands for the coordination of various targeted anions.

A common approach in the synthesis of macrocyclic receptors that possess amide clefts as an anion binding motif has been the use of pyridine based clefts in preference to phenyl derivatives. The increased stability of the *syn-syn* conformation of pyridine-2,6-dicarboxamides over the *anti-anti* and *syn-anti* geometries statistically increases macrocyclisation over polymerisation.[95]

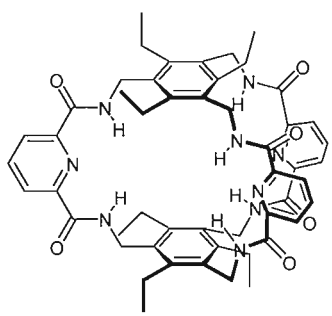

86

Fig 3.1: Ansyln's C_3-symmetric cyclophane **86** displays nitrate selectivity.

Ansyln and co-workers designed and synthesized a C_3-symmetric bicyclic cyclophane **86** for the complexation of nitrate (Fig 3.1).[96,97] Starting from the rigid precursors of 2,6-pyridine dicarbonyl chloride and 1,3,5-triaminomethyl-2,4,6-triethylbenzene, the resulting cyclophane was obtained in 40% yield.

Determination of stability constants was performed *via* ^{1}H NMR titration experiments in 25 % DCM/acetonitrile solution. In the case of all anions a 1:1 anion / receptor stoichiometry was observed with acetate bound most strongly. Significantly nitrate was bound only 2.6 less strongly than acetate but is 10^6 times less basic. This effect presumably arises from the optimal geometric arrangement of all six of the amide NH groups for this anion to allow nitrate encapsulation within the macrocyclic cavity.

The use of 2,6-pyridinedicarboxamide clefts in the formation of both mono- and bicyclic- anion receptors has been investigated in detail by Bowman-James (Fig 3.2).[98, 99] Tetra-amide **87** and tetra-thioamide **88** were prepared with the crystal structure of the sulfate complex of **87** obtained *via* crystallisation of the receptor in the presence of one equivalent of TBA hydrogen sulfate from $CHCl_3/Et_2O$. The dinegatively charged sulfate anion is sandwiched between two receptors molecules with each sulfate oxygen atom co-ordinated to two amide NH groups.

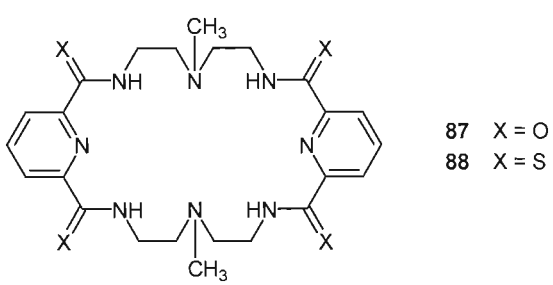

87 X = O
88 X = S

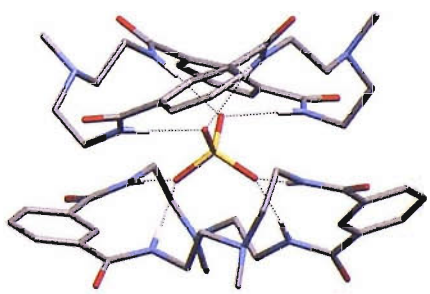

Fig 3.2: Bowman-James' monocyclic tetra-amide/thioamide receptors and the sulfate crystal structure of **87**.

Anion stability constants were elucidated through ^{1}H NMR titration experiments performed in DMSO-d_6. Tetra-thioamide **88** was found to bind dihydrogen phosphate, hydrogen sulfate and fluoride particularly strongly with 1:1 receptor / anion stoichiometry. Whilst dihydrogen phosphate was bound by **87** with a similar stability

constant, much weaker binding was detected with both hydrogen sulfate and fluoride, reflecting the reduction in the acidity of the amide NH protons relative to the thioamide analogue.

Subsequent investigations into the anion binding properties of analogous bicyclic receptors was later also performed by Bowman-James (Fig 3.3).[100-102] The introduction of two additional NH donor groups was intended to enable the formation of increased anion receptor interactions whilst the additional ring system provides additional rigidity to the structure.

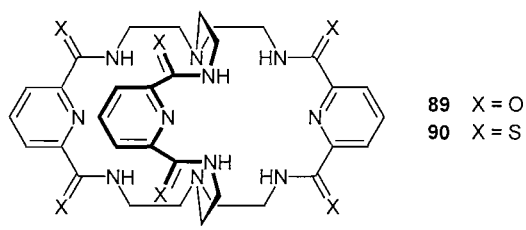

Fig 3.3: Bowman-James' bicyclic receptors **89** and **90** displayed enhanced fluoride selectivity.

Whilst investigations into the monocyclic receptors revealed that the thioamide receptors formed stronger complexes with anions than the amide derivatives analysis of the bicyclic systems revealed this to not be the case. A decrease in affinity of dihydrogen phosphate and hydrogen sulfate was observed in comparison to the monocyclic systems. This is attributable to the reduced ability of these anions to fit into the more defined and conformationally constricted cavity. Fluoride is small enough to fit into the cavity of both **89** and **90** and displays enhanced binding in these systems.

Structurally similar systems incorporating different linker units between the pyridine moieties have been investigated by Jurczak and co-workers (Fig 3.4).[103]

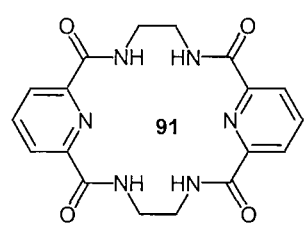

Fig 3.4: Jurczak's small cavity macrocyclic tetramide derivative.

Investigations into the anion complexation properties of macrocycle **91** were performed *via* ^{1}H NMR titration experiments performed in DMSO-d_6. These revealed that the macrocycle displayed selectivity for acetate, 2640 M^{-1}, and dihydrogen phosphate, 1680 M^{-1}. Although solution phase studies revealed a 1:1 binding stoichiometry *via* Job plot analysis, the acetate crystal structure adopts a 2:1 receptor anion stoichiometry with each receptor only able to satisfactorily accommodate a single oxygen atom of the acetate anion.

Sessler and co-workers have developed a range of novel 2,6-pyridine dicarboxamide receptors **92** & **93** that include dipyrrolemethane type moieties (Fig 3.5).[104,105] This type of hydrogen bonding motif has been shown in acyclic receptors to bind fluoride and dihydrogen phosphate with exceptionally high association constants in the highly competitive solvent mixture of DMSO-d_6/25% water.[57]

Generally receptors **92** and **93** bind tetrahedral anions strongly with high affinities for both hydrogen sulfate and dihydrogen phosphate reported. Whilst rigid receptor **93** binds sulfate, 10,800 M^{-1}, and phosphate, 29,500 M^{-1}, in 1:1 receptor anion stoichiometries, the more flexible receptor **92** binds sulfate more weakly, 64,000 M^{-1}. Additionally phosphate is bound in a 1:2 receptor anion stoichiometry with values of the two stability constants of 342,000 & 26,000 M^{-1}. These results indicate that the locked conformation of receptor **93** not only makes the receptor more suitable for selectively coordinating sulfate but additionally the rigidity prevents the formation of more complex equilibria in solution with phosphate.

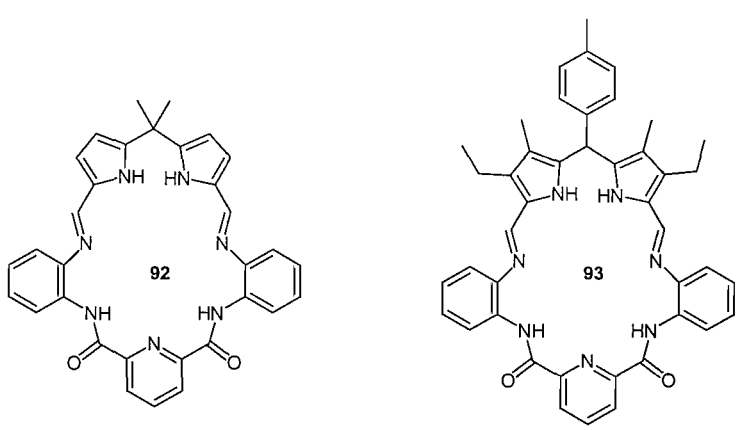

Fig 3.5: Sessler's dipyrrolemethane/2,6-pyridinedicarboxamide macrocycles **92** and **93** displayed varying anion selectivities

3.2. CYCLIC AND ACYCLIC AMIDO / UREA HYBRID ANION RECEPTORS.

Taking inspiration from the multiple examples of anion binding macrocycles that employ amide clefts as binding motifs, a target macrocycle was designed that combined both urea and amide functionalities and could act as a novel anion binding receptor.

Relatively few examples have been reported where the anion binding of a macrocycle had been compared to the behaviour exhibited by its components. As such it was decided to more investigate how the coordination properties of a macrocycle differ to those displayed by its fragments (Fig 3.6). Therefore both the constituent acyclic components and the macrocycle were synthesized and examined to determine the binding properties with coordinating anions.

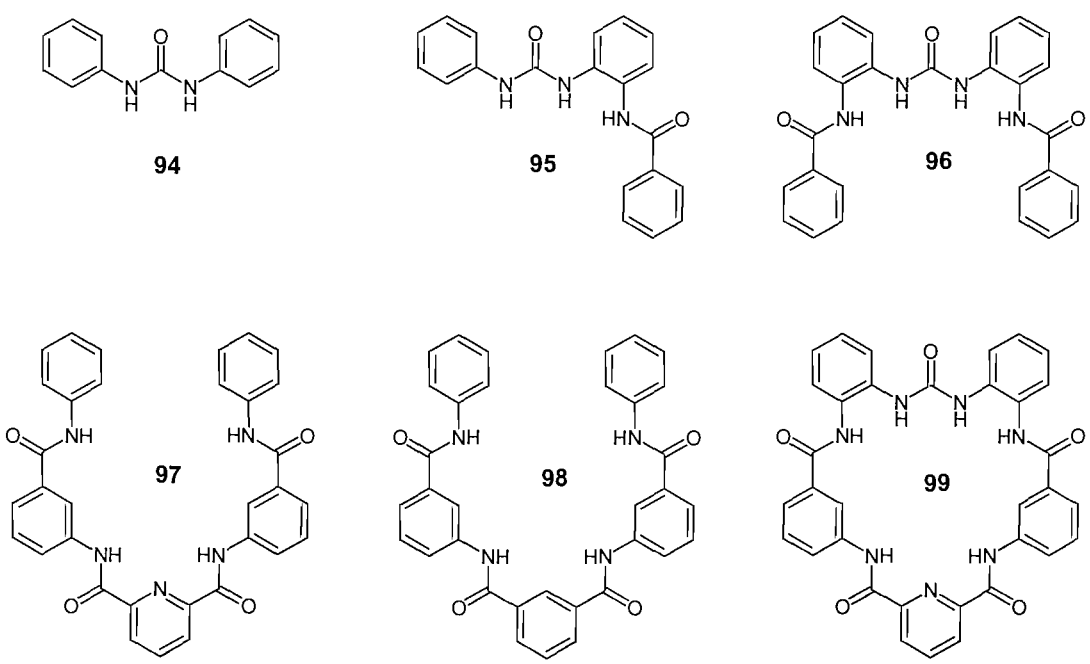

Fig 3.6: Acyclic and cyclic anion receptors **94-99** were synthesized in order to investigate the changes in anion selectivity induced through the geometrical locking of the macrocyclic receptor.

3.3. AMIDO-UREA FRAGMENTS AS ANION RECEPTORS.

3.3.1. SYNTHESIS AND CHARACTERISATION.

Urea derivatives **94** - **96** were synthesized in an attempt to determine the how the anion binding properties of the urea moiety is affected by the introduction of pendent amide groups. Receptor **94** was synthesized according to literature procedures.[106] Compound **100** was synthesised *via* literature procedures before reaction with phenylisocyanate **85** in dichloromethane yielded **95** in 97 % yield (Scheme 3.1).

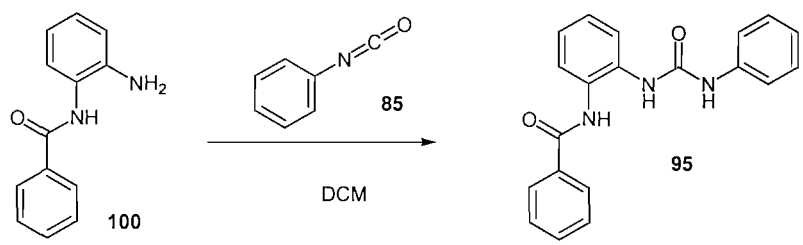

Scheme 3.1: Reaction scheme for the synthesis of urea-mono amide **95**.

Bis-amidourea **96** had been previously been synthesized, however its anion complexation properties had not been reported.[107] Synthesis of this fragment was achieved from a differing method from that in the literature by Miss Pamela Coles. Reaction of the diamine **101** with benzoyl chloride **102** in the presence Et_3N and DMAP in DCM affording **96** in 49 % yield (Scheme 3.2).

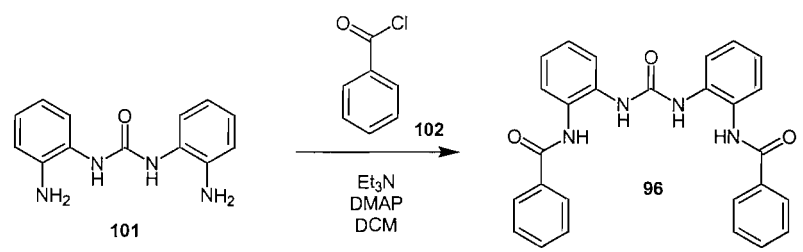

Scheme 3.2: Reaction scheme for the synthesis of urea-bis amide **96**.

X-ray quality crystals of the compound **96** were obtained *via* slow evaporation of an acetonitrile solution of **96**. The resulting white residue was then recrystalized from THF to afford single crystals of the acetonitrile solvate of **96**. The resulting structure reveals four independent molecules in the asymmetric cell with one acetonitrile molecule (Fig 3.7). Of the four molecules of the free ligand, two are arranged so that the pendent arms are pointing in the same direction, as drawn in the diagram above, whilst two are arranged in an up-down configuration (Fig 3.8).

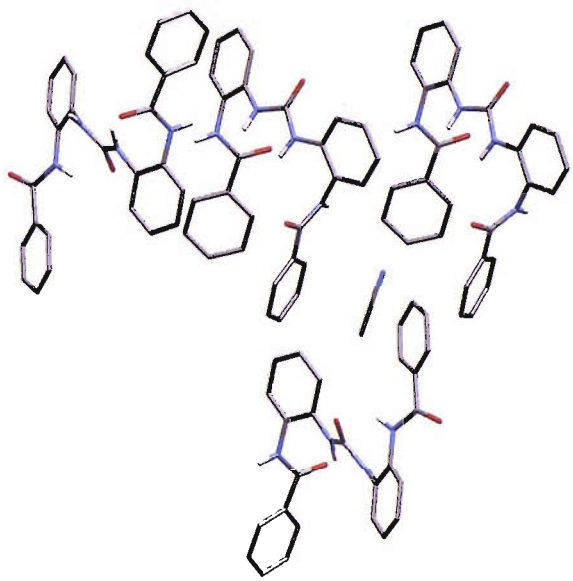

Fig 3.7: The unit cell contains four crystallographically independent molecules of **96**.

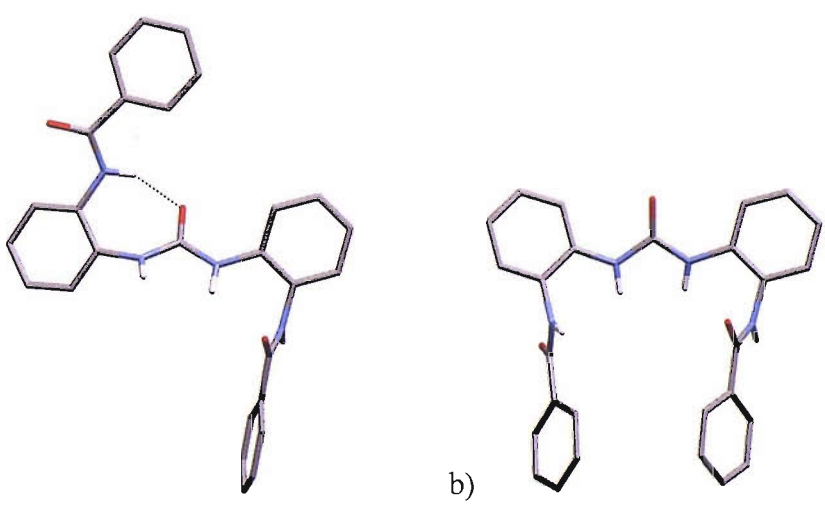

Fig. 3.8: Two of the geometries adopted by **96** in the acetonitrile solvate.

3.2.2. SOLUTION PHASE ANALYSIS.

3.2.2.1. ^{1}H NMR titration data.

Determination of the stability constants of receptors **94** – **96** with a variety of putative anionic guests was performed *via* ^{1}H NMR titration experiments in DMSO-d_6 / 0.5% water (Table 3.1).

Table 3.1: Stability constants for compounds **94** - **96** were determined in DMSO-d_6 / 0.5% water. Anions titrated in the form of their TBA salts at 298 K. All data fitted to a 1:1 binding model using WINEQNMR.[92] All errors <15%.

Anion	94	95	96
Chloride	31	<10	<10
Dihydrogen Phosphate	523	1286	1649
Acetate	1261	2364	2475
Benzoate	674	606	784

Compound **94** in which the only functionality that is able to interact with the anion is the urea NH groups shows oxo-anion selectivity with dihydrogen phosphate, acetate and benzoate all bound with appreciable strength. Additionally a relatively weak interaction can be determined with chloride.

Compound **95** in which one additional amide group has been introduced displays a significant improvement in both acetate and dihydrogen phosphate binding. Unusually benzoate is bound marginally weaker by this receptor and maybe the result of steric interactions between the aryl groups of the receptor and anion offsetting the stabilising additional amide / anion interaction.

Addition of two amide groups as in receptor **96** results in a further enhancement of anion / receptor complex stability with marginal improvements detected for all of the remaining anions. Whilst dihydrogen phosphate, acetate and benzoate are all bound more strongly than mono-amide **95** the differences in stability constants are small, potentially reflecting the difficulty of both amide groups simultaneously coordinating to a single

anion due to steric interactions. As a result anions may be bound by this receptor through a combination of both of the conformations that were previously determined in the acetonitrile solvate of **96**. In order to further investigate the interaction between **96** and benzoate both the change in chemical shifts of both the urea and amide proton resonances of **96** were determined (Graph 3.1).

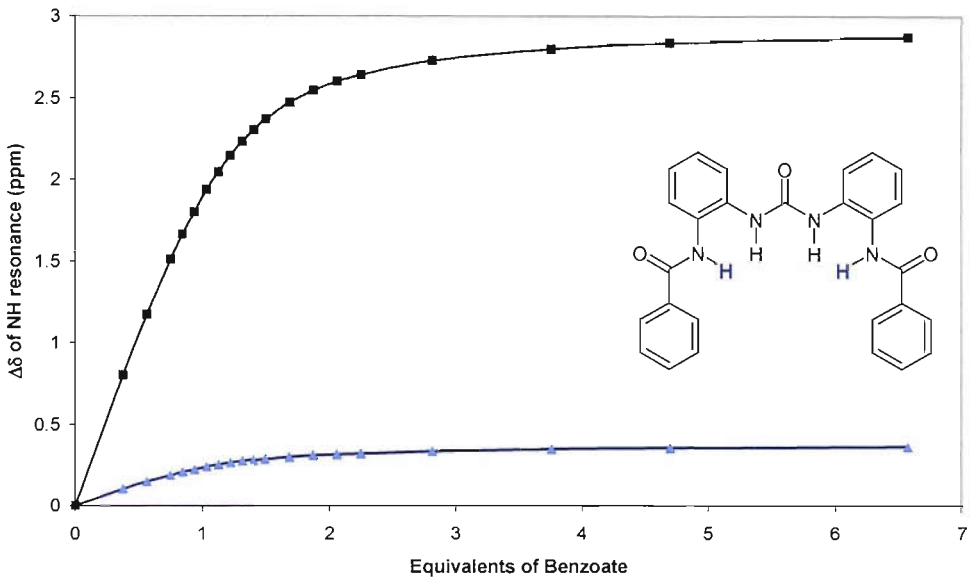

Graph 3.1: Graph showing effect of increasing benzoate concentration against change in amide (blue) and urea (green) NH proton chemical shift of receptor **96**.

An increase in the benzoate concentration causes urea and amide NH protons to undergo a downfield shift in the ^{1}H NMR spectrum, an effect consistent with both of these protons being involved in the formation of anion-receptor hydrogen bonds. Interestingly in this case the total change in chemical shift of the urea proton resonance is ten times greater than the total shift corresponding to the amide protons. This observation once more suggests that the urea protons interact with the benzoate anion more strongly than the amide protons and therefore are responsible for the primary interaction in this motif.

3.4. EXTENDED AMIDE CLEFTS AS ANION RECEPTORS.

3.4.1. SYNTHESIS AND CHARACTERISATION.

Novel anion receptors **97** and **98** were prepared to allow analysis of how the presence of additional appended amide moieties in an 'extended' amide cleft would affect the stability of anion complexes (Scheme 3.3). Both receptors were prepared in a similar fashion from compound **103** which itself was prepared *via* literature procedure.[107]

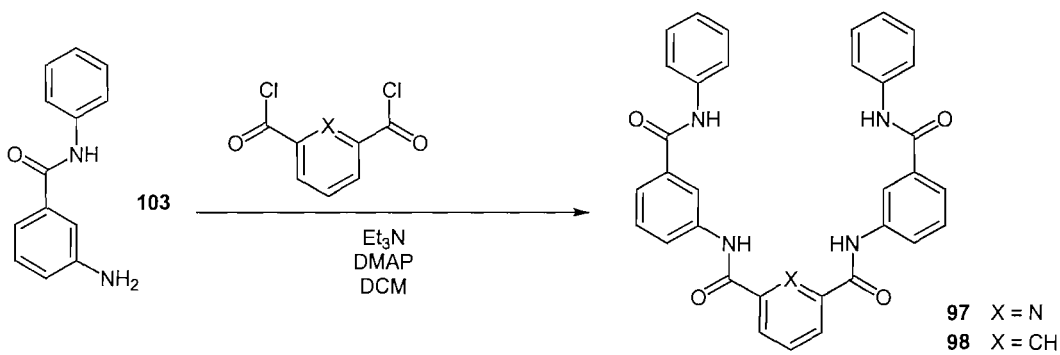

Scheme 3.3: Reaction scheme for the synthesis of isophthalamide-type receptors **97** and **98**.

Due to solubility issues the reaction scheme was based around initial synthesis of the pendent arms with the final step being the condensation amide coupling reaction to yield the products. Following the coupling, further purification of the bis-coupled product from mono-substituted side product was obtained *via* refluxing the crude product in acidic ethanol for 16 h, in order to convert any remaining acid residues to the more soluble ester. A final filtration of the hot ethanolic suspension left the product as a filtrate and allowed isolation of compounds **97** and **98** in 52 and 54 % respective yields.

3.3.2. SOLUTION PHASE ANALYSIS.

3.3.2.1. ^{1}H NMR titration data.

In order to determine the stability constants of receptors **97** and **98** with a variety of anions, ^{1}H NMR titration experiments were performed in DMSO-d_6 / 0.5 % water (Table 3.2).

Table 3.2: Stability constants for compounds **97** & **98** were determined in DMSO-d_6/0.5% water. Anions titrated in the form of their TBA salts at 298 K. Data fitted to 1:1 and 1:2 binding models using WINEQNMR.[92] All errors <15%.

Anion	97	98
Chloride	<10	$K_1 = 38$ $K_2 = 10$
Dihydrogen Phosphate	681	294
Acetate	419	137
Benzoate	101	71

The amide cleft based receptors **97** and **98** both demonstrated selectivity for oxo-anions under experimental conditions with the determined values considerably lower than those obtained for the urea and amidourea derivatives **94-96**.

In comparison to one another higher stability constants were obtained for the pyridine based receptor **97** for the investigated oxo-anions, with values approximately double those of the analogous isophthalamide based receptor **98**. This effect is consistent with the pyridine cleft being more pre-organized into an amide cleft conformation due to the stabilization of the *syn-syn* conformation in comparison to the other geometries.

As in the case of the amidourea fragments, the effect of the anion upon the change in chemical shifts of the amide NH groups was investigated in order to gain insight into the anion-receptor interaction (Graph 3.2).

The dominant receptor: anion interaction in this class of compound appears to be that of the isophthalamide/2,6-pyridinedicarboxamide cleft protons. Whilst both amide

NH protons are shifted downfield upon the addition of anions, the resonance equating to the cleft NH groups shift the most, suggesting that the major interaction with the anion occurs through this group. The pendant amide NH protons shift to a lesser extent with a total shift similar to that exhibited by the equivalent protons in receptor **96**. There is therefore less overall interaction with the anion which is reflected in the lower stability constants of **97** and **98**.

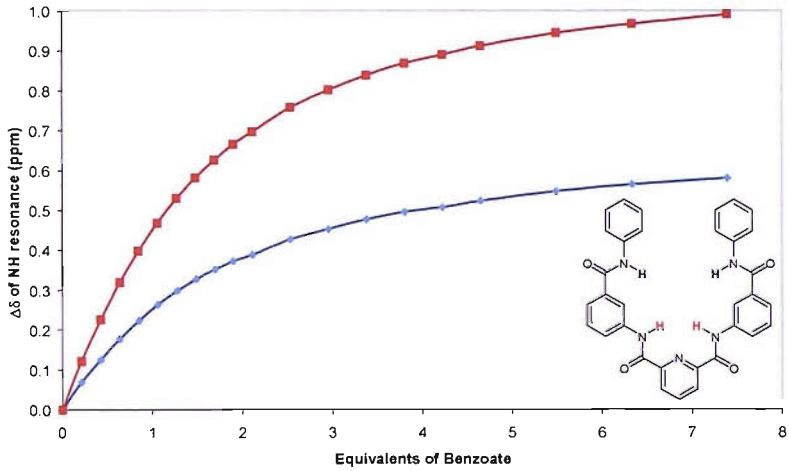

Graph 3.2: Effect of increasing benzoate concentration upon chemical shift of cleft (red) and pendent (blue) amide NH proton resonance of receptor **97**.

Conformation of the receptor: anion stoichiometry of receptor **97** in the solution phase was confirmed by Job plot in which a maximum was observed at 0.5 molar equivalents for benzoate (Fig 3.9).

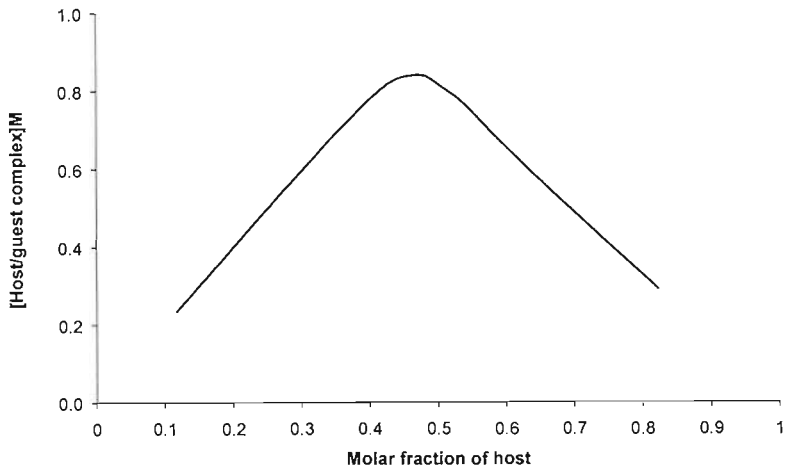

Fig 3.9: Job plot of **97** with benzoate in DMSO-d_6/ 0.5 % water.

3.4.3. SOLID PHASE ANALYSIS.

X-ray quality crystals of both the benzoate and chloride complexes of receptor **98** have been obtained through slow evaporation of saturated acetonitrile solutions containing an excess of either TBA benzoate or TBA chloride respectively.

The structure of the benzoate complex reveals a 2:1 anion / receptor stoichiometry in which each benzoate anion is bound to the receptor by two hydrogen bonds through similar hydrogen bonding motifs (Fig 3.10). One of these interactions arises from an isophthalamide NH group [N2···O7 2.786(4) Å & N3···O5 2.923(4) Å] with the second coming from the pendent amide NH groups [N1···O8 3.021(4) Å & N4···O6 2.880(4) Å].

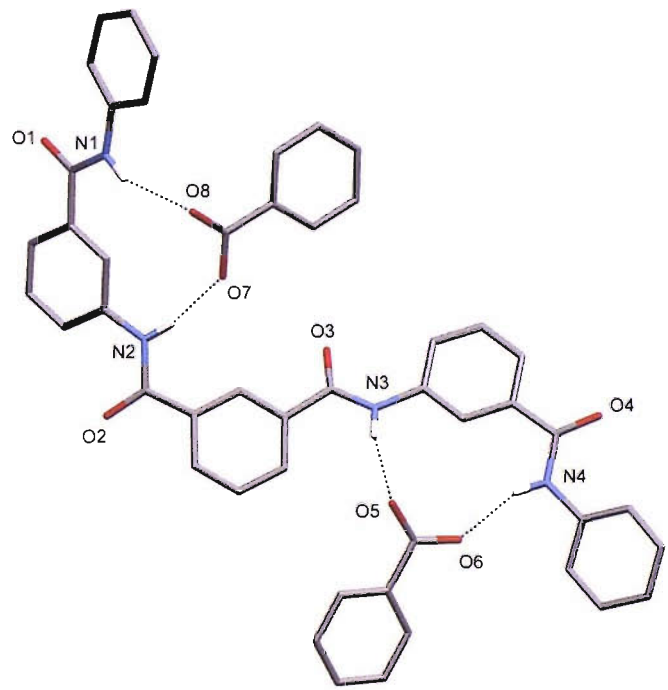

Fig 3.10: The benzoate complex of **98** has a 2:1 anion receptor stoichiometry. Non-acidic protons and TBA cations are omitted for clarity.

The chloride complex of **98** also has an overall 1:2 receptor / anion stoichiometry in the solid-state (Fig 3.11). One of the chloride anions is bound in the isophthalamide cleft in through two hydrogen bonds from each of the isophthalamide NH groups [N2···Cl3 3.386(4) Å & N3···Cl3 3.289(4) Å]. The remaining receptor bound chloride

anion interacts with the pendent amide groups of two adjacent receptor molecules [N1···Cl1 3.325(4) Å & N4···Cl1 3.412(4) Å] with these interactions facilitating the formation of a hydrogen bonded chain. A further chloride anion is included in the structure but is not bound by the receptor, instead there is evidence of a weak aryl CH···Cl interaction and interaction with an included water molecule [O5···Cl2 3.168(5) Å] (Fig 3.12).

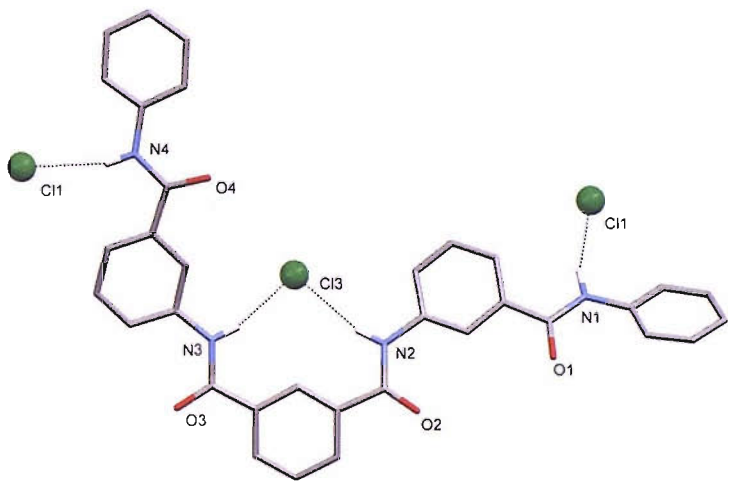

Fig 3.11: The chloride complex of **98.** Non-acidic protons, TBA cations, non-bound chloride anions and water molecules are omitted for clarity.

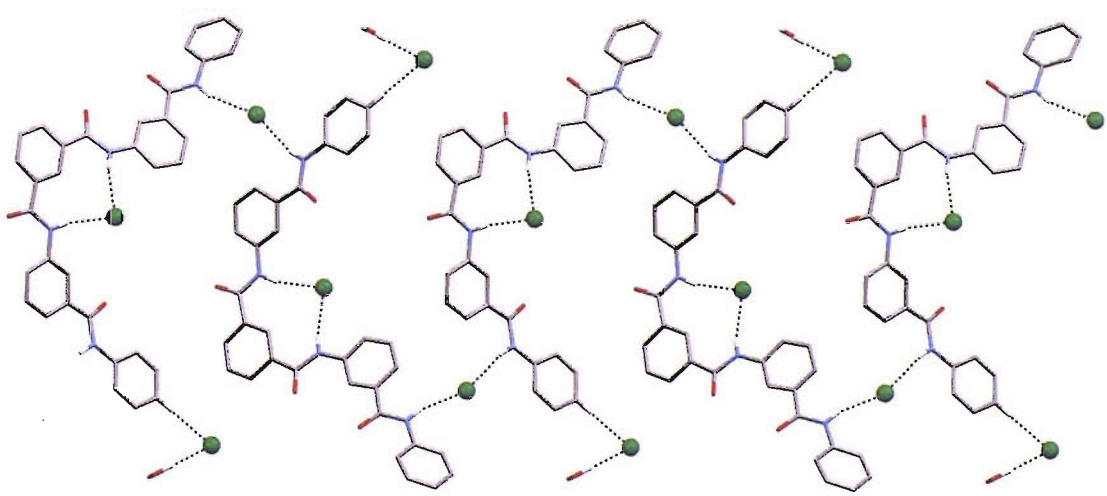

Fig 3.12: The extended chloride structure of **98** showing the additional non-receptor bound chloride anion. Non-acidic protons and TBA cations are omitted for clarity.

3.5. 2,6-PYRIDINEDICARBOXAMIDE/UREA MACROCYCLE.

3.5.1. SYNTHESIS AND CHARACTERISATION.

In order to synthesize the parent pyridine-based macrocycle, a stepwise procedure was followed, based initially on the synthesis of bis-amidourea component **99** (Scheme 3.4). Functionality was introduced through the replacement of benzoic acid with 3-nitrobenzoic acid which was subsequently reduced through a hydrazine reduction on palladium on carbon to provide the bis-amine **106**.

The low solubility of this precursor led to the use of TBA acetate in the final step of the synthesis, this allowed both the reaction to proceed in weakly coordinating dichloromethane and for a potential templating effect arising from the acetate coordinating not only to the urea functionality but also the pendant amide arms, resulting in the conformation in which both the amide arms are positioned so that macrocyclisation is likely to occur.

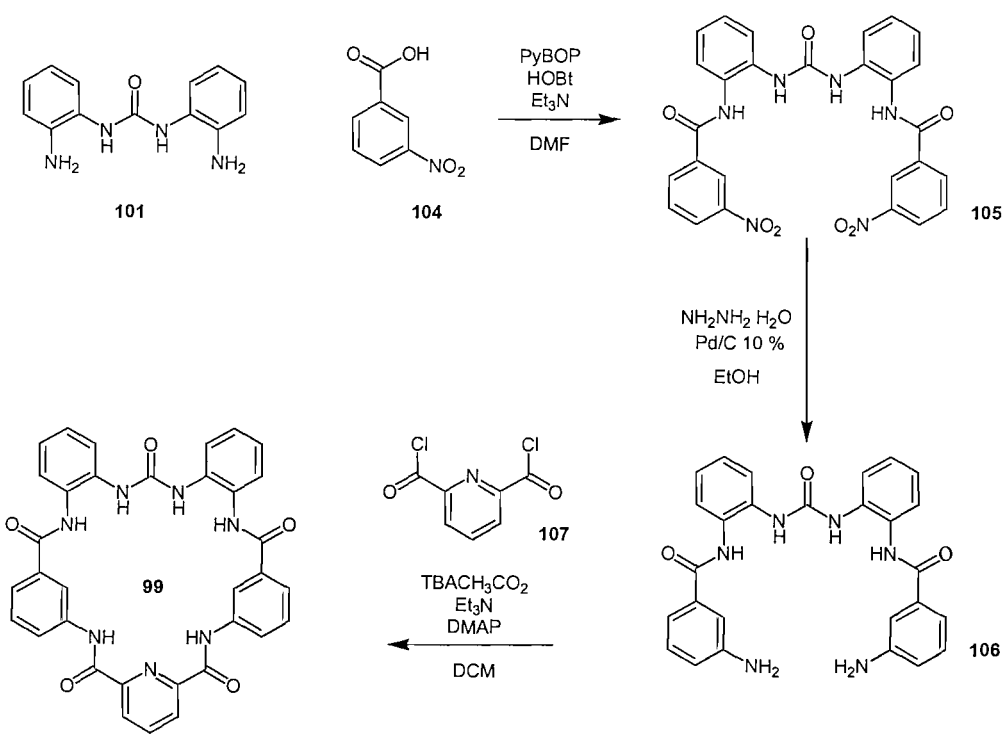

Scheme 3.4: Reaction scheme for the synthesis of isophthalamide based macrocycles.

3.5.2. SOLUTION PHASE ANALYSIS

3.5.2.1. ^{1}H NMR titration data.

In order to determine association constants for **99** with a variety of anions, ^{1}H NMR titration experiments were performed in DMSO-d_6 / 0.5% water and in cases where binding constants were particularly high, with DMSO-d_6 / 5.0% water (Table 3.3).

Table 3.3: Macrocyclic receptor **99** stability constants were determined in [a]DMSO-d_6/0.5% water and [b]DMSO-d_6/5.0% water at 298 K (M^{-1}). Data fitted to a 1:1 binding model in all cases using WINEQNMR.[92] All errors < 15 %.

Anion	99[a]	99[b]
Chloride	194	42
Bromide	10	-
Hydrogen Sulfate	115	-
Dihydrogen Phosphate	141	51
Nitrate	<10	-
Acetate	16520	5170
Benzoate	6432	1834

Attempts to elucidate stability constants of **99** with TBA fluoride were unsuccessful due to an inability to fit data to a binding model. The stability constants obtained for receptor **99** in DMSO-d_6/ 0.5 % water, reflect the an increase in stability constants when compared to its fragments acyclic derivatives **94-98** analogues, with a ten-fold increase in carboxylate stability constants in comparison to the highest observed for the acyclic components.

Interestingly with the exception of dihydrogen phosphate, all of the anions investigated show a significant improvement in stability constants with detectable, but weak, binding observed with bromide and nitrate, and a moderately high constant for hydrogen sulfate. Dihydrogen phosphate actually displayed a dramatic reduction in

stability constant with **99** in comparison to the constants obtained with the acyclic component fragments, indicating that the macrocycle has an inherent selectivity for carboxylates.

The stability constant acquired for **99** with acetate in particular is exceptionally high and approaching the limit of accuracy that can be determined using this method, therefore stability constants were also obtained in a more competitive solvent mixture of DMSO-d_6 / 5.0% water, which as expected reduced the association constants for all the anions investigated by approximately an equal amount.

As previously investigated for the acyclic components, we wished to examine how the introduction of a coordinating anion affected the chemical shifts of the NH protons, in order to attempt to elucidate information into the manner in which the receptor co-ordinates anions (Fig 3.13).

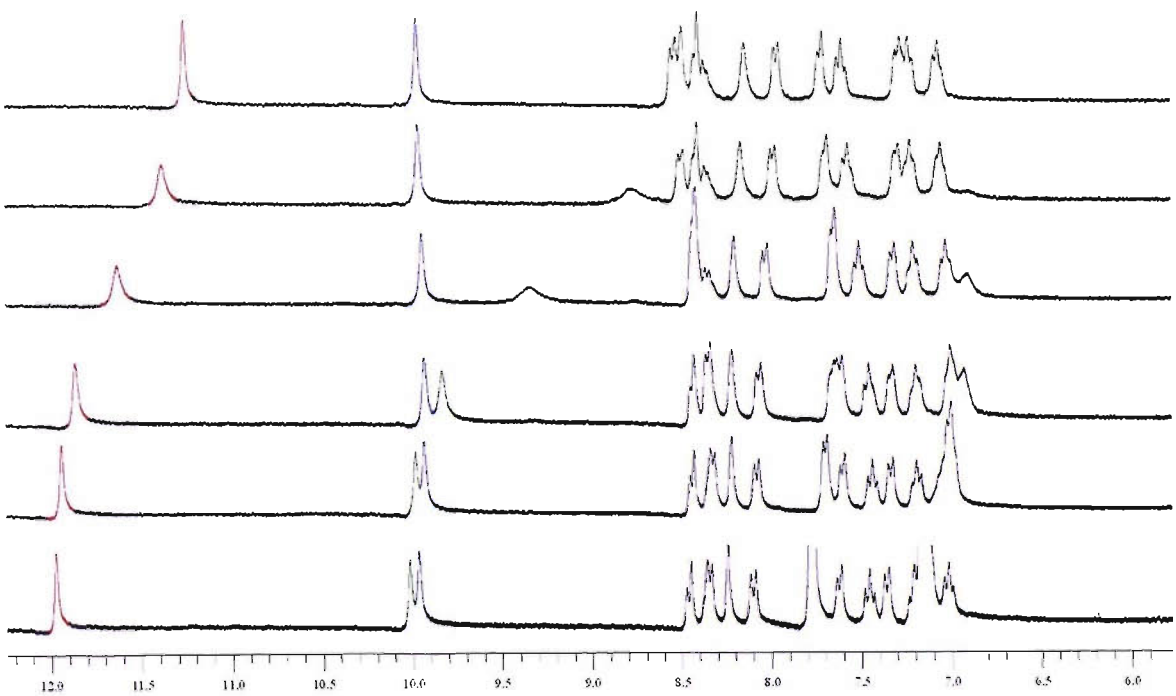

Fig 3.13: Stack plot of **68** showing the change in resonance of both the cleft (red) and linker (blue) amide NH protons and urea (green) NH protons upon increasing benzoate concentrations. Spectra recorded at 0.0, 0.20, 0.61, 1.01, 1.52 and 3.06 equivalents of benzoate.

Upon the addition of TBA benzoate to a solution of **99** both urea and cleft NH protons undergo downfield shifts, behaviour that is consistent with the formation of receptor / anion hydrogen bonds. Once again the most significant change in resonance is attributed to the urea NH proton with a large change also observed for the cleft amide NH resonances.

Interestingly the protons of linkage amide display an initial upfield shift upon the addition of benzoate before slowly returning downfield, however the final value obtained reflects an overall upfield shift, behaviour that is inconsistent with this proton being involved in anion coordination (Graph 3.4).

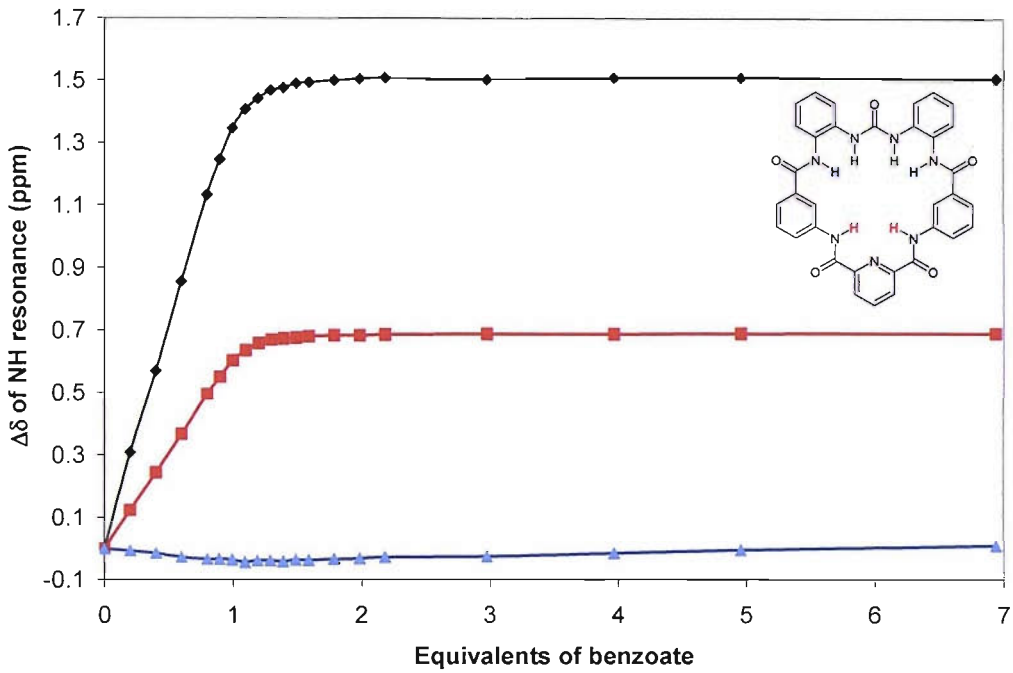

Graph 3.4: Graph showing the effect of increasing benzoate concentration upon the chemical shift of the urea (green), cleft amide (red) and pendent amide (blue) resonances of receptor **99**.

In order to determine that the unusual behaviour exhibited by the linkage amide proton did not reflect the formation of higher order coordination in solution, Job plots of both acetate and benzoate were obtained revealing a maximum at 0.5 molar equivalents of anion and thus confirming the 1:1 stoichiometry (Fig 3.14).

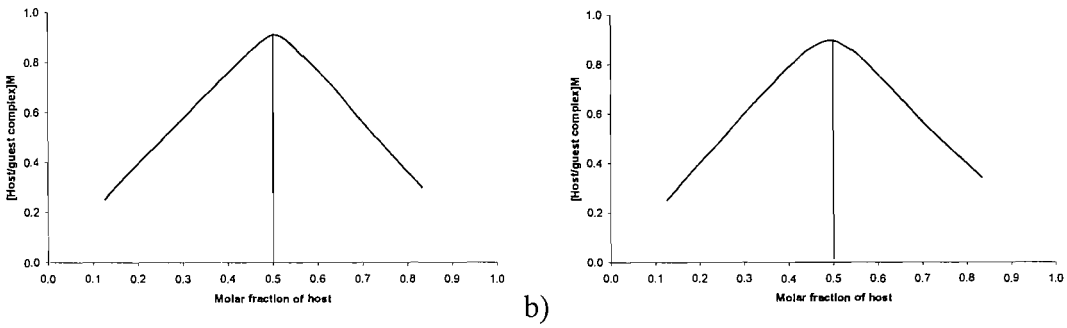

Fig 3.14: Job plots of **99** with a) acetate and b) benzoate reveal a 1:1 binding stoichiometry in DMSO-d_6/ 0.5 % water.

This behaviour may be explained by considering that the binding mode adopted by the receptor with carboxylate may display an interaction in which a bridging interaction between the carboxylate residue and the urea and cleft amide NH could exclude interactions with the linkage NH protons.

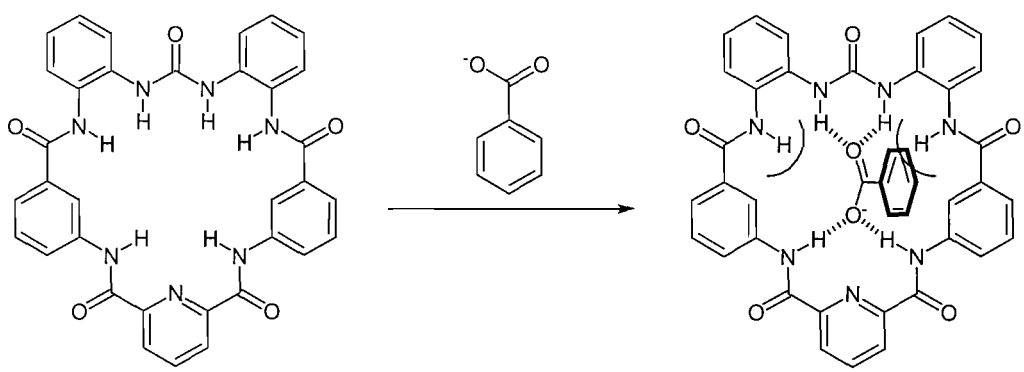

Fig 3.15: Potential bridging mode of macrocycle **99** with benzoate.

The upfield shift observed by the protons of the amide linkage could therefore be the result of a desolvation process in which disordered solvent included within the cavity is excluded upon the introduction of coordinating anion (Fig 3.15). As the linkage amide could be solvated in the free receptor, but unsolvated and not involved in anion coordination in the anion complex, the net effect for this proton would be the removal of hydrogen bonding to solvent molecules upon anion complexation and therefore an upfield shift in the proton resonance would be observed.

The change in the chemical resonance of the three differing NH groups differs between each of the anions investigated and therefore may provide insight into the way in which each interacts with the receptor.

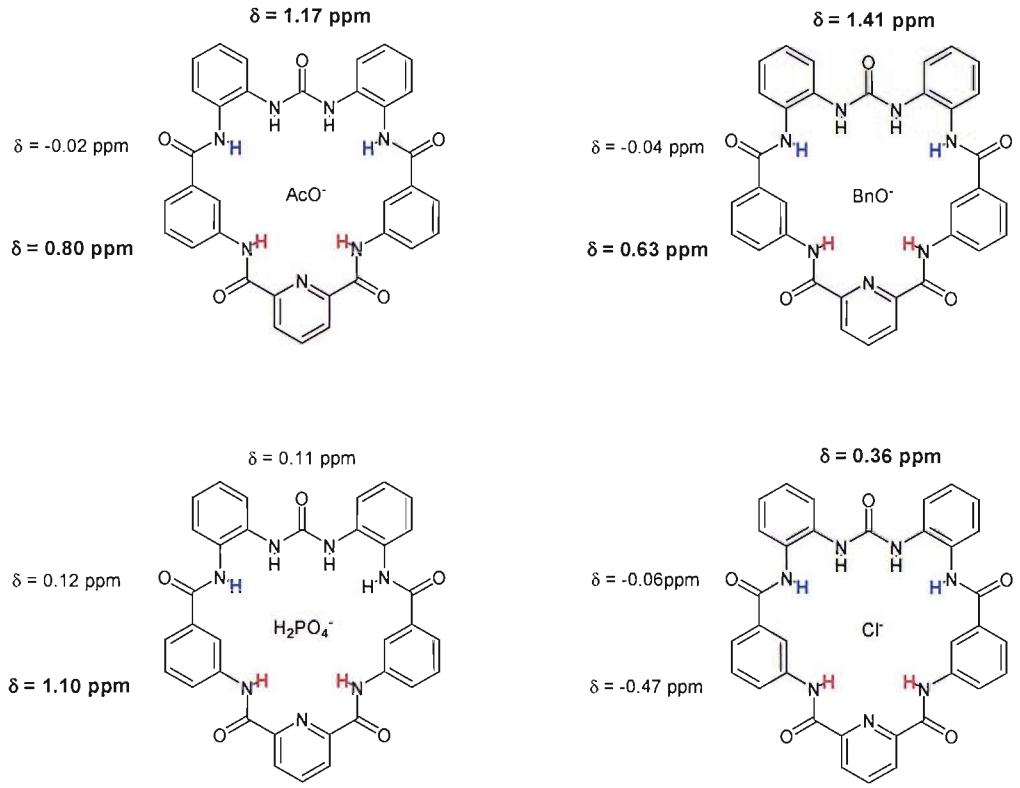

Fig 3.16: Change in chemical shift of urea and amide NH protons of **99** upon addition of 1.0 equivalents of acetate, benzoate, dihydrogen phosphate and chloride in DMSO-d_6 /0.5% water.

Both acetate and benzoate cause significant downfield chemical shifts to both the urea and amide cleft protons consistent with the formation of a bridging mode in solution between the urea and cleft amide protons, with desolvation of the linkage amide groups occurring as outlined previously.

Interesting dihydrogen phosphate and chloride interact with the receptor differently. Downfield shifts, consistent with anion receptor hydrogen bond formation, are observed with all three types of proton upon the addition of dihydrogen phosphate however the cleft protons are observed to shift downfield most significantly.

Chloride causes significant downfield shifts of the urea protons whilst upfield shifts of both sets of amide protons are observed. This suggests that the urea group is more suitable for binding chloride than the cleft with desolvation processes occurring at the remaining amide NH groups upon anion coordination. Data obtained from the ^{1}H NMR titration data of **94** showed that a higher stability constant with chloride was obtained for the free urea group than any of the appended amide cleft receptors **97** and **98**.

3.5.3. SOLID PHASE ANALYSIS.

Slow evaporation of a saturated methanol solution of **99** in the presence of excess TMA acetate afforded X-ray quality crystals of the hydrated acetate complex of **99** (Fig 3.16). Macrocyclic receptor **99** binds a single acetate anion through both of the pyridine amide NH groups [N4···O7 2.975(5) Å & N6···O7 3.321(5) Å] and through one of the linkage amide moieties [N7···O6 2.804(5) Å]. Both of the urea NH protons are involved in the formation of hydrogen bonds to a single water molecule [N1···O8 2.983(6) Å & N2···O8 2.857(6) Å]. The remaining linkage amide group is involved in hydrogen bonding to an adjacent macrocycle through an interaction with one of the pyridine cleft carbonyl oxygen atoms [N3···O3 3.130(5) Å] an interaction that is reciprocated by the same molecule. Numerous hydrogen bonds arising from the included water molecules are also present.

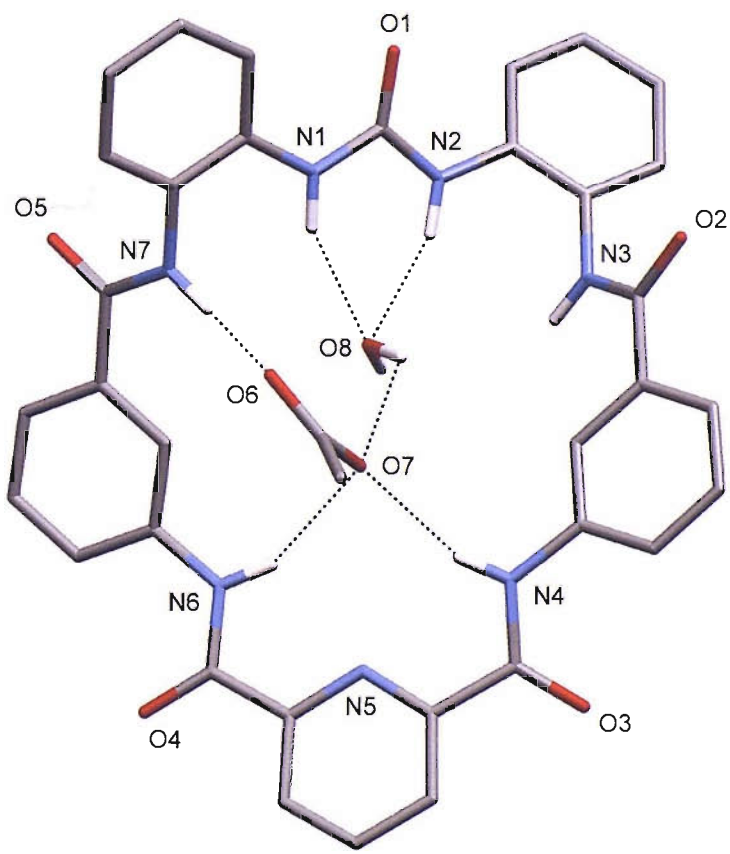

Fig 3.16: The acetate complex of **99**. Non-acidic protons, TMA cations and exocyclic water molecules omitted for clarity.

X-ray quality crystals of the carbonate complex of **99** were obtained *via* slow evaporation of a DMSO solution in the presence of excess TBA fluoride (Fig 3.17). The fixation of carbonate in the formation of hydrogen carbonate from basic DMSO solutions is a phenomenon that has been reported previously. The resulting structure shows the carbonate is bound centrally in the receptor with all six NH groups coordinating to the carbonate anion. One of the carbonate oxygen atoms is co-ordinated to both of the pyridine clefts amide NH groups [N4···O7 2.840(11) Å & N6···O7 2.806(11) Å].

The linkage amide groups [N3···O6 2.750(13) Å & N7···O8 2.831(12) Å] and the urea group [N1···O8 2.725(13) Å & N2···O6 2.767(13) Å] co-ordinate to the remaining two carbonate oxygen atoms so that each of the carbonate acceptor groups is bound by two hydrogen bonds.

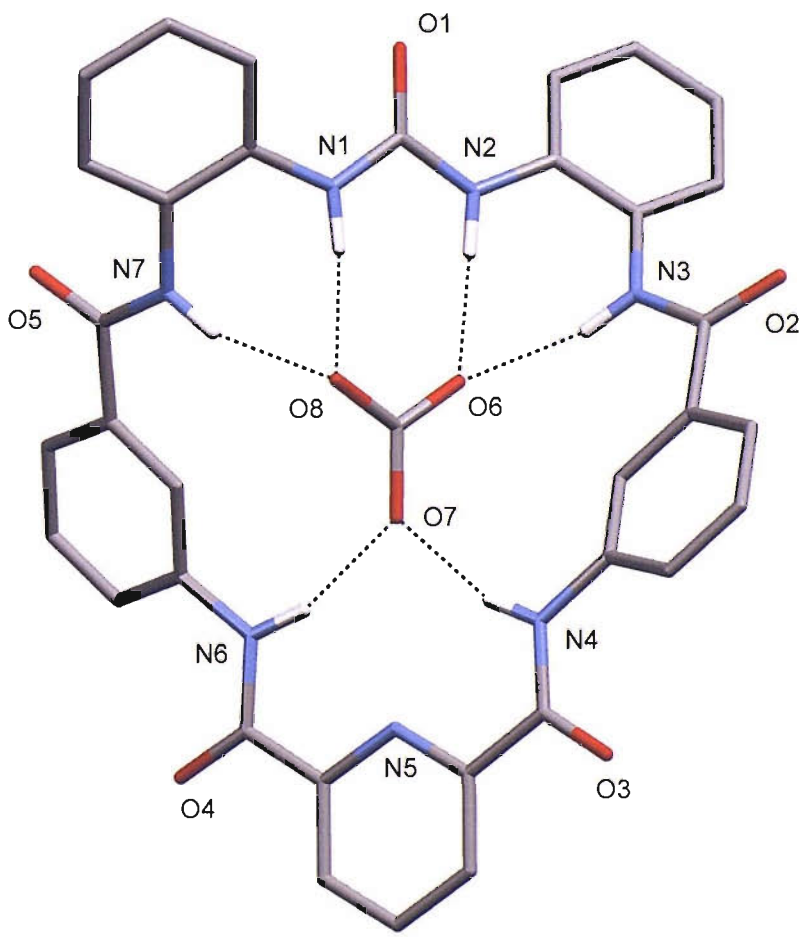

Fig. 3.17: Carbonate complex of **99**. TBA and fluoride counter ions, exocyclic water and DMSO molecules omitted for clarity.

Exocyclic to the macrocycle, fluoride is included in the extended structure in which four water molecules are seen to form a hydrogen bonded ring [O9···F1 2.621(7) Å] around the fluoride, whilst each of the water molecules also forms a hydrogen bond to one of the pyridine cleft oxygen atoms [O9···O3 2.940 Å] (Fig 3.15). Furthermore the extended structure reveals that clusters of this motif produce a porous structure in which disordered DMSO molecules are located in channels that run through the structure, with an overall 14% porosity (Fig 3.19).

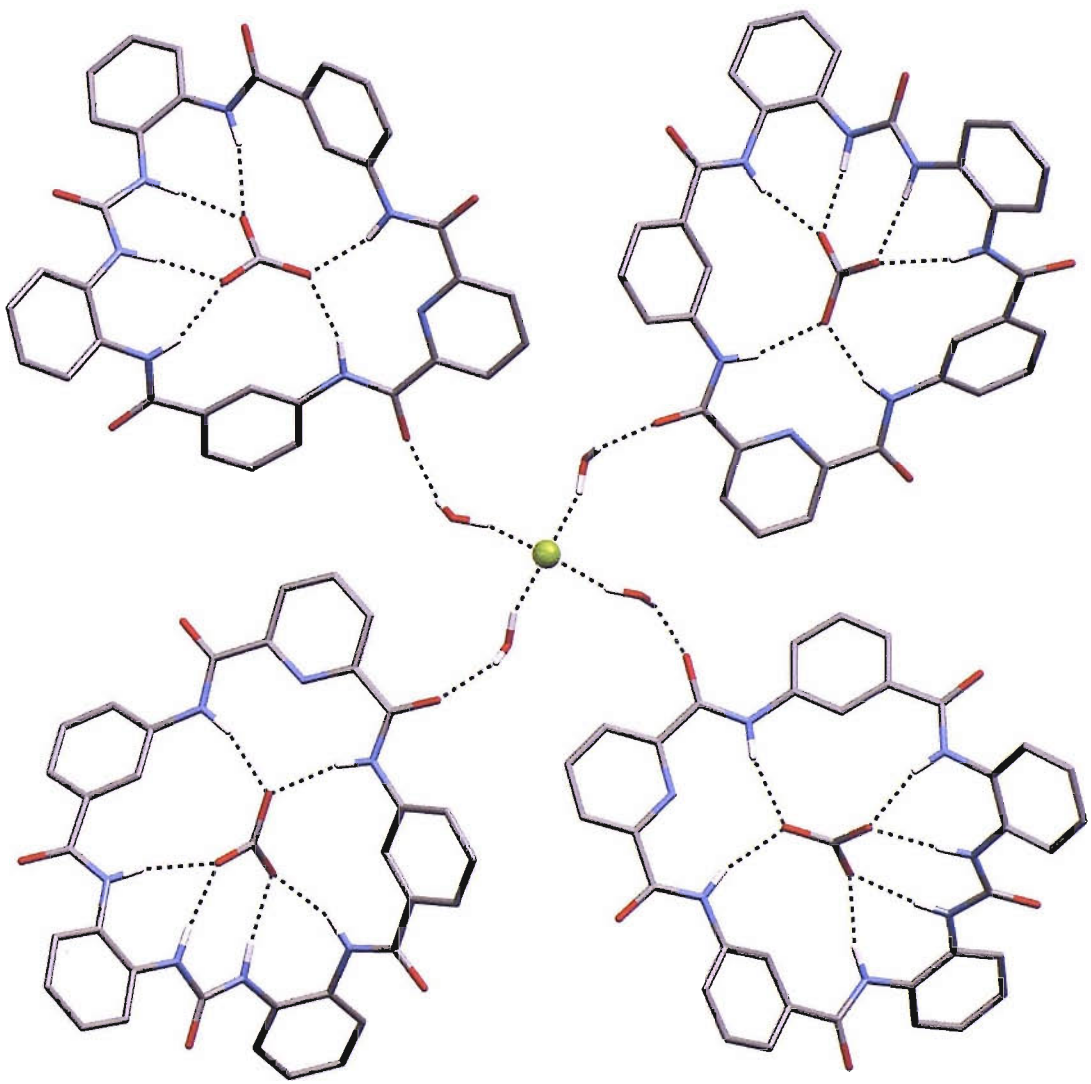

Fig 3.18: Charge parity is achieved by the inclusion of three TBA cations and one fluoride anion for every macrocyclic bound carbonate anion. Non-acidic hydrogen atoms are excluded for clarity.

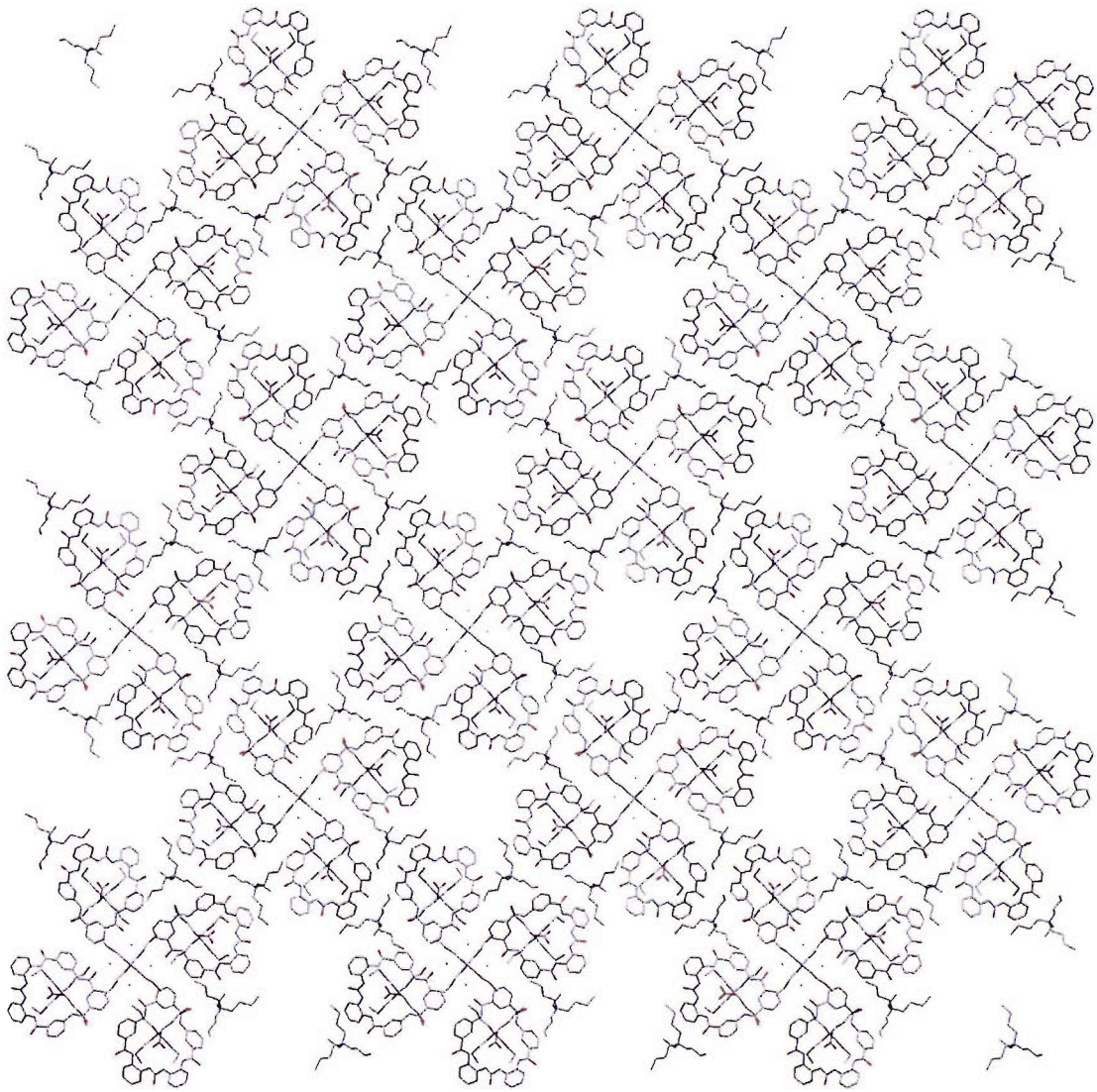

Fig. 3.19: Porous structure adopted by the **99** carbonate/fluoride extended crystal structure.

3.6. CONCLUSION.

A class of new amidourea anion receptors **94 - 96** has been synthesized and their anion coordination properties have been investigated by ^{1}H NMR titration techniques. The receptors reveal oxo-anion selectivity in particular for carboxylates and dihydrogen phosphate. Interestingly although the presence of one additional amide group does result in an increase in anion stability constants the improvement upon the addition of a second amide group is small. This suggests that the primary interaction between anion and the receptor occurs through the urea functionality. This conclusion is backed up by examination of the shifts of both the urea and amide protons during titrations that reveals that the urea protons shift significantly further during the titration.

Furthermore a new motif based upon amide appended isophthalamide **98** and pyridine-2,6-dicarboxamide **97** receptors has been investigated. Analysis of their anion coordination properties performed *via* the same method revealed generally weaker stability constants than the previously investigated. The presence of a central pyridine unit has been demonstrated to improve anion binding presumably through a combination of a greater acidity of the cleft amide protons and higher pre-organisation of the receptor into a binding conformation.

Novel macrocycle **99** has been synthesized using TBA acetate as both a method of solubilising the precursor into DCM solution and also a potential template for the macrocyclisation. Examination of the anion complexation properties indicates a significant improvement in the strength of carboxylate complexes in comparison to the acyclic fragments. A reduction in stability of complexes with dihydrogen phosphate when compared to the macrocyclic components reveal an improvement in phosphate / acetate selectivity by two-orders of magnitude.

Additionally in the presence of basic aqueous solution the receptor is able facilitate the fixation of atmospheric carbon dioxide in the form of carbonate. Further examination of this motif may provide new methods of controlling carbon dioxide levels under certain conditions or as a method of storage.

4. 1,3-ANTHRAQUINONE DERIVATIVES - ANION RECEPTORS AND ELECTROCHEMICAL SENSORS.

4.1 INTRODUCTION.

In Nature, quinones play a pivotal role in a variety of processes that include electron-proton transfer during oxidative phosphorylation and photosynthesis.[108,109] Extensive studies into the electrochemical behaviour of this redox system in the presence of various hydrogen bond donating solvents have been performed by numerous research groups.[110-112]

Generally it has been observed that quinone systems undergo two-step reduction and oxidation processes through the radical anion and dianion species (Fig 4.1). It has been shown that the electrochemical behaviour of the quinone system is largely dependent upon the nature of the solvent in which the studies are performed. In the case of acidic systems, protonation of the radical anion and the dianion can prevent the reversibility of the system, whilst the presence of strong hydrogen bond donor solvents such as methanol and ethanol have been observed to stabilise the reduced forms so that the reduction process is able to occur at more positive potentials.

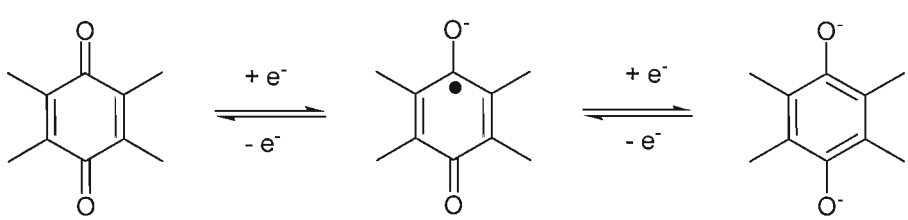

Fig 4.1: The reversibility of the quinone redox system through quinone (left), radical anion (centre) and dianion (right) has been employed by numerous systems in Nature.

Anion sensors based upon anthraquinone derivatives have been described in the literature and have been demonstrated to provide a reliable way of both binding anions, through the use of various appended hydrogen bond donor groups, and sensing anions through changes in UV/vis spectra or electrochemical properties. One of the earliest reported examples of anthraquinone being employed in an anion sensor was that by Martínez-Máñez and co-workers (Fig 4.2).[113] In this case substitution in both the 1- and 5 positions of the anthraquinone with urea **108** and thiourea **109** groups respectively yielded receptors that were observed to display selectivity for fluoride.

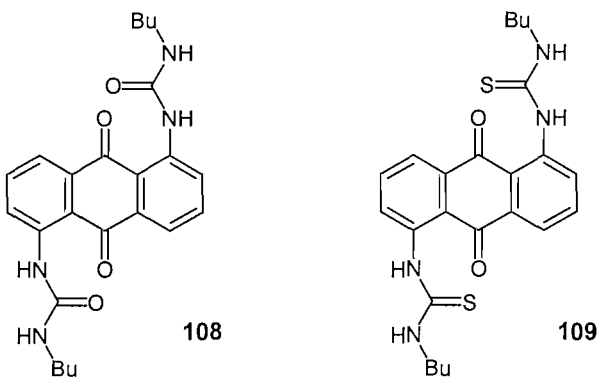

Fig 4.2: Martínez-Máñez's 1,5-diurea **108** and thiourea **109** anthraquinone based anion sensors.

Upon the introduction of 100 equivalents of anion to an acetonitrile solution of **108**, significant colour changes were observed for fluoride, dihydrogen phosphate, cyanide, acetate and benzoate. The addition of 10 equivalents of fluoride to an equivalent solution of **109** resulted in a colour change of orange to brown, with the appearance of a new band centred at 670 nm. Unfortunately attempts to calculate stability constants for the resulting complexes were unsuccessful due to the presumable coexistence of different anion-ligand stoichiometries in solution.

Nam and co-workers have investigated substitution in the 1- and 8 positions of the anthraquinone core, producing receptors based upon 1,8-diamino-4,5-dihydroxy anthraquinone and examined their anion binding affinities by ^{1}H NMR titration experiments performed in DMSO-d_6 (Fig 4.3).[114]

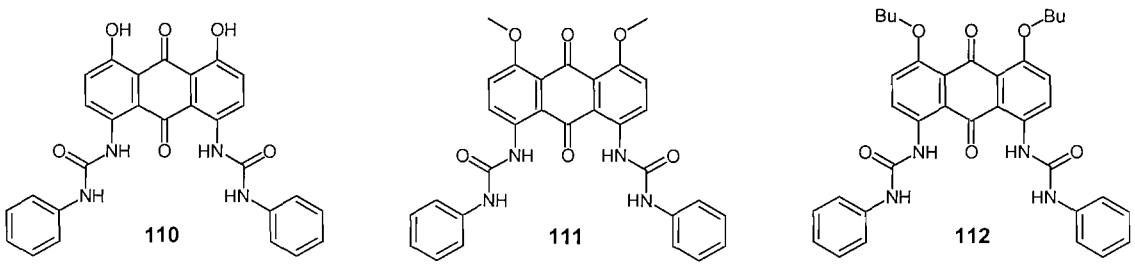

Fig 4.3: Nam's 1,5-diurea based anthraquinone receptors display a remarkable affinity for dihydrogen phosphate in DMSO/water mixtures.

Compounds **110-112** all display high association constants for dihydrogen phosphate with values of 11,000, 10,100 and 9830 M^{-1} determined respectively. Additionally acetate was found to bind strongly with both alkylated receptors **111** and **112** (5320 and 5100 M^{-1}). Interestingly **110** displayed an association constant an order of magnitude lower with acetate attributed to competitive deprotonation processes with the hydroxy protons. Analysis of these compounds *via* UV/vis experiments showed chromophoric shifts upon the addition of anions. Addition of acetate to a DMSO solution of **110** resulted in a colour change of purple to blue (λ_{max} 558 & 590 nm $\rightarrow$ 638 & 689 nm), with a similar colour change observed upon the addition of dihydrogen phosphate (λ_{max} 558 & 590 nm $\rightarrow$ 631 & 682 nm). Interestingly addition of weak bases such as triethylamine and pyridine caused similar shifts to those observed and as a result the colour changes of compound **110** could be attributed to proton abstraction rather than anion binding. A DMSO solution of **111** when exposed to acetate, chloride and hydrogen sulfate underwent no colour changes however addition of phosphate caused a shift in λ_{max} from 490 nm $\rightarrow$ 460 nm with an accompanied orange to pale yellow colour change. This unusual hypsochromic shift upon addition of anion has been attributed to the destabilisation of the electronically excited state relative to that of the ground state.

Analysis of the effects of anion binding upon the redox potentials of the anthraquinone system were subsequently performed by Nam and co-workers (Fig 4.4).[115] Electrochemical analysis of **113** revealed the typical two-step reduction and oxidation processes with the first reduction peak at -0.697 V followed by a second at -1.280 V. Upon the addition of dihydrogen phosphate, large cathodic shifts in the peaks were

observed, consistent with the formation of an anion complex, which overall has a net negative charge, therefore reducing the stability of the reduced species.

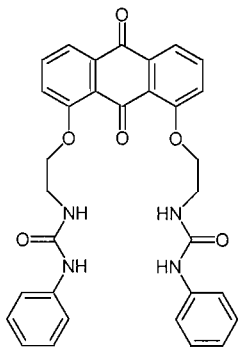

113

Fig 4.4: Compound **113** displays cathodic shifts of reduction and oxidation peaks upon addition with dihydrogen phosphate.

An alternative 1,2-disubstituted anthraquinone system has recently been explored by Das and co-workers (Fig 4.5).[116] Analysis of the anion binding behaviour displayed by these compounds was performed primarily using UV/vis spectroscopy methods. Addition of fluoride to a DMSO/acetonitrile (1:9 v/v) solution of **114** at room temperature resulted in no colour change even after a period of 24 h. However upon heating the solution to 60 °C, the solution took upon a pale red colouration.

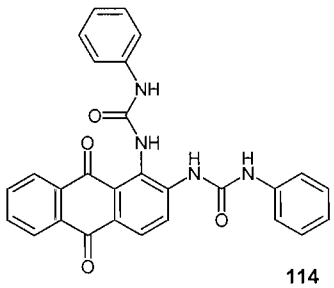

114

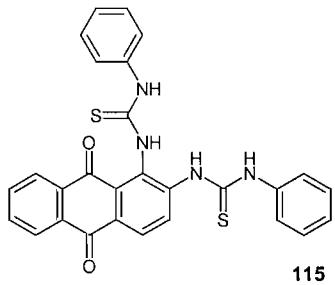

115

Fig 4.5: 1,2-diurea based anthraquinone derivatives.

UV/vis analysis of this phenomena revealed that the maximum at 422 nm disappears whilst a new peak at 530 nm appears, with two isosbestic points at 369 and 460 nm. Addition of alternative halide anions resulted in no colour changes. Addition of

fluoride to **115** at room temperature resulted in a sharp colour change (λ_{max} = 459 nm → 561 nm) with two isosbestic points once again being observed at 380 and 500 nm. Stoichiometry of the complex in solution was determined *via* Job plots performed at room temperature in DMSO/acetonitrile (1:9 v/v) in the presence of fluoride and revealed a 1:1 host/guest binding stoichiometry. Association constants for **114** and **115** with fluoride were determined *via* UV/vis titration data and gave values of 4.4×10^5 and 8.2×10^5 M^{-1} respectively.

Investigation into the affinity for oxo-anion of these compounds was later performed, with analysis of the binding constants with acetate, dihydrogen phosphate, benzoate and hydroxide performed once more in DMSO/acetonitrile (1:9 v/v) solution. [117] The results showed exceptionally high association constants with dihydrogen phosphate with 1:2 host guest stoichiometries observed for both compounds **114** and **115** (1.3×10^4 and 1.0×10^6 M^{-1} respectively).

4.2 1,3-ANTHRAQUINONEDICARBOXAMIDE ANION RECEPTORS.

4.2.1 SYNTHESIS AND CHARACTERISATION.

The synthesis of 1,3-anthraquinone-dicarboxylic acid was performed *via* literature procedures.[118] The production of the subsequent bis-amides were performed *via* reaction of the bis-acid chloride **117** with the appropriately substituted aniline, in the presence of triethylamine and a catalytic quantity of DMAP in DCM, with compounds **118-121** acquired in 43, 43, 36 and 6% respective yields (Scheme 4.1).

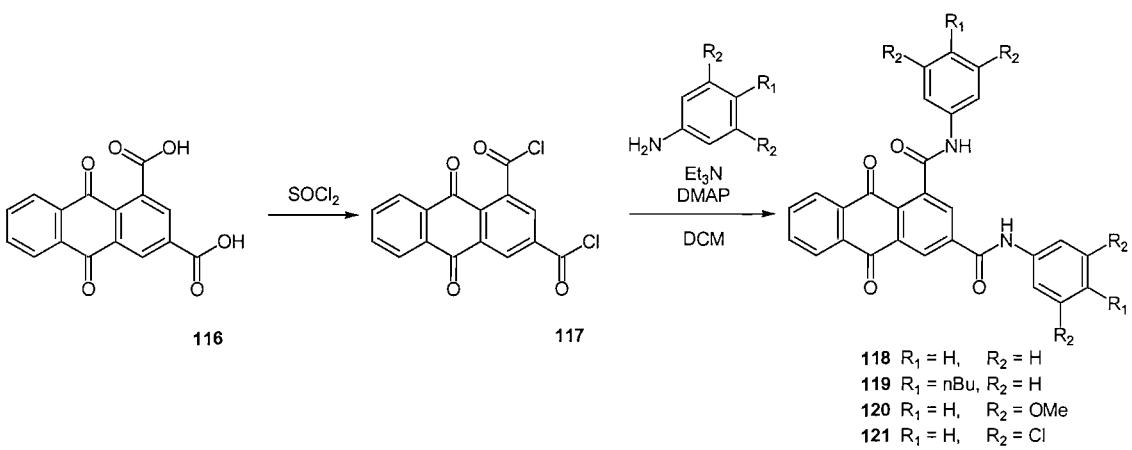

Scheme 4.1: Reaction scheme for the synthesis of 1,3-dicarboxamidoanthraquinone aryl derivatives.

All four compounds displayed poor solubility properties in organic solvents with the crude reaction product containing small quantities of mono-substituted amide side products. In order to remove the side products the remaining acid group was esterified by refluxing the product in acidic ethanol for 16 h and the remaining suspended bis-substituted product was removed by filtering the suspension whilst hot.

A more soluble derivative **122** was synthesized *via* an acid chloride condensation reaction between 1,3-anthraquinone dicarbonyl chloride **117** and *n*-butylamine **123** in the presence of triethylamine and DMAP in DCM, with **122** being isolated in 39% yield.

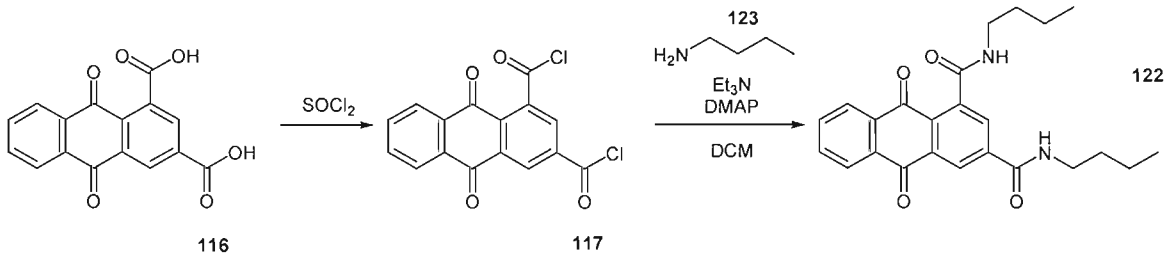

Scheme 4.2: Reaction scheme for the synthesis of compound **122**.

X-ray quality crystals of the DMSO solvate of **118** were obtained *via* slow evaporation of a saturated hot solution of **118** (Fig 4.6). The extended hydrogen bonded structure reveals the presence of hydrogen bonding through amide donor / acceptor interactions with both groups co-ordinated to an adjacent molecule with the result being the formation of a hydrogen bonded chain [N1···O3^{i} 2.922(3) Å & N2···O4^{i} 2.845(3) Å].

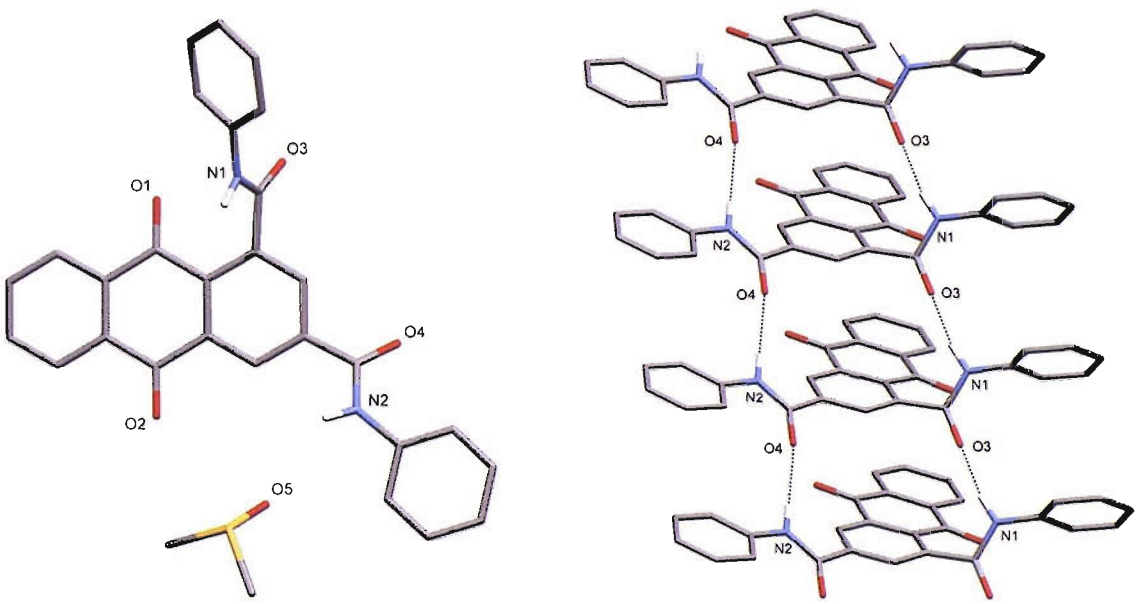

Fig 4.6: The solid state structure of **118** reveals extensive intermolecular hydrogen bonding. Non-acidic protons and in the case of the extended structure DMSO molecules omitted for clarity.

Crystals of **119** suitable for X-ray analysis were obtained *via* slow evaporation of a saturated acetonitrile solution (Fig 4.7). The structure reveals extensive intermolecular

amide donor / acceptor hydrogen bonds in which each of the hydrogen bonds is formed to a different adjacent molecule [N1···O4^{i} 2.863 Å & N2···O3^{ii} 2.838(4) Å]. An interesting feature of this structure is the out-of-plane deformation that the amide in the 1-position exhibits (≈ 80°) whilst the amide in the 3-position is essentially almost in plane relative to the anthraquinone aryl system.

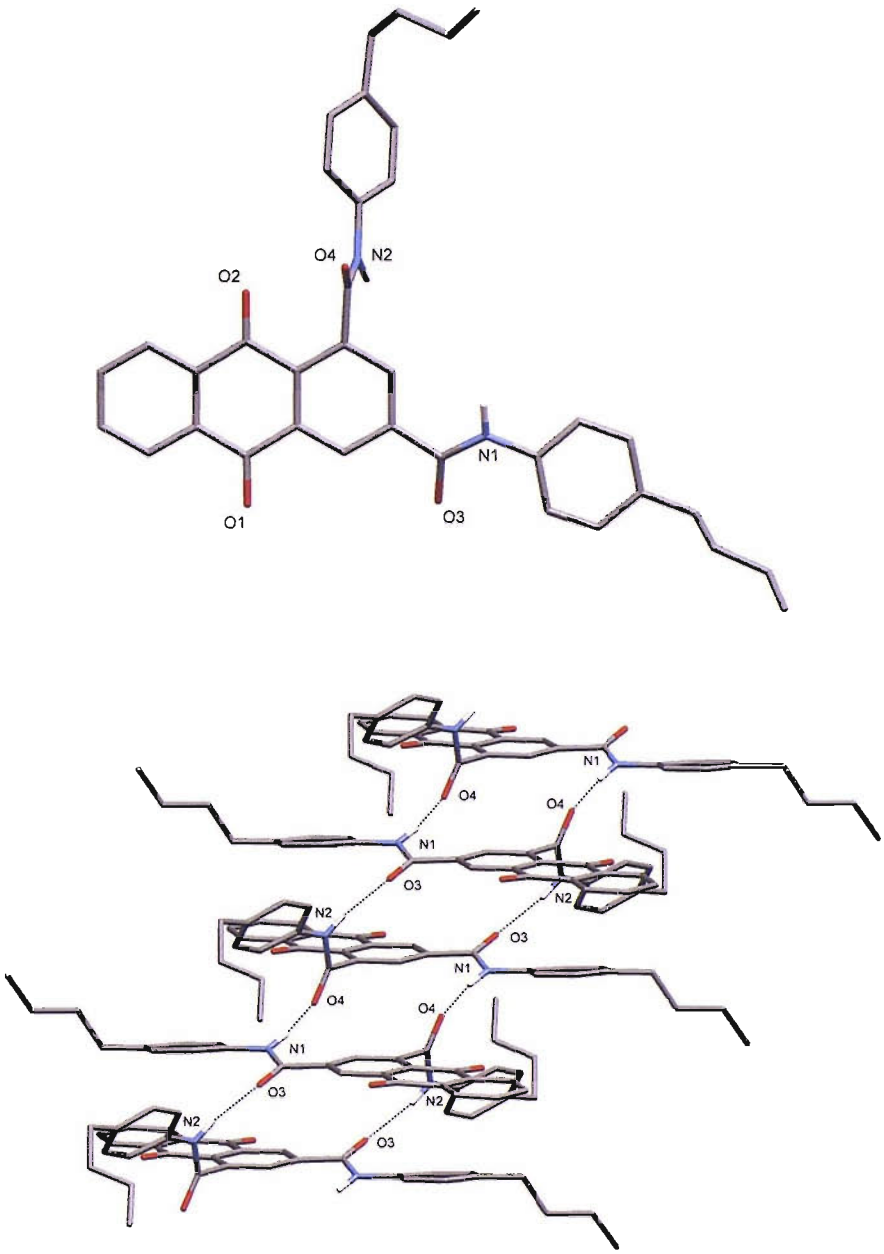

Fig 4.7: The amide in the 1-position of **119** adopts an almost perpendicular conformation from the anthraquinone system in the solid state. Non-acidic protons omitted for clarity.

Slow evaporation of a saturated acetonitrile solution of **120** yielded X-ray quality crystals (Fig 4.8). The unit cell in this case contains two crystallographically independent molecules of **120**. The molecules arrange themselves into a similar hydrogen bonding array as has previously been observed in the structure of **119** with extensive intermolecular hydrogen bonding present [N1···O14 2.851(5)Å, N3···O6 2.845(5) Å, N2···O3^{i} 2.942(5) Å & N4···O11^{ii} 2.877(5) Å].

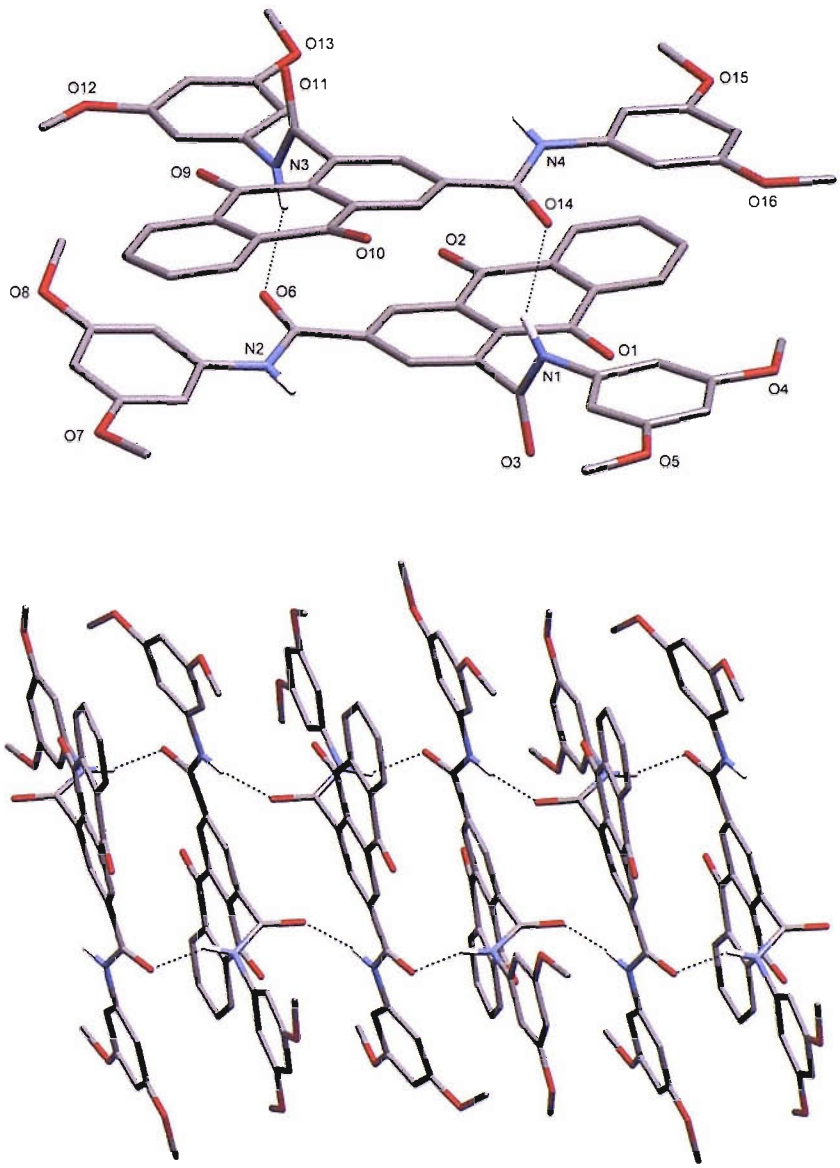

Fig 4.8: The unit cell of **120** contains two crystallographically independent molecules. Non-acidic protons omitted for clarity.

X-ray quality crystals of **122** were obtained *via* slow evaporation of a saturated acetonitrile solution of **122** (Fig 4.9). The presence of extensive hydrogen bonding is once more observed in this structure [N1···O4^{i} 2.8563(18) Å & N2···O3^{ii} 2.9006(18) Å], along with the out-of-plane geometry of the amide in the 1-position. The presence of this deformation provides evidence that the anthraquinone carbonyl group is providing steric interactions that cause a twisting of the amide cleft in these systems.

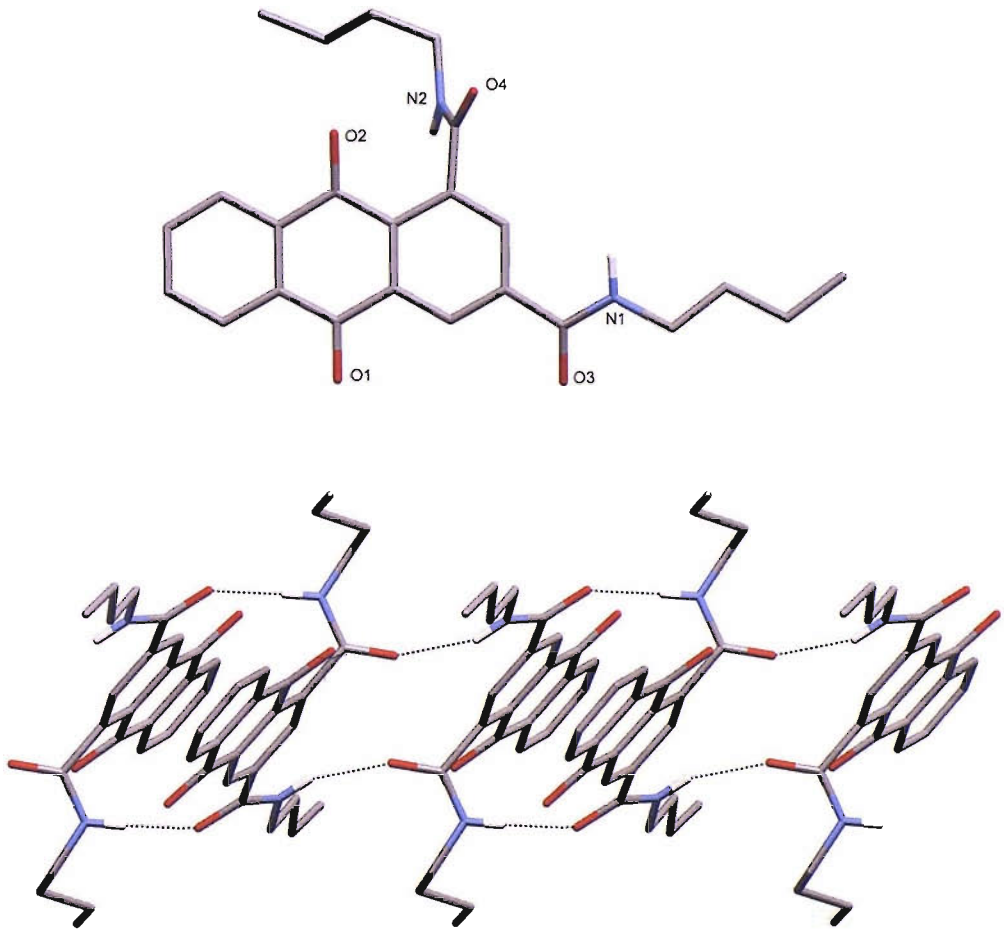

Fig 4.9: The extended hydrogen bonded structure of **122** reveals the formation of a hydrogen bonded chain in the solid state. Non-acidic protons omitted for clarity.

4.2.2. SOLUTION PHASE STUDIES.

4.2.2.1 ^{1}H NMR titration data.

In order to determine the strength of anion affinities for a variety of anions, ^{1}H NMR titration experiments were performed. A general lack of solubility of **118-121** meant that constants could only be determined in DMSO/water mixtures rather than less strongly coordinating solvents.

Table 4.1: Association constants for compounds **118-121** in DMSO/0.5% H_2O at 298 K were determined *via* ^{1}H NMR titration techniques (M^{-1}). All binding stoichiometries unless otherwise stated were 1:1 with binding curves fitted using WINEQNMR.[92] Anions titrated in the form of the TBA salt with all errors < 15%.

Anion	118	119	120	121
Chloride	-	<10	-	13
Dihydrogen Phosphate	198	120	214	$K_1 = 1520$, $K_2 = 65$
Acetate	30	24	35	-[a]
Benzoate	17	15	26	160

Titrations with bromide and hydrogen sulfate gave no change in ^{1}H NMR signals indicating interactions too weak to be determined *via* this technique. Titration with fluoride gave complicated curves that could not be fitted to a binding model and may arise from deprotonation of the amide group.

Overall the determined anion constants and selectivity arising from these values are broadly similar for compounds **118 - 120** indicating that these compounds are likely to co-ordinate anions in the same manner. The presence of the electron-donating methoxy groups of compound **120** appears to have little effect upon the anion binding relative to non-functionalized compound **118**, with an expected reduction in binding affinity resulting from less basic amide protons not observed. Compound **119**

incorporates electron-donating alkyl substituents onto the pendent aryl rings, resulting in an observable reduction in the anion binding.

The introduction of electron withdrawing chlorine substituents onto the pendent aryl groups in the 3- and 5-positions in compound **121** has a significant beneficial effect upon the anion affinity of the motif. The chemical shift of the amide NH protons of **121** (11.00 & 10.77 ppm) can be used to determine their comparative acidity when compared to non-functionalized receptor **118** (10.75 & 10.37 ppm). The downfield shift of these protons therefore is a reflection of their enhanced acidity, increasing their ability in the formation of anion / receptor hydrogen bonds.

An increase of an order of magnitude is observed for benzoate with **121** whilst a significant improvement in association with dihydrogen phosphate is observed with 1:2 host/guest binding stoichiometry determined. In the case of acetate, detection of new peaks during the titration meant that the data could not be satisfactorily fitted to a binding model and may indicate a deprotonation process due to the enhanced acidity of the amide NH groups. The oxo-anion selectivity that is observed in these systems could be due to the twisted nature of the amide cleft resulting in a less convergent hydrogen bonding array (Fig 4.10). In this case the amide NH groups adopt a more parallel hydrogen bonding array that a more suitable for oxo-anion binding.

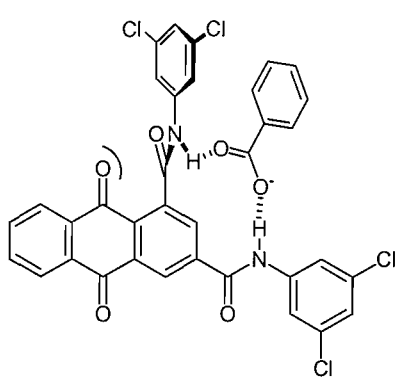

Fig 4.10: Potential binding mode of **121** with benzoate arising from twisting of the amide cleft.

The bis-butylamide derivative **122** was titrated in CD_2Cl_2 in order to allow a more accurate determination of *oxo*-anion selectivity by allowing comparison with halide

anions, given that the interactions with halides in DMSO-d_6 were too weak to allow association constants to be determined.

Table 4.2: : Association constants for compounds **122** in CD_2Cl_2 at 298 K were determined *via* ^1H NMR titration techniques (M^{-1}). All binding stoichiometries unless otherwise stated were 1:1 with binding curves fitted using WINEQNMR.[92] Anions titrated in the form of the TBA salt with all errors < 15%.

Anion	**122**
Chloride	127
Bromide	69
Hydrogen Sulfate	31
Dihydrogen Phosphate	93
Acetate	247
Benzoate	181

Examining the binding association in non-polar solvents allows the measurement of constants for halides, in which the interaction in DMSO is too low to be determined. Unfortunately titration of fluoride gave titration curves that could not be fitted to a binding model. In this solvent mixture there is a relatively large increase in the ability of the receptor motif to co-ordinate both chloride and bromide anions. Chloride in particular is found to bind more strongly than dihydrogen phosphate, the most strongly co-ordinated anion in DMSO, however as there is also a decrease in phosphate binding in this titration, this effect could be largely the result differing solvation properties in this system.

Both carboxylate anions that were investigated displayed enhanced binding properties relative to the more competitive DMSO conditions, with the motif retaining oxo-anion selectivity in this less competitive solvent mixture.

4.2.2.2. Electrochemical experiments.

Electrochemical studies in this section were performed in collaboration with Dr P. Birkin of the Electrochemistry Department at the University of Southampton.

As outlined previously, Nam and co-workers have demonstrated that upon addition of coordinating anions to a redox active anthraquinone-based anion receptor, cathodic peak shifts are observed, consistent with the formation of a negatively charged complex which is more difficult to reduce.[118]

We therefore wished to investigate the effect of the introduction of coordinating anions upon the peak shift of the anthraquinone-1,3-dicarboxamide redox system. Any peak shifts that would be observed could offer a method for the electrochemical sensing of anions.

Initially we investigated the redox properties of non-functionalized anthraquinone in DMSO solution and revealed that two single-step reduction processes could be detected (**A** and **B**) at -1.32 and -2.03 V.

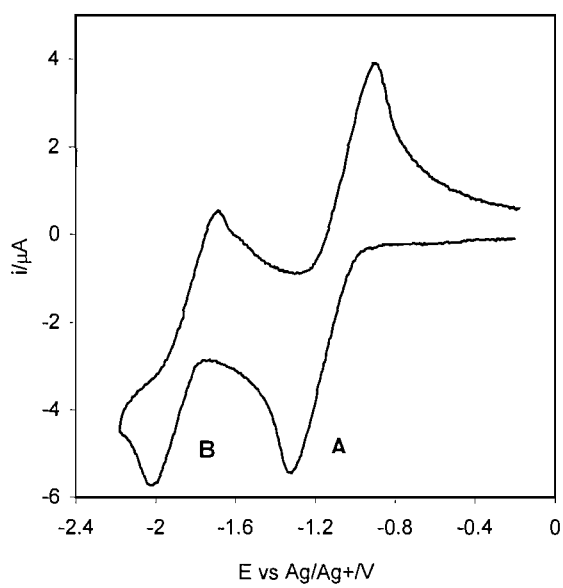

Fig 4.11: Plot showing the CV recorded for a 1 mmol dm-3 solution of anthraquinone. Voltammogram recorded in a 0.1 mmol dm^{-3} $TBAPF_6$/DMSO electrolyte at a 3 mm diameter glassy carbon electrode. The data was recorded at a sweep rate of 50 mVs. Reference electrode = $Ag/AgNO_3$.

Subsequently investigations under the same conditions were performed using **118** in order to determine the effect that the presence of the anion binding unit has upon the electrochemical behaviour of the system.

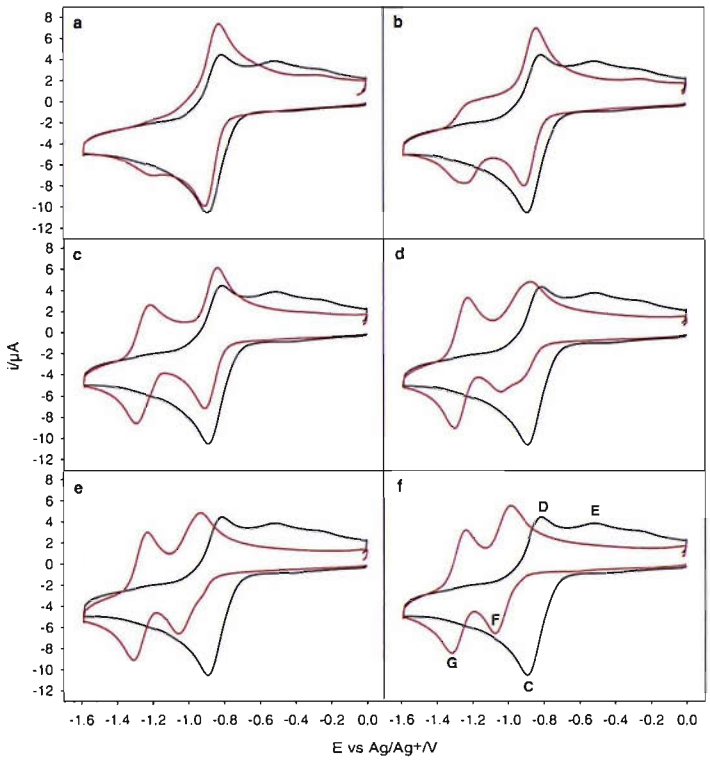

Fig 4.12: Plot showing the CVs recorded for a 1 mmol dm^{-3} solution of **118** (black line) and 1 mmol dm^{-3} solution of **118** (red line) in the presence of 2.0, 3.9, 5.8, 10.1, 15.2 and 20.4 equivalents of fluoride for plots (a)-(f) respectively. All voltammograms were recorded in a 0.1 mmol dm^{-3} $TBAPF_6$/DMSO electrolyte at a 3 mm diameter glassy carbon electrode. The data was recorded at a sweep rate of 50 mVs. Reference electrode = $Ag/AgNO_3$.

In the absence of coordinating anions, the CV (Fig 4.12) reveals behaviour that is atypical of the usual two-step reduction that characterizes anthraquinone electrochemistry. Reduction of the compound down to -1.60 V reveals only one sharp peak, whilst scanning the potential lower than this only reveals signals that correspond to the electrochemical decomposition of the solvent, therefore only the window 0.00 V → -1.60 V was used during these experiments.

A single reduction peak, labelled **C** in frame (f) on the cathodic sweep is followed by two subsequent oxidation peaks (labelled **D** and **E** respectively) on the anodic sweep. This unusual behaviour is in contrast to that observed previously of quinone species in DMSO, in which typically two separate redox species can be detected, attributed to two single-electron redox steps.

The difference from the data in the literature regarding quinone reductive behaviour, combined with the fact that the typical two-peak redox system can be observed upon the addition of fluoride, to be discussed later, and the fact that the integral value of the single reduction peak is twice that of the two oxidation peaks, strongly indicates that the behaviour exhibited in this system is much more complex.

In the few cases where similar electrochemical behaviour has been reported it has been in the presence of strong proton donor agents, such as methanol, however in this case this seems an unlikely step considering the conditions employed.[111]

The hypothesis to explain this unusual electrochemical behaviour is caused by the formation of strong intramolecular or intermolecular hydrogen bonding interactions (Fig 4.13). These interactions would provide stabilising interactions for the quinone system and both are possible in solution.

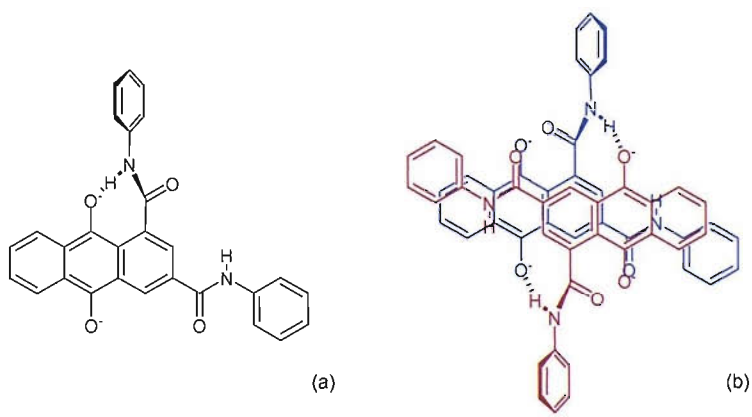

Fig 4.13: Potential stabilizing interactions through the formation of either intramolecular (a) or intermolecular (b) hydrogen bonds.

An intramolecular stabilisation effect is available for both the semi-reduced radical anion and the fully reduced dianion, however the electrochemical evidence appears to show that the dianion is stabilized by this effect to a greater degree. It is

therefore possible to propose two mechanisms that can account for the cathodic behaviour observed, either an ECE or a DISP type mechanism could be responsible for the reduction step. If an ECE type mechanism is considered then the reduction could proceed via an initial reduction step, followed separately by a conformational rearrangement resulting in stabilisation through the formation of a hydrogen bond to the quinone group. This stabilised species would act differently in solution to its non-stabilized conformer and would likely see the second reduction occur at a much more positive potential.

A = neutral anthraquinone receptor.

1) $A + e^- \leftrightarrow A^{\bullet -}$

2) $A^{\bullet -} \leftrightarrow A^{\bullet -}(NH)$

3) $A^{\bullet -}(NH) + e^- \leftrightarrow A^{2-}(NH)$

Addition of fluoride to the solution appears to result in disruption of the system through the removal of the stabilizing intramolecular hydrogen bonding interactions. Frame (a)-(f) in Fig 4.12 show the effect of increasing fluoride concentration (red) against the original, anion free situation (black).

Table 4.1: The potential of the peaks observed as a function of fluoride concentration.

[Fluoride] (mmol)dm^{-3}	Equivalents	$-E^1_{pc}$ (V vs. Ag/Ag^+)	$-E^2_{pc}$ (V vs. Ag/Ag^+)
0.0	0.0	0.898	-[a]
2.0	2.0	0.913	1.199
3.9	3.9	0.913	1.241
5.9	5.8	0.915	1.299
10.2	10.1	1.047	1.306
15.4	15.2	1.060	1.310
20.6	20.4	1.078	1.320

[a] The second reduction peak only became observable following the first addition of TBA fluoride.

Following the addition of approximately six equivalents of fluoride (Table 4.1), the CV has taken the typical appearance expected for anthraquinone redox systems, with two separate reduction (first reduction = E^1_{pc} and second reduction = E^2_{pc}) and oxidation peaks observable, with the integral of each reduction peak approximately equal to half that of the original reduction peak observed in the absence of fluoride.

Addition of further equivalents of fluoride results in the peak potentials shifting to more negative potentials, behaviour consistent with the increased difficulty expected for reducing a complex that already possesses a net negative charge in comparison to the reduction of a neutral receptor.

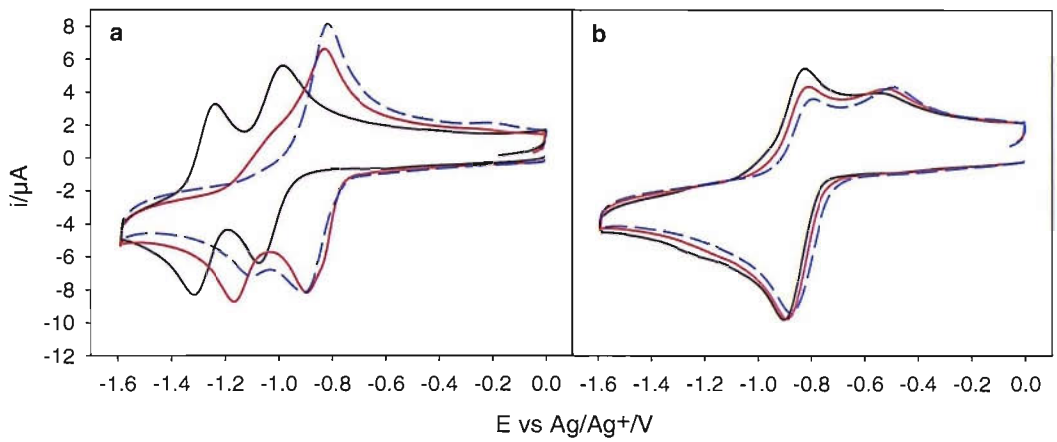

Fig 4.14: Plot showing the CVs recorded for: (a) 1mmol dm^{-3} solution of **118** in the presence of 20.4 equivalents of fluoride and (b) 1 mmol dm^{-3} of **118** alone as a function of varying ethanol concentration (0 (black), 1.78 (red) and 3.84 (blue) M). All voltammograms were recorded in a 0.1 mmol dm^{-3} $TBAPF_6$/DMSO electrolyte at a 3 mm diameter glassy carbon electrode. The data was recorded at a sweep rate of 50 mVs. Reference electrode = $Ag/AgNO_3$.

Previous electrochemical experiments into the anthraquinone species revealed that the addition of a proton-donating solvent such as ethanol can act so as to stabilize the reduced semiquinone and dianion *via* intermolecular hydrogen bonding. Therefore we decided to investigate the observable effects of this phenomenon in the case of both the free ligand, and in the case of a solution containing the ligand and excess TBA fluoride (Fig 4.14).

Upon addition of ethanol to a solution of **118** in the presence of excess TBA fluoride (**a**), the electrochemistry of the **118** begins to revert back to that observed in the absence of fluoride. This effect could arise from the introduction of either additional hydrogen bonding to the quinone oxygen atoms due to the nature of the ethanol or arise from sequestering of the fluoride ions by the ethanol itself. This second effect would allow the reformation of stabilising NH hydrogen bonds.

In the case of a solution **118** in the absence of fluoride (**b**), the addition of ethanol has a much less dramatic effect, however a small but noticeable shift in the potential of the reduction peak is observed. This movement is towards more positive potentials and is consistent with the presence of additional hydrogen bonding between the solvent and the receptor that can act to stabilize the reduced forms, making the reduction process able to occur at less negative potentials.

4.2.3. SOLID STATE BEHAVIOUR

Slow evaporation of a DMSO solution of **121** in the presence of excess TBA fluoride yielded X-ray quality crystals of the fluoride complex of **121** (Fig 4.15). An interesting dimeric structure is observed in the solid state in which the fluoride anions are separated by 5.37 Å and are bound by hydrogen bonding interactions from both of the receptor molecules.

Two hydrogen bonds from each receptor molecule to the respective fluoride anions are observed [N1···F1 2.577(7) Å, N4···F1 2.594(7) Å, N2···F2 2.615 (6) Å & N3···F2 2.574(6) Å]. Additionally there are also a total of four potential aryl CH hydrogen bonds [C17···F1 2.789(8) Å, C41···F1 3.034(8) Å, C24···F2 3.061(7) Å & C13···F2 3.062 Å] with the acidic protons from both the electron-deficient anthraquinone system and pendent aryl groups involved.

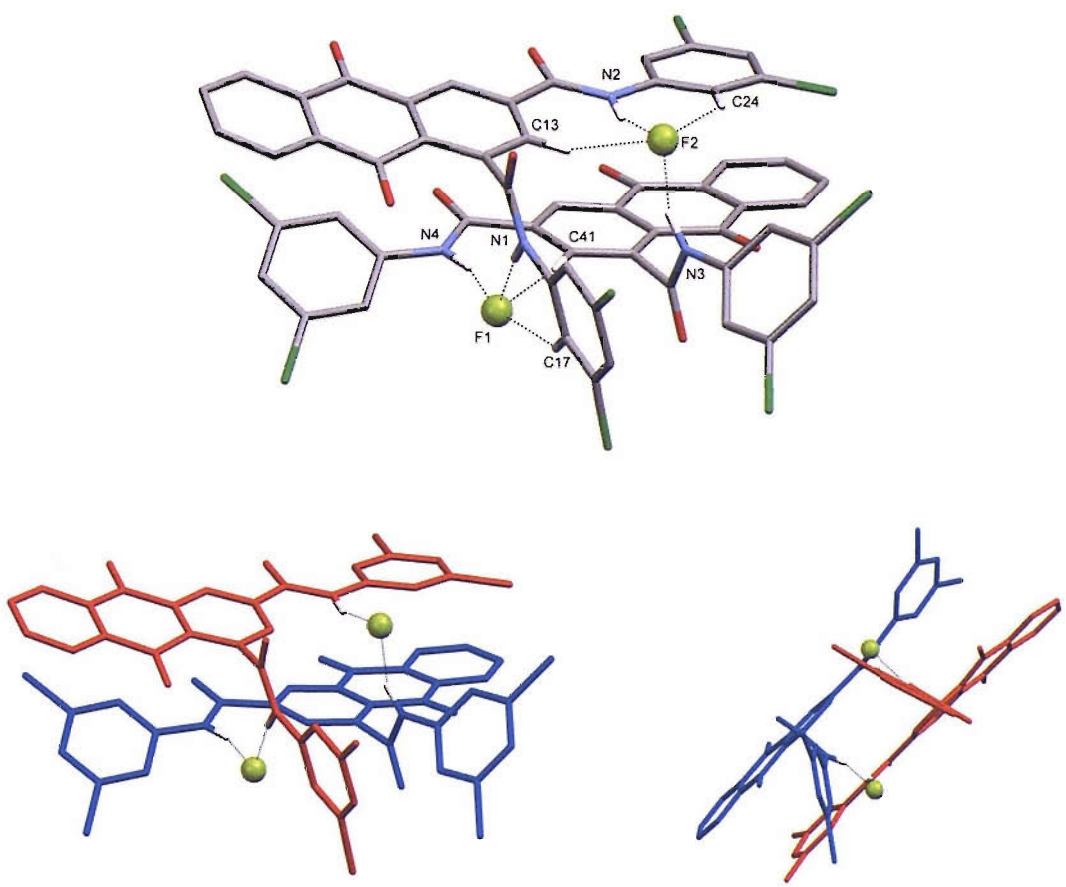

Fig 4.15: The fluoride complex of **121**. Non-acidic protons and TBA counter ions omitted for clarity.

4.3. CONCLUSION.

A new class of anthraquinone-based receptors **118-122** that incorporate amide cleft anion binding sites have been synthesized and their anion-binding properties have been investigated *via* ^{1}H NMR titration techniques.

In DMSO the receptors **118-121** displayed generally weak interactions with anions, with selectivity for phosphate observed in comparison to carboxylates. The introduction of electron-withdrawing substituents onto the receptor **121** was shown to significantly enhance the ability of the receptor to co-ordinate anions, however the increase in acidity may lead to deprotonation of the receptor in solution upon the addition of sufficiently basic anions such as acetate.

Determination of stability constants of butylamide derivative **122** was performed in more weakly coordinating DCM solution. In this solvent the presence of halide binding could be determined and was shown to be enhanced relative to oxo-anion binding. Whilst dihydrogen phosphate was observed to co-ordinate more weakly in this system higher association constants for carboxylates could be observed.

Evaluation of the electrochemical properties of **118** were obtained *via* cyclic voltammetry experiments performed in DMSO and revealed that an unusual hydrogen bonded stabilized system was formed upon the electrochemical reduction. Upon the addition of fluoride, this hydrogen bond is sequestered through interactions with the more basic anion and a typical two step reduction process for the anthraquinone system is revealed.

X-ray structure determination of the fluoride complex of **121** reveals the presence of a 2+2 hydrogen bonded dimer in which both of the receptor molecules co-ordinate to the two fluoride anions.

Future analysis of anthraquinone systems is likely to produce more strongly coordinating receptors for anions whilst finding new methods of protecting the anthraquinone system from solvent and hydrogen bonding events is likely to make receptors based upon this system more simple to interpret and produce more viable electrochemical sensors.

5. ANTHRACENE BASED ANION SENSORS: SELECTIVITY THROUGH HYDROGEN BONDING MOTIF VARIATION.

5.1 INTRODUCTION.

Changes in the fluorescence emission of an anion sensor that incorporates a fluorophore into its structure upon anion recognition, has provided the anion coordination chemist with a highly efficient and sensitive tool for determining the presence and concentration of anions.[119-121] A commonly used fluorophore is anthracene, due in part to the synthetic accessibility of derivatives that possess a variety of substitution patterns. This versatility allows various anion binding motifs to be appended from the anthracene scaffold.

Derivatization through the 1- and 8-positions of the anthracene group has allowed Kim and Yoon to develop a number of novel anion binding receptors in which the binding sites are separated from the anthracene unit through methylene bridging units. These sensors display not only interesting anion binding properties but also significant fluorescence quenching upon anion coordination (Fig 5.1).[122]

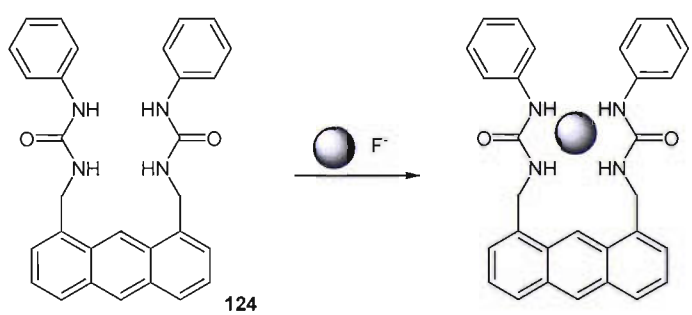

124

Fig 5.1: *Bis*-urea anthracene receptor **124** displays high selectivity for fluoride anions.

Bis-urea based anion receptor **124** was synthesized in a simple reaction between the diamine and phenylisocyanate in 72% yield. The anion binding properties of receptor **124** with halide anions were investigated *via* analysis of fluorescence quenching upon addition of the anion, performed in acetonitrile: DMSO (9:1) solution. These studies revealed that the receptor showed a high selectivity for fluoride with a stability constant of 71,270 M^{-1} obtained while the subsequently most strongly bound anion, chloride, displayed a constant of 614 M^{-1}, a reduction by a factor of 100. A 1:1 binding stoichiometry was observed between **124** and fluoride, with a probable binding mode involving all four urea NH groups coordinating to the anion.

An alternative approach using the same 1,8-substitution pattern was further exploited by Yoon and Kim. In this case the anion-receptor interaction was supplied by introducing imidazolium residues in which the strong $(C\text{-}H)^{+}\cdots X^{-}$ charged hydrogen bonding interaction between the moiety and the anion is employed as an anion binding mode (Fig 5.2). The syntheses of both acyclic **125** and cyclic **126** imidazolium derivatives have been reported, with the macrocyclic derivative reported in notably high yield.[76,123] The more rigid nature of the macrocyclic receptor **126**, would it was hoped result in a conformationally locked, highly preorganised receptor that would display enhanced stability constants in comparison with its acyclic analogue.

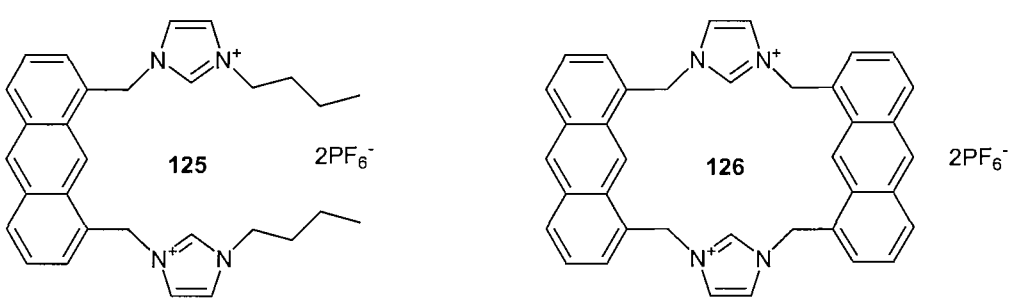

Fig 5.2: Kim and Yoon's imidazolium based sensors **125** and **126** coordinate anions through charged hydrogen bond interactions with the imidazolium CH.

The anion binding properties of receptors **125** and **126** were elucidated through both fluorescence titration experiments and ^{1}H NMR experiments which were performed in acetonitrile:DMSO (9:1) and actonitrile-d_3:DMSO-d_6 (9:1) respectively. These

experiments revealed that specifically in the case of macrocyclic **126**, dihydrogen phosphate selectivity was observed for which a stability constant of 1.3×10^6 M^{-1} was reported, reflecting a 200-fold selectivity over the other anions reported.

Significant advances in the area of PET chemosensors for anions that employ anthracene as the fluorophore, have been made by Gunnlaugsson and co-workers (Fig 5.3).[46,124-126] Most significantly functionalisation of the 9- and 10-positions of the anthracene group through methylene linkages has allowed the development of sensor design that incorporates a *receptor-spacer-fluorophore-spacer-receptor* motif. This design has successfully been demonstrated to bind complex anions, which have two separate binding sites in solution.

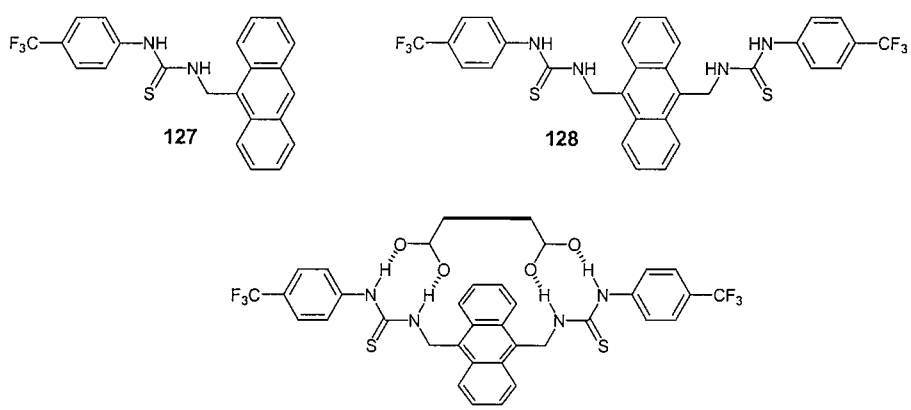

Fig 5.3: Gunnlaugsson's 9 and 9,10 functionalised anthracene receptors **127** and **128** and the bridging hydrogen bonding motif for anions such as dicarboxylates and pyrophosphate.

Both **127** and **128** can coordinate anions through the pendent thiourea groups, whilst additionally the presence of electron-deficient pendent aryl groups is intended to increase the acidity of the NH protons and therefore allow stronger anion – receptor interactions. The mono-functionalised sensor **127** displays a significant affinity for acetate typical with the 1:1 anion / receptor interaction that typifies carboxylate – thiourea interactions. Receptor **128** displays enhanced binding of dicarboxylates and pyrophosphate in comparison to mono-functionalized **127**, behaviour consistent with the formation of cooperative simultaneous binding through both of the thiourea binding sites.

A further development in the use 9-functionalized anthracene units has been demonstrated by Suzuki and co-workers. Tripodal receptor **130** was produced in an attempt to determine whether strong affinities with tripodal anions such as dihydrogen phosphate would be observed with potential interactions between each of the thiourea groups and three of the oxygen atoms of the anion (Fig 5.4).[127]

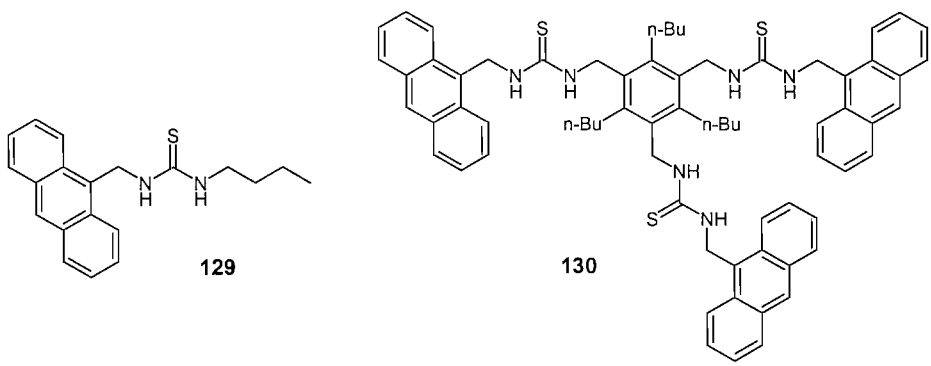

Fig 5.4: Suzuki and co-worker's synthesized a tripodal receptor **130** utilising fluorophore sensing.

Stability constants for compound **130** were determined *via* UV/vis titration performed in acetonitrile, revealing that dihydrogen phosphate binds with a constant of 1.9×10^4 M^{-1} and acetate with a value of 1.4×10^4 M^{-1}.

In comparison to its component fragment **129**, these values indicated a significant increase in stability constants (c.f. 6.7×10^2 & 2.9×10^3 M^{-1} for phosphate and acetate respectively) whilst also an increase in phosphate selectivity over acetate, consistent with the formation of a tripodal binding mode of **130** with dihydrogen phosphate in this system. This behaviour was also reflected in the fluorescence spectra with significant reduction in fluorescence emission of **130** only observed upon the addition of dihydrogen phosphate.

5.2 ANTHRACENE-DICARBOXAMIDO CLEFTS.

The appendage of NH donor groups from differing positions about the anthracene core has been demonstrated to produce varying selectivities that are dependent upon the binding conformation that the coordinating groups can adopt. In previous chapters we had investigated both the effects of 'twisting' an isophthalamide type amide cleft through in the introduction of additional steric effects as well as the anion binding properties of receptors based upon 1,2-phenylenediamine.

We wished to gain a more direct comparison into the anion complexation properties of both isophthalamide and 1,2-phenylenediamine type clefts to allow insight into the differing selectivities and strength of complex that each motif would afford. Therefore bis-amide receptors based upon 1,3-anthracene (to produce amide cleft type receptors) and 1,2-anthracene were synthesized.

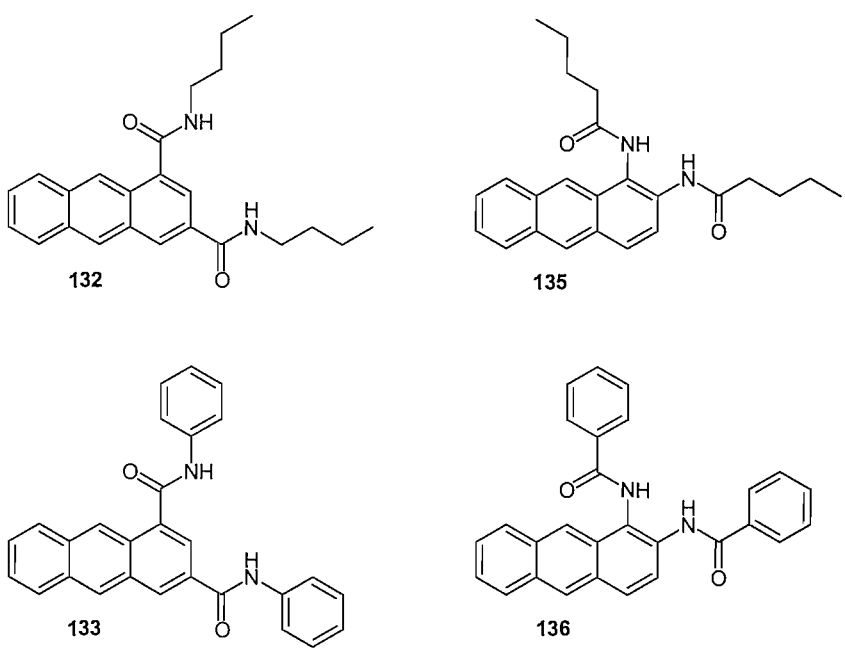

Fig 5.5: 1,2- and 1,3 anthracene bis-amide based receptors.

5.2.1 SYNTHESIS AND CHARACTERISATION.

Two new anthracene diamide clefts **132** and **133** have been synthesised (Scheme 5.1). Diethyl anthracene-1,3-dicarboxylate **131** was prepared following literature procedures,[117, 128] and was reacted with a slight excess of either *n*-butylamine or aniline in the presence trimethylaluminium solution in dry DCM to afford the desired products **132** and **133** in 32 and 82 % respective yields.

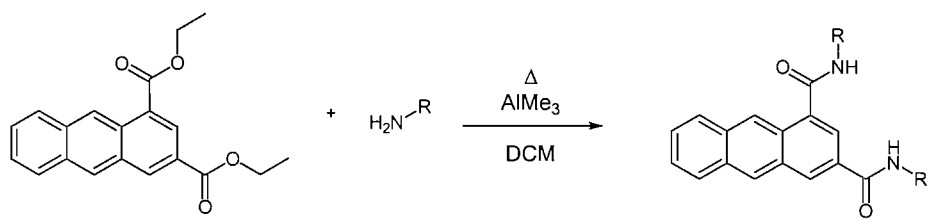

Scheme 5.1: Synthesis of 1,3-dicarboxamidoanthracene receptors **132** and **133**.

Two additional anthracene diamide clefts **135** and **136** in which the amide is attached to the anthracene moiety through the 1 and 2 positions were also synthesised (Scheme 5.2). 1,2-Diaminoanthracene **134** was prepared through reduction of 1,2-diaminoanthraquinone in the presence of excess sodium borohydride. Reaction of diamine **134** with a slight excess of either valeroyl chloride or benzoyl chloride in the presence of DMAP and triethylamine afforded **135** and **136** in 39 and 82 % yields respectively.

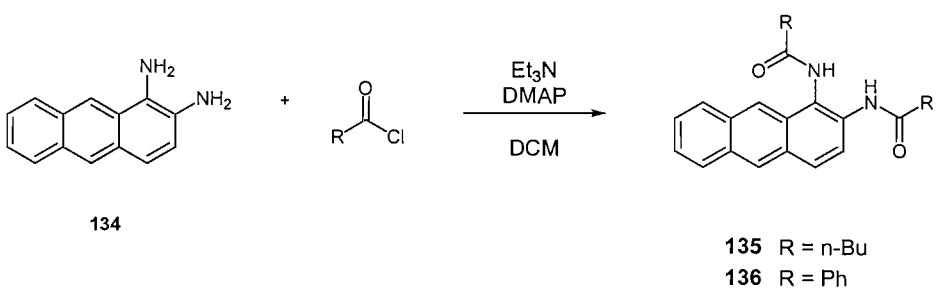

Scheme 5.2: Synthesis of 1,2-dicarboxamidoanthracene receptors **135** and **136**.

Slow evaporation of an ethanol solution of **135** afforded X-ray quality crystals of **135** (Figure 5.5). The structure reveals intermolecular hydrogen bonding between adjacent receptor molecules through amide donor-acceptor interactions [N1···O1^{i} 2.8441(19) Å & N2···O2^{i} 2.910(2) Å] with both interactions in the same direction.

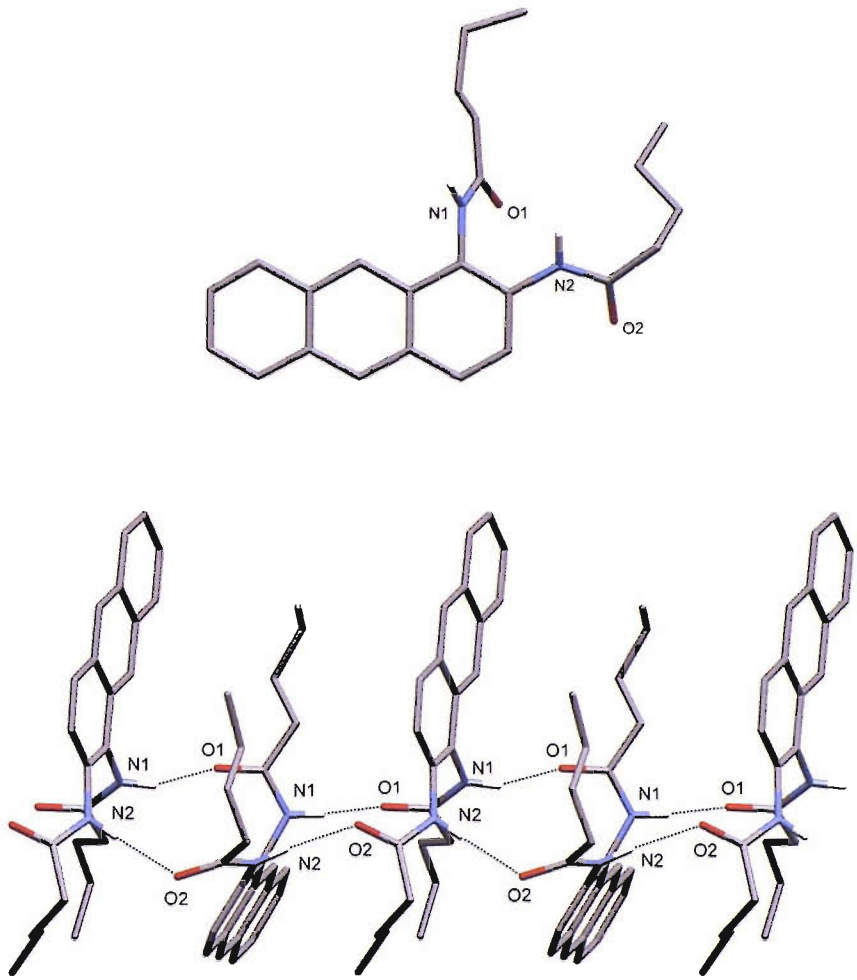

Fig 5.6: The solid state structure of **135** obtained from ethanol solution, reveals extensive hydrogen bonding interactions in the solid state. Non-acidic protons omitted for clarity.

5.2.2 SOLUTION PHASE ANALYSIS.

5.2.2.1. ^{1}H NMR titration data.

The presence of appended alkyl chains in both receptors **132** and **135** facilitated study of their anion binding properties in weakly coordinating DCM-d_2 solution (Table 5.1). Due to the lower competitive nature of this solvent mixture relative to DMSO/water mixtures, stability constants with a variety of anions, such as bromide and hydrogen sulfate, for which stability constants are difficult to obtain, could be elucidated.

Table 5.1: Anion stability constants for compounds **132** and **135** were determined in DCM-d_2 solution at 298 K (M^{-1}). Anions titrated in the form of their TBA salts. All data fitted to a 1:1 binding model using WINEQNMR.[92] All errors < 15%.

Anion	132	135
Chloride	257	238
Bromide	92	67
Hydrogen Sulfate	16	14
Dihydrogen Phosphate	52	128
Benzoate	173	709

Titrations were performed with fluoride, however unfortunately the data could not be fitted to a binding model.

As might be expected the two anion binding motifs display differing selectivities that reflect different anion binding conformations that each receptor can adopt (Fig 5.7). The amide NH groups of receptor **132** are able to form arrays in the form of those exhibited by isophthalamide derivatives. The convergent arrangement of the NH groups make them highly suitable for coordination of small singly charged anions such as halides.

This effect is reflected in the observed stability constants for **132** with both chloride and bromide being bound relatively strongly by the receptor. In comparison

both hydrogen sulfate and dihydrogen phosphate interact relatively weakly, whilst benzoate is bound more weakly than chloride.

In comparison the amide NH groups of compound **135** can adopt a conformation in which the two groups are less convergent and more parallel to one another. This effect allows the two NH groups to effectively coordinate to separate atoms, such as oxygen atoms in oxo-anions simultaneously and therefore alters the selectivity in favour of anions of this type. This can be seen in the observed stability constants for **135** which are similar stability constants for halides as **132**, but significantly displays improvements for dihydrogen phosphate and benzoate.

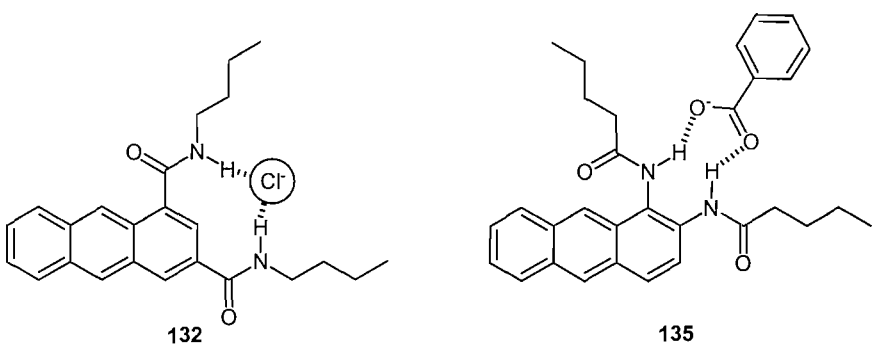

Fig 5.7: The differing selectivities of **132** and **135** can be explained by differing anion binding geometries in solution.

Comparison of the two differing anion motifs reveals differences in anion selectivities between the two receptors, however when considering which motif binds anions more strongly the relative acidities of the amide NH groups are an important factor. Receptor **132** contains NH groups that are appended directly to the electron-donating alkyl chain (δ = 6.45 & 6.35 ppm), which has the effect of reducing the acidity of the group whilst the amide NH groups in receptor **135** are linked to the electron-deficient aryl system (δ = 8.28 & 8.10 ppm). The effect of this is that the NH groups of **135** are more suitable for coordinating anions due to their greater acidity.

In order to provide further insight into how the differing arrangement of amide NH groups affects the observed anion stability constants, binding studies for receptors **132-133** & **135-136** were performed in DMSO-d_6 / 0.5% water solution (Table 5.2).

Table 5.2: Anion stability constants for compounds **132-133** and **135-136** were determined in DMSO-d_6 / 0.5% water solution at 298 K (M^{-1}). Anions titrated in the form of their TBA salts. All data fitted to a 1:1 binding model using WINEQNMR.[92] All errors < 15%.

Anion	**132**	**133**	**135**	**136**
Chloride	<10	<10	<10	<10
Dihydrogen Phosphate	19	122	64	63
Acetate	13	37	85	28
Benzoate	<10	21	44	34

Titrations were performed with both bromide and hydrogen sulfate, however in these cases interactions were too weak to allow stability constants to be determined.

In the more highly competitive solvent mixture of DMSO-d_6 / 0.5 % water, the observed stability constants are considerably lower than those observed in the less polar DCM solution.

In stark comparison to the previous studies in DCM, receptors **132** and **133** based on amide cleft motifs show highest affinities for oxo-anions with halide binding with chloride on the limits of detection. In the case of **132** very poor stability constants with all investigated anions are observed, whilst improvements are observed with receptor **133** consistent with the more acidic amide NH groups forming stronger binding interactions with the anions.

The differences between **135** and **136** are much smaller as expected considering the smaller affect in change of NH acidity. Whilst once more poor anion coordination properties are observed, in this case rather than the aryl-substituted receptor **136** coordinating anions more strongly, the reverse is observed with receptor **135** displaying higher stability constants. This effect could be due to the phenyl groups providing unfavourable steric interactions with the anions that destabilise the complex.

5.3. ANTHRACENE- BISUREA CLEFTS.

Investigation into the anion coordination properties of diamide receptors **132**, **133**, **135** and **136** had shown that the differing receptor motifs could coordinate anions with varying selectivities that were shown to be both an effect of the receptor and the solvent. Unfortunately even in non-competitive solvent systems, the strength of complexes formed with anions are relatively weak limiting the usefulness of these systems in developing fluorescence sensors.

In an attempt to develop more strongly coordinating receptors, we decided to produce receptors based upon the bis-urea receptor design, as detailed in chapter 2 (Fig 5.8). This motif has been demonstrated to coordinate oxo-anions in competitive solvent mixtures such as DMSO/water mixtures whilst solid-state structures with carboxylates have shown that all four of the urea NH donor groups are able to simultaneously coordinate to the anion oxygen atoms. It was therefore hoped that the more effective oxo-anion binding site of this motif would allow for the production of more sensitive anion sensors.

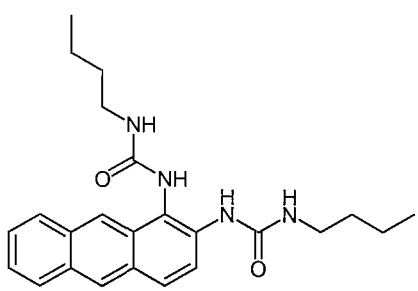

137

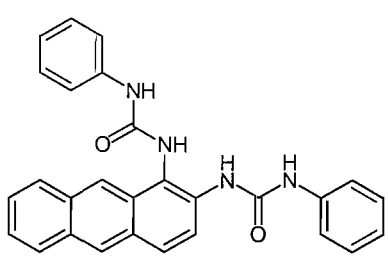

138

Fig 5.8: Bis-urea receptors **137** and **138**.

5.3.1. SYNTHESIS AND CHRACTERISATION.

Two novel anthracene bisurea clefts **137** and **138** have been synthesised (Scheme 5.3). 1,2-Diaminoanthracene **134** was prepared as previously, with the reaction of the diamine with a slight excess of either butylisocyanate or phenylisocyanate to afford receptors **137** and **138** in 39 and 82 % yields respectively.

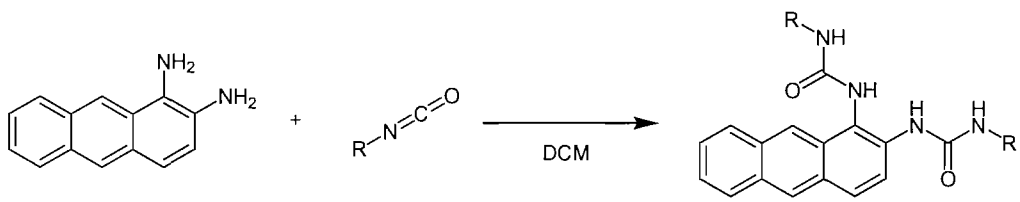

134

137 R = n-Bu
138 R = Ph

Scheme 5.3: Synthesis of 1,2-bisurea-anthracene receptors **137** and **138**.

5.3.2. SOLUTION PHASE ANALYSIS.

5.3.2.1. ^{1}H NMR titration data.

Anion stability constants for compounds **137** and **138** were elucidated *via* ^{1}H NMR titration experiments performed in DMSO -d_6/ 0.5 % water (Table 5.3). Titrations were also performed with fluoride, from which the data could not be fitted to a binding model, and with hydrogen sulphate with which shifts were insufficient to allow stability constants to be determined.

Both the alkyl derivative **137** and aryl derivative **138** demonstrate significantly higher binding constants for all of the anions reported compared to their dicarboxamido-anthracene analogues, consistent with the presence of an additional two NH moieties in the cleft of the receptor.

Table 5.3: Anion stability constants for compounds **137** and **138** were determined in DMSO-d_6 / 0.5% water solution at 298 K (M^{-1}). Anions titrated in the form of their TBA salts. All data fitted to a 1:1 binding model using WINEQNMR.[92] All errors < 15%.

Anion	137	138
Chloride	10	27
Bromide	-	<10
Dihydrogen Phosphate	370	1166
Acetate	277	2539
Benzoate	107	586

An improvement in the oxo-anion selectivity of receptors **137** and **138** is clearly apparent when comparing these values to those obtained previously (Table 5.2). Dihydrogen phosphate, acetate and benzoate stability constants all show large improvements in comparison to those observed with the simple 1,2- and 1,3-anthracene bis-amide systems.

Receptor **138** in which aryl groups are appended from the urea groups displays significantly higher anion stability constants over its alkyl derivative **137**. As previously discussed this effect can be largely explained through consideration of the acidity of the NH protons in these two systems. The internal NH groups in both receptors are attached to the anthracene aryl system, which has an electron-withdrawing effect thus enhancing their relative acidities and explaining why the receptors display high affinities in comparison to the bis-amide systems.

The presence of the additional external NH groups stabilize anion complexes in both cases. However this effect is enhanced further in **138** due to the external NH groups also being appended to an aryl group, thus increasing their acidity. Whilst the additional NH groups of **137** do enhance the stability of the anion complexes, they form weaker hydrogen bonds with the anion and therefore lower stability constants than **138** are obtained.

5.3.2.2. Photophysical experiments.

Initial qualitative experiments were performed with receptor **138** to determine its effectiveness as a fluorescent anion sensor. A 0.1 mM solution of **138** in DMSO was prepared, along with solutions of the same concentration of **138** but in the presence of 30 mM of dihydrogen phosphate, acetate and benzoate respectively these were excited at 365 nm with a resulting blue emission observed, this emission is visibly less in the presence of coordinating anions, with those coordinating more strongly quenching the emission to a greater degree (Fig 5.9).

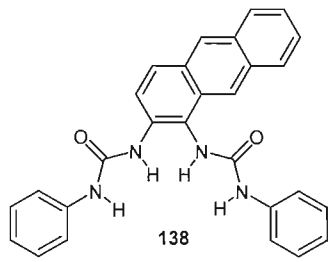

138

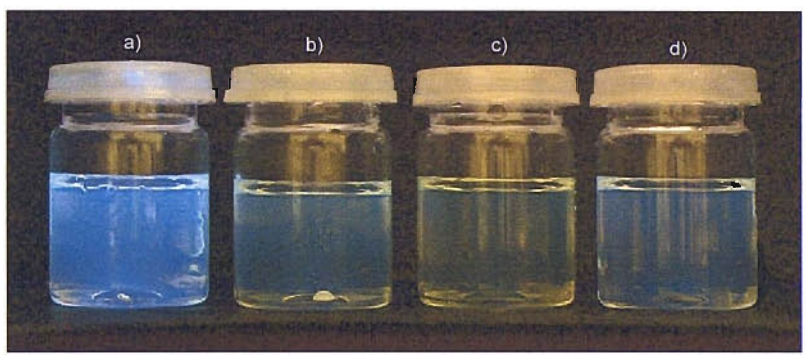

Fig 5.9: Solutions of 0.1 mM **138** in DMSO excited at 365 nm: a) in the absence of anions, b) 30 mM dihydrogen phosphate, c) 30 mM acetate and d) 30 mM benzoate.

In order to more fully evaluate the potential of bis-urea derived anthracene receptors as fluorescent anion sensors, both the ground state and excited state properties of **137** and **138** were investigated in DMSO solution in both the absence and presence of dihydrogen phosphate, acetate and benzoate. These anions were chosen in response to the high stability constants that had been determined previously by ^{1}H NMR titration experiments. The absorbance spectrum of **137** in the absence of anions reveals three

peaks located at 344, 362 and 393 nm with a determined extinction coefficient $\varepsilon = 5.0 \times 10^4$ cm^{-1} M^{-1} (Fig 5.10). Upon addition of TBA acetate relatively small changes in the absorbance spectrum is observed, with the two changes observed being an increase in absorbance in the range 320-340 nm can be attributed to changes in the electron density in the urea receptor. The second change occurs across the absorbance bands with a slight red-shift in both the centre of the absorbance and the intensity, consistent with the presence of the anion causing changes in the anthracene system through π-π interactions.

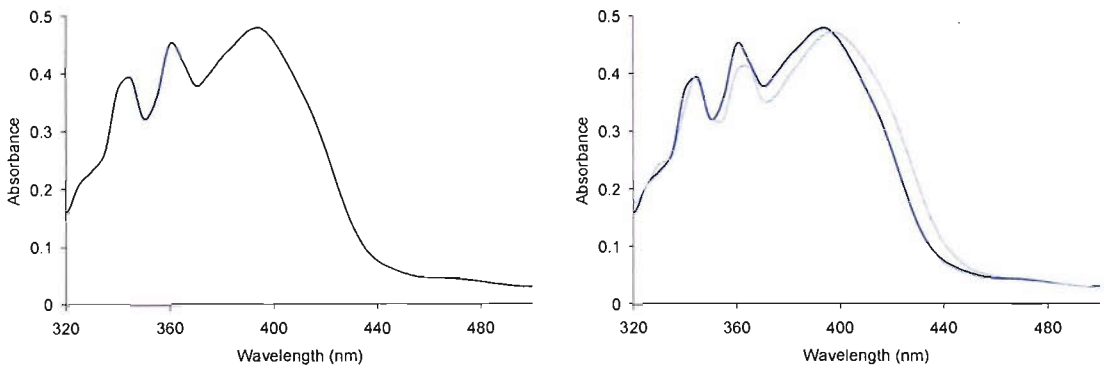

Fig 5.10: Absorbance spectra of **137** (0.1 mmol) (left) and upon addition of TBA acetate (30 mmol) (right) in DMSO.

The absorbance spectra of **138** is very similar to that obtained for **137**, with three distinct peaks observed at 346, 363 and 393 nm, with an extinction coefficient $\varepsilon = 5.7 \times 10^4$ cm^{-1} M^{-1} (Fig 5.11). As mentioned before the main changes in the spectrum occur in the lower range of the signal consistent with changes in electron density in the receptor.

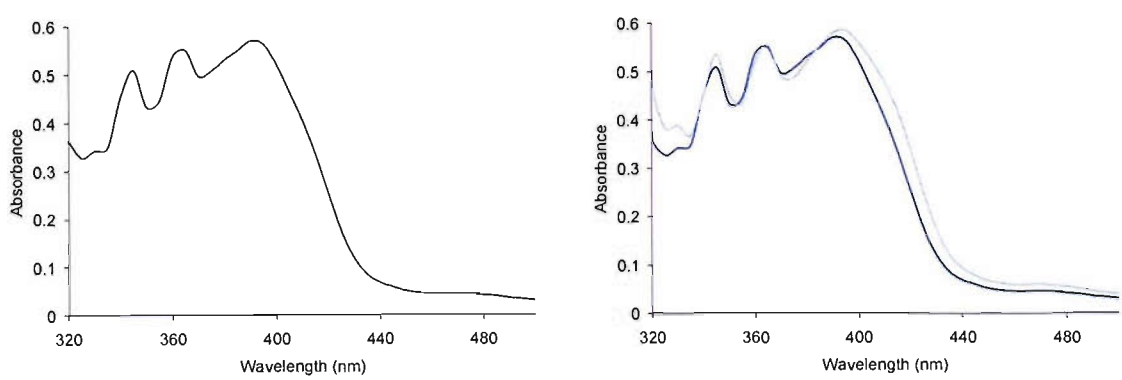

Fig 5.11: Absorbance spectra of **138** (0.1 mmol) (left) and upon the addition of TBA acetate (30 mmol) (right) in DMSO.

Excitation experiments performed with DMSO solutions of **137** and **138** revealed that a maximum emission was observed when **137** was excited at 368 nm, resulting in a maximum fluorescence emission peak centred at 493 nm (Fig 5.12). Upon addition of increasing concentrations of TBA acetate a quenching of the fluorescence intensity could be observed, with an insignificant shift in the emission.

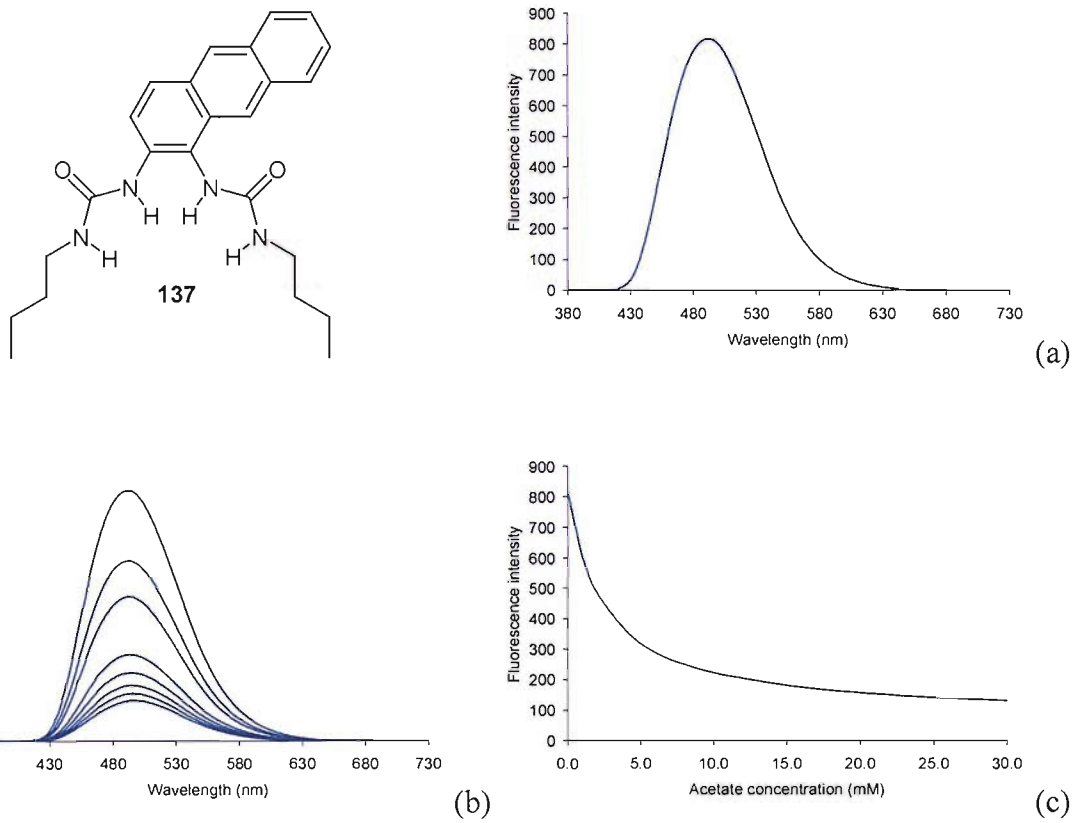

Fig 5.12: Emission spectra of **137** (0.1mM) in DMSO (a) in the absence of acetate, (b) upon the addition of TBA acetate (curves shown in (b) at 0, 0.2, 0.4, 0.9, 1.8, 3.3, 8.2 and 30 mmol acetate concentrations) and (c) fluorescence emission at 493 nm as a function of acetate concentration.

Maximum emission from a DMSO solution of **138** was observed upon excitation at 365 nm, with the emission peak centred at 477 nm (Fig 5.13). Upon addition of increasing concentrations of TBA acetate a quenching of the fluorescence emission could be observed.

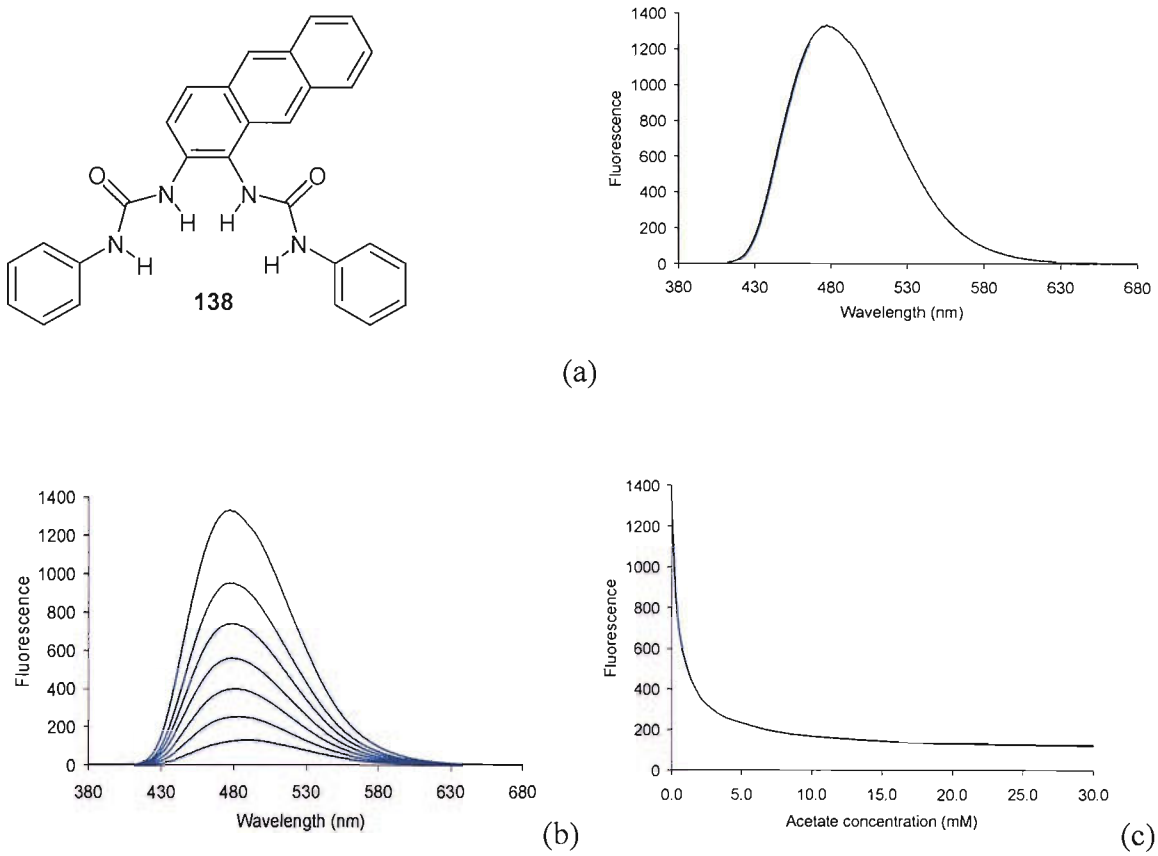

Fig 5.13: Emission spectra of **138** (0.1mM) in DMSO (a) in the absence of acetate, (b) upon the addition of TBA acetate (curves shown in (b) at 0, 0.2, 0.4, 0.9, 1.8, 3.3, 8.2 and 30 mmol acetate concentrations) and (c) fluorescence emission at 493 nm as a function of acetate concentration.

A comparison between the two quenching curves of **137** and **138** with acetate was made in order to allow comparison into the strength of the interaction between the respective receptors and the anion (Fig 5.14).

The sharper profile of the curve of **138** with acetate in comparison to that observed with **137** reflects a stronger interaction with the anion as supported by the ^{1}H NMR titration data.

A further comparison of the curves of acetate, dihydrogen phosphate and benzoate was performed (Fig 5.15). The shape of the titration curves indicate the strongest interaction is with acetate, with weaker interactions with both benzoate and dihydrogen phosphate.

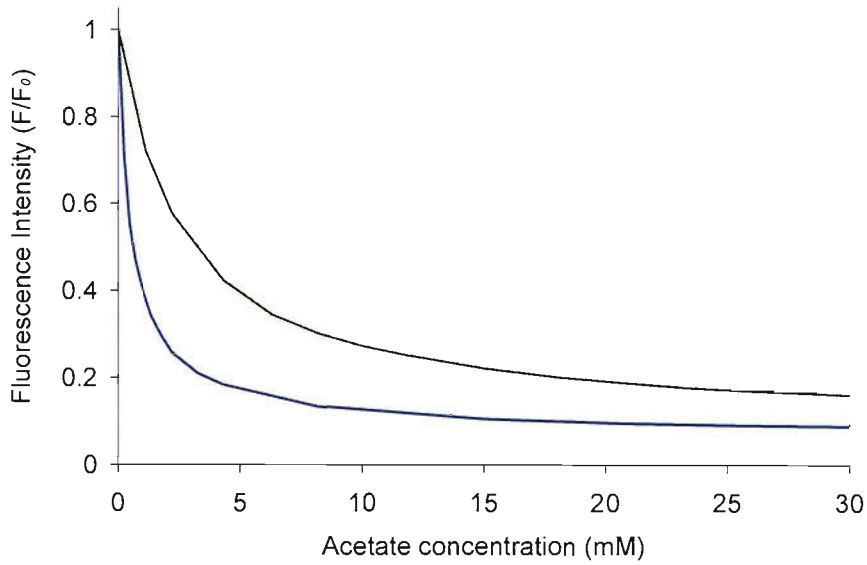

Fig 5.14: Comparison plot between the fluorescence quenching curves of **137** (green) and **138** (blue) (both 0.1 mmol) upon increasing acetate concentration.

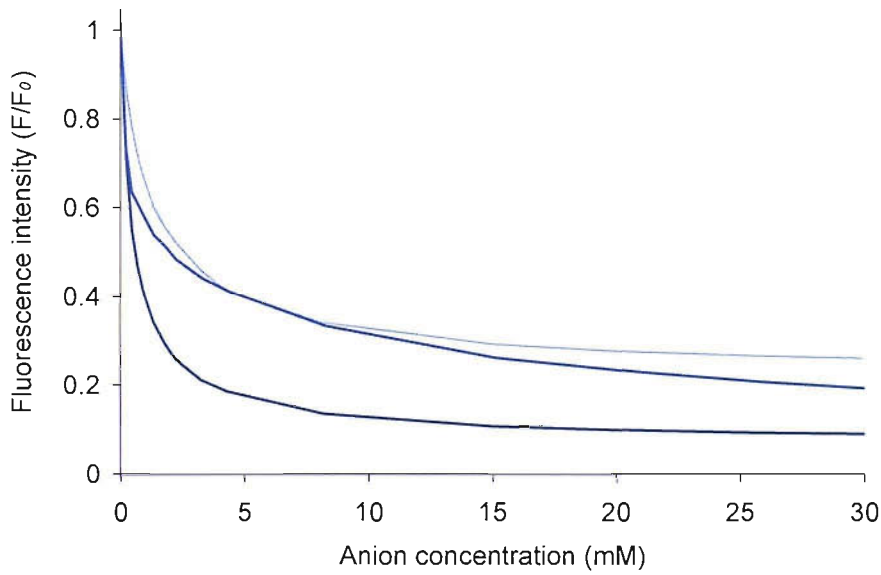

Fig 5.15: Fluorescence quenching curves of **138** (0.1 mmol) upon the addition of acetate (dark blue), dihydrogen phosphate (mid blue) and benzoate (light blue)

In order to quantify the fluorescence quenching experiments for both **137** and **138** with dihydrogen phosphate, acetate and benzoate, the data was fitted to a 1:1 binding model.

Table 5.4: Anion stability constants as calculated from fluorescence quenching experiments (M^{-1}) performed in DMSO. Data was fitted to a 1:1 binding model using Origin[129] Anions titrated in the form of their TBA salts. All errors less than 15%.

Anion	137	138
Dihydrogen Phosphate	368	1019
Acetate	400	1992
Benzoate	194	811

The stability constants with dihydrogen phosphate, acetate and benzoate were determined by fluorescence quenching experiments producing values that are remarkably consistent with those obtained through ^{1}H NMR titration experiments (Table 5.3). These results also indicate that the quenching mechanism of these receptors is almost certainly due to the bound anion providing an alternate non-radiative relaxation pathway.

Although the emission spectra demonstrates significant quenching upon addition of coordinating anions the UV/vis spectra only changes a relatively small amount which is surprising considering the fact the NH groups are directly appended to the anthracene unit. This phenomena is likely to be the result of a Twist Induced Charge Transfer (TICT) mechanism. In the absence of anions the urea groups are likely to lie out of plane with the anthracene unit and therefore the π-system of the urea group is unable to conjugate with the fluorophore. Upon addition of coordinating anions the urea groups are forced into a cleft conformation that places the groups in the plane of the anthracene moiety. As a result the charge differential of the receptor-anion groups is now able to communicate with the fluorophore and therefore a quenching of the fluorescence can be observed.

5.3.3. SOLID STATE ANALYSIS.

X-ray quality crystals of the benzoate complex of **138** were obtained *via* slow evaporation of an acetonitrile solution in the presence of excess TBA benzoate (Fig 5.16). A single benzoate anion is bound in the centrally with the bis-urea cleft, with both the internal urea NH groups [N1···O3 2.851(6) Å & N3···O4 2.839(6) Å] and external urea NH groups [N2···O3 2.890(6) Å & N4···O4 2.830(6) Å] coordinating through a total of four hydrogen bonds.

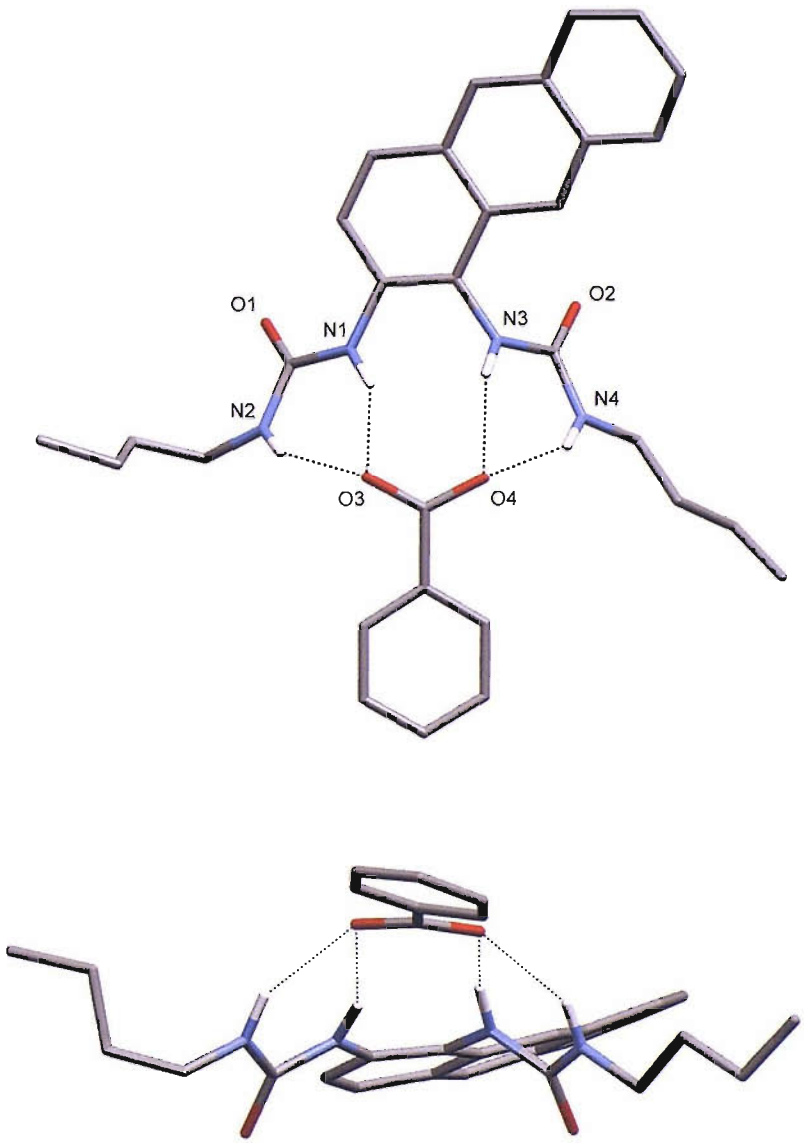

Fig 5.16: Benzoate complex of **138** reveals that the anion is bound simultaneously by all four NH donor groups.

5.4. CONCLUSION.

A series of novel anion receptors **132-133** and **135-136** based upon anthracene bis-amide derivatives have been synthesized and their anion binding properties investigated by ^{1}H NMR titration techniques. In both cases, although selectivity between both the amide cleft and 1,2-phenylenediamide motifs, for halide and oxo-anions respectively, could be observed, the overall strength of the complexes formed were low, particularly in DMSO/water mixtures.

In order to produce receptors that could form stronger complexes in solution, anthracene derived receptors **137** & **138**, both of which contain bis-urea clefts were synthesized. Evaluation of the receptors' stability constants with various anions were performed using ^{1}H NMR titration experiments. These revealed significant improvements in oxo-anion binding and selectivity in DMSO/water in comparison to the previously explored, two hydrogen bond donor, anthracene-dicarboxamide systems.

Photophysical investigations of **137** and **138** were performed in DMSO with the fluorescence emission significantly quenched upon the addition of coordinating oxo-anions. Titration of these anions produced curves that could be fitted to binding models, with values for stability constants in agreement to those obtained through ^{1}H NMR methods.

6. GENERAL CONCLUSION.

This thesis has outlined a number of strategies that have been undertaken towards the development of receptors that utilize hydrogen-bonding as their primary method of coordinating anions.

The use of bis-urea derivatives based upon 1,2-phenylenediamine provides a highly effective method for coordinating oxo-anions and in particular carboxylates. Whilst the high level of association with these anions is clearly a pleasing result, it is the ease at which these compounds can be obtained from commercially available starting materials in almost quantitative yields that make them highly interesting to study, and perhaps may facilitate their use within commercial applications. The solid-state behaviour of carboxylate complexes of these compounds have been shown to provide a reliable synthon. More complex 2- and 3-dimensional structures could be obtained either through the use of more complicated receptors containing three or four bis-urea units or more substituted carboxylates.

The synthesis and anion-binding properties of a more complicated macrocyclic receptor has been reported in chapter three and has demonstrated a high affinity for carboxylate anions, however in this case the selectivity over other oxo-anions such as dihydrogen phosphate is vastly increased. Interestingly the receptor demonstrates differing interactions between each of the NH donor groups depending upon the anion in question and in the future this may provide a means for anion identification through the attachment of different sensing groups, i.e. chromophores, to each of the NH groups. As the anion is varied, the effect upon each of the chromophores will depend upon how

strongly the anion interacts with each of the NH groups creating in effect a 'fingerprint' signal that could only be observed with that particular anion.

The use of anthraquinone as a redox active centre that can be incorporated into anion sensors has been explored in chapter 4. It is clear that although this class of receptor binds anions quite poorly there remains much scope to improve the current system through the use of more highly coordinating anion binding motifs. Unfortunately the exposed nature of the quinone system leads it to be susceptible to solvation effects which can overwhelm the response observed upon anion binding, particularly in the presence of strongly hydrogen-bonding solvents. A potential method of overcoming this problem is to 'insulate' the redox system from the effect of the solvent through the use of a rotaxane system in which both quinone oxygen atoms could be bound within a macrocycle. Anion binding groups could be attached to the anthraquinone system as before with the large sterically bulky terminating groups employed to prevent the macrocycle from slipping off the rotaxane axle.

Luminescent anion sensors provide highly sensitive methods of determining the presence of anions. The use of anthracene as a fluorophore gives a highly effective and synthetically versatile building block for anion receptor synthesis. Ultimately the use of fluorophores that have sharp and well defined emission spectra at different wavelengths may provide methods for employing multiple fluorophores in a single sensor in order to obtain information into the host/guest interaction at non-equivalent locations within the receptor.

The future of anion receptor chemistry could be described as rapidly approaching a crossroads. The area which was initially relatively underdeveloped has been explored by a number of great scientists and numerous designs and strategies have been developed for the coordination of anions. The overlap of anion coordination chemistry with the areas of biology, physics and material engineering provides a host of real world applications making the subject ideally located to exploit and, as the area develops further, it will influence these related areas in an increasingly profound manner.

7. EXPERIMENTAL METHODS.

7.1. SOLVENT AND REAGENT PRETREATMENT.

Where necessary solvents were purified prior to use. DCM and ethanol was distilled over calcium hydride. Anhydrous acetonitrile (water <0.003 %) was purchased from Fischer. Anhydrous DMSO was purchased from Fischer and dried further over 4Å activated molecular sieves. Triethylamine was distilled from KOH and stored under nitrogen in the presence of KOH pellets. Thionyl chloride was distilled from 10% (w/w) triphenyl phosphate and stored under nitrogen. Commercial grade reagents have been used without further purification. Reagents prepared in accordance to the literature have been so referenced. All syntheses have been performed under an inert atmosphere of nitrogen. TBA salts of the anions used for ^{1}H NMR titration experiments, electrochemical and fluorescence analyses have been thoroughly dried overnight under high vacuum.

7.2. INSTRUMENTAL METHODS.

NMR data were recorded on Bruker AV300 and DPX400 spectrometers. The data were referenced internally using the residual protio-solvent (^{1}H) or the signals of the solvent (^{13}C) with the chemical shifts reported in ppm. Low resolution mass spectra were recorded on a Micromass Platform single quadrupole spectrometer, whereas high resolution mass spectra were recorded on a VG 70-250-SE normal geometry double focusing mass spectrometer by the mass spectrometry service at the University of Southampton. Elemental analyses were performed by Medac Ltd. UV/vis spectra were recorded on a UNicam UV1 spectrometer with IR spectra Mattson Satellite (ATR) FTIR

and are reported in wavenumbers (cm^{-1}). Melting points were recorded in open capillaries on a Gallenkamp melting point apparatus and are uncorrected.

7.2.1. Electrochemical methods.

Analysis of the simple 1,3-diphenyl substituted receptor **118** was performed using cyclic voltammetry recorded using a home built potentiostat interfaced with a PC through an ADC card (Measurement Computing, PCI-DAS 1602/16) and software written in house. The solutions consisted of 0.1 mol dm^{-3} TBA hexafluorophosphate in DMSO (Fischer, 99.99%) as base electrolyte. The DMSO was dried prior to use by drying over activated molecular sieves (Aldrich, 4Å). Platinum wire served as the counter electrode and a Ag/Ag^{+} system (0.1 mmol dm^{-3} $AgNO_3$ (Fischer, 99.9%), 0.1 mol dm^{-3} TBA hexafluorophosphate in DMSO) was used as the reference electrode. Absolute ethanol (Fischer) was dried over $CaSO_4$ prior to use. Voltammetry was recorded at a 3mm diameter glassy carbon electrode sealed in glass. This electrode was polished on 0.3μm alumina and washed in dry DMSO prior to insertion into the cell. All electrolyte solutions were sparged with argon prior to use in an effort to remove oxygen from the solutions. Experiments were performed at ambient temperature (20-23 °C). The cell was baked prior to use.

7.2.2. Fluorescence methods.

Absorbance spectra for **137** and **138** were recorded on a Hitachi U-2001 spectrophotometer whilst fluorescence spectra were obtained using a Hitachi F-2000 spectrofluorimeter with a 150W xenon lamp. The photomultiplier voltage was set to 400 volts with excitation and emission slits set to 2.5 mm. Emission spectra were obtained by exciting at 370 nm, with the emission monitored over 380-600 nm, using a scan speed of 60 nm/min. The sample solutions consisted of 0.1 mM of receptor in DMSO, with titrated anion solutions consisting of 0.1 mM of receptor and 100 mM of anion in the form of its TBA salt.

7.3 SYNTHETIC PROCEDURES.

7.3.1 Synthetic schemes included in chapter 2.

1,1′-(4,5-dichloro-1,2-phenylene)bis(3-phenylurea) (69):

Phenylisocyanate (0.61 mL, 5.7 mmol) was added dropwise to a stirring solution of 4,5-dichloro-1,2-phenylenediamine (0.50 g, 2.8 mmol) in DCM (100 mL) over a five minute period. Following the addition the reaction was heated to reflux for 18 h after which time the product had precipitated and after allowing the reaction to cool to ambient temperature was removed via filtration. In order to purify the product further the crude solid was resuspended in DCM (50 mL) and was washed with aqueous HCl solution (3 × 20 mL, pH = 3), in order to remove any of the remaining mono-substituted amine side-product. The organic phase was retained with the solvent removed *in vacuo* before recrystalisation was performed from hot acetone, yielding the isolated white solid product, which was subsequently dried under high vacuum. Mass of product = 0.98 g. Yield = 82%. ^{1}H NMR 300 MHz in DMSO-d_6 δ (ppm): 6.99 (t, 2H, J = 7.0 Hz, ArH), 7.29 (t, 4H, J = 7.7 Hz, ArH), 7.47 (d, 4H, J = 8.4 Hz, ArH), 7.93 (s, 2H, ArH), 8.20 (s, 2H, NH), 9.14 (s, 2H, NH). ^{13}C NMR 75 MHz in DMSO-d_6 δ (ppm): 118.3 (CH), 122.1 (CH), 124.5 (CH), 125.2 (C) 128.8 (CH), 131.3 (C), 139.1 (C), 152.8 (CO). IR (cm^{-1}): 3315, 3056, 1697, 1623, 1581, 1562, 1528, 1441, 1223, 880. LRMS (ES-): 494.9 $(M+2MeCN–H)^-$, 527.0 $(M+TFA–H)^-$. Microanalysis for $C_{20}H_{16}Cl_2N_4O_2$: Calc. (%) C = 57.54, H = 4.01, N = 13.46. Found (%) C = 57.85, H = 3.88, N = 13.48. m.p. (acetone) = decomp. 271-273 °C.

1,1′-(1,2-phenylene)bis(3-(4-nitrophenyl)urea) (70):

Powdered 4-nitrophenylisocyante (1.67 g, 9.3 mmol) was slowly added to a stirring solution of 1,2-phenylenediamine (0.50 g, 4.6 mmol) in DCM (100 mL) over a period of 15 m before the reaction was heated to reflux for 18 h. After this time the product had formed as a yellow precipitate which after allowing the reaction to cool to ambient temperature was removed from the suspension via filtration. The yellow product was washed with DCM (3 × 20 mL) and air dried before being dried further under high

vacuum. Mass of product = 1.98 g. Yield = 98%. ^{1}H NMR 300 MHz in DMSO-d_6 δ (ppm): 7.16 (m, 2H, ArH), 7.62 (m, 2H, ArH), 7.71 (m, 4H, ArH), 8.18 (m, 4H, ArH), 8.29 (s, 2H, NH), 9.81 (s, 2H, ArH). ^{13}C NMR 75 MHz in DMSO-d_6 δ (ppm): 117.5 (CH), 124.5 (CH), 124.7 (CH), 125.1 (CH), 131.0 (C), 141.0 (C), 146.4 (C), 152.7 (CO). IR (cm^{-1}): 3322, 3296, 3214, 1728, 1591, 1491, 1301, 1169, 1105, 846. LRMS (ES-): 549.0 $(M+TFA-H)^-$, 998.8 $(2M+TFA-H)^-$. Microanalysis for $C_{20}H_{16}N_6O_6$: Calc. (%) C = 55.05, H = 3.70, N = 19.26. Found (%) C = 55.17, H = 3.69, N = 19.25. m.p. (DCM) = 278 °C.

1,1′-(1,2-phenylene)bis(3-(2-nitrophenyl)urea) (71):

Powdered 2-nitrophenylisocyanate (1.00 g, 6.1 mmol) was added slowly to a stirring solution of 1,2-phenylenediamine (0.33 g, 3.1 mmol) in DCM (75 mL) over a period of 15 m before the reaction was heated to reflux for 18 h. After this the product had formed as a yellow precipitate, which after allowing the reaction to cool to ambient temperature was removed from suspension via filtration. The yellow product was washed with DCM (3 × 20 mL) and air dried before being dried further under high vacuum. Mass of product = 1.31 g, 3.00 mmol. Yield = 98%. ^{1}H NMR 300 MHz in DMSO-d_6 δ (ppm): 7.13, (m, 2H, ArH), 7.21 (m, 2H, ArH), 7.60 (m, 2H, ArH), 7.69 (m, 2H, ArH), 8.07 (m, 2H, ArH), 8.24 (m, 2H, ArH), 9.45 (s, 2H, NH), 9.72 (s, 2H, NH). ^{13}C NMR 75.4 MHz in DMSO-d_6 δ (ppm): 122.4 (CH), 122.9 (CH), 124.5 (CH), 124.6 (CH), 125.3 (CH), 130.9 (C), 134.6 (C), 134.8 (CH), 138.1 (C), 152.6 (CO). IR (cm-1): 3277, 3108, 1662, 1637, 1589, 1562, 1501, 1340, 1280, 1225, 1149. LRMS (ES-): 470.8 $(M+Cl)^-$, 907.1 $(2M+Cl)^-$. Microanalysis for $C_{20}H_{16}N_6O_6$: Calc. (%) C = 55.05, H = 3.70, N = 19.25. Found (%) C = 54.96, H = 3.69, N = 19.17. m.p. (DCM) = 253 °C.

1,1′-(4,5-dichloro-1,2-phenylene)bis(3-(2-nitrophenyl)urea) (72):

Powdered 2-nitrophenylisocyanate (0.93 g, 5.6 mmol) was added slowly to a stirring solution of 4,5-dichloro-1,2-phenylenediamine (0.50 g, 2.8 mmol) in DCM (100 mL) over a period of 15 m before the reaction was heated to reflux for 18 h. After this time the product had formed as a yellow precipitate which was removed from suspension via filtration. In order to purify the product further the crude solid was resuspended in

DCM (50 mL) and was washed with aqueous HCl solution (3 × 20 mL, pH = 3), in order to remove any of the remaining mono-substituted amine side-product. The organic phase was retained with the solvent removed *in vacuo* before recrystalisation was performed from hot acetone, yielding the isolated white solid product, which was subsequently dried under high vacuum. Mass of product = 0.97 g. Yield = 68%. ^{1}H NMR 300 MHz in DMSO-d_6 δ (ppm): 7.25 (m, 2H, ArH), 7.71 (m, 2H, ArH), 7.71 (m, 2H, ArH), 7.91 (s, 2H, ArH), 8.08 (m, 2H, ArH), 8.21 (m, 2H, ArH), 9.37 (s, 2H, NH), 9.77 (s, 2H, NH). ^{13}C NMR 75.4 MHz in DMSO-d_6 δ (ppm): 122.9 (CH), 123.2 (CH), 125.0 (CH), 125.3 (CH), 125.8 (C), 130.8 (C), 134.1 (C), 134.8 (CH), 138.4 (C), 152.4 (CO). IR (cm^{-1}): 3353, 3295, 1728, 1664, 1579, 1492, 1431, 1338, 1262, 1184, 1141. LRMS (ES-): 616.9 (M+TFA–H)$^{-}$. Microanalysis for $C_{20}H_{14}Cl_2N_6O_6$ + 0.50 H_2O. Calc. (%) C = 46.71, H = 2.94, N = 16.34. Found (%) C = 46.98, H = 2.78, N = 16.19. m.p. (acetone) = decomp. 264-267 °C.

_N,N'_-(2,2'-(1,2-Phenylenebis(azanediyl))bis(oxomethylene)bis(azanediyl)bis(2,1-phenylene)dibenzamide (74):

Benzoyl chloride (0.74 mL, 6.4 mmol) was added slowly over a period of 15 m to a stirring solution of 1,1'-(1,2-phenylene)bis(3-(2-aminophenyl)urea) **76** (1.20 g, 3.2 mmol), triethylamine (0.76 mL, 7.1 mmol) and DMAP (0.01g, cat.) in DMF (50 mL). After the addition the reaction was left stirring at ambient temperature for a further 18 h, after which the precipitated triethylamine hydrochloride was removed via filtration. The solvent was removed from the filtrate via reduced pressure distillation to afford an oily brown residue that was then added to DCM (50 mL). The organic solution was then washed with water (3 × 50 mL) and dried with anhydrous $MgSO_4$ before the removal of solvent *in vacuo*. The resulting brown solid was washed with ethyl acetate (10 mL) to produce a white solid that was triturated further with hot ethyl acetate (3 × 10 mL) affording the final product was a white solid that was further dried under high vacuum. Mass of product = 0.55 g. Yield = 29%. ^{1}H NMR 400 MHz (DMSO-d_6) δ (ppm): 10.02 (s, 2H, NH), 8.58 (s, 2H, NH), 8.44 (s, 2H, NH), 8.00 (app d, 4H, J = 7.0 Hz, ArH), 7.77 (dd, 2H, J = 8.0 & 1.0 Hz, ArH), 7.50 (m, 10H, ArH), 7.20 (td, 2H, J = 7.9 & 1.1 Hz, ArH), 7.04 (m, 4H, ArH). ^{13}C NMR - 100 MHz (DMSO-d_6) δ (ppm): 165.6 (CO), 153.8

(CO), 134.2 (C), 133.9 (C), 131.1 (CH), 128.6 (C), 128.4 (CH), 127.7 (CH), 126.9 (CH), 126.1 (CH), 124.0 (CH), 123.0 (CH), 122.5 (CH). IR (cm^{-1}): 3288, 3057, 1654, 1596, 1507, 1439, 1309, 1206, 757. LRMS (ES): 619.3 $[M+Cl]^-$, 697.2 $[M+TFA-H]^-$, 1203.6 $[2M+Cl]^-$, 1281.1 $[2M+TFA-H]^-$. Microanalysis for $C_{34}H_{28}N_6O_4$. Calc. (%) C = 69.85, H = 4.83, N = 14.37. Found (%) C = 69.54, H = 4.81, N = 14.38. m.p. (ethyl acetate) = 220-222 °C.

3,3′-(1,2-Phenylenebis(azanediyl))bis(oxomethylene)bis(azanediyl)bis(N-phenylbenzamide) (75):

Aniline (0.40 mL, 4.1 mmol) was dissolved in dry DCM (40 mL) with 2M trimethylaluminium in hexanes (2.03 mL, 4.06 mmol) added dropwise with the reaction then left stirring 30 m before the addition of 1,1′-(1,2-phenylene)bis(3-[3-ethylcarboxylatephenyl]urea) **80** (1.00 g, 2.03 mmol). Following the addition the reaction was heated to reflux for 5 days after which time the reaction was allowed to cool to ambient temperature before addition of 2M aqueous HCl solution. The addition continued until the reaction ceased bubbling with a further 20 mL of water added with the biphasic mixture, in which the product had precipitated in the organic phase, left stirring for a further 15 m. The organic phase was removed and washed with water (3 × 50 mL) with the precipitated product removed via filtration affording the product as a white solid that was washed with Et_2O (3 × 20 mL) and air dried before drying further under high vacuum. Mass of product = 0.94 g. Yield = 94%. ^1H NMR 300 MHz (DMSO-d_6) δ (ppm): 10.22 (s, 2H, NH), 9.33 (s, 2H, NH), 8.15 (s, 2H, NH), 8.00 (s, 2H, ArH), 7.76 (m, 6H, ArH), 7.63 (m, 2H, ArH), 7.56 (m, 2H, ArH), 7.43 (t, 2H, J = 7.7 Hz, ArH), 7.35 (t, 4H, J = 7.7 Hz, ArH), 7.11 (m, 4H, ArH).. ^{13}C NMR - 75 MHz (DMSO-d_6) δ (ppm): 165.6 (CO), 153.2 (CO), 140.1 (C), 139.2 (C), 135.8 (C), 131.3 (C), 128.8 (CH), 128.6 (CH), 124.2 (CH), 124.1 (CH), 123.6 (CH), 121.1 (CH), 120.8 (CH), 120.3 (CH), 117.6 (CH). IR (cm^{-1}): 3351, 3250, 2980, 1724, 1648, 1555, 1462, 1280, 1217, 1103, 1026, 752. LRMS (ES): 619.1 $[M+Cl]^-$, 696.9 $[M+TFA-H]^-$, 1203.4 $[2M+Cl]^-$, 1281.3 $[2M+TFA-H]^-$, 1787.9 $[3M+Cl]^-$. Microanalysis for $C_{34}H_{28}N_6O_4$ + 0.40 CH_2Cl_2. Calc. (%) C = 66.79, H = 4.69, N = 13.59. Found (%) C = 66.60, H = 4.90, N = 13.58. m.p. (Et_2O) = 227 °C.

1,1′-(1,2-Phenylene)bis(3-(2-aminophenyl)urea) (76):

1,1′-(1,2-phenylene)bis(3-(2-nitrophenyl)urea) **71** (1.33 g, 3.0 mmol) was suspended in EtOH (200 mL) before the addition of 10% Pd/C (0.04 g, 0.1 mmol) and hydrazine monohydrate (1.40 mL). Following the addition the reaction was heated to reflux and after 2 hours a further addition of 10% Pd/C (0.04 g, 0.1 mmol) was performed with the reaction left at reflux for a further 16 h. After this time the reaction was then removed from reflux and allowed to cool to ambient temperature with the resulting white precipitate and remaining Pd/C removed via filtration. The crude product was dissolved in a small volume of DMF (5 mL) and filtered to remove the remaining Pd/C from the reduction. The filtrate was retained and the DMF was removed by reduced pressure distillation to yield the product was a white precipitate in a green oil. The product was removed via filtration and washed with water (3 × 10 mL) followed by MeOH (3 × 10 mL) before the white product was dried under high vacuum. Mass of product = 0.88 g. Yield = 78%. ^{1}H NMR - 400 MHz (DMSO-d_6) δ (ppm): 8.37 (s, 2H, NH), 8.29 (s, 2H, NH), 7.64 (dd, 2H, J = 5.6 & 3.4 Hz, ArH), 7.36 (d, 2H, J = 7.9 Hz, ArH), 7.02 (dd, 2H, J = 5.6 & 3.8 Hz, ArH), 6.82 (t, 2H, J = 7.1 Hz, ArH), 6.71 (d, 2H, J = 7.5 Hz, ArH), 6.55 (t, 2H, J = 7.5 Hz, ArH), 4.90 (bs, 4H, NH_2). ^{13}C NMR – 100 MHz (DMSO-d_6) δ (ppm): 153.7 (CO), 140.8 (C), 131.1 (CH), 124.5 (CH), 124.2 (C), 123.7 (C), 123.2 (CH), 116.4 (CH), 115.5 (CH). IR (cm^{-1}): 3353, 3295, 1728, 1664, 1579, 1492, 1431, 1338, 1262, 1184, 1141. LRMS (ES+): 376.9 $[M+H]^+$, 398.9 $[M+Na]^+$, 439.9 $[M+Na+MeCN]^+$, 753.1 $[2M+H]^+$, 775.1 $[2M+Na]^+$, 1129.2 $[3M+Na]^+$, 1152.3 $[3M+Na]^+$. HRMS (ES+): Calculated Mass = 377.1721. Observed Mass = 377.1721. Δ = 0.06 ppm. m.p. (MeOH) = decomp. 221 °C.

1,1′-(1,2-phenylene)bis(3-(3-ethylcarboxylatephenyl)urea) (80):

3-Ethylisocyanatobenzoate (2.16 mL, 13.1 mmol) was added dropwise to a stirring solution of phenylenediamine (0.71 g, 6.5 mmol) in dry DCM (150 mL) with MeOH (5 mL) to prevent gelation. The reaction was left at ambient temperature for a further 16 h following which the solvent was removed from reaction via rotary evaporation. The product was then recrystalized from boiling MeOH and washed with Et_2O (3 × 20 mL) to afford a white solid that was air dried before drying further under

high vacuum. Mass of product = 2.74 g. Yield = 86%. ^{1}H NMR 300 MHz (DMSO-d_6) δ (ppm): 9.35 (s, 2H, NH), 8.15 (s, 2H, ArH), 8.07 (s, 2H, NH), 7.70 (m, 2H, ArH), 7.60 (m, 2H, ArH), 7.55 (m, 2H, ArH), 7.41 (t, 2H, J = 7.9 Hz, ArH), 7.11 (dd, 2H, J = 6.0 & 3.8 Hz, ArH), 4.30 (q, 4H, J = 7.1 Hz, CH_2), 1.31 (t, 6H, J = 7.1 Hz, CH_3). ^{13}C NMR - 100 MHz (DMSO-d_6) δ (ppm): 166.2 (CO), 153.7 (CO), 140.7 (C), 131.8 (C), 130.9 (C), 129.6 (CH), 124.7 (CH), 124.7 (CH), 123.1 (CH), 122.9 (CH), 119.0 (CH), 61.2 (CH_2), 14.6 (CH_3). IR (cm^{-1}): 3351, 3245, 2980. 1724, 1652, 1559, 1458, 1280, 1251, 1217, 1103, 752. LRMS (ES): 491.3 $[M+H]^+$, 513.3 $[M+Na]^+$, 100.3 $[2M+Na]^+$. Microanalysis for $C_{26}H_{26}N_4O_6$. Calc. (%) C = 63.66, H = 5.34, N = 11.42. Found (%) C = 63.46, H = 5.34, N = 11.34. m.p. (Et_2O) = 208 °C.

1-Phenyl-3-[3,3',4'-tris-(3-phenyl-ureido)-biphenyl-4-yl]-urea (82):

Phenylisocyanate (0.75 mL, 6.9 mmol) was added dropwise to a stirring solution of 3,3′-diaminobenzidine (0.34g, 1.6 mmol) in anhydrous DMF (40 mL). The reaction was then heated to 80 °C for 72 h before being allowed to cool to ambient temperature. Upon cooling the white product was precipitated from solution and was removed from suspension via filtration. The product was then washed with both DCM, (3 × 20 mL), and water (3 × 20 mL) and air dried before drying further under high vacuum. Mass of solid = 0.64 g. Yield = 58%. ^{1}H NMR 400 MHz (DMSO-d_6) δ (ppm): 9.10 (s, 4H, NH), 8.15 (s, 2H, NH), 8.12 (s, 2H, NH), 7.71 (d, 2H, J = 8.4 Hz, ArH), 7.49 (d, 8H, J = 8.4 Hz, ArH), 7.38 (dd, 2H, J = 8.4 & 2.2 Hz, ArH), 7.28 (m, 8H, ArH), 6.96 (m, 4H, ArH). ^{13}C NMR - 100 MHz (DMSO-d_6) δ (ppm): 153.3 (CO), 153.1 (CO), 139.8 (C), 135.4 (C), 131.5 (C), 130.6 (C), 128.8 (CH), 124.2 (CH), 121.9 (CH), 121.8 (CH), 118.2 (CH), 118.2 (CH). IR (cm^{-1}): 3269, 3051, 1695, 1624, 1600, 1561, 1441, 1216. LRMS (ES): 380.5 $[M+2Cl]^{2-}$, 502.7 $[M+3MeCN+2Cl]^{2-}$. Microanalysis for $C_{40}H_{34}N_8O_4$. Calc. (%) C = 69.55, H = 4.96, N = 16.22. Found (%) C = 69.24, H = 4.95, N = 16.10. m.p. (H_2O) > 300 °C.

7.3.2. Synthetic schemes included in chapter 3.

_N_-(2-(3-Phenyl-ureido)-phenyl)-benzamide (95):

_N_-(2-amino-phenyl)-benzamide (0.54 g, 2.5 mmol) was dissolved in dry DCM (40 mL) with phenyl isocyanate (0.28 mL, 2.5 mmol) added dropwise. The reaction was then left stirring for 16 h at ambient temperature after which time the resulting white precipitate was removed via filtration and washed with DCM and Et_2O to afford the product as a white powder. Mass of product = 0.82 g. Yield = 97%. ^{1}H NMR 300 MHz in DMSO-d_6 δ (ppm): 9.21 (s, 1H, NH), 8.08 (s, 1H, NH), 8.04 (d, 2H, J = 1.4 Hz, ArH), 8.01 (s, 1H, NH), 7.57 (m, 3H, ArH). ^{13}C NMR 75 MHz in DMSO-d_6 δ (ppm): 165.8 (CO), 152.9 (CO), 139.7 (C), 134.5 (C), 134.1 (C), 131.7 (CH), 128.8 (CH), 128.4 (CH), 128.1 (C), 127.8 (CH), 127.3 (CH), 126.3 (CH), 122.7 (CH), 122.1 (CH), 121.8 (CH), 118.2 (CH). LRMS (ES-): 393.0 $[M+2MeOH-H]^-$, 409.9 $[M+Br]^-$, 444.0 $[M+TFA-H]^-$, 743.0 $[2M+Br]^-$, 775.1 $[2M+TFA-H]^-$. IR (cm^{-1}): 3350, 3200, 3143, 3044, 2995, 1638, 1565, 1478, 1438, 1322, 1226, 748. Microanalysis for $C_{20}H_{17}N_3O_2$ + 0.05 CH_2Cl_2. Calc. (%) C = 71.75, H = 5.14, N = 12.52. Found (%) C = 71.99, H = 5.17, N = 12.57. m.p. (Et_2O) = 198 °C.

1,3-Bis-(2-benzanilide-phenyl)-urea (96):

A solution of 1,3-Bis-(2-amino-phenyl)-urea (0.35 g, 1.5 mmol), triethylamine (0.43 mL, 3.1 mmol) and DMAP (0.002 g cat.) in dry DCM (30 mL) was stirred for 15 m. After this benzoyl chloride (0.34 mL, 2.9 mmol) was added to the reaction dropwise with the reaction then left stirring for a further 18 h after which time the solvent was removed via a rotary evaporator. The crude product was purified using flash column chromatography using DCM / 95:5 DCM /MeOH eluent. The white product obtained was further purified by recrystalisation from hot EtOH which yielded the product as a white powder. Mass of product = 0.39 g. Yield = 49%. ^{1}H NMR 300 MHz in DMSO-d_6 δ (ppm): 10.00 (s, 2H, NH), 8.61 (s, 2H, NH), 7.99 (m, 4H, ArH), 7.75 (dd, 2H, J = 7.9 & 1.1 Hz, ArH), 7.50 (m, 8H, ArH) 7.22 (td, 2H, J = 7.5 & 1.5 Hz, ArH), 7.11 (td, 2H, J = 7.6 & 1.5 Hz, ArH). ^{13}C NMR 75 MHz in DMSO-d_6 δ (ppm): 165.6 (CO), 153.7 (CO), 134.3 (C), 133.5 (C), 131.6 (CH), 129.0 (C), 128.4 (CH), 127.7 (CH), 126.8 (CH), 126.0

(CH), 123.3 (CH), 122.9 (CH). LRMS (ES-): 562.9 $[M+TFA-H]^-$, 934.9 $[2M+Cl]^-$, 1386.2 $[3M+Cl]^-$. IR (cm^{-1}): 3239, 3058, 3027, 1704, 1638, 1593, 1514, 1472, 1437, 1296, 1261 Microanalysis for $C_{27}H_{22}N_4O_3$. Calc. (%) C = 71.99, H = 4.92, N = 10.65. Found (%) C = 71.75, H = 4.87, N = 12.36. m.p. (EtOH) = 198 °C.

Pyridine-2,6-dicarboxylic acid bis-[(3-phenylcarbamoyl-phenyl)-amide]) (97):

A solution of 3-aminobenzanilide (0.48 g, 2.26 mmol), triethylamine (0.35 mL, 2.49 mmol) and DMAP (a few mg, cat.) in dry DCM (50 mL) was stirred for 15 m before adding 2,6-pyridinedicarbonyl chloride (0.23 g, 1.13 mmol). The reaction was left stirring at ambient temperature for 18 h after which the resulting white precipitated product was removed by filtration was washed with DCM and water with the product isolated as a white solid. Mass of product = 0.32 g. Yield = 52%. ^{11}H NMR 300 MHz in DMSO-d_6 δ (ppm): 11.25 (s, 2H, NH), 10.34 (s, 2H, NH), 8.47 (m, 2H, ArH), 8.45 (s, 2H, ArH), 8.34 (dd, 1H, J = 8.7 & 6.78 Hz, ArH), 8.19 (m, 1H, ArH), 8.16 (m, 1H, ArH), 7.80 (m, 6H, ArH), 7.62 (t, 2H, J = 7.9 Hz, ArH), 7.37 (m, 4H, ArH), 7.12 (m, 2H, ArH). ^{13}C NMR 75 MHz in DMSO-d_6 δ (ppm): 165.4 (CO), 162.0 (CO), 148.7 (C), 140.1 (CH), 139.1 (C), 138.3 (C), 135.8 (C), 128.9 (CH), 128.6 (CH), 125.6 (CH), 124.2 (CH), 123.8 (CH), 123.4 (CH), 120.7 (CH), 120.5 (CH). LRMS (ES+): 578.1 $[M+Na]^+$, 1133.4 $[2M+Na]^+$, 1163.7 $[2M+MeOH+Na]^+$. IR (cm^{-1}): 3235, 3135, 3058, 1646, 2584, 1528, 1422, 1324, 1237, 1142, 1079, 998, 902. Microanalysis for $C_{33}H_{25}N_5O_4$ + 0.25 CH_3OH. Calc. (%) C = 70.86, H = 4.65, N = 12.43. Found (%) C = 70.72, H = 4.43, N = 12.50. m.p. (H_2O) = 194 °C.

***N,N'*-Bis-(3-phenylcarbamoyl-phenyl)-isophthalamide (98).**

A solution of 3-aminobenzanilide (1.00 g, 4.7 mmol), triethylamine (0.72 mL, 5.2 mmol), DMAP (0.003 g cat) in dry DCM (30 mL) was stirred for 30 m before adding isophthaloyl dichloride (0.48 g, 2.3 mmol). The reaction was left stirring at ambient temperature for 16 h before the precipitated white product was removed by filtration and subsequently washed with DCM (2 × 10 mL) followed by water (2 × 10 mL). The precipitated was dried under high vacuum, however ^1H NMR analysis revealed approximately 10% of mono substituted isophthalic acid side product. The crude product

was further purified by suspending in acidic MeOH (100 mL) solution and refluxing for 18 h. After this time reaction suspension was filtered hot and washed with MeOH (2 × 20 mL) with the product obtained as a white solid. Mass of product = 0.65 g. Yield = 54%. ^{1}H NMR 400 MHz in DMSO-d_6 δ (ppm): 10.63 (s, 2H, NH), 10.28 (s, 2H, NH), 8.33 (t, 2H, J = 1.8 Hz, ArH), 8.21 (dd, 2H, J = 8.0 & 1.8 Hz, ArH), 8.07 (m, 2H,ArH), 7.78 (m, 4H, ArH), 7.72 (m, 3H, ArH), 7.54 (t, 2H, J = 7.7 Hz, ArH), 7.36 (m, 4H, ArH), 7.10 (m, 2H, ArH). ^{13}C NMR 100 MHz in DMSO-d_6 δ (ppm): 165.5 (CO), 165.1 (CO), 139.2 (C), 139.1 (C), 135.7 (C), 134.9 (C), 130.8 (CH), 128.7 (CH), 128.6 (CH), 127.1 (CH), 123.7 (CH), 123.3 (CH), 122.7 (CH), 120.4 (CH), 120.0 (CH). IR (cm^{-1}): 3288, 3061, 1689, 1645, 1534, 1451, 1326, 1253. LRMS (ES-): 725.2 $[M+TFA+Acetone-H]^-$. (ES+): 555.0 $[M+H]^+$. IR (cm^{-1}): 3288, 3061, 1589, 1645, 1534, 1451, 1326, 1253. Microanalysis for $C_{34}H_{26}N_4O_4$. Calc. (%) C = 73.19, H = 4.65, N = 10.35. Found (%) C = 73.24, H = 4.68, N = 9.97. m.p. (MeOH) >300 °C.

Macrocycle (99):

A solution of DCM (500 mL) with triethylamine (0.49 mL, 3.43 mmol) and a small catalytic quantity 4-dimethylaminopyridine (0.01 g) was set up and left stirring whilst two additional solutions were prepared. The first solution contained 1,3-bis-(2-(3-amino)-benzanilide-phenyl)-urea (1.50 g, 3.12 mmol) and TBA acetate (1.50 g, 4.97 mmol) in dry DCM (50 mL), whilst the second 2,6-pyridinedicarbonyl chloride (0.64 g, 3.12 mmol) in dry DCM (50 mL). Both additional solutions were introduced into the reaction vessel using a motor-driven syringe pump over a period of 6 h. After the addition the reaction was left stirring at ambient temperature for a further 72 h. Following this the volume of solvent was reduced by approximately ¾ and reaction was extracted with water (3 × 200 mL). The retained organic phase was dried with $MgSO_4$ before removal of solvent under rotary evaporator. The light grey residue was dissolved in a small volume of 92:8 DCM/MeOH before purification by flash column chromatography. The white coloured solid was further purified by trituation from hot ethyl acetate to afford the product as a white powder. Mass of solid = 0.32 g. Yield = 17%. ^{1}H NMR 400 MHz in DMSO-d_6 δ (ppm): 11.26 (s, 2H, amide NH), 9.99 (s, 2H, amide NH), 8.54 (d, 2H, J = 8.3 Hz, ArH), 8.50 (s, 2H, urea NH), 8.43-8.32 (m, 3H,

ArH), 8.16 (s, 2H, ArH), 7.97 (d, 2H, J = 8.3 Hz, ArH), 7.72 (d, 2H, J = 8.3 Hz, ArH), 7.60 (t, 2H, J = 7.9 Hz, ArH), 7.31-7.21 (m, 4H, ArH), 7.07 (t, 2H, J = 7.5 Hz, ArH). ^{13}C NMR - 100 MHz (DMSO-d_6) δ (ppm): 166.9 (CO), 161.6 (CO), 153.2 (CO), 148.5 (C), 140.4 (CH), 138.0 (C), 136.0 (C), 134.9 (C), 129.1 (CH), 128.3 (C), 127.3 (CH), 126.5 (CH), 125.2 (CH), 123.4 (CH), 122.9 (CH), 122.8 (CH), 120.8 (CH). LRMS (ES-): 646.3 $[M+Cl]^-$, 673.3 $[M+2MeOH-H]^-$, 724.4 $[M+TFA-H]^-$, 1284.8 $[2M+2MeOH-H]^-$. Rf: 0.45 (96:4 DCM/MeOH). Microanalysis for $C_{34}H_{25}N_7O_5$ + 0.50 CH_2Cl_2. Calc. (%) C = 63.35, H = 4.01, N = 14.99. Found (%) C = 63.19, H = 4.17, N = 14.96. m.p. (ethyl acetate) = decomp. 235 °C.

1,3-Bis-(2-(3-nitro)-benzanilide-phenyl)-urea (105):

A solution of 3-nitrobenzoic acid (3.13 g, 18.73 mmol), triethylamine (2.81 mL, 20.60 mmol), PyBOP (9.75 g, 18.73 mmol) and HOBt (0.01g) in anhydrous DMF (40 mL) was stirred for 15 m before 1,3-bis-(2-aminophenyl)urea (2.27 g, 9.37 mmol) was slowly added. The reaction was left stirring at ambient temperature for 72 h, after which time the solvent was removed using reduced pressure distillation to afford a brown solid residue. The residue was re-suspended in MeOH (50 mL) and filtered before being further washed with Et_2O. The product was obtained as a white solid. Mass of product = 3.70 g. Yield = 52%. ^{1}H NMR 400 MHz in DMSO-d_6 δ (ppm): 10.37 (s, 2H, NH), 8.78 (s, 2H, NH), 8.52 (s, 2H, NH), 8.39 (m, 4H, ArH), 7.84 (dd, 4H, J = 8.3 & 1.5 Hz, ArH), 7.75 (t, 2H, J = 7.9 Hz, ArH), 7.40 (dd, 2H, J = 7.5 & 1.1 Hz, ArH), 7.25 (m, 2H, ArH), 7.10 (m, 2H, ArH). ^{13}C NMR 100 MHz in DMSO-d_6 δ (ppm): 163.6 (CO), 153.3 (CO), 147.7 (C), 135.7 (C), 134.1 (CH), 130.0 (CH), 128.1 (C), 127.1 (CH), 126.5 (CH), 126.1 (CH), 123.1 (CH), 122.6 (CH), 122.4 (CH). IR (cm^{-1}): 3379, 3231, 1641, 1517, 1346, 1316, 751. LRMS (ES-): 653.1 $[M+TFA-H]^-$, 1193.7 $[2M+TFA-H]^-$, 1733.4 $[3M+TFA-H]^-$. IR (cm^{-1}): 3380,3231, 1641, 1517, 1348, 1316. Microanalysis for $C_{27}H_{20}N_5O_7$. Calc. (%) C = 60.00, H = 3.73, N = 15.54. Found (%) C = 59.70, H = 3.83, N = 15.60. m.p. (Et_2O) = 217 °C.

1,3-Bis-(2-(3-amino)-benzanilide-phenyl)-urea (106):

A stirring suspension of 1,3-bis-(2-(3-nitro)-benzanilide-phenyl)-urea (0.50 g, 0.93 mmol) in ethanol (150 mL) was produced to which was added Pd/C 10% (0.01 g, cat.) and hydrazine monohydrate (0.10 mL) dropwise. The reaction was then heated to reflux and left stirring for 16 h after which the reduced product was removed via filtration. The product was dissolved in DMF and filtered to remove Pd/C after which time the solvent was removed via reduced pressure distillation, resuspended in DCM and washed with water to remove remaining DMF. The white precipitated product was removed via filtration and washed with MeOH. Mass of product = 0.40 g. Yield = 89%. ^{1}H NMR 300 MHz in DMSO-d_6 δ (ppm):9.79 (s, 2H, amide NH), 8.62 (s, 2H, urea NH), 7.65 (dd, 2H, J = 7.9 & 1.5 Hz, ArH), 7.49 (dd, 2H, J = 7.5 & 1.5 Hz, ArH), 7.22-7.09 (m, 10H, ArH), 6.75 (m, 2H, ArH), 5.27 (s, 4H, NH_2). ^{13}C NMR 75 MHz in DMSO-d_6 δ (ppm): 166.1 (CO), 153.9 (CO), 148.8 (C), 135.1 (C), 132.9 (C), 129.7 (C), 128.8 (CH), 126.4 (CH), 125.7 (CH), 123.5 (CH), 123.1 (CH), 116.9 (CH), 114.5 (CH), 113.2 (CH). LRMS (ES-): 515.2 $[M+Cl]^-$, 542.1 $[M+2MeOH-H]^-$, 559.1 $[M+Br]^-$, 593.3 $[M+TFA-H]^-$, 995.4 $[2M+Cl]^-$, 1041.4 $[2M+Br]^-$, 1073.6 $[2M+TFA-H]^-$. IR (cm^{-1}): 3312, 3285, 1641, 1509, 1441, 1308, 1293, 1275, 1233. Microanalysis for $C_{27}H_{24}N_5O_3$ + 0.25 CH_3OH. Calc. (%) C = 67.00, H = 5.16, N = 17.20. Found (%) C = 66.80, H = 5.11, N = 17.06. m.p. (MeOH) = 194 °C.

7.3.3. Synthetic schemes included in chapter 4.

9,10-dihydro-9,10-dioxo-N^1,N^3-diphenylanthracene-1,3-dicarboxamide (118):

Aniline (1.00 g, 10.8 mmol), triethylamine (1.66 mL, 11.9 mmol) and DMAP (a few mg cat.) were dissolved in dry DCM (30 mL) and stirred together for 15 m, before the slow addition of anthraquinone-1,3-dicarbonylchloride (1.78 g, 5.4 mmol) to the reaction over the course of a further 15 m. The reaction was left stirring at ambient temperature for 18 h after which the resulting yellow precipitate was removed from suspension via filtration and washed with DCM and water. The product was further purified by titration from hot acetonitrile and dried under high vacuum to afford the product as a yellow solid. Mass of product = 1.03 g. Yield = 43%. ^{1}H NMR 400 MHz in DMSO-d_6 δ (ppm): 10.75 (s, 1H, NH), 10.36 (s, 1H, NH), 8.89 (d, 1H, J = 1.9 Hz, ArH), 8.47 (d, 1H, J = 1.9 Hz, ArH), 8.29 (m, 1H, ArH), 8.19 (m, 1H, ArH), 7.98 (m, 2H, ArH), 7.82 (d, 2 H, J = 7.9 Hz, ArH), 7.72 (d, 2H, J = 7.9 Hz, ArH), 7.40 (overlapping t, 4H, J = 7.5 Hz, ArH), 7.14 (m, 2H, ArH). ^{13}C NMR DMSO-d_6 (100 MHz): δ (ppm) 181.8 (CO), 166.6 (CO), 166.0 (CO), 139.3 (C), 139.1 (C), 138.7 (C), 138.6 (C), 135.0 (CH), 134.8 (CH), 133.7 (C), 133.4 (C), 132.5 (C), 132.1 (CH), 132.0 (CH), 128.8 (CH), 128.7 (CH), 127.1 (CH), 126.9 (CH), 126.9 (CH), 124.3 (CH), 123.6 (CH), 120.7 (CH), 119.5 (CH). IR (cm^{-1}): 3250, 2325, 1644, 1527, 1267, 752. LRMS (ES+): 447.1 $(M+H)^+$, 893.3 $(2M+H)^+$, 915.2 $(2M+Na)^+$. HRMS (ES-): Calc. = 481.0960. Observed = 481.0949. Δ = 2.4 ppm. (ES+): Calc. = 447.1339. Observed = 447.1336. Δ = 0.8 ppm. Microanalysis for $C_{23}H_{18}N_2O_4$. Calc. (%) C = 75.33, H = 4.06, N = 6.27. Found (%) C = 74.99, H = 4.09, N = 6.21. m.p. (acetonitrile) = decomp. 278-283 °C.

N^1,N^3-bis(4-butylphenyl)-9,10-dihydro-9,10-dioxoanthracene-1,3-dicarboxamide (119):

4-Butylaniline (1.72 mL, 10.9 mmol) was stirred with triethylamine (1.66 mL, 11.9 mmol) and DMAP (a few mg) in dry DCM (80 mL) for 15 m before the portionwise addition of anthraquinone-1,3-dicarbonylchloride (1.82g, 5.4 mmol). Reaction was left stirring at ambient temperature for 18 h. The precipitated product was removed by filtration and washed with DCM and water, before purifying by refluxing in acidic EtOH

and filtering hot. Product was isolated as a yellow powder. Mass of product = 1.32 g. Yield = 43%. ^{1}H NMR DMSO-d_6 (400 MHz) δ (ppm): 10.68 (s, 1H, NH), 10.27 (s, 1H, NH), 8.87 (d, 1H, J = 1.9 Hz, ArH), 8.44 (d, 1H, J = 1.9Hz, ArH), 8.27 (m, 1H, ArH), 8.18 (m ,1H, ArH), 7.97 (m, 2H, ArH), 7.72 (d, 2H, J = 8.7 Hz, ArH), 7.62 (d, 2H, J = 8.6 Hz, ArH), 7.21 (d, 2H, J = 3.0 Hz, ArH), 7.19 (d, 2H, J = 3.0 Hz, ArH). 2.55 (m, 4H, CH_2), 1.57 (m, 4H, CH_2), 1.32 (m ,4H, CH_2), 0.91 (m, 6H, CH_3). ^{13}C NMR DMSO-d_6 (100 MHz) δ (ppm): 181.9 (CO), 166.5 (CO), 162.9 (CO), 139.2 (C), 138.9 (C), 138.5 (C), 137.6 (C), 137.1 (C), 136.3 (C), 135.1 (CH), 134.8 (CH), 133.8 (C), 133.5 (C), 132.6 (C), 132.1 (CH), 131.9 (C), 128.6 (CH), 128.5 (CH), 127.1 (CH), 126.9 (CH), 120.8 (CH), 119.6 (CH), 34.3 (CH_2), 33.2 (CH_2), 21.7 (CH_2), 13.8 (CH_3). IR (cm^{-1}): 3241, 3185, 3118, 3058, 2950, 2920, 2851, 1675, 1661, 1642, 1598, 1509, 1402, 1329, 1156, 1000, 911, 834. LRMS (ES-): 639.1 $[M+Br]^-$, 1195.8 $[2M+Br]^-$, 1755.1 $[3M+Br]^-$. Microanalysis for $C_{36}H_{34}N_2O_4$. Calc. (%) C = 77.40, H = 6.13, N = 5.01. Found (%) C = 77.13, H = 6.09, N = 4.93. m.p. (EtOH) = 267 °C.

9,10-dihydro-N^1,N^3-bis(3,5-dimethoxyphenyl)-9,10-dioxoanthracene-1,3-dicarboxamide (120):

3,5-Dimethoxyaniline (1.90 g, 12.2 mmol) was stirred with triethylamine (1.29 g, 12.8 mmol) and DMAP (a few mg cat.) in dry DCM (80 mL) for 15 m before the portionwise addition of anthraquinone-1,3-dicarbonylchloride (2.02 g, 6.1 mol) over 15 m. The reaction was left stirring at ambient temperature for 18 h. The precipitated product was removed from suspension via filtration and washed with DCM and water. Product was further purified by multiple crystallisations from hot acetonitrile. Product was isolated as a yellow solid. Mass of product = 1.23 g. Yield = 36%. ^{1}H NMR DMSO-d_6 (400 MHz) δ (ppm): 10.64 (s, 1H, NH), 10.31 (s, 1H, NH), 8.86 (d, 1H, J = 1.5 Hz, ArH), 8.44 (d, 1H, J = 1.5 Hz, ArH), 8.29 (m, 1H, ArH), 8.19 (m, 1H, ArH), 7.98 (m, 2H, ArH), 7.13 (d, 2H, J = 2.2 Hz, ArH), 6.96 (d, 2H, J = 2.2 Hz, ArH), 3.76 (s, 6H, CH_3), 3.75 (s, 6H, CH_3). ^{13}C NMR DMSO-d_6 (100 MHz) δ (ppm): 181.7 (CO), 166.6 (CO), 163.0 (CO), 160.6 (C), 160.4 (C), 140.9 (C), 140.3 (C), 138.9 (C), 138.6 (C), 134.9 (C), 134.7 (C), 133.6 (C), 133.4 (C), 132.5 (C), 132.0 (C), 131.9 (C), 127.1 (CH), 126.9 (CH), 126.8 (CH), 98.8 (CH), 97.8 (CH), 96.3 (CH), 96.5 (CH), 55.2 (CH_3), 55.1 (CH_3).

IR (cm^{-1}): 3225, 3085, 2949, 2842, 2650, 2325, 1676, 1596, 1276, 1198. LRMS (ES-): 601.2 $(M+Cl)^-$, 1167.5 $(2M+Cl)^-$. HRMS (ES-): Calc. = 601.1383. Observed = 601.1365. Δ = 2.9 ppm. (ES+): Calc. = 567.1762. Observed = 567.1758. Δ = 0.6 ppm. Microanalysis for $C_{32}H_{26}N_2O_8$. Calc. (%) C = 67.84, H = 4.63, N = 4.94. Found (%) C = 67.69, H = 4.63, N = 5.01. m.p. (acetonitrile) = decomp. 283-284 °C.

N^1,N^3-bis(3,5-dichlorophenyl)-9,10-dihydro-9,10-dioxoanthracene-1,3-dicarboxamide (121):

3,5-Dichloroaniline (1.92 g, 11.6 mmol) was stirred with triethylamine (1.29 g, 12.8 mmol) and DMAP (a few mg cat.) in dry DCM (80 mL) for 15 m before the portionwise addition of anthraquinone-1,3-dicarbonylchloride (1.94 g, 5.8 mol) over 15 m. The reaction was left stirring at ambient temperature under N_2 for 18 h. The precipitated product was removed from suspension via filtration and washed with DCM and water. Product was further purified by multiple crystallisations from hot acetonitrile. Product was isolated as a yellow solid. Mass of product = 0.21 g. Yield = 6%. ^{1}H NMR DMSO-d_6 (400 MHz) δ (ppm): 10.99 (s, 1H, NH), 10.77 (s, 1H, NH), 8.89 (d, 1H, J = 1.5 Hz, ArH), 8.45 (d, 1H, J = 1.5 Hz, ArH), 8.28 (m, 1H, ArH), 8.19 (m, 1H, ArH), 7.98 (m, 2H, ArH), 7.93 (d, 2H, J = 1.9 Hz, ArH), 7.76 (d, 2H, J = 1.9 Hz, ArH), 7.38 (m, 2H, ArH). ^{13}C NMR DMSO-d_6 (100 MHz) δ (ppm): 181.8 (CO), 181.6 (CO), 167.1 (CO), 163.4 (CO), 141.5 (CH), 141.0 (C), 138.4 (C), 137.8 (C), 1351 (CH), 134.9 (CH), 134.3 (C), 134.0 (C), 133.8 (C), 133.2 (C), 132.5 (C), 132.2 (C), 132.0 (CH), 127.2 (CH), 127.2 (C), 126.9 (CH), 123.5 (CH), 122.9 (CH), 118.7 (CH), 117.6 (CH). IR (cm^{-1}): 3213, 3177, 3077, 1677, 1650, 1589, 1275, 849, 706. LRMS (ES-): 618.9 $(M+Cl)^-$, 699.0 $(M+2MeCN+Cl)^-$, 1202.5 $(2M+Cl)^-$. HRMS (ES-): Calc. = 616.9402. Observed = 616.9395. Δ = 1.1 ppm. Microanalysis for $C_{28}H_{14}Cl_4N_2O_4$ + 0.33 CH_2Cl_2: Calc. (%) C = 55.72, H = 2.61, N = 4.53. Found (%) C = 55.68, H = 2.99, N = 4.32. m.p. (acetonitrile) = decomp. 281-284 °C.

N^1,N^3-dibutyl-9,10-dihydro-9,10-dioxoanthracene-1,3-dicarboxamide (122):

n-Butylamine (0.67 mL, 6.7 mmol) was stirred with triethylamine (1.03 mL, 7.4 mmol) and DMAP (a few mg) in dry DCM (40 mL) for 15 m before the portionwise addition of anthraquinone-1,3-dicarbonylchloride (1.12 g, 3.4 mmol) over 15 m. Reaction was left stirring at ambient temperature for 18 h. The precipitated product was removed by filtration and washed with DCM (3 × 5 mL). Product was isolated as a yellow powder. Mass of product = 0.47 g. Yield = 34%. ^{1}H NMR DMSO-d_6 (400 MHz) δ (ppm): 8.97 (t, 1H, J = 5.3 Hz. NH), 8.70 (d, 1H, J = 1.9 Hz, ArH), 8.26-8.14 (m, 3H, ArH & NH), 8.12 (d, 1H, J = 1.9 Hz, ArH), 7.95 (m, 2H, ArH), 3.29 (m, 4H, CH_2), 1.54 (m, 4H, CH_2), 1.39 (m, 4H, CH_2), 0.93 (m, 6H, CH_3). ^{13}C NMR DMSO-d_6 (100 MHz) δ (ppm): 181.90 (CO), 181.58 (CO), 168.00 (CO), 163.73 (CO), 139.52 (C), 138.58 (C), 134.87 (CH), 134.48 (CH), 133.60 (C), 132.44 (C), 131.68 (CH), 126.87 (CH), 126.68 (CH), 125.86 (CH), 39.14 (CH_2), 38.82 (CH_2), 30.94 (CH_2), 30.76 (CH_2), 19.68 (CH_2), 19.61 (CH_2), 13.73 (CH_3), 13.64 (CH_3). LRMS (ES-): 519.2 $[M+TFA-H]^-$, 847.2 $[2M+Cl]^-$, 925.1 $[2M+TFA-H]^-$, 1253.3 $[3M+Cl]^-$, 1331.6 $[3M+TFA-H]^-$. Microanalysis for $C_{24}H_{26}N_2O_4$. Calc. (%) C = 70.92, H = 6.45, N = 6.89. Found (%) C = 70.70, H = 6.43, N = 6.79. m.p. (DCM) = 258 °C.

7.3.4. Synthetic schemes included in chapter 5.

N^1,N^3-dibutylanthracene-1,3-dicarboxamide (132):

n-Butylamine (0.43 mL, 4.4 mmol) was dissolved in dry DCM (25 mL) before the dropwise addition of 2M trimethylaluminium solution in hexane (2.2 mL, 4.4 mmol) with the solution left stirring for 30 m. Addition of 1,3-anthracenedimethyl ester (0.64 g, 2.2 mmol) proceeded heating to reflux for 5 days. Reaction mixture was allowed to cool before the addition of aqueous HCl solution (1:10 v/v) until bubbling ceased. A further 50 mL of water was added and the reaction was stirred for a further 30 m before partition performed with water (3 × 50 mL) with organic phase containing the suspended compound retained. The remaining solvent was removed *in vacuo* with compound dried under high vacuum. Product was isolated as a pale yellow solid. Mass of product = 0.26 g. Yield = 32%. ^{1}H NMR $CDCl_3$-d_1 (300 MHz) δ (ppm): 8.65 (s, 1H, NH), 8.02 (s, 1H, NH), 7.99 (s, 1H, ArH), 7.86 (d, 1H, J = 8.4 Hz, ArH), 7.68 (d, 1H, J = 8.4 Hz, ArH), 7.62 (d, 1H, J = 1.1 Hz, ArH), 7.40 (m, 2H, ArH), 6.79 (m, 2H, ArH), 3.50 (q, 2H, J = 7.0 Hz, CH_2), 3.40 (q, 2H, J = 6.9 Hz, CH_2), 1.64 (m, 4H, overlapping CH_2), 1.43 (m, 4H, overlapping CH_2), 0.97 (m, 6H, overlapping CH_3). ^{13}C NMR $CDCl_3$-d_1 (75 MHz) δ (ppm): 169.3 (CO), 167.4 (CO), 134.9 (C), 133.0 (C), 131.8 (C), 130.3 (C), 130.0 (CH), 129.9 (C), 128.7 (CH), 128.3 (C), 128.2 (CH), 128.0 (CH), 126.6 (CH), 126.3 (CH), 124.6 (CH), 122.2 (CH), 40.2 (CH_2), 40.0 (CH_2), 31.8 (CH_2), 20.4 (CH_2), 13.9 (CH_3). IR (cm^{-1}): 3247, 2954, 1654, 1624, 1553, 1294, 1250, 1157, 875, 733. LRMS (ES-): 489.0 $(M+TFA-H)^-$, 865.2 $(2M+TFA-H)^-$. Microanalysis for $C_{24}H_{28}N_2O_2$ + 0.17 CH_2Cl_2. Calc. (%) C = 74.30, H = 7.31, N = 7.17. Found (%) C = 74.23, H = 7.41, N = 7.15. m.p. (H_2O) = 173 ° C.

N^1,N^3-diphenylanthracene-1,3-dicarboxamide (133):

Aniline (0.54 g, 5.8 mmol) was dissolved in dry DCM (30 mL) before the dropwise addition of 2M trimethylaluminium solution in hexane (2.9 mL, 5.8 mmol) with the solution left stirring for 30 m. Addition of 1,3-anthracenedimethyl ester (0.85g, 2.9mmol) proceeded heating to reflux for 5 days. The reaction mixture was allowed to cool before the addition of aqueous HCl solution (1:10 v/v) until bubbling ceased. A

further 75 mL of water was added and the reaction was stirred for a further 30 m before partition performed with water (3 × 50 mL) with organic phase containing the suspended compound retained. Remaining solvent was removed *in vacuo* with compound dried under high vacuum. Product was isolated as a pale yellow solid. Mass of product = 0.99 g. Yield = 82%. ^{1}H NMR DMSO-d_6 (300 MHz) δ (ppm): 10.77 (s, 1H, NH), 10.56 (s, 1H, NH), 8.92 (m, 2H, ArH), 8.89 (m, 1H, ArH), 8.20 (m, 2H, ArH), 7.87 (m, 4H, ArH), 7.61 (m, 2H, ArH), 7.40 (m, 4H, ArH), 7.16 (m, 2H, ArH). ^{13}C NMR DMSO-d_6 (75 MHz) δ (ppm): 166.9 (CO), 164.8 (CO), 139.3 (C), 139.1 (C), 134.8 (C), 132.6 (C), 131.6 (C), 131.2 (CH), 130.3 (C), 130.3 (C), 128.8 (CH), 128.7 (CH), 128.6 (CH), 128.1 (CH), 127.0 (CH), 126.5 (CH), 124.2 (CH), 123.9 (CH), 123.5 (CH), 120.5 (CH), 120.0 (CH). IR (cm^{-1}): 3274, 3126, 1638, 1594, 1526, 1491, 1317, 1247, 893, 865. LRMS (ES-): 529.0 $(M+TFA-H)^-$, 945.1 $(2M+TFA-H)^-$, 1362.9 (3M+TFA-H). Microanalysis for $C_{28}H_{20}N_2O_2$ + 0.20 CH_3CN. Calc. (%) C = 80.32, H = 4.89, N = 7.26. Found (%) C = 80.02, H = 4.81, N = 6.92. m.p. (H_2O) = decomp. 243-248 °C.

N^1,N^2-dibutylanthracene-1,2-dicarboxamide (135):

Anthracene-1,2-diamine (0.50 g, 2.4 mmol), triethylamine (0.74 mL, 5.3 mmol) and DMAP (a few mg. cat) were stirred together for 15 m in dry DCM (15 mL) before the dropwise addition of valeroyl chloride (0.56mL, 4.8 mmol). The reaction was left stirring at ambient temperature for 18 h. After this time the reaction solvent was washed with water (3 × 25 mL) before the remaining solvent was removed *in vacuo*. Recrystalized from hot ethyl acetate before crude reaction was purified by flash column chromatography (90:10 DCM:MeOH), with product isolated as a yellow/beige solid. Mass of product = 0.35 g. Yield = 39%. ^{1}H NMR DMSO-d_6 (300 MHz) δ (ppm): 9.75 (s, 1H, NH), 9.21 (s, 1H, NH), 8.57 (s, 1H, ArH), 8.46 (s, 1H, ArH), 8.04 (m, 3H, ArH), 7.80 (d, 1H, J = 9.1 Hz, ArH), 7.52 (m, 2H, ArH), 2.59 (t, 2H, J = 7.2 Hz, CH_2), 2.39 (t, 2H, J = 7.2 Hz, CH_2), 1.71 (m, 2H, CH_2), 1.62 (m, 2H, CH_2), 1.46 (m, 2H, CH_2), 1.37 (m, 2H, CH_2), 0.97 (t, 3H, J = 7.5 Hz, CH_3), 0.93 (t, 3H, J = 7.5 Hz, CH_3). ^{13}C NMR DMSO-d_6 (75 MHz) δ (ppm): 173.6 (CO), 172.83 (CO), 131.78 (C), 131.3 (C), 130.0 (C), 129.3 (C), 128.4 (CH), 128.0 (CH), 127.8 (CH), 127.6 (CH), 126.8 (CH), 126.0 (CH), 125.8 (CH), 123.7 (C), 123.5 (CH), 121.3 (CH), 37.1 (CH_2), 36.6 (CH_2), 28.3 (CH_2), 27.8

(CH_2), 22.6 (CH_2), 22.5 (CH_2), 14.0 (CH_3), 13.9 (CH_3). IR (cm^{-1}): 3241, 2953, 2933, 2868, 1652, 1530, 1425, 1289, 1185, 1093, 880, 736. LRMS (ES-): 411.0 $[M+Cl]^-$, 438.0 $[M+2MeOH-H]^-$, 489.1 $[M+TFA-H]^-$, 787.4 $[2M+Cl]^-$, 814.0 $[2M+2MeOH-H]^-$, 865.3 $[2M+TFA-H]^-$. R_f: 0.56 (90:10 DCM/MeOH). Microanalysis for $C_{24}H_{28}N_2O_2$. Calc. (%) C = 76.56, H = 7.50, N = 7.44. Found (%) C = 76.50, H = 7.50, N = 7.42. m.p. (DCM/MeOH) = 176 °C.

N^1,N^2-diphenylanthracene-1,2-dicarboxamide (136):

Anthracene-1,2-diamine (0.77 g, 3.7 mmol), triethylamine (1.12 mL, 8.14 mmol) and DMAP (a few mg, cat.) were stirred together for 15 m in dry DCM (75 mL) before the dropwise addition of benzoyl chloride (0.86mL, 7.4 mmol). Reaction was left stirring at ambient temperature under N_2 for 18 h after which the precipitated product was removed via filtration and washed with DCM, water and Et_2O. Product was isolated as a yellow powder. Mass of product = 1.26 g. Yield = 82%. ^1H NMR DMSO-d_6 (300 MHz) δ (ppm): 10.42 (s, 1H, NH), 10.06 (s, 1H, NH), 8.66 (s, 1H, ArH), 8.59 (s, 1H, ArH), 8.14 (m, 5H, ArH), 7.92 (m, 3H, ArH), 7.57 (m, 8H, ArH). ^{13}C NMR DMSO-d_6 (75 MHz) [in the presence of 5 equivalents TBACl] δ (ppm): 165.7 (CO), 165.0 (CO), 133.9 (C), 131.8 (CH), 131.8 (CH), 131.2 (CH), 129.8 (C), 128.7 (C), 128.4 (CH), 128.3 (CH), 128.1 (CH), 127.8 (CH), 127.7 (CH), 126.9 (CH), 16.3 (CH), 125.8 (CH), 125.5 (CH), 124.7 (CH), 122.5 (CH), 57.54 (TBA CH_2), 23.1 (TBA CH_2), 19.2 (TBA CH_2), 13.4 (TBA CH_3). IR (cm^{-1}): 3247, 3037, 1647, 1519, 1459, 1289, 894. LRMS (ES-): 450.9 $[M+Cl]^-$, 477.9 $[M+2MeOH-H]^-$, 529.0 $[M+TFA-H]^-$, 862.5 $[2M+MeOH-H]^-$, 945.7 $[2M+TFA-H]^-$. Microanalysis for $C_{28}H_{20}N_2O_2 + 0.40\ CH_2Cl_2$. Calc. (%) C = 75.73, H = 4.65, N = 6.22. Found (%) C = 75.98, H = 4.63, N = 6.22. m.p. (Et_2O) = decomp. 251-255 °C.

1,2-Anthracene bis-butylurea (137).

Anthracene-1,2-diamine (0.20 g, 1.0 mmol) was dissolved in dry DCM (40 mL), with butylisocyanate (0.22 mL, 2.0 mmol) added dropwise. The reaction was left stirring at ambient temperature for 18 h. Solvent was removed in vacuo before redissolving in 90:10 DCM:MeOH and purifying by flash column chromatography. The product was

further purified by recrystalisation from EtOH. Product obtained as a brown solid. Mass of product = 0.21 g. Yield = 54%. ^{1}H NMR DMSO-d_6 (300 MHz) δ (ppm): 8.49 (s, 1H, NH), 8.20 (m, 2H, NH & ArH), 7.92 (m, 4H, ArH), 7.46 (m, 2H, ArH), 7.08 (t, 1H, J = 5.1 Hz, NH), 6.30 (br s, 1H, NH), 3.12 (m, 4H, CH_2), 1.45 (m, 4H, CH_2), 1.34 (m, 4H, CH_2), 0.90 (m, 6H, CH_3). ^{13}C NMR DMSO-d_6 (75 MHz) δ (ppm): 15.7.0 (CO), 155.2 (CO), 131.3 (C), 130.1 (C), 129.9 (C), 128.6 (C), 127.9 (CH), 127.7 (CH), 126.4 (CH), 126.2 (CH), 125.7 (CH), 124.8 (CH), 122.3 (CH), 120.0 (CH), 39.22 (CH_2), 38.9 (CH_2), 32.0 (CH_2), 31.8 (CH_2), 19.6 (CH_2), 19.5 (CH_2), 13.7 (CH_3), 13.6 (CH_3). IR (cm^{-1}): 3268, 2953, 2924, 2858, 1637, 1561, 1458, 1239, 882, 741. LRMS (ES-): 441.5 $[M+Cl]^-$, 519.5 $[M+TFA-H]^-$, 848.4$[2M+Cl]^-$, Microanalysis for $C_{24}H_{30}N_4O_2$. Calc. (%) C = 70.91, H = 7.44, N = 13.78. Found (%) C = 70.61, H = 7.35, N = 13.58. m.p. (EtOH) = decomp. 186-188 °C.

1,2-Anthracene bis-phenylurea (138).

Anthracene-1,2-diamine (0.35 g, 1.7 mmol) was dissolved in dry DCM (40 mL), with phenylisocyanate (0.37 mL, 3.4 mmol) added dropwise. The reaction was left stirring at ambient temperature for 18 h. The precipitated product was removed via filtration and washed with DCM (3 × 10 mL) and MeOH (3 × 10 mL). Product was isolated as a green solid. Mass of product = 0.37 g. Yield = 49%. ^{1}H NMR DMSO-d_6 (300 MHz) δ (ppm): 9.50 (s, 1H, NH), 9.15 (s, 1H, NH), 8.57 (s, 1H, NH), 8.28 (d, 2H, J = 8.8 Hz, ArH), 8.09-8.01 (m, 3H, ArH & NH), 7.52-7.45 (m, 6H, ArH), 7.29 (t, 4H, J = 7.3 Hz), 6.98 (td, 2H, J = 7.3 & 0.7 Hz, ArH). ^{13}C NMR DMSO-d_6 (75 MHz) δ (ppm): 154.1 (CO), 152.7 (CO), 140.1 (C), 139.7 (C), 133.8 (C), 131.5 (C), 130.2 (C), 129.9 (C), 128.8 (CH), 128.7 (CH), 127.9 (CH), 126.9 (CH), 126.4 (CH), 125.9 (CH), 122.4 (CH), 121.9 (CH), 121.7 (CH), 120.1 (CH), 119.9 (C), 118.3 (CH), 118.2 (CH). IR (cm^{-1}): 3261, 3045, 1598, 1563, 1443, 1313, 1222, 874, 727. LRMS (ES-): 559.3 $[M+TFA-H]^-$, 927.6 $[2M+Cl]^-$, 1005.0 $[2M+TFA-H]^-$, 1373.7 $[3M+Cl]^-$. Microanalysis for $C_{24}H_{28}N_2O_2$ + 0.25 CH_2Cl_2. Calc. (%) C = 72.54, H = 4.85, N = 11.98. Found (%) C = 72.48, H = 5.17, N = 11.70. m.p. (DCM/MeOH) = decomp. 261-264 °C.

REFERENCES.

1. Fischer, E. *Ber. Dtsch. Chem. Ges.* **1894,** 2985.
2. Beijer, F. H.; Sijbesma, R.P.; Kooijman, H.; Spek, A .L.; Meijer, E. W. *J. Am. Chem. Soc.* **1998,** 120, 6761.
3. Lafitte, V. G. H.; Aliev, A. E.; Hailes, H. C.; Bala, K.; Golding, P. *J. Org. Chem.* **2005,** 70, 2701.
4. Steed, J. W.; Atwood, J. L. *Supramolecular Chemistry.* Wiley. **2000.**
5. Luecke, H.; Quiochio, F. A. *Nature.* **1990,** 347, 402.
6. Pflugrath, J. W.; Quiochio, F. A. *Science.* **1991,** 251, 1497.
7. Park, C. H.; Simmons, H. E. *J. Am. Chem. Soc.* **1968,** 90, 2431.
8. Bell, R. A.; Christoph, G. G.; Fronczek, F. R.; Marsh, R. E. *Science.* **1975,** 190, 151.
9. Schmuck, C.; Heil, M. *Chembiochem.* **2003,** 4, 1232.
10. Kubik, S.; Kirchner, R.; Nolting, D.; Seidel, J. *J. Am. Chem. Soc.* **2002,** 124, 12752.
11. Casnati, A.; Pirondini, L.; Pelizzi, N.; Ungaro, R. *Supramol. Chem.* **2000,** 12, 53.
12. Kavallieratos, K.; Bertao, C. M.; Crabtree, R. H. *J. Org. Chem.* **1999,** 64, 1675.
13. Ayling, A. J.; Pérez-Payán, M. N.; Davis, A. P. *J. Am. Chem. Soc.* **2001,** 123, 12716.
14. Sasaki, S.-I.; Mizuno, M.; Naemura, K.; Tobe, Y. *J. Org. Chem.* **2000,** 65, 275.
15. Menif, R.; Reibenspies, J.; Martell, A. E. *Inorg. Chem.* **1991,** 30, 3446.
16. Hossain, M. A.; Liljegran, J. A.; Powell, D.; Bowman-James, K. *Inorg. Chem.* **2004,** 43, 3751.
17. Murakami, Y.; Kikuchi, J.-I.; Ohno, T.; Hirayama, T.; Hisaeda, Y.; Nishimura, H.; Snyder, J. P. Steliou, K. *J. Am. Chem. Soc.* **1991,** 113, 8229.
18. Lehn, J.-M.; Méric, R.; Vigneron, J.-P.; Bkouche-Waksman, I.; Pascard, C. *J. Chem. Soc. Chem. Commun.* **1991,** 62.
19. Heyer, D.; Lehn, J.-M. *Tetrahedron Lett.* **1986,** 27, 5869.
20. Dietrich, B.; Hosseini, M. W.; Lehn, J.-M. Sessions, R. B. *J. Am. Chem. Soc.* **1981,** 103, 1282.

21. Schmidtchen, F. P. *Angew. Chem. Int. Ed.* **1977,** 16, 720.
22. Worm, K.; Schmidtchen, F. P. *Angew. Chem. Int. Ed.* **1994,** 34, 65.
23. Nation, D. A.; Reibenspies, J.; Martell, A. E. *Inorg. Chem.* **1996,** 40, 4710.
24. Verschueren, K. H. G.; Seljee, F.; Rozeboom, H. J.; Kalk, K. H.; Dijkstra, B. W. *Nature.* **1993,** 363, 693.
25. Pacal, R. A.; Spergel, J. J.; VanEngen, D. *Tetrahedron Lett.* **1986**, 27, 4099.
26. Valiyateetil, S.; Engbersen, J. F. J.; Verboom, W.; Reinhoudt, D. N. *Angew. Chem. Int. Ed.* **1993,** 32, 900.
27. Choi, K.; Hamilton, A. D. *J. Am. Chem. Soc.* **2001,** 123, 2456.
28. Choi, K.; Hamilton, A. D. *J. Am. Chem. Soc.* **2003,** 125, 10241.
29. Kavallieratos, K.; de Gala, S.R.; Austin, D. J.; Crabtree, R. H. *J. Am. Chem. Soc.* **1997,** 119, 2325.
30. Kavallieratos, K.; Hwang, S.; Crabtree, R. H. J. *Inorg. Chem.* **1999,** 38, 5184.
31. Chang, S.-K.; Hamilton, A. D. *J. Am. Chem. Soc.* **1988,** 110, 1318.
32. Hughes, M. P.; Smith, B. D. *J. Org. Chem.* **1997,** 62, 4492.
33. Prohens, R.; Tomas, S.; Morey, J.; Deya, P. M.; Ballester, P.; Costa, A. *Tetrahedron Lett.* **1998,** 39, 1063.
34. Kubik, S.; Goddard, R.; Kirchner, R.; Nolting, D.; Seidel, J. *Angew. Chem. Int. Ed.* **2001,** 40, 2648.
35. Szumna, A.; Jurczak, J. *Eur. J. Org. Chem.* **2001**, 4031.
36. Yang, Y. S.; Ko, S. W.; Song, I. H.; Ryu, B. J.; Nam, K. C. *Bull. Korean. Chem. Soc.* **2003,** 24, 681.
37. Budka, J.; Lhoták, P.; Michlová, V.; Stilbor, I. *Tetrahedron Lett.* **2001,** 42, 1583.
38. Sansone, F.; Baldini, L.; Casnati, A.; Lazzarotto, M.; Ugozzoli, F.; Ungaro, R. *Proc. Natl. Acad. Sci. USA.* **2002,** 99, 4842.
39. Lankshear, M. D.; Cowley, A. R.; Beer, P .D. *Chem. Commun.* **2006,** 612.
40. Khatri, V. K.; Upreti, S.; Pandey, P. S. *Org. Lett.* **2006,** 8, 1755.
41. Davis, A. P.; Perry, J. J.; Williams, R. P. *J. Am. Chem. Soc.* **1997,** 119, 1793.
42. Gómez, D. E.; Fabbrizzi, L.; Licchelli, M.; Monzani, E. *Org. Biomol. Chem.* **2005,** 3, 1495.
43. Hughes, M. P.; Shang, M.; Smith, B. D. *J. Org. Chem.* **1996,** 61, 4510.

44. Gunnlaugsson, T.; Kruger, P. E.; Lee, T.C.; Parkesh, R. P.; Pfeffer, F. M.; Hussey, G. M. *Tetrahedron Lett.* **2003,** 44, 6575.

45. Pfeffer, F. M.; Buschgen, A. M.; Barnett, N. W.; Gunnlaugsson, T.; Kruger, P. E. *Tetrahedron Lett.* **2005,** 46, 6579.

46. Gunnlaugsson, T.; Davis, A. P.; Glynn, M. *Chem. Commun.* **2001**, 2556.

47. Gunnlaugsson, T.; Kruger, P. E.; Jensen, P.; Pfeffer, F. M.; Hussey, G. M. *Tetrahedron Lett.* **2003,** 44, 8909.

48. Pratt, M. D.; Beer, P. D. *Polyhedron.* **2003,** 22, 649.

49. Kondo, S.; Nagamine, M.; Yano, Y. *Tetrahedron Lett.* **2003,** 44, 8801.

50. Pfeffer, F. M.; Gunnlaugsson, T.; Jensen, P.; Kruger, P. E. *Org. Lett.* **2005,** 7, 5357.

51. Haino, T.; Nakamura, M.; Kato, N.; Hiraoka, M.; Fukazawa, Y. *Tetrahedron Lett.* **2004,** 45, 2281.

52. Kyne, G. M.; Light, M. E.; Hursthouse, M. B.; de Mendoza, J.; Kilburn, J. D. *J. Chem. Soc., Perkin Trans. 1.* **2001**, 1258.

53. Rossi, S.; Kyne, G. M.; Turner, D. L.; Wells, N. J.; Kilburn, J. D. *Angew. Chem. Int. Ed.* **2002,** 41, 4233.

54. Otón, F.; Tárraga, A.; Espinosa, A.; Velasco, M. D.; Molina, P. *J. Org. Chem.* **2006,** 71, 4590.

55. Sessler, J. L.; Mody, T. D.; Ford, D. A.; Lynch, V. *Angew. Chem. Int. Ed.* **1992,** 104, 461.

56. Shevchuk, S. V.; Lynch, V. M.; Sessler, J. L. *Tetrahedron* **2004,** 60, 11283.

57. El Drubi Vega, I.; Gale, P. A.; Hursthouse, M. B.; Light, M. E. *Org. Biomol. Chem.* **2004,** 2, 2935.

58. Schmuck, C.; Bickert, V. *Org. Lett.* **2003,** 5, 4579.

59. Coles, S. J.; Gale, P. A.; Hursthouse, M. B. *CrystEngComm* **2001**, 53.

60. Gale, P. A.; Camiolo, S.; Chapman, C. P.; Light, M. E.; Hursthouse, M. B. *Tetrahedron Lett.* **2001,** 42, (30), 5095-5097.

61. Camiolo, S.; Gale, P. A.; Hursthouse, M. B.; Light, M. E.; Shi, A. J. *Chem. Commun.* **2002,** 7, 758.

62. Camiolo, S.; Gale, P. A.; Hursthouse, M. B.; Light, M. E. *Org. Biomol. Chem.* **2003,** 4, 741.
63. Camiolo, S.; Gale, P. A.; Hursthouse, M. B.; Light, M. E. *Tetrahedron Lett.* **2002,** 43, 6995.
64. Sessler, J. L.; Dan Pantos, G.; Gale, P. A.; Light, M. E. *Org. Lett.* **2006,** 8, 1593.
65. Schmuck, C.; Heil, M. *Org. Lett.* **2001,** 3, 1253.
66. Schmuck, C.; Geiger, L. *Chem. Commun.* **2004,** 1698.
67. Schmuck, C. *J. Org. Chem.* **2000,** 65, 2432.
68. Schmuck, C.; Geiger, L. *J. Am. Chem. Soc.* **2004,** 126, 8898.
69. Chmielewski, M. J.; Charon, M.; Jurczak, J. *Org. Lett.* **2004,** 6, 3501.
70. Piatek, P.; Lynch, V. M.; Sessler, J. L. *J. Am. Chem. Soc.* **2004,** 126, 16073.
71. Sato, K.; Arai, S.; Yamagishi, T. *Tetrahedron Lett.* **1999,** 40, 5219.
72. Ihm, H.; Yun, S.; Kim, H. G.; Kim, J. K.; Kim, K. S. *Org. Lett.* **2002,** 4, 2897.
73. In, S.; Kang, J. *Tetrahedron Lett.* **2005,** 46, 7165.
74. Kim, H.; Kang, J. *Tetrahedron Lett.* **2005**, 46, 5443.
75. Yuan, Y.; Gao, G.; Jiang, Z.-L.; You, J.-S.; Zhou, Z.-Y.; Yuan, D.-Q.; Xie, R.-G. *Tetrahedron* **2002,** 58, 8993.
76. Kim, S. K.; Kang, B.-G.; Koh, H. S.; Yoon, Y. J.; Jung, S. J.; Jeong, B.; Lee, K.-D.; Yoon, J. *Org. Lett.* **2004,** 6, 4655.
77. Wong, W. W. H.; Vickers, M. S.; Cowley, R. A.; Paul, R. L.; Beer, P. D. *Org. Biomol. Chem.* **2005,** 3, 4201.
78. Schazmann, B.; Alhashimy, N.; Diamond, D. *J. Am. Chem. Soc.* **2006,** 128, 8607.
79. Bondy, C. R.; Gale, P. A.; Loeb, S. J. *J. Am. Chem. Soc.* **2004,** 126, 5030.
80. Bühlmann, P.; Nishizawa, S.; Xiao, K. P.; Umezawa, Y. *Tetrahedron.* **1997,** 53, 1647.
81. Snellink-Ruël, B. H. M.; Antonisse, M. M. G.; Engbersen, J. F. J.; Timmerman, P.; Reinhoudt, D. N. *Eur. J. Org. Chem.* **2000,** 1, 165.
82. Cho, E. J.; Moon, J. W.; Ko, S. W.; Lee, J. Y.; Kim, S. K.; Yoon, J.; Nam, K. C. *J. Am. Chem. Soc.* **2003,** 125, 12376.
83. Turner, D. R.; Paterson, M. J.; Steed, J. W. *J. Org. Chem.* **2006,** 71, 1598.

84. Amedola, V.; Boiocchi, M.; Esteban-Gómez, D.; Fabbrizzi, L.; Monzani, E. *Org. Biomol. Chem.* **2005,** 3, 2632.

85. Kavallieratos, K.; de Gala, S. R.; Austin, D. J.; Crabtree, R. J. *J. Am. Chem. Soc.* **1997,** 119, 2325.

86. Gale, P. A.; Camiolo, S.; Tizzard, G. J.; Chapman, C. P.; Light, M. E.; Coles, S. J.; Hursthouse, M. B. *J. Org. Chem.* **2001,** 66, , 7849.

87. Shivanyuk, A.; Rissanen, K.; Körner, S. K.; Rudkevich, D. M.; Rebek Jr, J. R. *Helv. Chim. Acta.* **2000,** 83, 1778.

88. Yin, Z.; Li, Z.; Yu, A.; He, J.; Cheng, J.-P. *Tetrahedron Lett.* **2004,** 45, 6803.

89. Bruce, M. I.; Zwar, J. A *Proc. Roy, Soc. (London), Ser. B.* **1966,** 165, 245.

90. Camiolo, S.; Coles, S. J.; Gale, P. A.; Hursthouse, M. B.; Tizzard, G. J. *Supramol. Chem.* **2003,** 15, 231.

91. Denuault, G.; Gale, P. A.; Hursthouse, M. B.; Light, M. E.; Warriner, C. N. *New. J. Chem.* **2002,** 26, 811.

92. Hynes, M. J. *Dalton Trans.* **1993**, 311.

93. Hassan, A. A.; E., M. A.-F.; El-shaieb, K. M.; Abou-Zied, A. H.; Dopp, D. *Heteroatom Chem.* **2003,** 14, 535.

94. Mataka, S.; Irie, T.; Ikezaki, Y.; Tashiro, M. *Chem. Ber.* **1993,** 126, 1819.

95. Alott, C.; Adams, H.; Bernard Jr, P. L. *Chem. Commun.* **1998**, 2449.

96. Bisson, A. P.; Lynch, V.; Monahan, M.-K. C.; Ansyln, E. V. *Angew. Chem. Int. Ed.* **1997,** 36, 2340.

97. Niikura, K.; Bisson, A. P.; Ansyln, E. V. *J. Chem. Soc. Perkin Trans 2.* **1999**, 1111.

98. Hossain, M. A.; Llinares, J. M.; Powell, D.; Bowman-James, K. *Inorg. Chem.* **2001,** 40, 2936.

99. Hossain, M. A.; Kang, S. O.; Powell, D.; Bowman-James, K. *Inorg. Chem.* **2003,** 42, 1397.

100. Hossain, M. A.; Kang, S. O.; Llinares, J. M.; Powell, D.; Bowman-James, K. *Inorg. Chem.* **2003,** 42, 5043.

101. Kang, S. O.; Llinares, J. M.; Powell, D.; VanderVelde, D.; Bowman-James, K. *J. Am. Chem. Soc.* **2003,** 125, 10152.

102. Kang, S. O.; VanderVelde, D.; Powell, D.; Bowman-James, K. *J. Am. Chem. Soc.* **2004,** 126, 12272.
103. Szumna, A.; Jurczak, J. *Helv. Chim. Acta.* **2001,** 84, 3760.
104. Sessler, J. L.; Katayev, E.; Dan Pantos, G.; Ustynuk, Y. A. *Chem. Commun.* **2004,** 1276.
105. Sessler, J. L.; Katayev, E.; Dan Pantos, G.; Scherbakov, P.; Reshetova, M. D. *J. Am. Chem. Soc.* **2005,** 126, 11442.
106. Sitzmann, M. E.; Gilligan, W. H. *J. Org. Chem.* **1985**, 50, 5879.
107. Awad, W. I.; Nossier, M. H.; Doss, N. L.; Ishak, E. A. *J. Prakt. Chem.* **1973**, 1152.
108. Frigaard, N. U.; Tokita, S.; Matsuura, K. *Biochimica et Biophysica Acta - Bioenergetics.* **1999,** 252
109. Tokita, S.; Frigaard, N. U.; Hirota, M.; Shimada, K.; Matsuura, K. *Photochemistry and photobiology* **2000,** 72, 345.
110. Gupta, N.; Linschitz, H. *J. Am. Chem. Soc.* **1997,** 119, 6384.
111. Gómez, M.; González, F. J.; González, I. *Electroanalysis* **2003,** 15, 635.
112. Ashnagar, A.; Bruce, J. M.; Dutton, P. L.; Prince, R. C. *Biochimica et Biophysica Acta.* **1984**, 351
113. Jiménez, D.; Martínez-Máñez, R.; Sancenón, F.; Soto, J. *Tetrahedron Lett.* **2002,** 43, 2823.
114. Kang, S. O.; Jeon, S.; Nam, K. C. *Supramol. Chem.* **2002,** 14, 405.
115. Jeon, S.; Park, D. H.; Lee, H. K.; Park, J. Y.; Kang, S. O.; Nam, K. C. *Bull. Korean. Chem. Soc.* **2003,** 24, 1465.
116. Jose, D. A.; Kumar, D. K.; Ganguly, B.; Das, A. *Org. Lett.* **2004,** 20, 3445.
117. Jose, D. A.; Kumar, D. K.; Ganguly, B.; Das, A. *Tetrahedron Lett.* **2005,** 46, 5343.
118. Leon, J. W.; Whitten, D. G. *J. Am. Chem. Soc.* **1995,** 117, 2226.
119. Mei, M.; Wu, S. *New. J. Chem.* **2001,** 25, 471.
120. Chen, Q.-Y.; Chen, C.-F. *Tetrahedron Lett.* **2004,** 45, 6493.
121. Jun, W. J.; Swamy, M. K.; Bang, H.; Kim, S.-J.; Yoon, J. *Tetrahedron Lett.* **2006,** 47, 3103.

122. Kim, S. K.; Yoon, J. *Chem. Commun* **2002**, 770.

123. Kim, S. K.; Singh, N. J.; Kim, S. J.; Kim, H. G.; Kim, J. K.; Lee, J. W.; Kim, K. S.; Yoon, J. *Org. Lett.* **2003,** 5, 2083.

124. Gunnlaugsson, T.; Davis, A. P.; Hussey, G. M.; Tierney, J.; Glynn, M. *Org. Biomol. Chem.* **2004,** 2, 1856.

125. Gunnlaugsson, T.; Davis, A. P.; O'Brien, J. E.; Glynn, M. *Org. Lett.* **2002,** 4, 2449.

126. Gunnlaugsson, T.; Davis, A. P.; O'Brien, J. E.; Glynn, M. *Org. Biomol. Chem.* **2005,** 3, 48.

127. Sasaki, S.-I.; Citterio, D.; Ozawa, S.; Suzuki, K. *J. Chem. Soc., Perkin Trans. 2.* **2001**, 2309.

128. Sukharevsky, A. P.; Read, I.; Linton, B.; Hamilton, A. D.; Waldeck, D. H. *J. Phys. Chem. B.* **1998,** 102, 5394.

129. Origin v7.0383. Originlab Corporation. 1991-2002.

APPENDIX 1. ^{1}H NMR TITRATION CURVES.

Where reported, anion stability constants have been elucidated through ^{1}H NMR titration experiments in which the anions in the form of their tetrabutylammonium salts at 298 K either in DMSO-d_6/water mixtures or CD_2Cl_2.

Data from these titration experiments has been fitted to the appropriate binding model with the resulting experimental and calculated titration profiles reported for completeness.

CHAPTER 2.

N^1,N^2-Phenylene-bis-acetamide (66) in DMSO-d_6/0.5% water.

Acetate.
$K_a = 98$
Error = 2.0 %

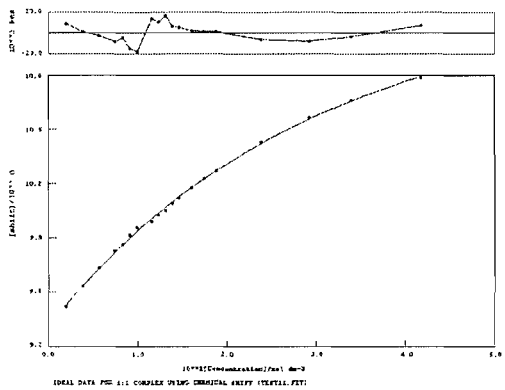

Benzoate.
$K_a = 43$
Error = 1.7 %

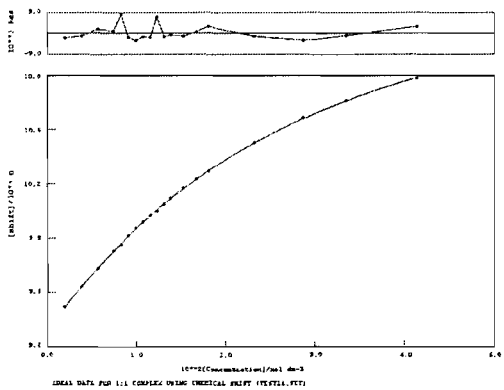

Chloride.
$K_a = 13$
Error = 4.0 %

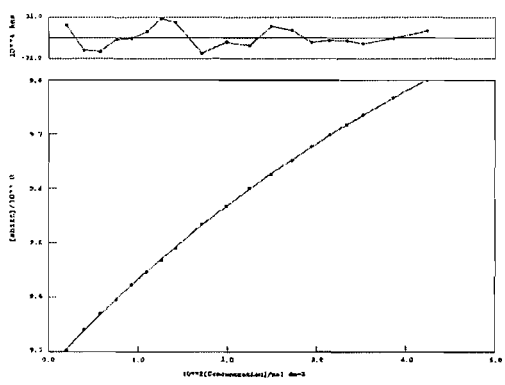

Dihydrogen Phosphate.
$K_a = 149$
Error = 2.1 %

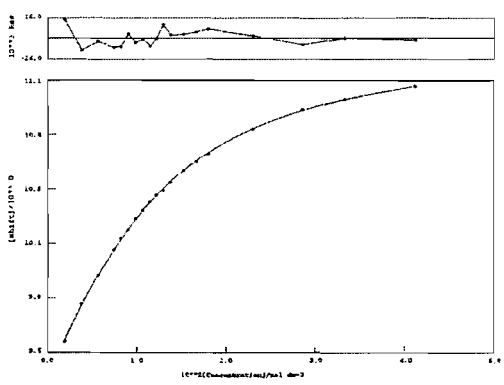

N-(2-(1H-pyrrole-2-carboxamido)phenyl)-1H-pyrrole-2-carboxamide (67) in DMSO-d_6/0.5% water.

Acetate.
$K_a = 251$
Error = 2.4 %

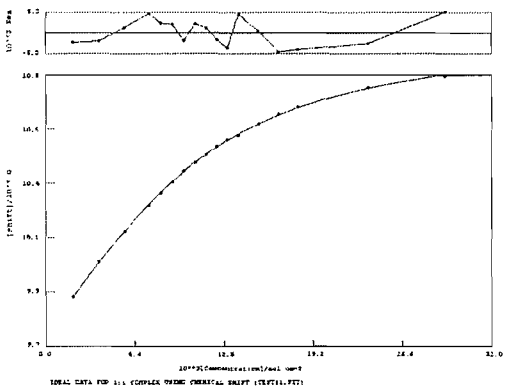

Benzoate.
$K_a = 113$
Error = 1.4 %

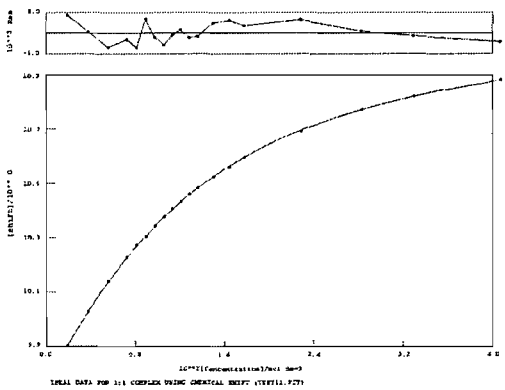

Chloride.
$K_a = 12$
Error = 4.8 %

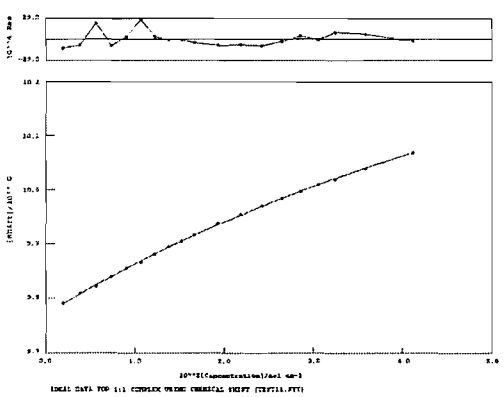

Dihydrogen Phosphate
$K_a = 295$
Error = 2.5 %

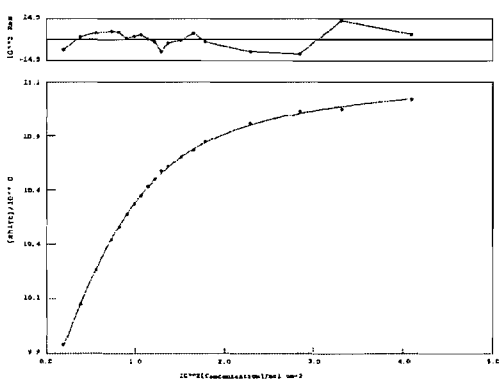

1,1′-(1,2-Phenylene)bis(3-phenylurea) (68) in DMSO-d_6/0.5% water.

Acetate.
K_a = 3211
Error = 6.3 %

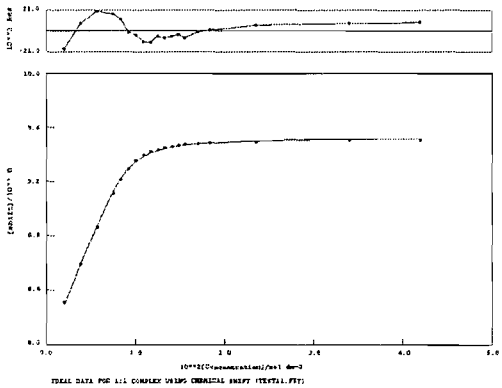

Benzoate.
K_a = 1329
Error = 1.9 %

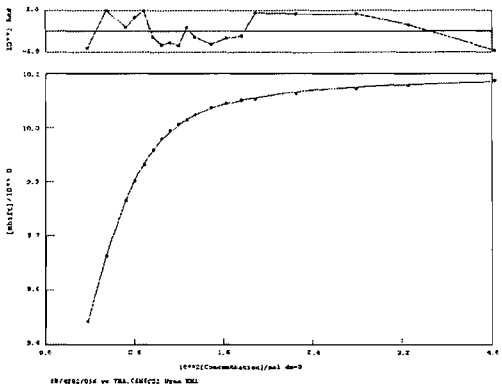

Bromide.
K_a = <10
Error = 17.6 %

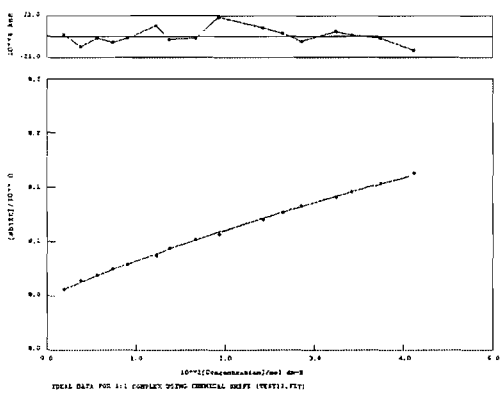

Chloride.
K_a = 43
Error = 2.0 %

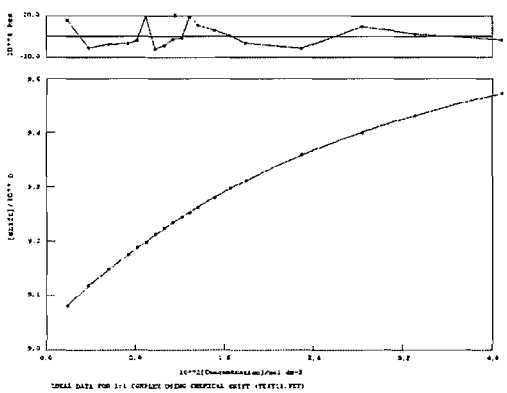

Dihydrogen Phosphate.
K_a = 732
Error = 6.5 %

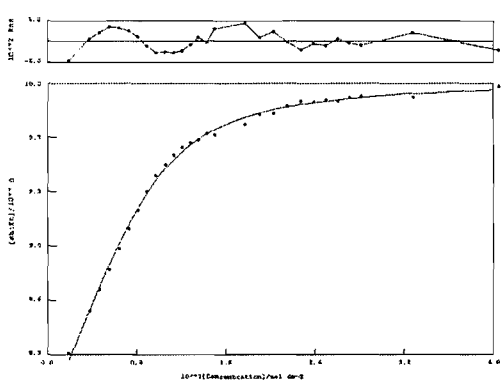

Hydrogen Sulfate.
K_a = 10
Error = 10.2 %

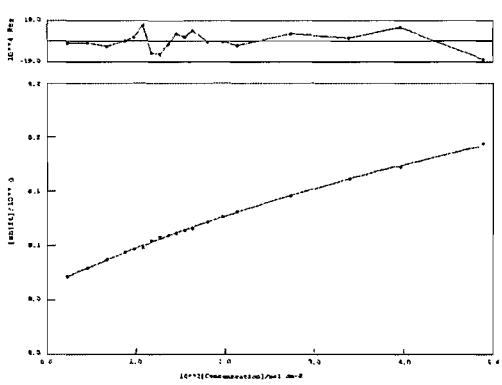

1,1′-(4,5-dichloro-1,2-phenylene)bis(3-phenylurea) (69) in DMSO-d_6/0.5% water.

Acetate.
K_a = 8079
Error = 5.7 %

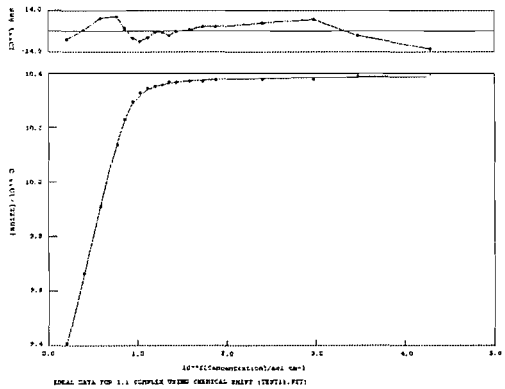

Benzoate.
K_a = 2248
Error = 7.8 %

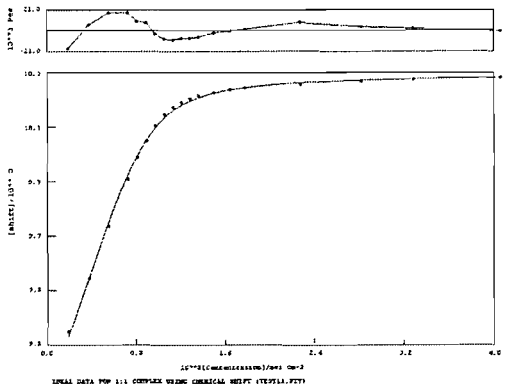

Bromide.
K_a = <10
Error = 17.9 %

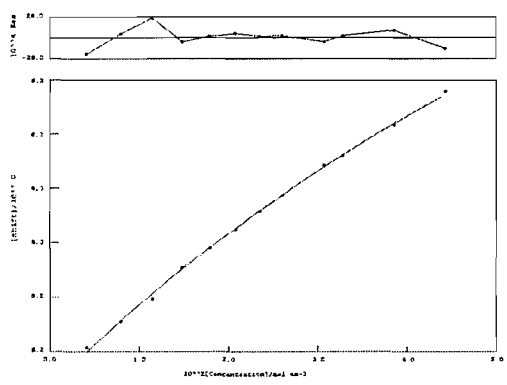

Chloride.
K_a = 67
Error = 1.6 %

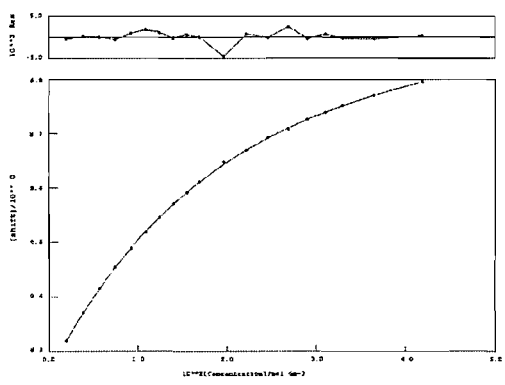

Dihydrogen Phosphate.
K_a = 4724
Error = 3.8 %

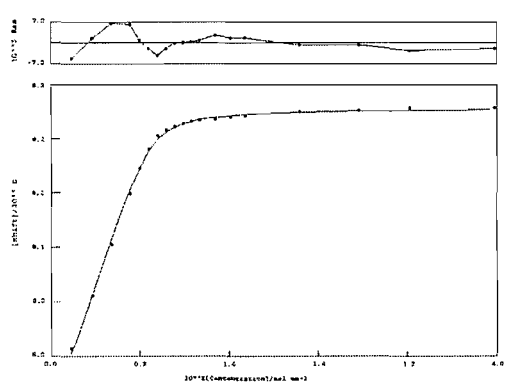

Hydrogen Sulfate.
K_a = <10
Error = 16.6 %

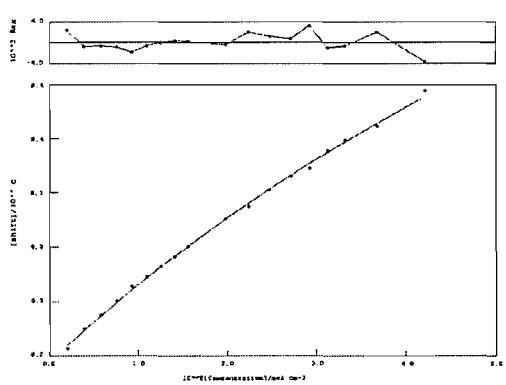

1,1′-(1,2-phenylene)bis(3-(4-nitrophenyl)urea) (70) in DMSO-d_6/0.5% water.

Acetate.
K_a = 4018
Error = 9.3 %

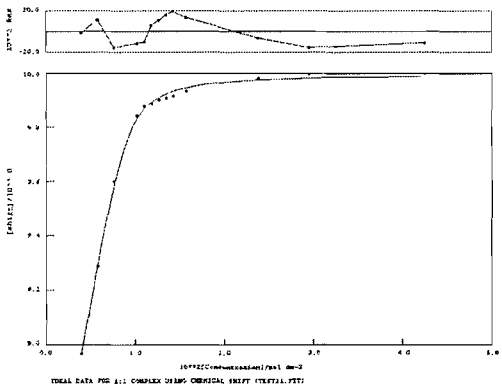

Benzoate.
K_a = 1399
Error = 9.3 %

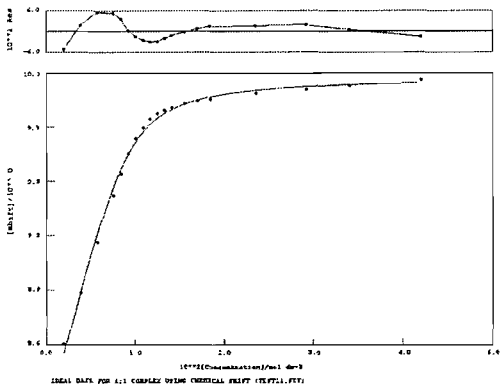

Bromide.
K_a = <10
Error = 14.9 %

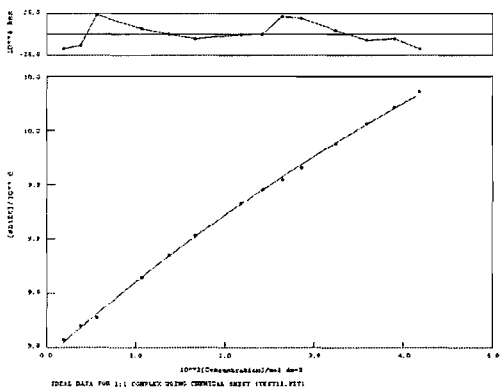

Chloride.
K_a = 78
Error = 1.2 %

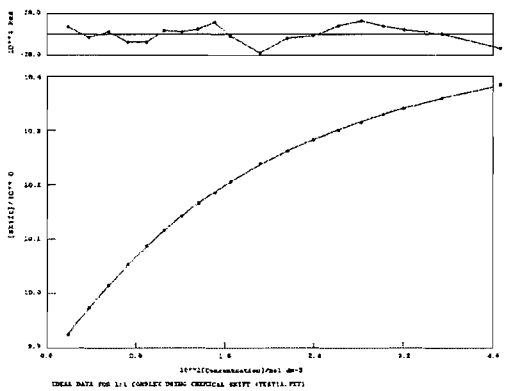

Dihydrogen Phosphate.
K_a = 666
Error = 8.5 %

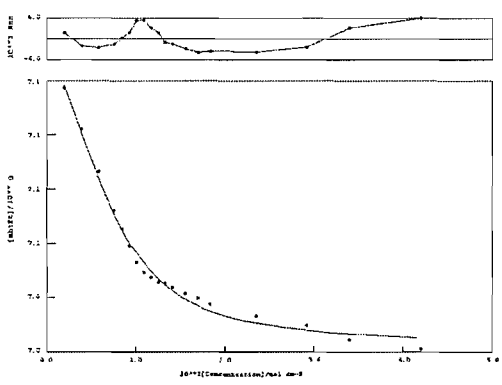

Hydrogen Sulfate.
K_a = 11
Error = 8.5 %

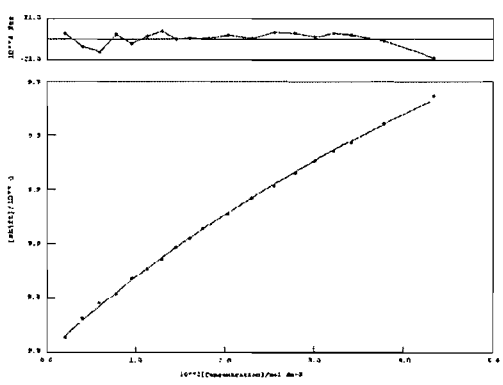

1,1′-(1,2-phenylene)bis(3-(2-nitrophenyl)urea) (71) in DMSO-d_6/0.5% water.

Acetate.
K_a = 1976
Error = 3.5 %

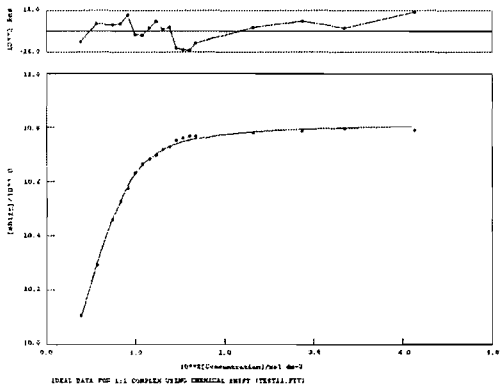

Benzoate.
K_a = 541
Error = 2.6 %

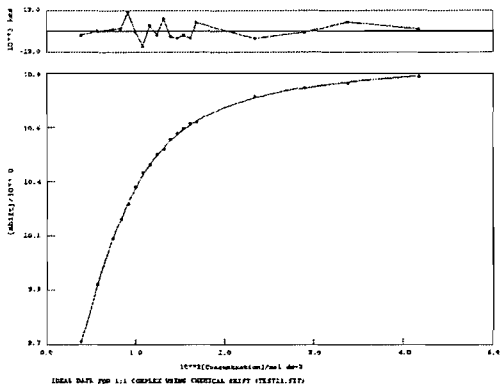

Dihydrogen Phosphate.
K_a = 349
Error = 3.4 %

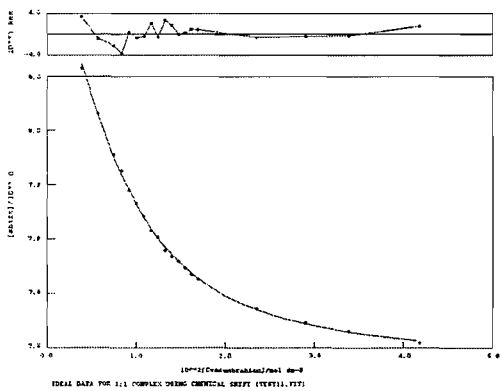

1,1′-(4,5-dichloro-1,2-phenylene)bis(3-(2-nitrophenyl)urea) (72) in DMSO-d_6/0.5% water.

Benzoate.
K_a = 1249
Error = 5.7 %

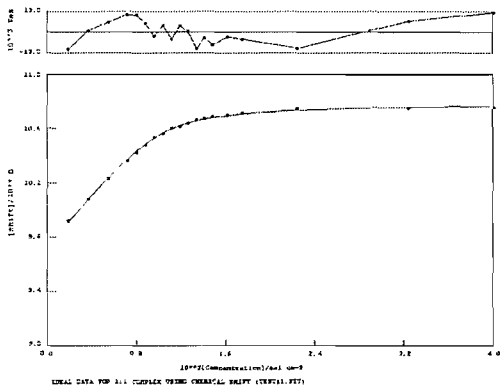

Chloride.
K_a = 18
Error = 9.9 %

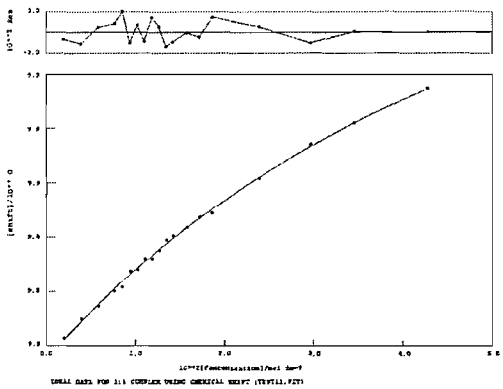

Dihydrogen Phosphate.
K_a = 1637
Error = 4.4 %

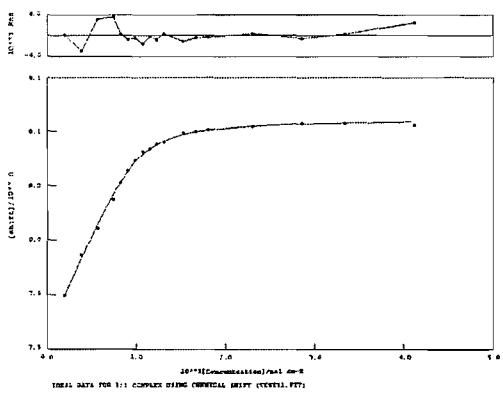

1,1′-(1,2-Phenylene)bis(3-phenylthiourea) (73) in DMSO-d_6/0.5% water.

Acetate.
$K_a = 188$
Error = 9.4 %

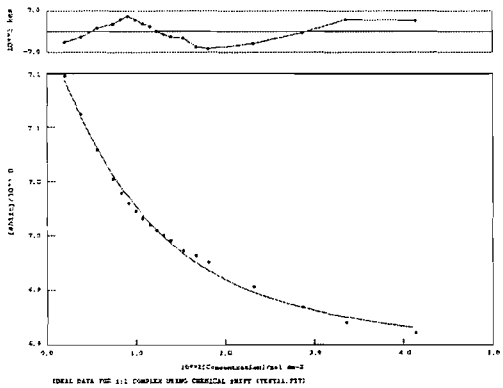

Benzoate.
$K_a = 233$
Error = 4.8 %

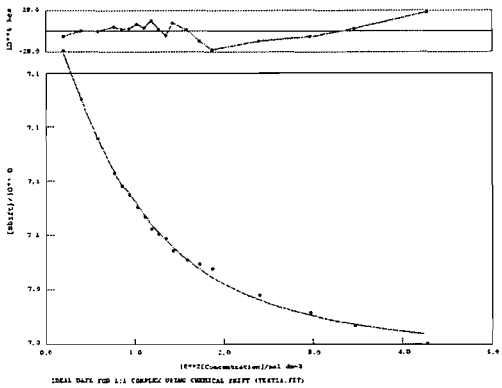

Chloride.
$K_a = 18$
Error = 3.4 %

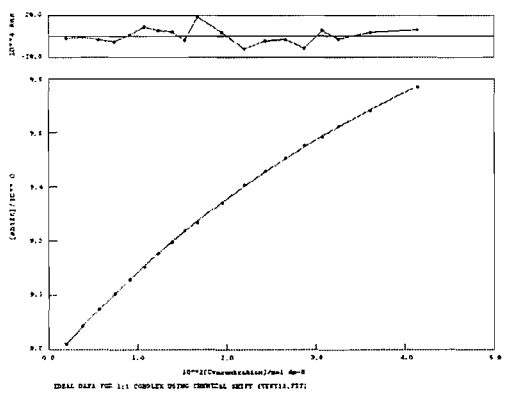

Dihydrogen Phosphate.
$K_a = 1490$
Error = 6.2 %

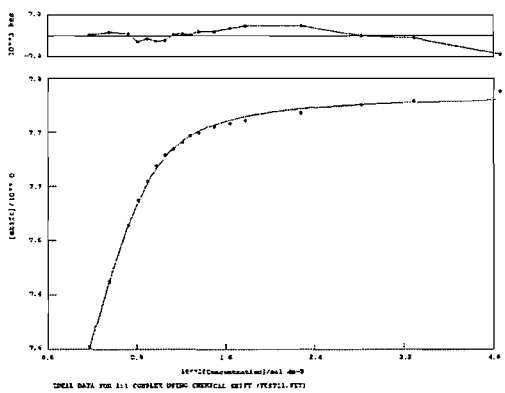

***N*,*N*′-(2,2′-(1,2-Phenylenebis(azanediyl))bis(oxomethylene)bis(azanediyl)bis(2,1-phenylene)dibenzamide (74) in DMSO-d_6/0.5% water.**

Acetate.
K_1 = 6008 K_2 = <10
K_{12} = 55230
Error = 2.2 & 3.2 %

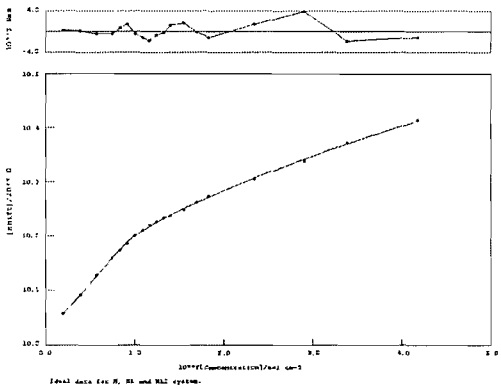

Benzoate.
K_1 = 10110 K_2 = <10
K_{12} = 16554
Error = 3.4 % & 12.5 %

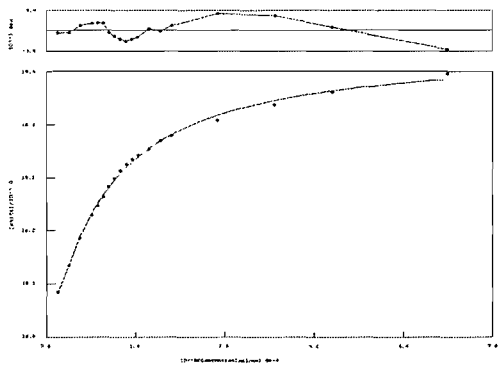

Chloride.
K_a = 17

Error = 4.7 %

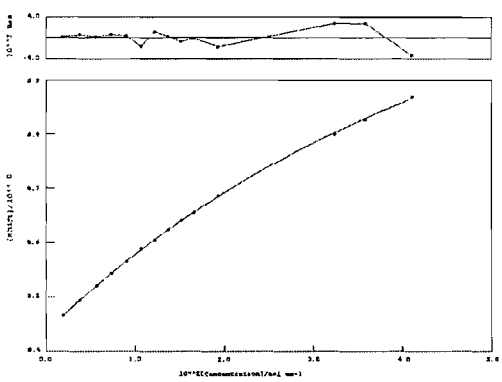

Dihydrogen Phosphate.
K_1 = 7777 K_2 = 24
K_{12} = 185149
Error = 5.7 & 4.0 %

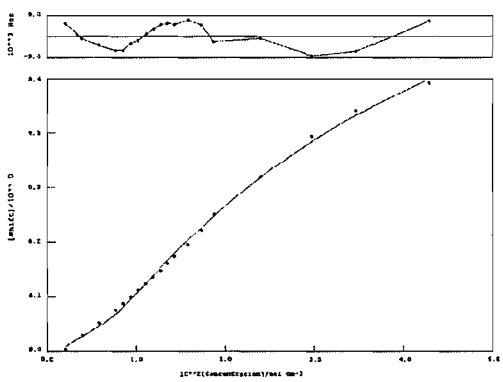

3,3′-(1,2-Phenylenebis(azanediyl))bis(oxomethylene)bis(azanediyl)bis(N-phenylbenzamide) (75) in DMSO-d_6/0.5% water.

Acetate.
$K_a = 3199$
Error = 7.2 %

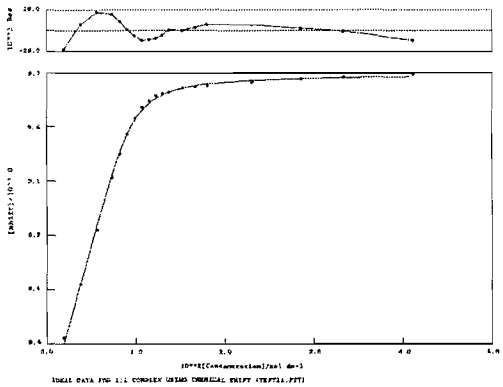

Benzoate.
$K_a = 974$
Error = 7.2 %

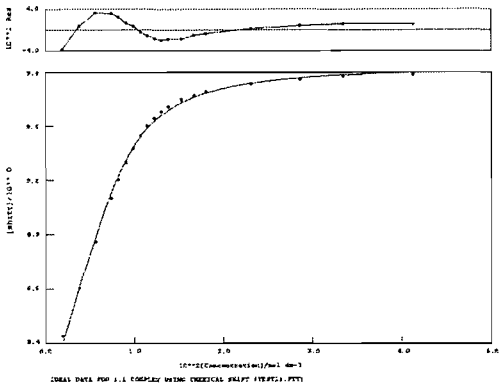

Chloride.
$K_a = 52$
Error = 1.0 %

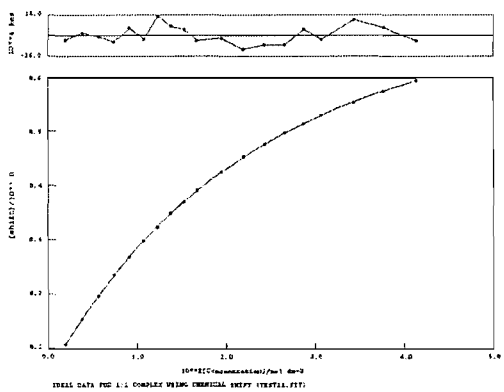

Dihydrogen Phosphate.
$K_a = 2289$
Error = 11.8 %

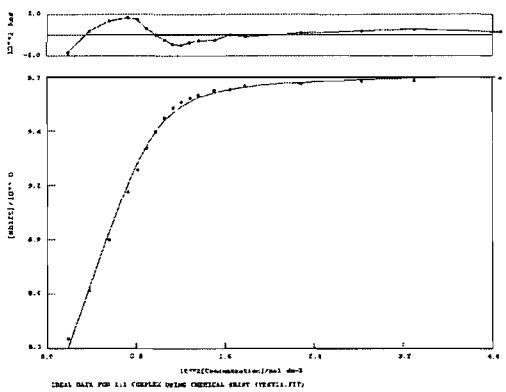

Hydrogen Sulfate.
$K_a = 12$
Error = 10.8 %

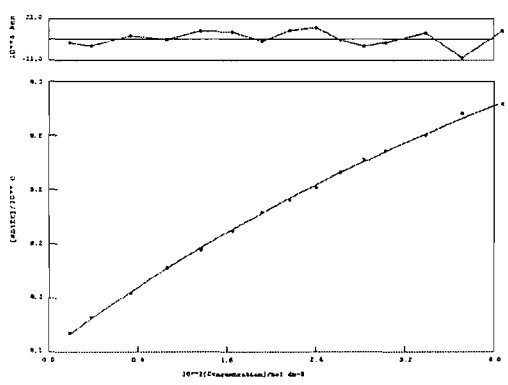

CHAPTER 3.

1,3-Diphenylurea (94) in DMSO-d_6/0.5 % water.

Acetate.
K_a = 1261
Error = 7.4 %

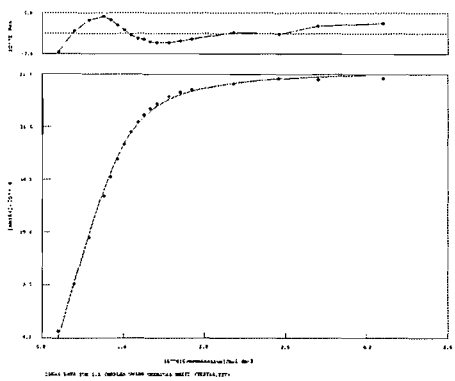

Benzoate.
K_a = 674
Error = 0.5 %

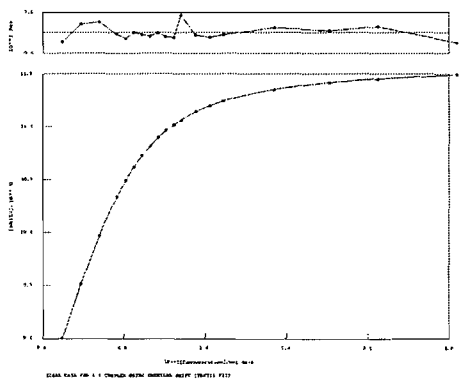

Chloride.
K_a = 31
Error = 0.8 %

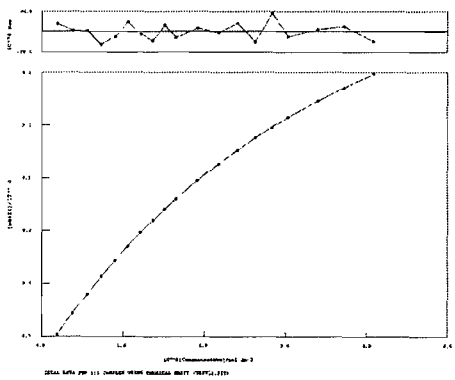

Dihydrogen Phosphate.
K_a = 523
Error =3.1 %

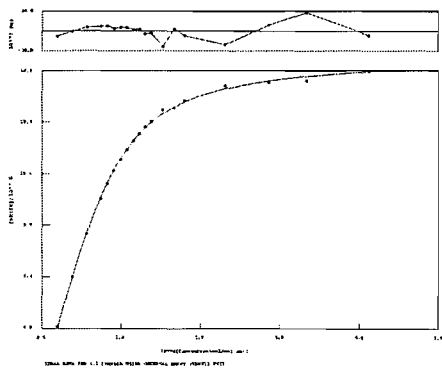

_N_-(2-(3-Phenyl-ureido)-phenyl)-benzamide (95) in DMSO-d_6/0.5% water.

Acetate.
K_a = 2364
Error = 3.9 %

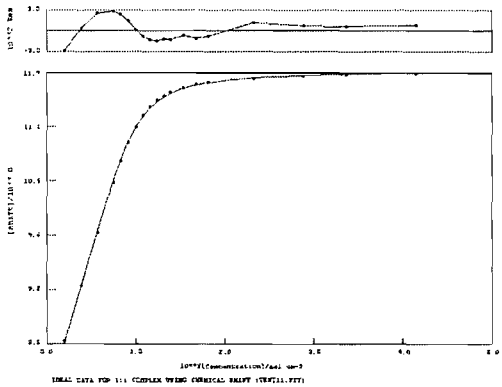

Benzoate.
K_a = 606
Error = 3.7 %

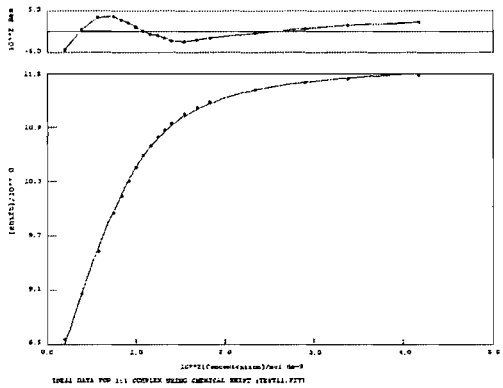

Chloride.
K_a = <10
Error = 3.8 %

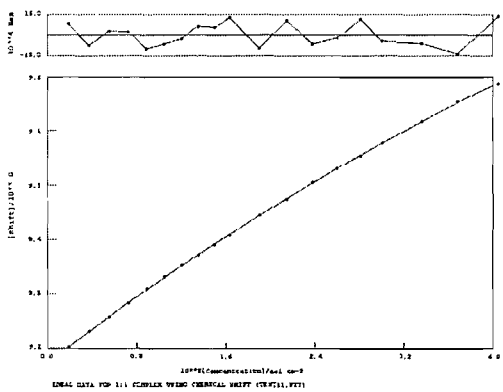

Dihydrogen Phosphate.
K_a = 1286
Error = 4.0 %

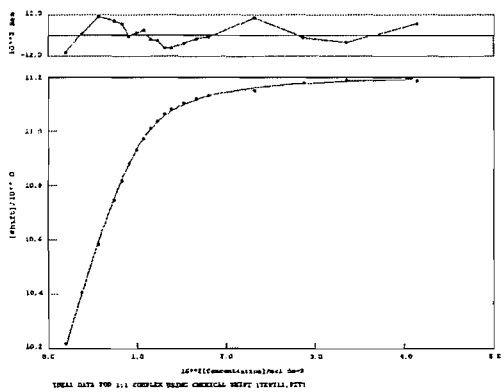

1,3-Bis-(2-benzanilide-phenyl)-urea (96) in DMSO-d_6/0.5% water.

Acetate.
K_a = 2475
Error = 4.6 %

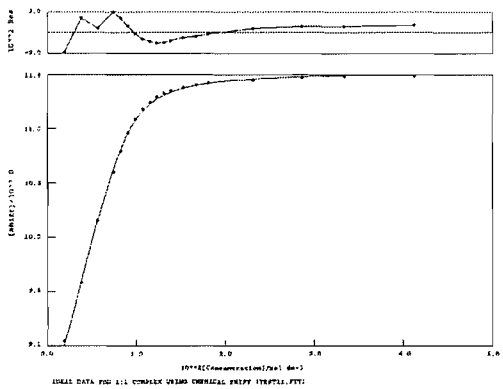

Benzoate.
K_a = 784
Error = 3.0 %

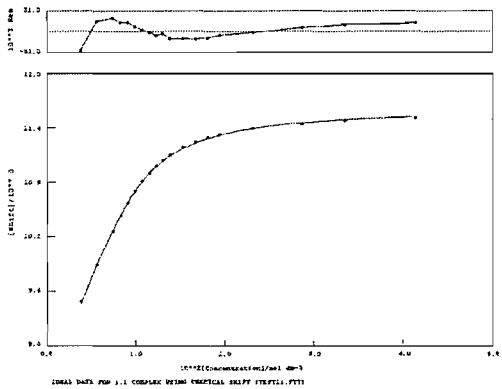

Chloride.
K_a = <10
Error = 13.8 %

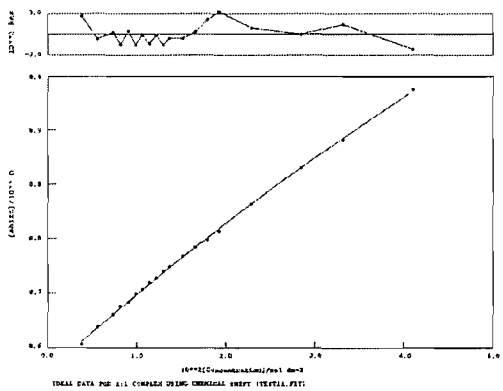

Dihydrogen Phosphate.
K_a = 1649
Error = 4.9 %

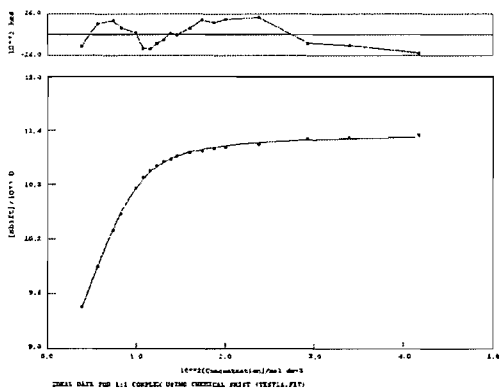

Pyridine-2,6-dicarboxylic acid bis-((3-phenylcarbamoyl-phenyl)-amide)) (97) in DMSO-d_6/0.5% water.

Acetate.
K_a = 419
Error = 1.8 %

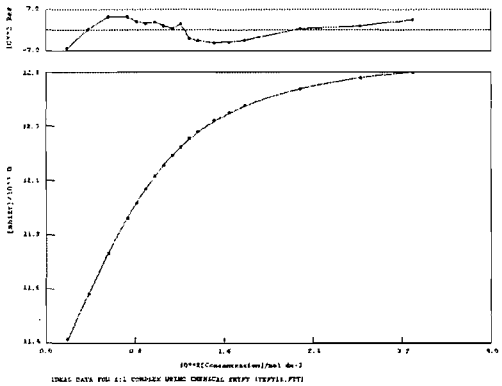

Benzoate.
K_a = 101
Error = 0.8 %

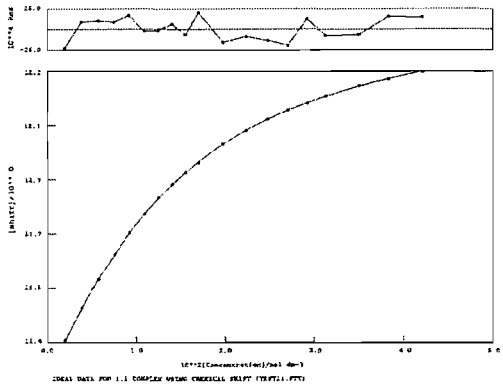

Chloride.
K_a = <10
Error = 11.2 %

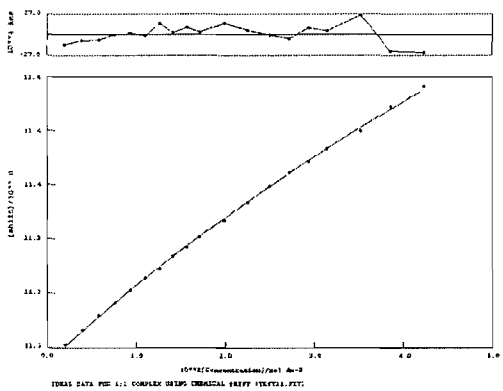

Dihydrogen Phosphate.
K_a = 681
Error = 4.5 %

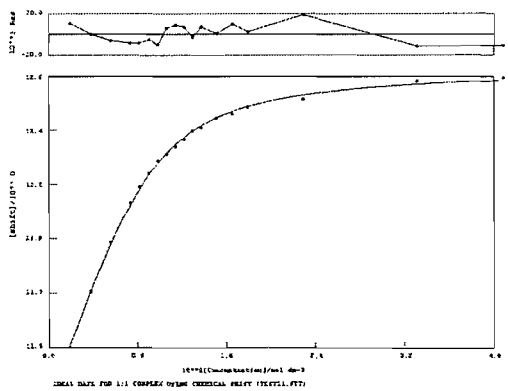

***N,N'*-Bis-(3-phenylcarbamoyl-phenyl)-isophthalamide (98) in DMSO-d_6/0.5% water.**

Acetate.
$K_a = 137$
Error = 1.3 %

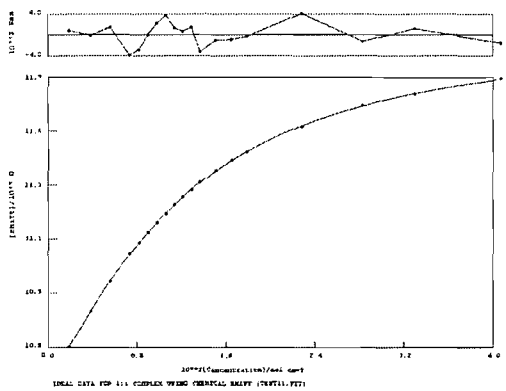

Benzoate.
$K_a = 71$
Error = 1.0 %

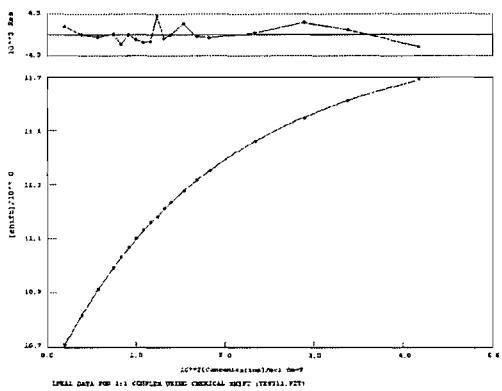

Chloride.
$K_a = 14$
Error = 3.1 %

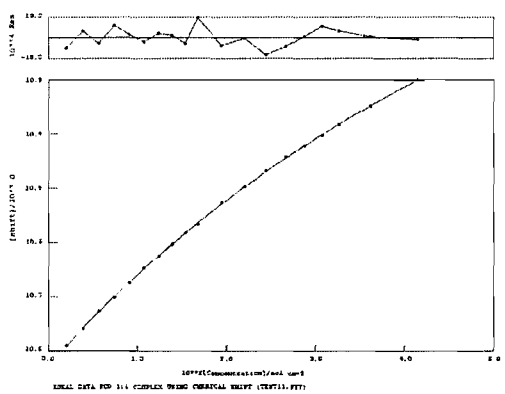

Dihydrogen Phosphate.
$K_a = 294$
Error = 3.9 %

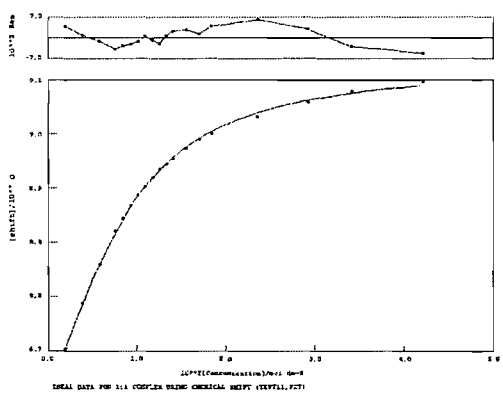

(99) in DMSO-d_6/0.5% water.

Acetate.
K_a = 16520
Error =3.2 %

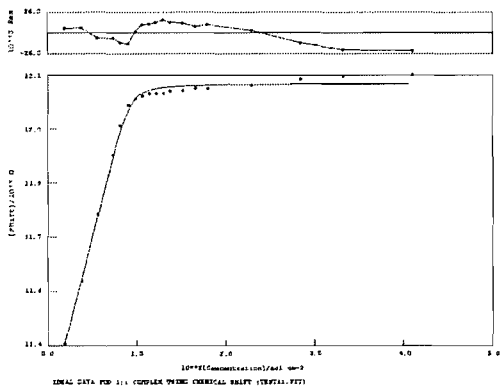

Benzoate.
K_a = 6432
Error = 11.2 %

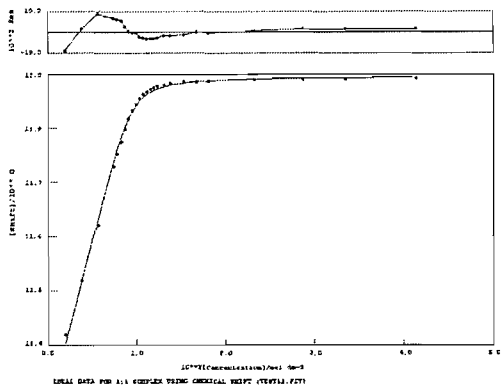

Bromide.
K_a = 10
Error =13.7 %

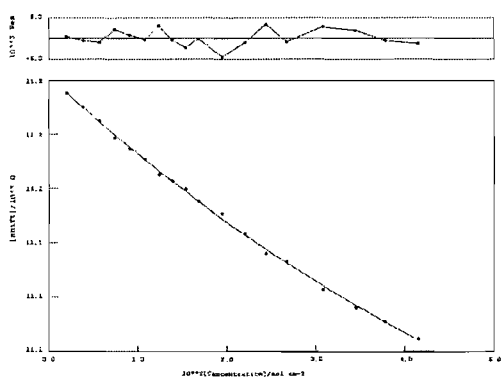

Chloride.
K_a = 194
Error = 1.5 %

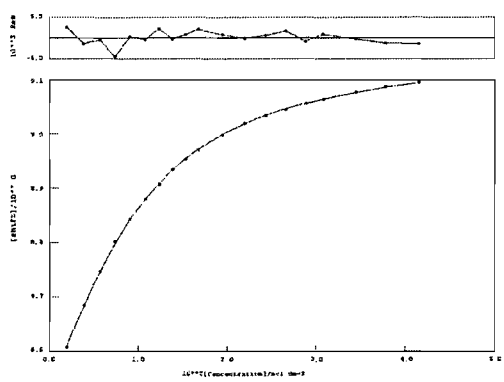

Dihydrogen Phosphate.
K_a = 141
Error = 13.4 %

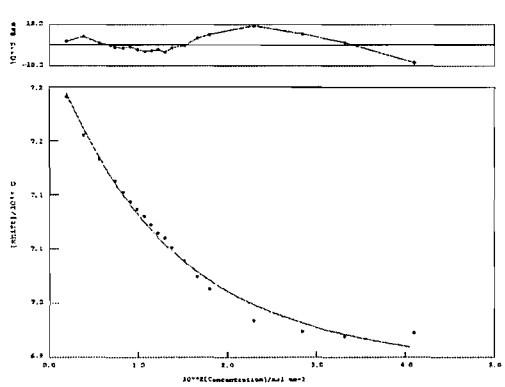

Hydrogen Sulfate.
K_a = 115
Error = 10.3 %

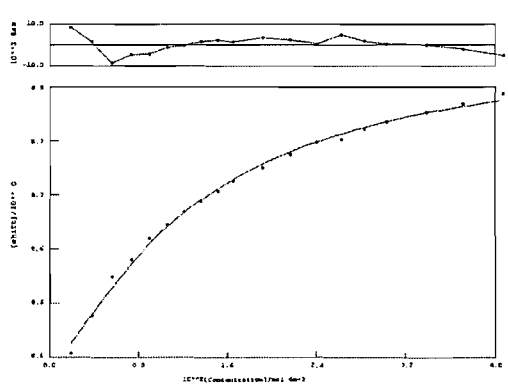

Nitrate.
$K_a = 9$
Error = 16.2 %

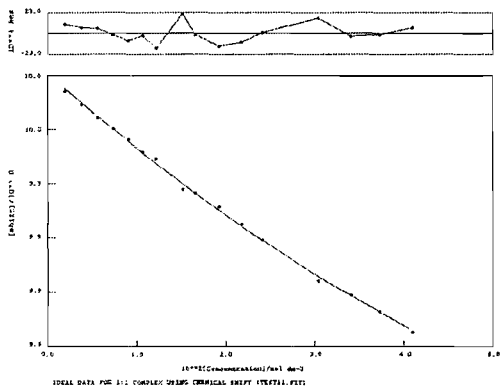

(99) in DMSO-d_6/5.0 % water.

Acetate.
$K_a = 5170$
Error = 4.4 %

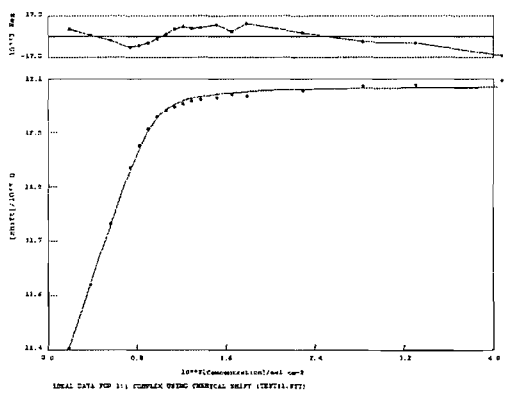

Benzoate.
$K_a = 1834$
Error = 5.4 %

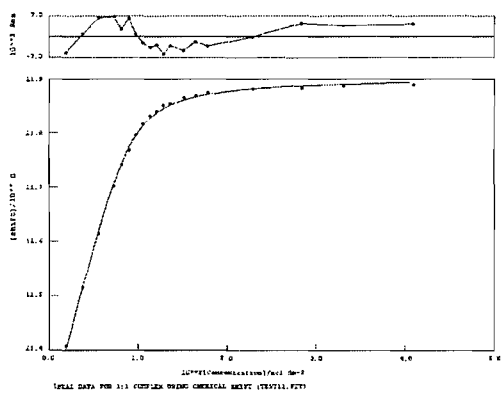

Chloride
$K_a = 42$
Error = 3.7 %

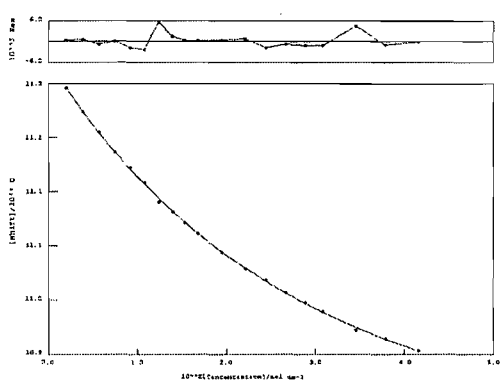

Dihydrogen Phosphate.
$K_a = 51$
Error = 8.3 %

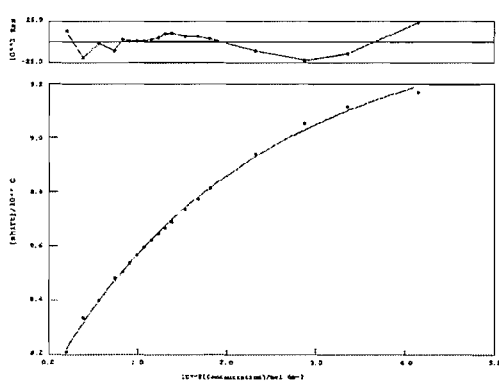

CHAPTER 4.

9,10-dihydro-9,10-dioxo-N^1,N^3-diphenylanthracene-1,3-dicarboxamide (118) in DMSO-d_6/0.5% water.

Acetate.
$K_a = 30$
Error = 3.6 %

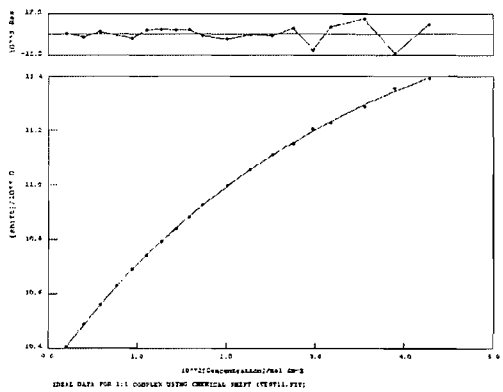

Benzoate
$K_a = 17$
Error = 7.8 %

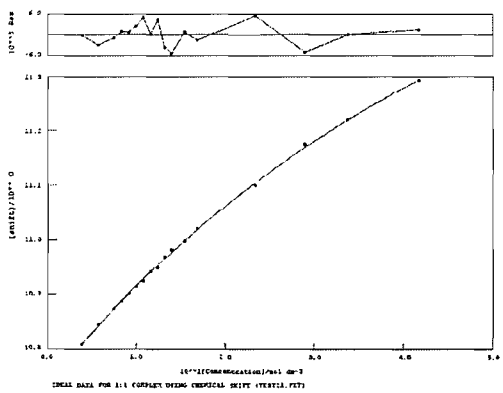

Dihydrogen Phosphate.
$K_a = 185$
Error = 7.6 %

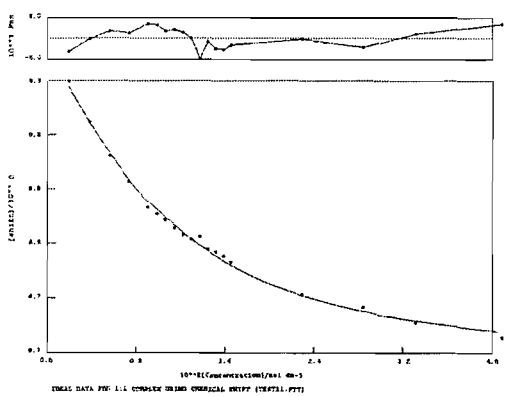

N^1,N^3-bis(4-butylphenyl)-9,10-dihydro-9,10-dioxoanthracene-1,3-dicarboxamide (119) in DMSO-d_6/0.5% water.

Acetate.
K_a = 24
Error = 3.8 %

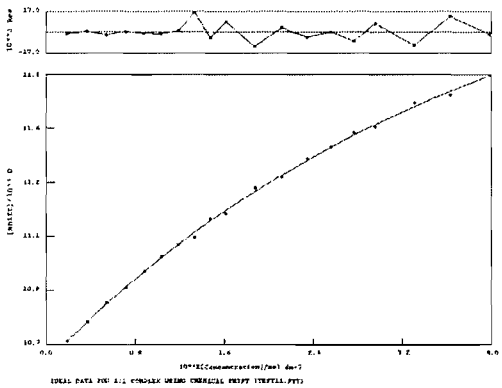

Benzoate.
K_a = 15
Error = 2.1 %

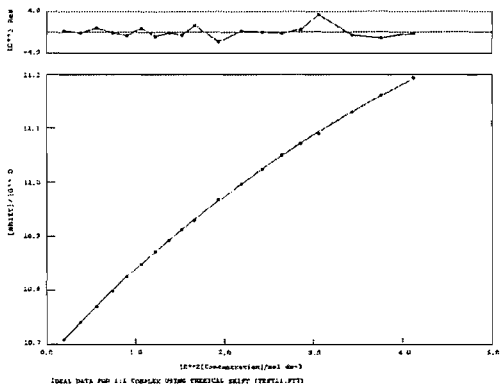

Chloride.
K_a = <10
Error = 33.1 %

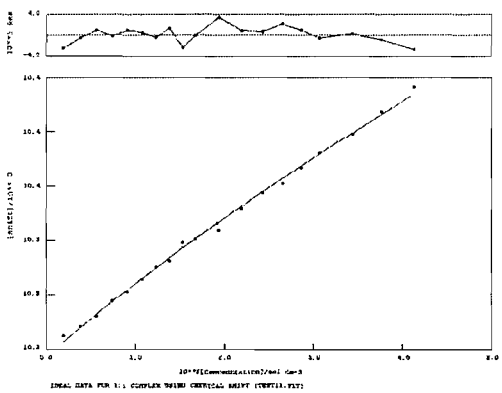

Dihydrogen Phosphate
K_a = 120
Error = 9.5 %

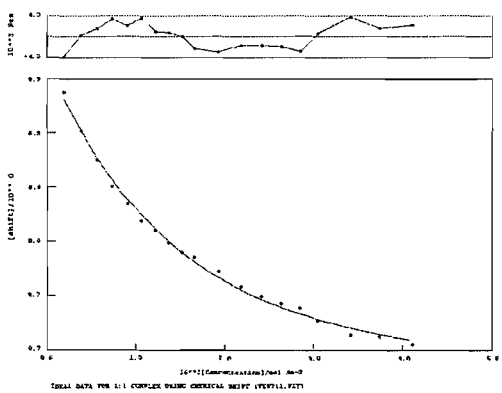

9,10-dihydro-N^1,N^3-bis(3,5-dimethoxyphenyl)-9,10-dioxoanthracene-1,3-dicarboxamide (120) in DMSO-d_6/0.5% water.

Acetate.
$K_a = 35$
Error = 4.1 %

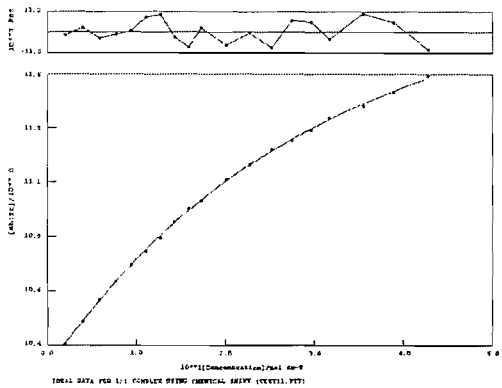

Benzoate
$K_a = 27$
Error = 8.0 %

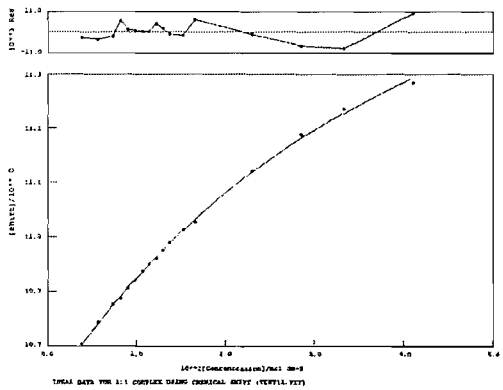

Dihydrogen Phosphate.
$K_a = 185$
Error = 7.6 %

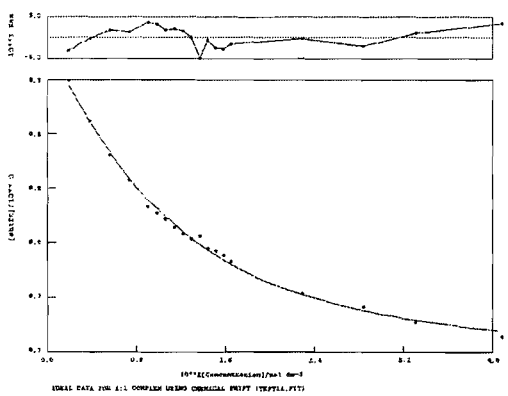

N^1,N^3-bis(3,5-dichlorophenyl)-9,10-dihydro-9,10-dioxoanthracene-1,3-dicarboxamide (121) in DMSO-d_6/0.5% water.

Benzoate.
K_a = 168
Error = 7.0 %

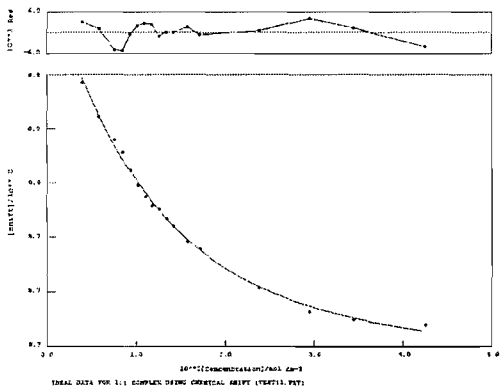

Chloride.
Ka = 11
Error = 9.6 %

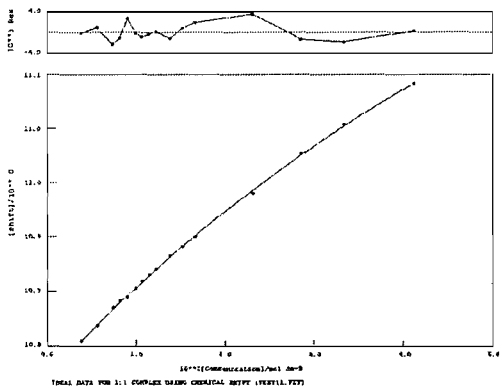

Dihydrogen Phosphate.
K_1 = 1689 K_2 = 41
Error = 0.4 % 2.7 %

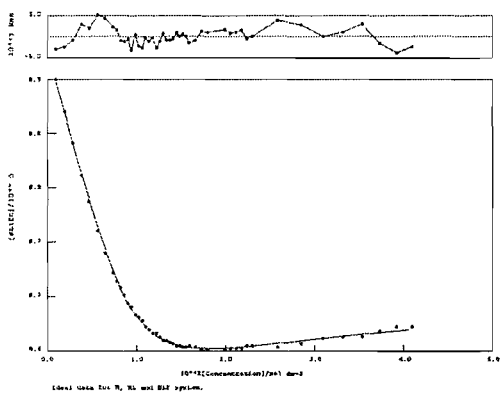

N^1,N^3-dibutyl-9,10-dihydro-9,10-dioxoanthracene-1,3-dicarboxamide (122) in CD_2Cl_2-d_2.

Acetate.
$K_a = 247$
Error = 9.9 %

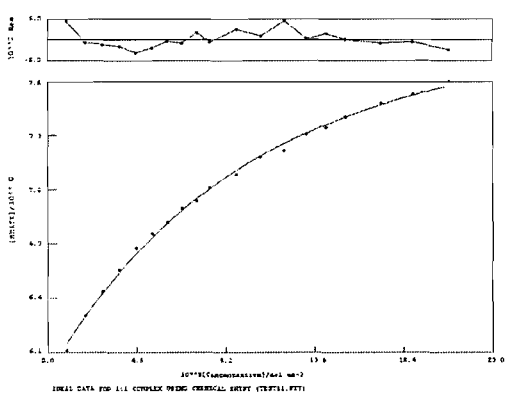

Benzoate.
$K_a = 181$
Error = 5.6 %

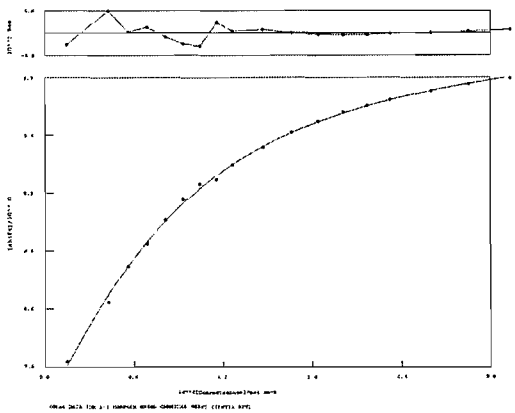

Chloride.
$K_a = 127$
Error = 8.6 %

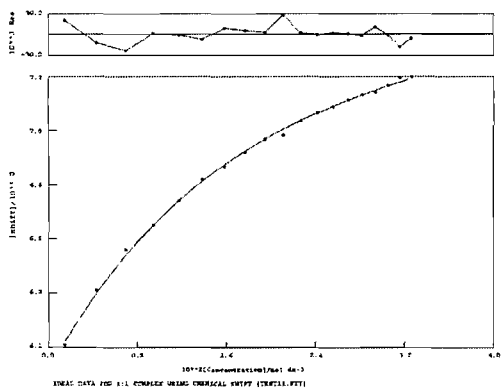

Bromide.
$K_a = 69$
Error = 6.3 %

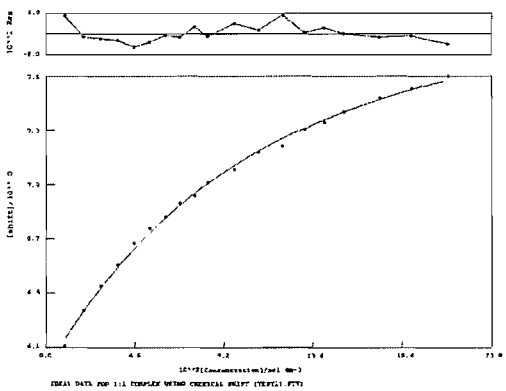

Dihydrogen Phosphate.
$K_a = 93$
Error = 6.1 %

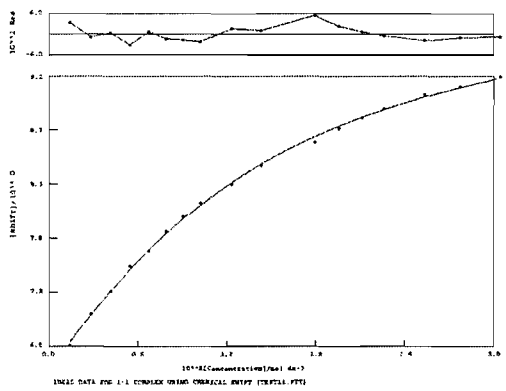

Hydrogen Sulfate.
$K_a = 31$
Error = 14.4 %

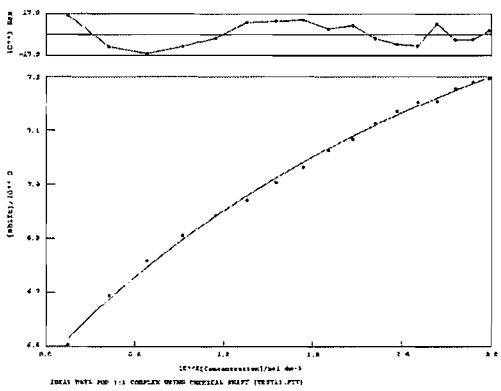

CHAPTER 5.

N^1,N^3-dibutylanthracene-1,3-dicarboxamide (132) in CD_2Cl_2-d_2.

Benzoate.
$K_a = 173$
Error = 2.2 %

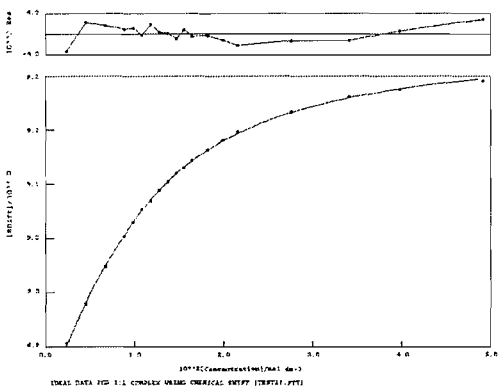

Bromide.
$K_a = 92$
Error = 2.0%

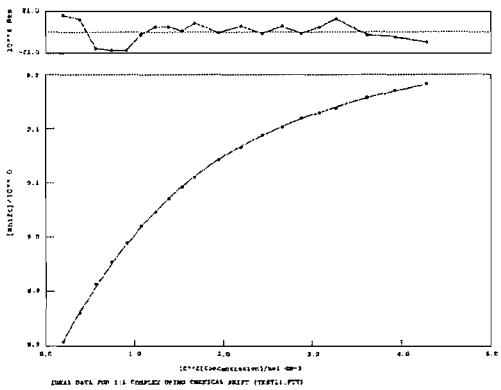

Chloride.
$K_a = 257$
Error = 4.7 %

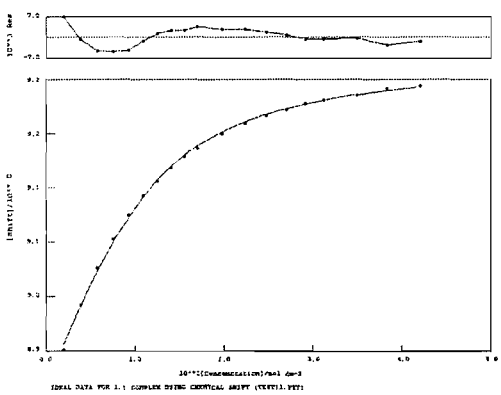

Dihydrogen Phosphate.
Ka = 52
Error = 2.9 %

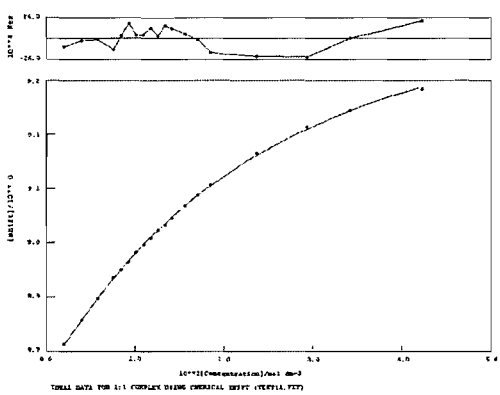

Hydrogen Sulfate.
$K_a = 16$
Error = 10.0 %

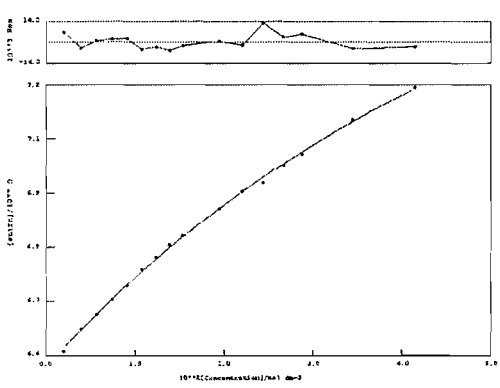

N^1,N^3-dibutylanthracene-1,3-dicarboxamide (132) in DMSO-d_6/0.5% water.

Acetate.
K_a = 13
Error = 5.8 %

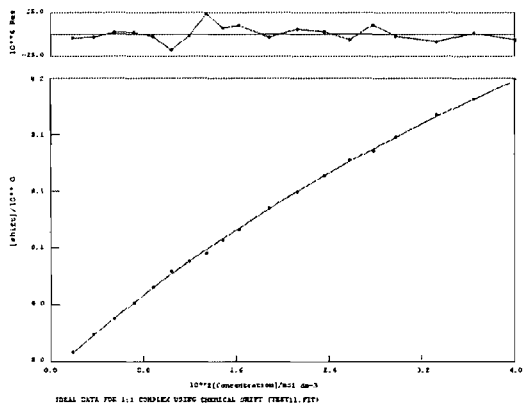

Benzoate.
K_a = <10
Error = 9.6 %

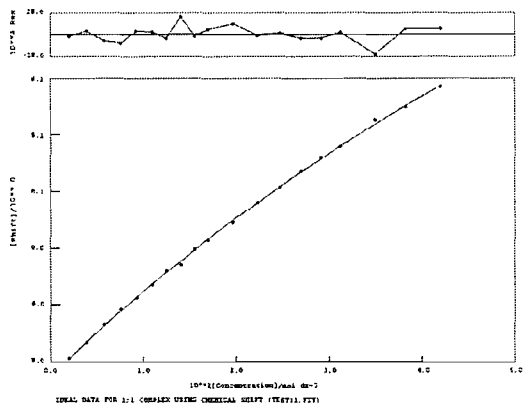

Chloride.
Ka = <10
Error = 33.0 %

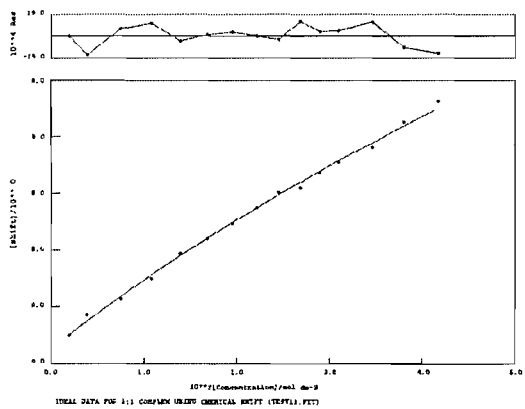

Dihydrogen Phosphate.
Ka = 19
Error = 10.9 %

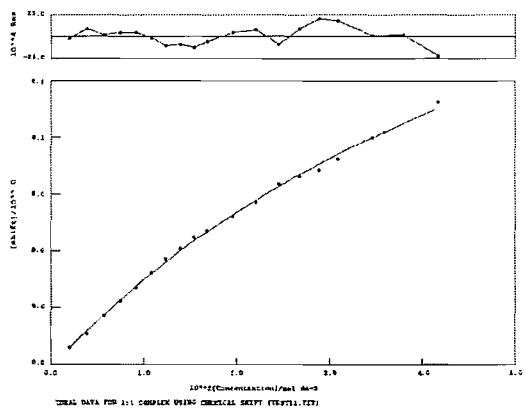

N^1,N^3-diphenylanthracene-1,3-dicarboxamide (133) in DMSO-d_6/0.5% water.

Acetate.
$K_a = 37$
Error = 3.3 %

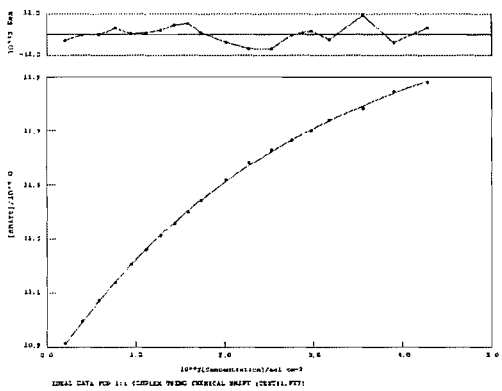

Benzoate.
$K_a = 21$
Error = 2.4 %

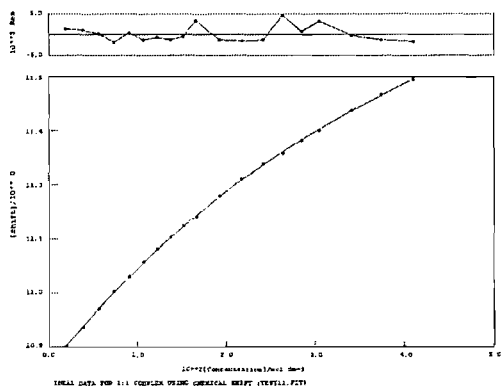

Chloride.
$K_a = <10$
Error = 7.1 %

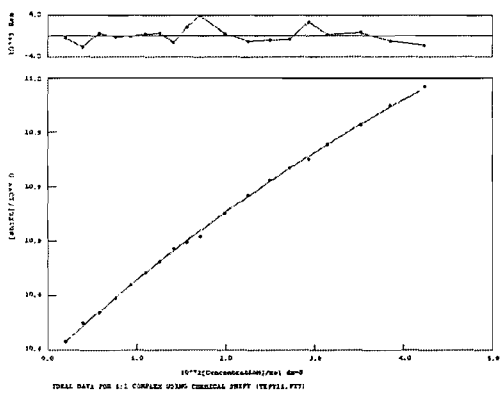

Dihydrogen Phosphate.
$K_a = 122$
Error = 6.6 %

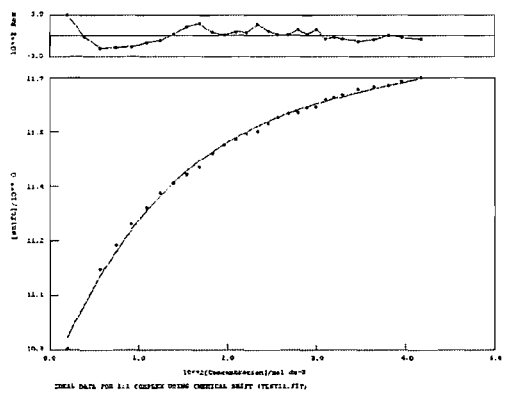

N^1,N^2-dibutylanthracene-1,2-dicarboxamide (135) in CD_2Cl_2-d_2.

Benzoate.
$K_a = 709$
Error = 1.6 %

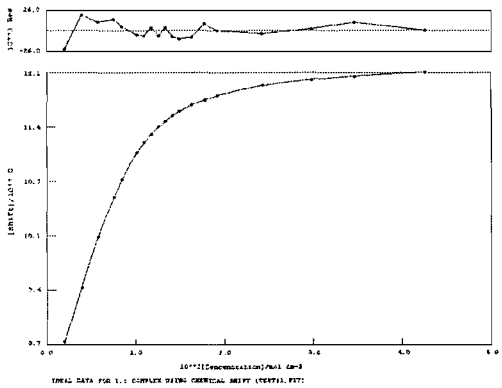

Bromide.
$K_a = 67$
Error = 1.4 %

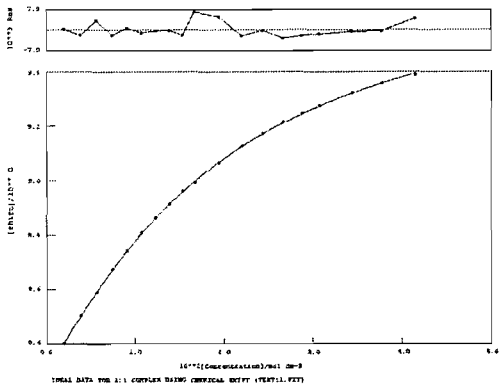

Chloride.
$K_a = 238$
Error = 1.4 %

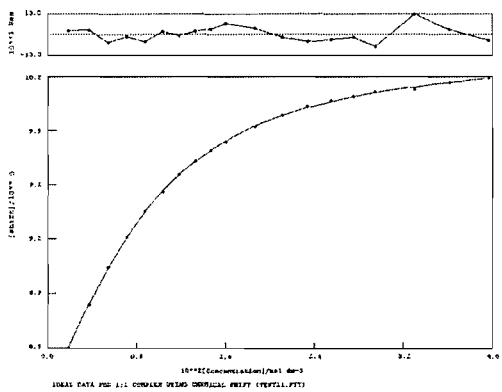

Dihydrogen Phosphate.
$K_a = 128$
Error = 2.3 %

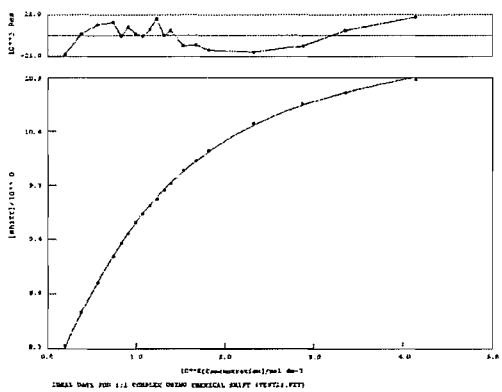

Hydrogen Sulfate.
$K_a = 14$
Error = 11.3 %

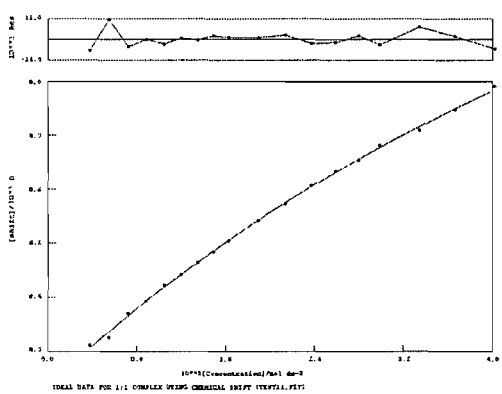

N^1,N^2-dibutylanthracene-1,2-dicarboxamide (135) in DMSO-d_6/0.5% water.

Acetate.
K_a = 85
Error = 0.9 %

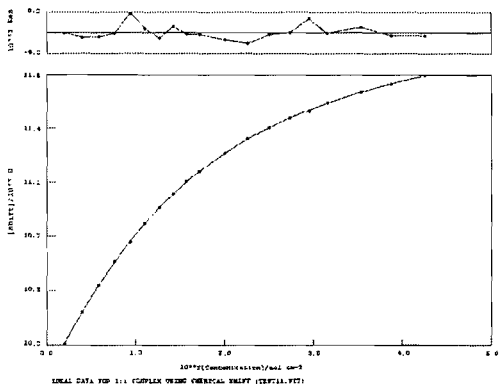

Benzoate.
K_a = 44
Error = 2.1 %

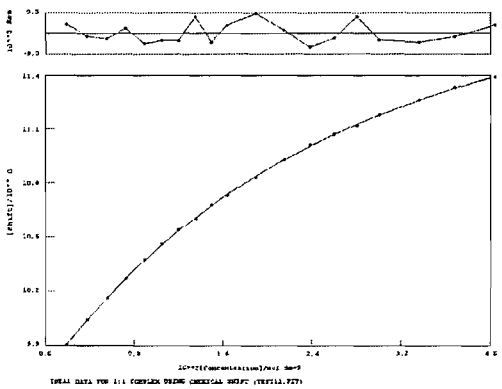

Chloride.
K_a = <10
Error = 4.5 %

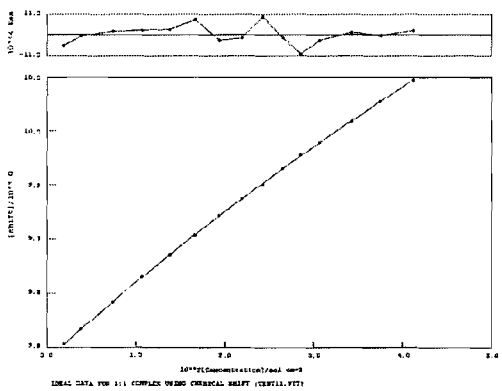

Dihydrogen Phosphate.
K_a = 64
Error = 5.4 %

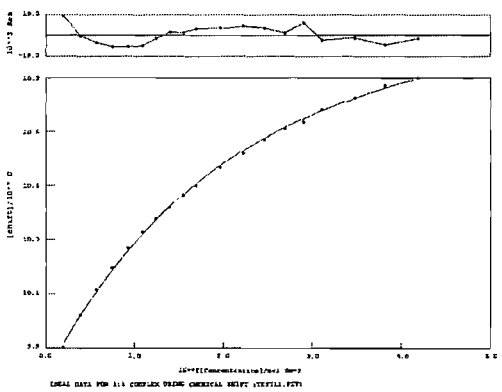

N^1,N^2-diphenylanthracene-1,2-dicarboxamide (136) in DMSO-d_6/0.5% H_2O.

Acetate.
$K_a = 28$
Error = 6.1 %

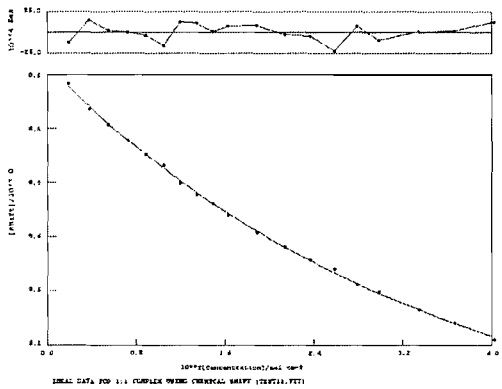

Benzoate.
$K_a = 34$
Error = 3.9 %

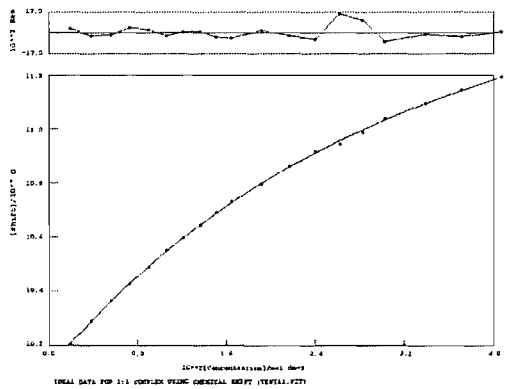

Chloride.
$K_a = <10$
Error = 10.7 %

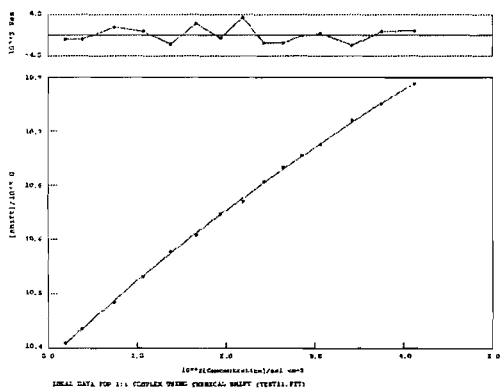

Dihydrogen Phosphate.
$K_a = 63$
Error = 4.1 %

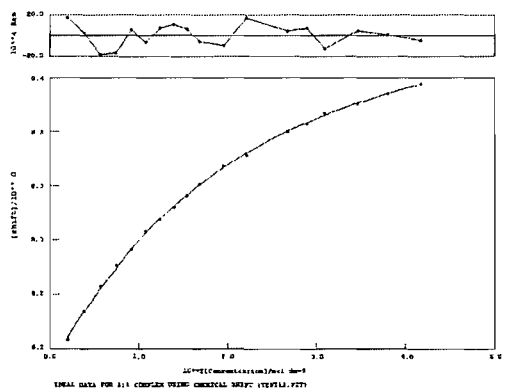

1,2-Anthracene bis-butylurea (137) in DMSO-d_6/0.5% water.

Acetate.
$K_a = 277$
Error = 1.0 %

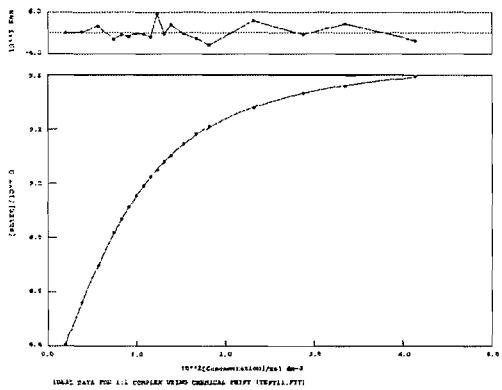

Benzoate.
$K_a = 107$
Error = 1.2%

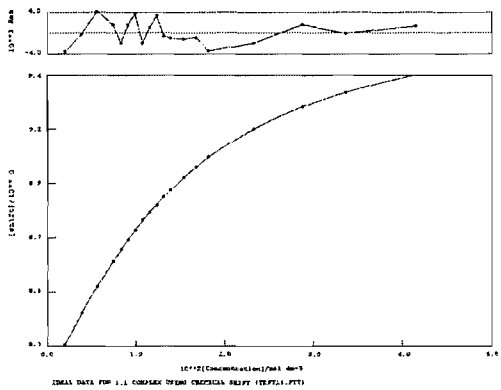

Chloride.
$K_a = 10$
Error = 13.2 %

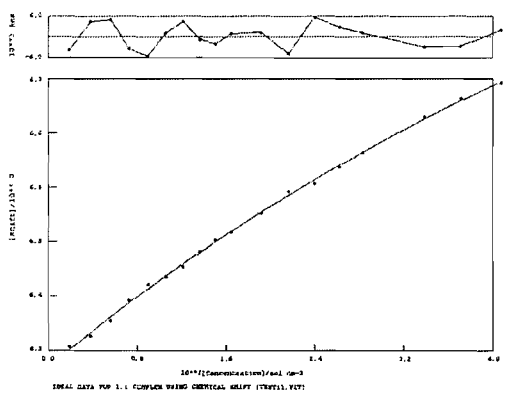

Dihydrogen Phosphate.
$K_a = 370$
Error = 2.1%

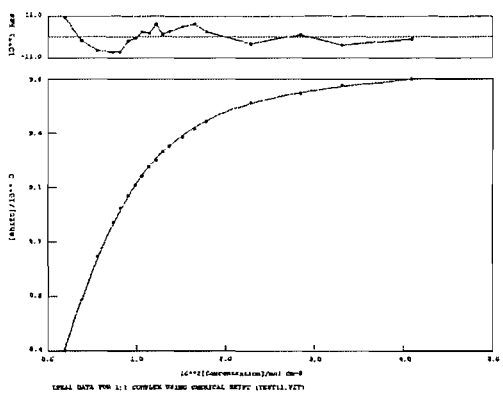

1,2-Anthracene bis-phenylurea (138) in DMSO-d_6/0.5% water.

Acetate.
K_a = 2539
Error = 1.4 %

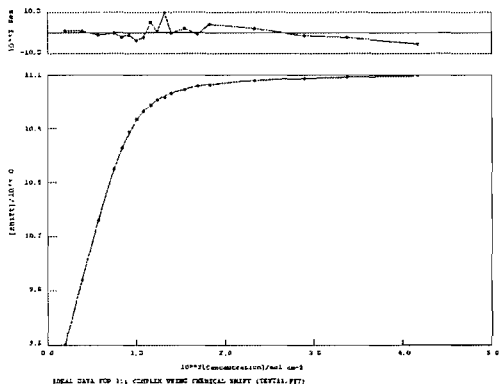

Benzoate.
K_a = 586
Error = 2.9 %

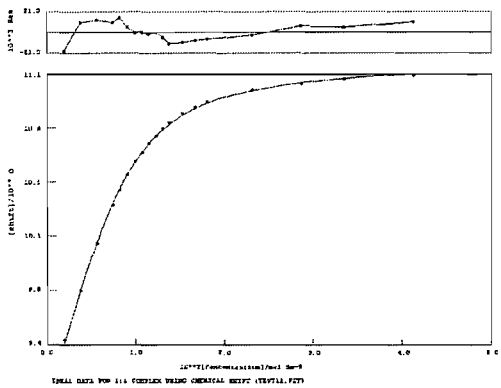

Bromide.
K_a = <10
Error = 29.9 %

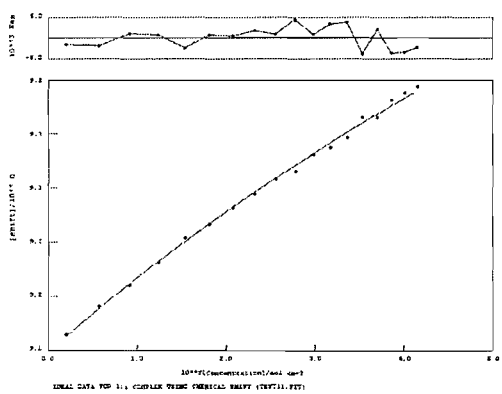

Chloride.
K_a = 27
Error = 2.4 %

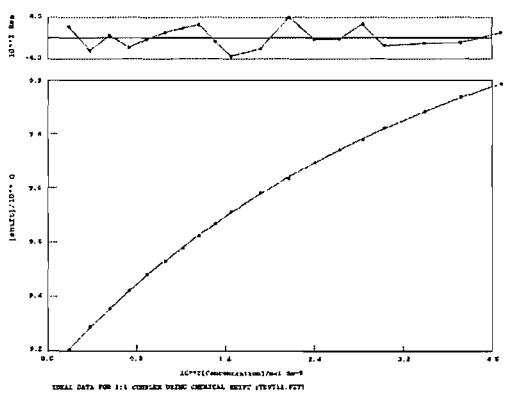

Dihydrogen Phosphate.
K_a = 1166
Error = 6.2 %

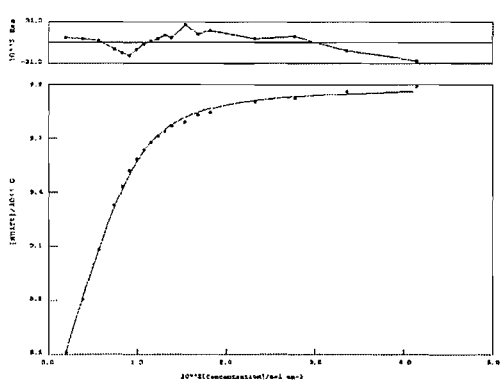

APPENDIX 2. FLUORESCENCE QUENCHING EXPERIMENTS.

FLUORESCENCE QUENCHING CURVES.

Data from fluorescence titrations fitted to a 1:1 binding model.

$$Y = B^{x}x/(1+(K^{x}x))$$

1,2-Anthracene bis-butylurea (137).

Acetate.

$K_a = 400$

Error = 0.6 %

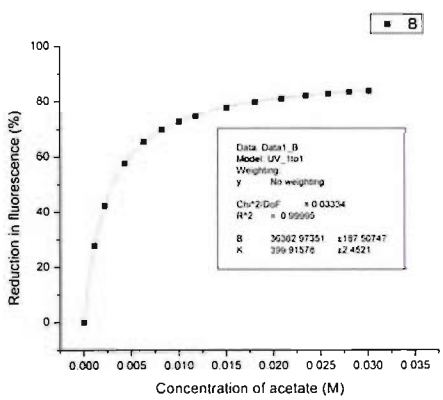

Benzoate.

$K_a = 194$

Error = 2.0 %

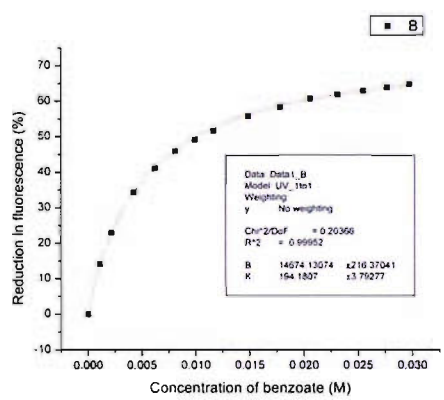

Dihydrogen Phosphate.

$K_a = 368$

Error = 6.2 %

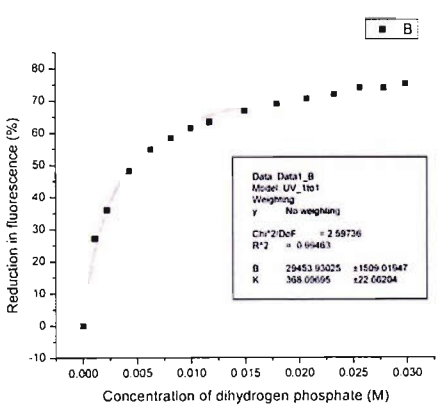

1,2-Anthracene bis-phenylurea (138).

Acetate.

K_a = 1992

Error =2.0 %

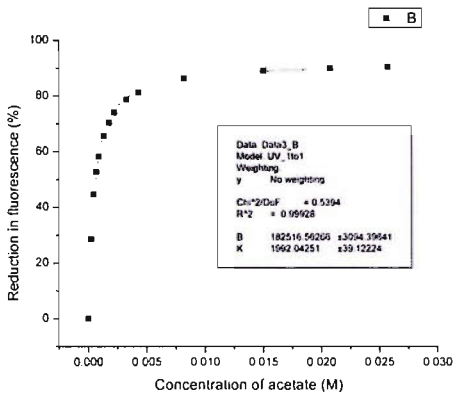

Benzoate.

K_a = 812

Error = 2.5 %

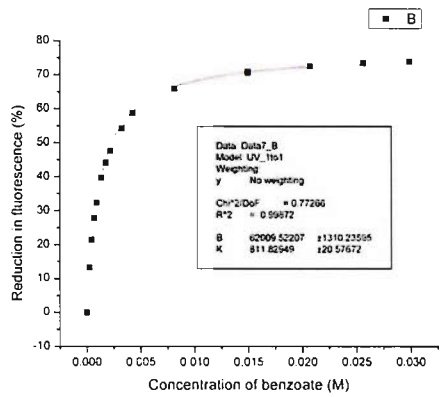

Dihydrogen Phosphate.

K_a = 1019

Error = 12.5 %